POLITECNICO DI TORINO

Collegio di Ingegneria Chimica e dei Materiali

Corso di Laurea Magistrale in
Ingegneria Chimica e dei Processi Sostenibili

Tesi di Laurea Magistrale

Heterogeneous catalysis for C–C coupling reactions: insights, main drawbacks and DFT modeling perspectives.

A comprehensive review

Relatore

Prof. Mauro Banchero

Candidato

Andrea Cassani

Ottobre 2020

In Collaboration with

CSIRO

Commonwealth Scientific and Industrial Research Organization

Manufacturing Business Unit

Research Way, Clayton VIC
3168, Australia

Research supervisor

Ivan Martinez Botella

A dreamer is one
who can only find his way
by moonlight,
and his punishment is that
he sees the dawn before the rest of the world.

Oscar Wilde

Abstract

The C–C cross-coupling reactions are organometallic condensation reactions between two organic groups, borne by two different substrates, and catalyzed by transition metal-based catalysts.
They were discovered in the 20^{th} century and gained great importance later, thanks to the agrochemical and pharmaceutical industries. Nowadays, these industries exploit the reactions for substituting complex and not eco-friendly steps of common organic synthesis paths, with greener ones. Indeed, once well-understood, this group of reactions allows to work under mild conditions, even with non-toxic solvents like water.
During the last years, the most utilized catalytic systems were in-solution solubilized homogeneous systems, namely phosphine-based complexes of palladium. Though, heterogeneous catalysis offers a valuable alternative, in terms of ease in recycling the catalyst, purifying the liquid phase and isolating the reaction product.
For this purpose the CSIRO laboratories patented new modular 3D-printed metallic structures, improving both the fluidodynamics of continuous reactors and the mechanical properties of the solid support, commonly used for heterogeneous catalysis applications. These structures are named Catalytic Static Mixers (CSMs).
Herein an analysis of the state-of-the-art regarding the heterogeneous catalysis of cross-coupling reactions, is performed. Then, the definition of the concept of "cocktail" catalysis helps understanding more deeply, the drawbacks linked to the leaching phenomenon, which decreases the efficiency of the solid-phase catalysts. Moreover, some insights on the DFT molecular modeling techniques complete the overview on the issues which may be encountered during such applications, and their causes.

List of Figures

List of Tables

Contents

0 Italian summary

0.1 Introduzione

Il lavoro, di seguito presentato, verte sull'applicazione di sistemi catalitici eterogenei alle reazioni organometalliche di accoppiamento incrociato C–C. In particolare, la natura bibliografica del rapporto di tesi ha permesso di sostituire l'esperienza che avrebbe dovuto essere condotta in laboratorio, il CSIRO di Clayton (Melbourne, Vic, Australia).
Il Commonwealth Scientific and Industrial Research Organization (CSIRO), è un laboratorio federale australiano, di fama mondiale, che si occupa di una vasta gamma di campi della ricerca, a partire dalla salute, passando per energia e materiali.
Nella sede di Melbourne si sarebbe dovuto svolgere lo stage finale per il conseguimento del doppio titolo Erasmus+.

Il gruppo di reazioni, di cui sopra, avrebbe dovuto essere studiato in batch e in continuo, attraverso la deposizione di catalizzatori a base di palladio, su supporti di vario tipo, tra cui i Catalytic Static Mixers (CSMs) brevettati dall'organizzazione, stessa. Un CSM consiste in una struttura modulare in metallo, ottenuta tramite stampa 3D, con dimensioni sbilanciate a favore della lunghezza.
Si tratta, quindi, di un supporto metallico su cui è possibile depositare uno strato di materiale catalitico, e che può essere facilmente inserito/rimosso nel/dal reattore, in particolare per applicazioni in reattori continui. L'ottenimento è facile e poco costoso e la sua natura monolitica permette di evitare il movimento delle componenti solide, riducendo dannosi fenomeni di degradazione e rottura meccanica durante la reazione, rispetto a un letto catalitico mobile. Risultano evidenti i vantaggi a livello di efficienza e contenimento dei costi. Inoltre, le forme ripetute che compongono la struttura, sono state ottenute, precedentemente alla brevettazione, tramite simulazioni di fluidodinamica computazionale, al fine di ottimizzare la suddetta, all'interno del reattore continuo utilizzato per le esperienze.
Per quanto riguarda il/i reattori da utilizzare, due sarebbero state le scelte possibili: Mark II e Mark IV (microfluidico). Dal momento che Mark IV non era disponibile al momento della preparazione delle prime esperienze in continuo, Mark II è stato scelto come soluzione.
In Figura 47 si può osservare il set up del reattore. Il corpo è costituito da un monolite in acciaio inossidabile, al cui interno sono stati ottenuti 12 canali cilindrici per l'inserimento dei CSMs catalitici e il passaggio della fase liquida. Il monolite è a sua volta incluso tra due testate fisse, anch'esse in acciaio inox, contenenti le scanalature per l'inversione di flusso e i fori d'entrata dei tubi di alimentazione/uscita e delle termocoppie, misuranti la temperatura nel corso del processo.
Infine, il riscaldamento/raffreddamento è effettuato tramite scambio di calore con un fluido all'interno di una camicia esterna, di termostatazione.

Tuttavia, a causa dell'emergenza sanitaria COVID-19, un solo mese su sei è stato speso *in situ* per la sperimentazione, con attenzione preliminare a reazioni in batch. Il resto è stato dedicato alla ricerca e compilazione di questo lavoro bibliografico.

0.2 Le reazioni di accoppiamento incrociato C–C

Le reazioni di accoppiamento C–C sono una classe di reazioni organometalliche, catalizzate da metalli di transizione, con l'intento di creare un nuovo legame carbonio-carbonio tra due gruppi organici introdotti tramite carriers che fungono da substrati per la reazione catalitica. L'accoppiamento può essere omogeneo, tra due molecole dello stesso reagente di partenza, o incrociato, tra substrati differenti. I meccanismi menzionati di seguito, sono sempre del tipo "accoppiamento incrociato".
Reazioni di questo tipo sono largamente utilizzate a livello industriale, specialmente nei settori agrochimico e farmaceutico, perché spesso permettono di lavorare in condizioni più "verdi" e ad alta efficienza, riducendo l'impatto ambientale e i rischi sulla salute umana. Tuttavia, più avanti, si approfondiranno i problemi di contaminazione dei prodotti farmaceutici, che rappresentano uno svantaggio consistente nel caso di utilizzo di gran parte dei sistemi catalitici.

Le reazioni di Suzuki-Miyaura, Mizoroki-Heck e Sonogashira sono le più sfruttate come step intermedi, di accoppiamento incrociato, nelle reazioni di sintesi dei prodotti farmaceutici. Tra questi compaiono molecole con almeno un gruppo bifenile, come in Figure 10-13 e Figura 15. Altri schemi prevedono la formazione di olefine o alchini intramolecolari (Figure 14).

Gli accoppiamenti incrociati C–C procedono secondo la reazione generica di condensazione $R^1X + R^2M \xrightarrow{[cat]} R^1{-}R^2 + MX$, dove R^1X e R^2M sono i due substrati contenenti i gruppi organici, condensati a fine reazione nel prodotto R^1–R^2. Tale reazione, da un punto di vista cinetico e termodinamico è rappresentata da un ciclo catalitico di rigenerazione delle specie catalitiche attive, dipendente dal tipo di substrati utilizzati.
Un ciclo catalitico di accoppiamento C–C, il più generale possibile, è composto da tre step principali: addizione ossidativa, transmetallazione e eliminazione riduttiva.
L'addizione ossidativa è la reazione di coordinazione del reagente R^1X, sul centro metallico. Il palladio è stato utilizzato nella maggior parte dei casi come metallo altamente attivo e sarà analizzato in questo studio, malgrado altri metalli di transizione siano stati studiati (Cu, Pt ecc.). L'addizione ossidativa causa l'ossidazione del palladio a Pd(II). Il substrato R^1X, è costituito comunemente da alogenuri alchilici/arilici, altrimenti, da pseudo-alogenuri (triflati, tosilati ecc). Tuttavia, l'esempio più lampante è rappresentato dagli alogenuri, che verranno citati lungo tutto il corpo della tesi. Riguardo a tali reagenti, alcune considerazioni sulla reattività sono necessarie. L'addizione ossidativa sarà favorita da legami R–X deboli, facilmente rotti in presenza di metalli di transizione. Perciò, la cinetica sarà più veloce in presenza di ioduri, rispetto ai cloruri, secondo la scala decrescente: $I > Br > Cl$. Per lo stesso motivo, in presenza di fenil alogenuri, la sostituzione del fenile con gruppi elettronaccettori favorisce la reazione, rispetto a gruppi donatori.
La prima tappa appena descritta, del ciclo di accoppiamento è supposta procedere secondo due possibili e competitivi meccanismi: concertato e bimolecolare.
Immediatamente seguente l'addizione ossidativa, in alcuni studi, è stato teorizzato un riarrangiamento del prodotto da conformero *cis* a *trans*, secondo calcoli di stabilità che ne suggerirebbero la necessità. É degno di nota, il fatto che, in diversi studi, intermedi/prodotti in forma anionica sono stati rilevati e teorizzati [3, 26]. Questi sembrerebbero provenire dalla sovra-coordinazione di complessi a base di Pd(II), tramite gruppi alogenuro o altri anioni presenti nel mezzo liquido. Perciò, la presenza nel mezzo reattivo, di complessi anionici pentacoordinati fu proposta, nei primi anni, per giustificare l'assenza di stabilizzazione tramite isomerizzazione. Tuttavia, la tappa di riarrangiamento è ancora discussa e il suo coinvolgimento, nel meccanismo di reazione, sembra essere dipendente dalle condizioni.
Indipendentemente dalla presenza o meno, di una tappa di isomerizzazione, la transmetallazione segue l'addizione ossidativa nei comuni cicli reperibili in letteratura. Lo step prevede una sostituzione del gruppo alogenuro con il secondo gruppo organico, sul palladio, tramite azione del reagente R^2M, la cui natura varia a seconda della reazione impostata (Suzuki, Heck, Sonogashira ecc.).
In taluni casi, molecole leganti elettrondonatrici potrebbero causare un rafforzamento del legame Pd–X e conseguentemente, un rallentamento della transmetallazione. Per questi motivi, addizione ossidativa e transmetallazione sono spesso individuate, alternativamente, come gli stadi cineticamente controllanti dell'intero ciclo.
Infine, l'eliminazione riduttiva, terzo e ultimo step del ciclo, è spesso una reazione facile, che prevede la condensazione dei due gruppi organici per formare il prodotto a partire da un complesso *cis*, ristabilendo lo stato d'ossidazione del palladio a Pd(0). Perciò, se si considerasse una tappa di isomerizzazione in seguito all'addizione ossidativa, un secondo riarrangiamento dovrebbe avvenire dopo la transmetallazione, dal momento che i prodotti *trans* della transmetallazione non permettono l'eliminazione. Tuttavia, si tratterebbe di un riarrangiamento altamente endoergonico, e perciò poco probabile.

0.2.1 La reazione di Suzuki-Miyaura

Come primo esempio di accoppiamento incrociato, la reazione di Suzuki avviene tra alogenuri alchilici/arilici e derivati organoboronici, la cui alta reattività, spesso, permette di lavorare in condizioni termiche più leggere, rispetto ad altre reazioni. La reazione è quasi sempre condotta in presenza di una base, organica o meno, anche se le basi inorganiche, e in particolare carbonati e fosfati hanno mostrato le migliori attività. I solventi possibili sono svariati e dipendono molto dalle tipologie di substrati, catalizzatore e base. In linea generale, i solventi polari protici (acqua ecc.) o aprotici (DMF ecc.) sembrano essere più efficienti in termini di attivazione e accelerazione della reazione, rispetto ai solventi apolari (toluene ecc.).

Fu per spiegare il meccanismo della reazione SMC che Amatore e Jutand, introdussero, nel 2000, la possibilità di formazione di complessi intermedi pentacoordinati e anionici, al fine di eliminare le due isomerizzazioni [3]. Tuttavia, la presenza di complessi pentacoordinati non fu mai dimostrata, tramite alcun rilevamento, e l'idea fu accantonata, anche se, tutt'oggi, la formazione di stati di transizione e/o prodotti anionici è una teoria largamente accettata, e composti simili sono stati spesso, isolati.

0.2.2 La reazione di Mizoroki-Heck

La seconda reazione più conosciuta è quella di Heck o Mizoroki-Heck, considerando che Heck è il nome conservato nel caso di alcune varianti come la reazione di Heck-Matsuda. Questo gruppo di reazioni fu il primo a essere scoperto e valse il premio Nobel a Richard Heck nel 2010.

Si tratta, di una condensazione tra il gruppo organico di un alogenuro arilico o alchilico insaturo e un'olefina.

A causa delle differenti reattività e proprietà chimiche degli alcheni rispetto agli organoborani, il ciclo catalitico risulta, nel complesso, leggermente differente rispetto allo schema classico precedentemente presentato (*vide supra*). Infatti, segue all'addizione ossidativa una tappa di inserzione dell'olefina, comunemente secondo una configurazione *syn*. L'intera regioselettività della reazione sembra dipendere da questa tappa, e può essere modulata variando le condizioni di reazione. Conseguentemente, il prodotto viene eliminato dal ciclo tramite uno step di β-eliminazione d'idruro e formazione di un alchene intramolecolare (Figura 6). Il ciclo si conclude con la riduzione del centro metallico tramite decoordinazione del legante alogenuro (X^-).

In aggiunta a quanto sopra esposto, tali reazioni, vengono spesso condotte a temperature relativamente alte ($> 100°C$), che favoriscono reazioni parassite indesiderate. Una tra tutte è la π-coordinazione non ossidativa dell'olefina, che finisce per occupare il sito catalitico senza donare prodotti di reazione, riducendo la resa del processo.

0.2.3 La reazione di Sonogashira

Infine, la reazione di Sonogashira permette la formazione di un alchino intramolecolare per condensazione tra un alchino terminale e un gruppo organico portato da un alogenuro. La reazione è spesso condotta in presenza di un co-catalizzatore a base di Cu(I), che permette l'attivazione del carbonio sp dell'alchino. Tuttavia, questa variante, anche se è la più conosciuta, riduce spesso la selettività del processo, favorendo reazioni di omoaccoppiamento, note come reazioni di Glaser-Hay (Figura 9(**a**)). Alternativamente, il co-catalizzatore può non essere utilizzato, ma ciò richiede un'attenzione particolare alla reattività dei substrati.

0.3 Il ruolo del solvente

Come accennato precedentemente, i componenti del sistema reattivo e le condizioni di reazione sembrano avere un impatto importante su conversione e selettività dei cicli catalitici di accoppiamento C–C. Il ruolo più importante è probabilmente giocato dal solvente, la cui azione non è stata ancora completamente compresa.

È noto che il solvente può controllare l'efficienza della reazione. In particolare, la polarità del solvente può favorire/disfavorire determinati meccanismi di reazione in soluzione, come nel caso dell'eliminazione dell'alogenuro, dove la solvatazione per mezzo delle molecole di solvente permettono di stabilizzare l'anione rimosso. Inoltre, molecole di solvente polari possono adsorbirsi debolmente sulla superficie solida di catalizzatori eterogenei. Qui, possono favorire il distacco locale di atomi o agglomerati di atomi di metallo, come il palladio, e addirittura la loro solubilizzazione. Questo fenomeno è noto come leaching, ed è stato dimostrato che viene favorito dall'utilizzo di solventi polari più che apolari. In concomitanza con questo effetto, anche la conversione sembra essere facilitata, nelle medesime condizioni, il che porta a chiedersi se non sia facilitata dal passaggio stesso di atomi di palladio in soluzione.

Così come le molecole di solvente possono adsorbirsi sulla superficie di un catalizzatore solido, ciò può avvenire alla superficie di nanoparticelle, introdotte per la sperimentazione, o prodotte *in situ*. Tali nanoparticelle possono, quindi, essere stabilizzate dagli effetti elettronici di formazione del doppio strato di cariche, di Stern e Guy-Chapman, cosi come prodotte per riduzione da anioni, anche in assenza di composti riducenti (idrazina, $NaBH_4$ ecc), in determinate condizioni. Le nanoparticelle così stabilizzate possono essere re-veicolate verso la superficie solida e re-adsorbirsi. In questo caso, una riduzione dell'efficienza è stata spesso misurata, per cristallizzazione incontrollata e ristrutturazione con perdita di superficie attiva, durante tale processo. D'altro canto, la re-deposizione di atomi di palladio su una superficie, può dare vita a adatomi, o atomi giacenti singolarmente su una superficie solida cristallina. Tali adatomi superficiali, sono siti di leaching preferenziale e sono considerati la causa prima di aumento dell'attività in soluzione.

La polarità dei solventi è spesso modulata attraverso l'aggiunta di acqua, per formare una miscela a polarità aumentata. Altrimenti, sistemi bifasici, come le microemulsioni sono stati testati per massimizzare la solubilità di molecole idrofile e idrofobe al tempo stesso, e gli scambi di materia tra fasi diverse. Per tali applicazioni, spesso, sali d'ammonio, noti anche come liquidi ionici (LI), sono stati utilizzati come surfattanti per la stabilizzazione delle interfacce solido-liquido.

I liquidi ionici sono anche adoperati come solventi, separatamente o in miscela con acqua, per aumentare le proprietà di stabilizzazione degli agglomerati/nanoparticelle metallici in soluzione e migliorare la riciclabilità di sistemi catalitici omogenei e eterogenei nonché la purificazione del solvente stesso. Del loro impatto sul processo di leaching, si parlerà più avanti.

Per concludere, sempre maggiore attenzione è stata dedicata ai cosiddetti solventi "green" come l'acqua, a impatto ambientale "zero", o ridotto. In questa categoria rientrano i solventi eutettici profondi, formati da due componenti, un donatore e un accettore di legami a idrogeno.

0.4 Catalisi - Generalità

In termini di catalisi, possono essere utilizzati sia sistemi omogenei a base di palladio, sia eterogenei, con risultati interessanti in termini di resa. Tuttavia, possono sopraggiungere problemi di contaminazione dei prodotti industriali.

I sistemi catalitici più utilizzati anche dall'industria farmaceutica, quelli omogenei, sono composti solubili nel mezzo di reazione, quali complessi metallorganici o sali di palladio. Ciò causa l'introduzione di metalli pesanti, e con forte probabilità di molecole tossiche, sotto forma di leganti del palladio, che rischiano di essere intrappolate nella struttura del prodotto in formazione, durante le tappe di purificazione. In questo caso si parla di contaminazione del prodotto, un fenomeno che è severamente regolamentato in molti settori, come quello farmaceutico.

Per quanto riguarda i sistemi eterogenei, questo discorso risulta ancora più complesso. Dal momento che, tali sistemi, seppur meno efficienti dei loro analoghi omogenei, sono introdotti per facilitare la separazione del catalizzatore e la riduzione del rischio di contaminazione, la presenza di fenomeni di leaching e solubilizzazione in fase liquida fanno venir meno i vantaggi di questo cambiamento di condizioni. Inoltre, la re-deposizione che può prodursi ad alte conversioni e l'enorme attività del palladio in soluzione, anche a basse concentrazioni, rendono complesso il rilevamento di contaminazioni della fase liquida, con conseguente aumento dei rischi.

Se in aggiunta, si considera l'elevato costo di fabbricazione dei complessi catalizzatori solidi, e delle tecnologie che spesso sono richieste per ridurre al minimo il leaching, tale utilizzo, non sembra essere così vantaggioso. La separazione del catalizzatore è in parte facilitata, ma operazioni di purificazione potrebbero essere richieste, in ogni caso, in presenza di leaching consistente.

Per questi svariati motivi, il comportamento dei catalizzatori solidi per reazioni di accoppiamento C–C, in contatto con una fase liquida, deve essere studiato nel dettaglio, prima di effettuare qualsiasi operazione di scale-up.

Per la standardizzazione dell'espressione dei risultati sperimentali, due grandezze sono le più usate negli studi di catalisi: numero e frequenza di turn-over, TON e TOF.
La frequenza di turn-over (TOF) rappresenta l'attività intrinseca di un catalizzatore nei confronti di un determinato substrato. Si tratta di una quantità espressa in $[h^{-1}]$ e calcolata, come la derivata del numero di cicli catalitici effettuati da un sito catalitico nell'unità di tempo. Parallelamente, il numero di turn-over (TON) definisce sia l'attività che la durabilità del catalizzatore, in quanto misura adimensionata dell'attività globale del catalizzatore fino a fine vita (disattivazione completa).

0.5 Catalisi omogenea

Come già spiegato, i catalizzatori più utilizzati sono sistemi omogenei, solubili nella fase liquida.
Una prima categoria è costituita dai semplici sali di palladio, sfruttati senza addizione di alcun tipo di molecola legante. Si tratta di composti del tipo $Pd(OAc)_2$, $PdCl_2$ ecc., altamente attivi anche a concentrazioni molto basse, ma che presentano ridotta e poco controllabile selettività verso il prodotto oltre a una certa sensibilità a fenomeni di coalescenza.
Considerando che è stato ormai dimostrato che la forma attiva del palladio è quella ridotta Pd(0), in quanto entra direttamente nel ciclo catalitico, anche il palladio ossidato Pd(II) necessita di riduzione *in situ*, prima di iniziare la reazione. Eppure, il Pd metallico è estremamente sensibile alla coalescenza, e quindi rischia di diminuire l'attività di tali sistemici catalitici, tramite formazione e precipitazione di aggregati di inattivi di Pd elementale, il "Pd black". Lo stadio prima della precipitazione di tali aggregati, prevede la formazione *in situ* di nanoparticelle, che spesso sono anche state considerate come le vere forme attive del palladio.
La coalescenza diventa importante anche, nel momento dell'acquisto di un determinato composto catalitico. Diversi studi hanno dimostrato che la contaminazione da nanoparticelle potrebbe essere la causa della grande differenza di efficacia tra composti dello stesso tipo, ma acquistati da produttori diversi. Infatti, la contaminazione da nanoparticelle sembra cambiare in funzione del produttore e agire sull'efficienza dei sistemi catalitici.
Tra le soluzioni ai problemi di instabilità del palladio, è interessante nominare l'utilizzo di sali d'ammonio (TBAB ecc.) in soluzione o la complessazione con molecole leganti. Tra i leganti più utilizzati, troviamo sicuramente, le fosfine. Si tratta di molecole organiche, donatrici di elettroni a base di fosforo, per cui gli elettroni messi a disposizione del palladio sono quasi sempre gli elettroni di non-legame o anti-legame del P. In quanto tali, si tratta di elettroni a relativamente basso potere di coordinazione che rendono il legame Pd–P fragile e facilmente spezzabile, da condizioni termiche più severe, per esempio. La rottura di tale legame, oltre ad aumentare il rischio di coalescenza del Pd(0) e diminuire l'efficienza dei catalizzatori omogenei può costituire una fonte di contaminazione del prodotto industriale, tramite molecole tossiche e sensibili ad atmosfere ossidanti come le fosfine.
D'altro canto, le fosfine sono composti relativamente poco costosi e molto studiati, di cui gli effetti elettronici e sterici sono facilmente modulabili, e che permettono di aumentare la densità elettronica del palladio per favorire le tappe di attacco nucleofilo su molecole come gli alogenuri (addizione ossidativa).
Altri leganti simili alle fosfine, possono essere prodotti a partire da gruppi a base di azoto, zolfo, arsenico, selenio, silicio ecc., in modo da aumentare la forza del legame con il palladio e ridurne le possibilità di rottura.
Alcune forme particolari di complessi metallorganici, sono i palladacicli e i carbeni N-eterociclici. Mentre i primi sono semplicemente forme cicliche di complessi del palladio, in cui quest'ultimo è incorporato in un eterociclo, i secondi coinvolgono un tipo di legame, il Pd–C, non ancora presentato. Tale legame, è stato spesso considerato più forte dei classici legami Pd–legante, anche se in alcuni casi fu dimostrato che questi complessi potevano comportarsi esattamente come forme di Pd non complessate, sottolineando la possibilità di rottura di tale legame. Si tratta, però, di composti progettabili e dalle proprietà

altamente modulabili. I leganti pre-coordinati possono, per esempio, essere debolmente legati al palladio, al fine di facilitare l'addizione ossidativa, per decoordinazione del legante, seppur stabilizzando il palladio.

0.6 Catalisi eterogenea

Il passaggio a catalizzatori eterogenei prevede l'immobilizzazione delle forme attive descritte, complessi e/o sali, su un supporto solido, in forma di letto mobile o fisso, o ancora sotto forma di colloidi disperdibili nella fase liquida.
Tuttavia, tale immobilizzazione, oltre a provocare modifiche, spesso negative, all'attività delle specie attive, crea resistenze non trascurabili al trasporto di materia. Infatti, al momento della formazione di un'interfaccia solido-liquido, i reagenti devono attraversare una serie di resistenze e barriere energetiche di adsorbimento/desorbimento, prima di effettuare la reazione vera e propria. Tutto ciò riduce l'efficacia del catalizzatore solido rispetto ad un sistema omogeneo (Figura 24).
Tra i supporti più conosciuti e utilizzati, quelli a base di carbonio sono, forse, i più famosi e apprezzati. Le prime sperimentazioni furono effettuate su carbone attivo, un supporto economico, ad elevata porosità e stabilità, a una vasta gamma di pH e condizioni di reazione. Tuttavia, la sua semplicità e difficoltà ad accedere alla funzionalizzazione della superficie, riduce la stabilità a lungo termine del sistema, con rischio elevato di sintering e leaching. Si parlerà più avanti e più approfonditamente di entrambi i fenomeni.
Al carbone attivo sono spesso preferiti i sistemi nano-dimensionati dei tipi: ossido di grafene ridotto (RGO), nanotubi di carbonio, nanoparticelle, fullereni ecc. Le dimensioni peculiari di tali carriers, oltre ad aumentare notevolmente la rapidità e l'attività catalitica, conferiscono, spesso, proprietà chimiche uniche. In aggiunta, il dopaggio a base di gruppi azotati, così come la presenza di gruppi ossigenati (carbonile, carbossile ecc.) sui fogli di RGO, è una tecnica che può essere sfruttata per aumentare l'aderenza dei metalli di transizione sulle superfici solide dei supporti, una metodologia spesso utilizzata anche in fabbricazione di elettrodi in elettrochimica.
Una classe di supporti altrettanto famosa è rappresentata dagli ossidi inorganici di silicio, alluminio, cerio, magnesio, zinco, zircone ecc. Si tratta di materiali solidi dalle proprietà chimiche estremamente varie e variabili, ma che, spesso, presentano problemi di stabilità per contatto con soluzioni acide o alcaline.
Negli ultimi anni, le strutture polimeriche sono state largamente utilizzate, probabilmente perchè sono le più facilmente modulabili in termini di proprietà chimiche. Variando le dimensioni e natura chimica dei monomeri, si possono produrre catene altamente diversificate, in termini di porosità e natura dei gruppi funzionali. Fanno parte di questa categoria le MOF e i dendrimeri, le prime, materiali ad elevata porosità utilizzati in altre applicazioni come setacci molecolari; gli ultimi, strutture supra-molecolari ad elevata simmetria, utilizzati per l'incapsulamento di specie a base di palladio, da diversi autori, in studi di catalisi delle reazioni di accoppiamento C–C.
Recentemente, alcuni biopolimeri come la cellulosa, la lignina e il chitosano sono stati utilizzati efficacemente in diverse applicazioni come supporti solidi per sistemi catalitici.

Per quanto riguarda i catalizzatori eterogenei, sono molte le combinazioni possibili, di natura chimica del palladio, tipo di supporto e condizioni di reazione. I primi studi furono effettuati sull'immobilizzazione di complessi di palladio su svariati supporti; si tratta di complessi a base di gruppi elettrondonatori, come le fosfine.
Come precedentemente anticipato, tali studi furono incentrati prevalentemente sul problema di decomposizione dei complessi e conseguente solubilizzazione del palladio. Svariati autori rilevarono rotture dei legami legante–Pd. Fra i vari studi la migliore possibilità sembrò, per un periodo, essere l'immobilizzazione di carbeni N-eterociclici, dal momento che il legame Pd–C appariva come il più stabile. Tuttavia, non tutti i ricercatori concordano sull'effettiva stabilità di tali legami con il palladio.
Al fine di ridurre la quantità di palladio perso per solubilizzazione e/o precipitazione di Pd black, molecole "scavengers", o sequestratori di palladio, sono state utilizzate per funzionalizzare le superfici solide dei supporti polimerici. Tale funzionalizzazione da' origine a catene laterali, spesso, a base di

zolfo, che permettono di sequestrare per complessazione le specie di Pd solubilizzate nella fase liquida.
La soluzione sembra, ora, solo parzialmente praticabile, in quanto efficace nel ridurre la concentrazione di palladio in soluzione soltanto in tempi lunghi, a causa di una cinetica di complessazione lenta. Inoltre, le condizioni di reazione sembrano avere un impatto sullo stato di ossidazione dello zolfo stesso, con rischio di decomposizione e perdita di siti attivi.
Dal momento che le perdite di palladio in soluzione sembrano inevitabili, diversi studi sono stati condotti sulla stabilizzazione delle specie disperse/solubilizzate e sui meccanismi di re-deposizione del palladio sulla superficie solida. Quest'ultima sarà trattata più approfonditamente di seguito.
Relativamente alla stabilizzazione, si è già accennato al ruolo dei sali di ammonio sottoforma di chelanti solubilizzati nella fase liquida o di liquidi ionici. Alternativamente, i dendrimeri possono essere sfruttati per l'incapsulazione del palladio con conseguente stabilizzazione.
Nonostante l'efficacia dei sistemi sopra descritti, la stabilizzazione eccessiva sembra comportare una consistente riduzione dell'attività catalitica del palladio, specialmente in presenza di nanoparticelle. Infatti, se si considerassero le nanoparticelle come riserve di palladio atomico effettivamente attivo e rilasciato tramite leaching, l'incapsulazione potrebbe ridurre il trasporto di materia delle specie attive e ridurne, quindi l'attività globale.
In alternativa, all'immobilizzazione di complessi di palladio, tale metallo può essere depositato sottoforma di Pd(II) o di nanoparticelle di Pd(0). Nel primo caso, tuttavia, data la presenza in fase liquida di molecole organiche o agenti riducenti e, in alcune applicazioni anche di semplici anioni o molecole di solvente, le specie ossidate possono essere facilmente ridotte a Pd(0).
Come anticipato, il palladio metallico è instabile e sensibile a coalescenza. Ciò comporta quindi, la formazione di agglomerati e nanoparticelle, senza possibilità di distinguere la prima tipologia di catalizzatori eterogenei, dalla seconda. L'aggregazione avviene principalmente per maturazione di Ostwald, per cui il potenziale delle superfici di nanoparticelle di dimensioni diverse dirige una migrazione a livello atomico, dalle particelle più piccole alle più grandi.
Malgrado queste similitudini tra l'immobilizzazione di palladio "nudo" (sottoforma di sali di Pd(II)) e nanoparticelle, è degno di nota citare una tecnologia recente che permette l'immobilizzazione di palladio metallico in forma atomica, raggiungendo livelli di uniformità molto elevati e interessanti. Dal momento che è proprio, la distribuzione disomogenea delle dimensioni delle particelle a causare la maturazione di Ostwald, l'ottenimento di atomi immobilizzati in modo "monodisperso" riduce la probabilità di coalescenza, stabilizzando le superfici dei catalizzatori. Si tratta dei SAC o catalizzatori a singolo-atomo [37].
Ciò che è stato appena esposto rende, a questo punto, necessario un approfondimento a riguardo delle nanoparticelle di Pd. Per anni, la natura catalitica di tali agglomerati di palladio è stata discussa. Molti autori le hanno indicate come specie effettivamente attive, che espleterebbero, perciò, un meccanismo eterogeneo di adsorbimento dei substrati e reazione superficiale (Figura 33). Alternativamente, le specie attive richiederebbero di passare nella fase liquida, per ottenere i prodotti di reazione tramite catalisi omogenea. Quest'ultimo meccanismo sembra essere il più plausibile, date le numerose prove di consistenti componenti omogenee di catalisi, in diverse applicazioni di catalisi eterogenea. Tuttavia, il contributo della catalisi eterogenea non può essere completamente escluso, anche se, in genere, meno significativo.
Le nanoparticelle sono strutture cristalline caratterizzate da impilaggio più o meno uniforme di atomi. Tali strutture sono caratterizzate, quindi, in termini di disposizione degli atomi, che vengono distinti in atomi di vertice, spigolo e faccia. Inoltre, impurità, come adatomi di palladio, possono facilmente depositarsi sulla superficie cristallina e altrettanto facilmente subire un distacco. Ciò accade perché gli adatomi presentano un basso numero di coordinazione, una grandezza caratterizzante ogni atomo facente parte di una struttura cristallina, comprese le impurità. Il numero di coordinazione rappresenta il numero di atomi appartenenti a una struttura cristallina, che circondano l'atomo di riferimento e con cui questo forma dei legami. Un numero di coordinazione più elevato significherebbe una maggiore barriera energetica, da superare per il distacco dell'atomo dalla struttura.
Diversi studi sono stati condotti sulla relazione tra leaching a partire da nanoparticelle e la direzione di crescita delle facce di tali particelle. Sembra che strutture che presentano una crescita estremamente

direzionata, siano più sensibili al leaching. Introducendo il formalismo degli indici di Miller, facce del tipo {111} o {100} sembrano essere più stabili di facce come {730} e {221}, a causa degli inferiori numeri di coordinazione degli atomi che le formano. Di conseguenza, facce più instabili saranno anche più sensibili alla ri-cattura delle specie solubilizzate nella fase liquida, con conseguente riduzione della contaminazione del mezzo reattivo da metalli pesanti [34].

In conclusione, prima di procedere all'approfondimento dei fenomeni di leaching e sintering, vale la pena citare due applicazioni interessanti di catalizzatori eterogenei. Si tratta delle nanoparticelle magneticamente riciclabili e delle leghe Au/Pd fotoattivabili.
Le prime sono nanoparticelle a base di magnetite, ricoperte da uno strato polimerico (lignina, chitosano ecc.) o a base di ossidi inorganici (silice ecc.). Tale strato ricopre sia un ruolo di protezione contro la coalescenza, di cui la magnetite soffre, anche a causa delle sue proprietà magnetiche, sia permette la funzionalizzazione della superficie delle particelle, con sistemi a base di palladio, tra cui complessi, carbeni ecc.
Le leghe di oro e palladio, invece, sono state recentemente scoperte come materiali metallici fotoattivabili. In particolare, un raggio di luce incidente sembrerebbe capace di separare un elettrone dalla sfera di valenza dell'oro per arricchire quella del palladio. Ciò comporterebbe un'addizione ossidativa dell'alogenuro, di tipo radicalico, per poi ristabilizzare lo stato di ossidazione del palladio a Pd(II) e condurre un ciclo catalitico ordinario.

0.7 Catalisi eterogenea - Catalisi "cocktail"

Finora, si è parlato di meccanismi di leaching, sintering, re-deposizione, una serie di fenomeni che contribuiscono ad aumentare la complessità delle applicazioni catalitiche in tema di accoppiamenti C–C. Tuttavia, è doveroso riordinare le idee e dare uno schema di correlazione tra i fenomeni citati. Ciò è possibile evocando un concetto noto nella catalisi eterogenea di queste tipologie di reazioni, come la catalisi "cocktail".
Il concetto si riferisce a una miscela di fenomeni che modificano la natura chimica e fisica delle diverse specie di palladio, nel corso della reazione, in uno scenario estremamente dinamico. In quest'ottica, le specie di palladio possono attivarsi/disattivarsi nel corso della reazione o subire una trasformazione da una forma all'altra, creando un sistema complesso formato da specie di natura chimica diversa, contemporaneamente attive, ma con efficienze diverse. Per diverse specie di palladio si intendono principalmente: palladio atomico in forma ossidata o metallico, complessi (anche sottoforma di oligomeri), agglomerati e nanoparticelle, nelle loro versioni in soluzione o immobilizzate.
Secondo il concetto di catalisi "cocktail", partendo dalla superficie si possono trovare specie ossidate di Pd(II) facilmente riducibili, come accennato in precedenza, a palladio metallico. A causa della loro instabilità, gli atomi di palladio immobilizzati possono coalescere, per migrazione o maturazione di Ostwald. Tale migrazione, può essere una delle cause del leaching, in quanto il momentaneo distacco dell'atomo dalla superficie può causarne la captazione da parte di molecole solvatanti e la conseguente solubilizzazione. Altrimenti, l'atomo può concludere la migrazione e formare nuovi aggregati/nanoparticelle.
A loro volta le nanoparticelle possono cambiare dimensioni, guidate da fenomeni di sintering per maturazione di Ostwald o migrazione di intere particelle. Di nuovo, la migrazione di particelle, può essere una causa di distacco e dispersione nel mezzo liquido reattivo. Dalla superficie di nanoparticelle immobilizzate, singoli atomi o nanoaggregati (clusters), possono subire un distacco, nel caso di facce cristalline più instabili.
Molecole di solvente o altre molecole chelanti (capping agents) in soluzione hanno la caratteristica di stabilizzare la maggior parte delle specie che si separano dalla superficie solida, e di allungarne la vita in soluzione, contro coalescenza e disattivazione per precipitazione di Pd black.
Una delle cause principali di leaching sembra, invece, essere la stessa addizione ossidativa. Sulle specie preridotte, spesso prima del leaching, l'attacco delle molecole di alogenuro causerebbe un distacco semi-definitivo e l'avvio del ciclo catalitico.
Per concludere, ad alte conversioni del reagente limitante, l'equilibrio di leaching/re-deposizione si

sposta verso quest'ultima, causando la ricristallizzazione delle specie di palladio disciolte/disperse nella fase liquida e re-immobilizzazione sulla superficie solida. Si tratterebbe, però, essendo un fenomeno difficilmente controllabile, di una delle cause di perdita dell'attività dei catalizzatori eterogenei, per aumento della polidispersione delle dimensioni degli aggregati e riduzione della superficie attiva.
Secondo uno studio approfondito, di Eremin e Ananikov del 2017, si parla di leaching da un agglomerato/nanoparticella nel caso di: distacco locale di atomi, separazione definitiva di atomi o agglomerati, e destrutturazione dell'agglomerato di partenza (Figura 41). In modo simile, la re-deposizione può essere orientata, "caotica" o ibrida (Figura 42).
Durante questi fenomeni di scambio di materia tra la fase solida e quella liquida, alterazioni locali di carica, possono anche verificarsi. Per esempio, un complesso metallorganico può subire la coordinazione di uno ione alogenuro o la perdita di tale gruppo, riducendosi o ossidandosi, rispettivamente. Allo stesso modo la formazione e crescita di nanoparticelle può modificare la polarizzabilità delle stesse, alterando le proprietà degli strati ionici di Stern e Guy-Chapman e originando svariate, e spesso uniche proprietà in termini di attività catalitica.

0.8 Meccanismi di disattivazione e sintering

A tutti gli elementi di complessità citati, si aggiungono i tipici meccanismi di disattivazione di catalizzatori solidi, in parte già menzionati. Oltre a leaching e sintering, si ricordano i fenomeni di deposizione di molecole o strati molecolari meno attivi, come strati polimerici o di altri metalli meno attivi del palladio, che riducono l'accessibilità dei siti attivi e l'attività; altri fenomeni di adsorbimento di molecole che possono avvelenare il catalizzatore, come i composti a base di zolfo; alterazioni meccaniche e/o ossidazione del componente attivo, il palladio. In quest'ultimo caso, diversi studi hanno dimostrato che l'utilizzo di condizioni aerobiche durante reazioni di accoppiamento catalizzate dal palladio, causano l'ossidazione della superfice a PdO. Tali specie sono particolarmente sensibili al leaching, in quanto più solubili del palladio metallico.
Alcune precisazioni sono necessarie nel caso della disattivazione per sintering. Se si considerano, come unici meccanismi di sintering, la maturazione di Ostwald e la migrazione particellare, tramite una semplice analisi della PSD, o curva di distribuzione delle dimensioni particellari, si possono trarre alcune informazioni utili. Infatti, il sintering causato principalmente dalla maturazione di Ostwald, presenta curve PSD crescenti verso le dimensioni maggiori, ma con valori di cut-off, ovvero dove la curva precipita, intorno a 1,3-1,5 volte la dimensione iniziale. Al contrario, nel caso di migrazione prevalente, delle code nella curva PSD possono essere osservate dalla parte delle dimensioni maggiori.
Perciò alcuni studi sono stati effettuati riguardo a tale fenomeno e al suo impatto sulle performance in condizioni di reazioni di accoppiamento C–C. La crescita delle nanoparticelle sembra essere caratterizzata da tre fasi distinte, in cui si riscontra una decrescita in dimensioni delle particelle più piccole nella fase iniziale, seguite da rallentamento di tale decrescita e sparizione definitiva delle particelle, intorno a determinate dimensioni. Apparentemente, le prime fasi del sintering sembrano essere causate principalmente dalla maturazione di Ostwald, o migrazione atomo per atomo, per poi lasciare il posto a fenomeni di migrazione prevalente.

0.9 Leaching - Tecniche di analisi

Solo dopo aver compreso nel dettaglio l'insieme delle trasformazioni che un sistema catalitico, come quelli citati, può subire, risulta più facile trarre conclusioni dalle analisi di tali sistemi bifasici. Spesso, a causa di mancanza di conoscenza al riguardo, i risultati sono stati male interpretati e le conclusioni tratte fuorvianti.
Tra le tecniche di analisi più utilizzate per tracciare una linea di demarcazione tra catalisi eterogenea e omogenea da leaching, si ricordano: l'analisi ICP della fase liquida, la filtrazione a caldo, i test da avvelenamento, di cui il più famoso è quello al mercurio Hg (0) e il 3-phase test.
Nel primo caso il mezzo di reazione viene analizzato, alla ricerca di impurità, palladio in questo caso specifico. Malgrado la grande sensibilità della tecnica, determinati limiti tecnologici di rilevamento sono imposti e possono falsare il risultato. Spesso, dal momento che il palladio risulta estremamente attivo

in soluzione (catalisi "omeopatica"), anche a concentrazioni molto basse (dell'ordine della ppm/ppb), la tecnica utilizzata potrebbe non dare risultati positivi riguardo la presenza di specie catalitiche attive disciolte. Eppure, queste potrebbero essere presenti e altamente attive.

Per quanto riguarda la tecnica di filtrazione a caldo, essa si basa sulla separazione del catalizzatore solido, mantenendo la fase liquida alla temperatura di reazione per evitare fenomeni di precipitazione o re-deposizione. Oltre alla complessità operativa di tale tecnica, bisogna tenere conto che a conversioni dei reagenti troppo elevate, i fenomeni di re-deposizione sono prevalenti rispetto al leaching e rischierebbero di dare falsi negativi. Perciò è necessario bloccare la reazione intorno a conversioni del 50% e, possibilmente, condurla con reagenti relativamente poco attivi in modo da lasciare il tempo di operare la separazione e le analisi della fase liquida.

In terzo luogo, si ricorda che le cinetiche di avvelenamento possono essere relativamente lente rispetto a quelle di reazione e non dare la possibilità di escludere completamente il contributo di catalisi eterogenea. In quest'ottica, l'avvelenamento da mercurio Hg (0), sembra essere il più performante. Tale metallo è capace di formare un amalgama con il palladio metallico e, teoricamente, disattivare tutte le fonti di tale forma di palladio, principalmente quelle eterogenee (Pd immobilizzato e nanoparticelle). Tuttavia, il mercurio sembra essere attivo anche verso alcuni complessi del palladio come i palladacicli. Ciò esclude, quindi, la possibilità di valutare correttamente l'intero contributo di catalisi omogenea.

Infine, il 3-phase test consiste nell'immobilizzazione di un reagente su un supporto solido. Riducendo la mobilità di uno dei substrati, teoricamente, solo le specie disciolte nella fase liquida possono raggiungere la nuova superficie solida e attivare il meccanismo di reazione. Tuttavia, se si considerasse l'addizione ossidativa come la principale causa di leaching e se si immobilizzasse l'alogenuro, piuttosto che il secondo substrato, si otterrebbe una conversione praticamente nulla. Ciò però, non escluderebbe la possibilità di ottenere un contributo in soluzione, in condizioni di reazione normali. Si può concludere riguardo a questi test, che occorre dedicare attenzioni particolari all'allestimento della tecnica di analisi e all'interpretazione dei risultati.

Negli ultimi anni, sono state proposte alcune tecniche più precise. Si tratta delle tecniche di split-test e dei ritratti di fase della selettività differenziale (SADS).

Nel primo caso un reattore catalitico a letto fisso (PBR) e un reattore a pistone (PFR) senza catalizzatore, vengono collegati in serie. Solo il primo contiene effettivamente specie attive, all'inizio della reazione. La possibilità di modulare la temperatura di reazione e, quindi, attivare o disattivare la cinetica di conversione, permette di ottenere informazioni sull'attività del catalizzatore, che sarà, spesso, sia omogenea che eterogenea nel PBR, e se esistente, solo omogenea nel PFR.

Nel secondo caso, invece, due reazioni competitive di accoppiamento C–C con un substrato in comune vengono lanciate in contemporanea e ne vengono calcolate le velocità di conversione (P_1 e P_2). Nel piano delle fasi $[P_1] vs. [P_2]$, si può definire un parametro noto come "selettività differenziale". Teoricamente, variazioni nella pendenza della curva, ottenuta per interpolazione dei dati, significano trasformazione delle specie attive nel corso della reazione. Tramite un controllo incrociato con specie omogenee pure, si può risalire a quali specie e in quale momento espletano la propria attività.

0.10 Modellazione molecolare DFT

Per concludere, uno strumento molto utile per la comprensione, spesso preliminare, di sistemi reattivi come le reazioni di accoppiamento C–C catalizzate dal palladio, è costituito dalla modellazione DFT (density functional theory), a livello molecolare. Si tratta di una metodologia per approssimare e risolvere l'equazione di Schrödinger dipendente dal tempo.

Più precisamente, al fine di definire le barriere energetiche legate a diversi fenomeni che si potrebbero produrre in tali sistemi reattivi, e quantificarne la probabilità, l'equazione omogenea agli autovalori, legata all'equazione di Schrödinger, deve essere risolta. La soluzione, sulla base del principio variazionale e dei due teoremi di Hohenberg e Kohn, sarà rappresentata dallo stato energetico stazionario fondamentale di un atomo/molecola. Altrimenti, attraverso metodologie più complesse anche gli stati eccitati possono essere calcolati, con una certa precisione.

Per fare ciò, l'equazione deve essere semplificata. Le teorie, prima di Hartree-Fock e poi di Kohn-Sham permettono di calcolare l'energia associata a una combinazione lineare di funzioni d'onda di singolo

elettrone, o determinanti di Slater, approssimante la funzione d'onda reale, dipendente da N elettroni, e che definisce lo stato quantico di un elettrone in ogni istante.
L'implementazione di tali teorie in programmi di simulazione quali Gaussian o Turbomole, prevede ulteriori approssimazioni delle funzioni d'onda così come la definizione del parametro chiave della DFT, dal nome, densità elettronica ($\rho(\vec{\mathbf{r}})$).
Infine, la tecnica detta di campo auto-coerente, basata sulla coincidenza tra valori di densità calcolati differentemente, viene normalmente utilizzata per valutare la convergenza di un metodo numerico approssimante la soluzione dell'equazione di Schrödinger omogenea, secondo il principio variazionale.
In letteratura, tali tecniche di simulazione sono state spesso usate per definire i meccanismi di reazioni più probabili, così come per calcolare le proprietà chimiche fondamentali dei composti coinvolti in reazioni di accoppiamento C–C.

0.11 Conclusioni e prospettive

Nel lavoro di tesi, sono stati presentati alcuni punti critici da valutare con attenzione al fine di migliorare la comprensione dei meccanismi complessi coinvolti nella catalisi eterogenea di reazioni di accoppiamento C–C. In sintesi, è necessario provvedere a monte, a una standardizzazione nel calcolo delle grandezze derivate (TOF, TON ecc.) e nelle metodologie seguite per raccogliere i risultati sperimentali. Si può, per esempio, notare nello studio della letteratura una profonda diversità nel metodo di presentazione dei risultati, che spesso causa uno sforzo consistente di riorganizzazione, a valle. Inoltre, trarre conclusioni troppo affrettate riguardo le analisi eseguite a fine reazione, può essere deleterio e condurre a risultati falsi e fuorvianti. Si consiglia di studiare nel dettaglio la natura e caratteristiche di tutte le tecniche di analisi e di condurre più esperimenti nelle stesse condizioni. In letteratura sono stati, spesso, definiti eterogenei, catalizzatori che, a un'analisi posteriore e più critica dei risultati, sembrerebbero non esserlo. Una conclusione tratta sulla base di poche analisi conclusive delle fasi liquida e solida (es. ICP, filtrazione a caldo, microscopia ecc.). Nella maggior parte dei casi, la ripetizione delle analisi e l'accoppiamento di più tecniche differenti sarebbe risultato un percorso più affidabile.
Potenti mezzi di simulazione sono disponibili e molto importanti per una comprensione preliminare della complessità dei sistemi reattivi catalizzati da metalli di transizione. Oltre ad offrire una prospettiva generale delle complessità agenti sui sistemi studiati, la modellazione, permette di valutare l'importanza relativa di quest'ultimi e di semplificare le operazioni di raccolta dei dati sperimentali.
Per concludere, resta molto da comprendere riguardo alle cause del leaching e al legame tra questo e i diversi componenti del sistema catalitico. La speranza per il futuro è di trovare catalizzatori eterogenei puri, ma che ciò sia possibile è ancora da stabilire. Una soluzione che potrebbe essere proposta, alla luce della teoria raccolta, nel lavoro di tesi appena descritto, è di lavorare su meccanismi di stabilizzazione in soluzione e re-deposizione controllata. Tutto ciò, al fine di ridurre le perdite di attività catalitica da un ciclo al seguente, e aumentare la riciclabilità del catalizzatore, così come ridurre la contaminazione del mezzo di reazione.

1 Introduction

The present work consists of a bibliographical study about the state of the art on C–C cross-coupling reactions catalyzed by Pd-based heterogeneous catalysts. They, actually are organometallic condensation reactions between two organic groups R^1 and R^2, born by two different substrates. Indeed, the prefix "cross" stands for different substrates, both acting to give the product.

Herein, an experimental work which should have been performed at the Commonwealth Scientific and Industrial Research Organization (CSIRO) laboratories in Melbourne (Victoria, Australia), is replaced by a review of the literature. The CSIRO is an Australian federal government agency responsible for scientific research. The agency was founded in 1916 with the intent of improving the scientific knowledge, and is now well known worldwide. Yet, due to the COVID-19 health emergency, only 1 month out of 6 was performed on site. The remaining months have been spent on this bibliographical work with the supervision of the Manufacturing Business Unit (BU) represented by the researcher Ivan Martinez Botella.

This study was part of a greater research project led by the BU on the CSMs (Catalytic Static Mixers), patented by CSIRO. A CSM is, in brief, a modular metallic structure, manufactured by metallic 3D printing, and used as catalyst support for several catalytic applications, namely hydrogenation and cross-coupling reactions. Some more details will be provided in the appendix, that contains information about the continuous-flow reactor and the CSMs.

On the whole, the experimental work was organized into two phases, with a significant degree of freedom about the choice of the reaction conditions to test, but a common objective: the understanding and optimization of that category of reactions. The two phases consisted of testing the same, or similar, reaction conditions in batch, using a round-bottom flask, and in a CSIRO-manufactured continuous-flow reactor, Mark II. The batch experience was intended to give some hints on the common issues related to the reaction and on how to avoid them. Though, not every detail could be understood, due to the completely different set-up between round-bottom flask and Mark II. In addition, the batch experience was characterized by catalysis by Pd/C (or Pd/Al_2O_3 etc) coils, rather than 3D modular structures like the CSMs.

Once a preliminary knowledge on cross-couplings was achieved, the plan would be to switch to the continuous-flow reactor and to finally test the CSMs. Despite, no experiment was performed in-flow, the present work helps clarifying the general functioning of Pd-based catalysts towards cross-coupling reactions and facilitating the continuous flow experiments (conception and practice).

One could sum up the study with the question "Is the exploitation of heterogeneous catalysts advantageous over homogeneous catalysis?". Thus, herein some tools will be provided in order to get an overview on the topic, by warning the reader about several details to care of, while performing such reactions, and without excessively concentrating on a theoretical knowledge which is still not completely established.

The review introduces firstly the cross-couplings, their kinetics and thermodynamics with a focus on a bunch of known reactions belonging to the group, namely the Suzuki, Heck and Sonogashira reactions. Then, the first section will be ended with a focus on some interesting pharmaceutical applications of such reactions, in order to understand their importance.

Since the subject deals with catalyzed organometallic chemistry, the section will necessarily hint at catalysis-related issues, namely the leaching phenomenon. Indeed, the several components of the reactive system, namely the solvent, seem to have an impact both on the performance of the reaction and on the degradation of the catalyst. Thereby, some considerations on the role of some components of the reactive system, will be provided. This leads to deal with the characteristics of homogeneous and heterogeneous catalysis. The first one is used for comparison's purpose and to talk about the thermosensitivity of most of Pd complexes.

Besides, together with some generalities on heterogeneous catalysis, the concepts of "cocktail" and "homeopathic" catalysis will be explained. One defines a dynamic scenario according to which different active or inactive species of Pd, turn into the others during the whole reaction, so that several species may be active at the same time.

Pd activity is also said to be "homeopathic" since very little amounts (even of the order of the ppm)

of palladium, namely dissolved, may catalyze the whole reaction and lead the conversion to 100%.
Then, another section will deal with the recyclability properties of heterogeneous catalysts, in particular, on the degradation mechanisms, namely sintering and leaching, as well as with the analysis techniques used by the researchers for quantifying them.
Finally an extremely powerful tool is introduced: the DFT (Density Functional Theory) modeling. Based on the principles of quantum mechanics, such simulations would help the comprehension of a system, by calculating typical energy barriers of the main phenomena involved in cross-coupling reactions. In this way, the behavior of the catalyst and substrates would be forecast, prior to spending other efforts on the experimental optimization.

2 Homogeneous cross-coupling kinetics

Cross-coupling reactions have been widely studied including Pd, Ni, Co and Cu-based catalytic systems. The present study will focus on the commonly used albeit rare and expensive palladium, as a great source of catalytic activity for such reactions. Pd is often incorporated into precatalysts in the oxidized form Pd(II), in order to enhance the palladium stability, and then reduced *in situ* during the catalytic coupling cycle [32].

The purpose of cross-couplings is to form a new C–C bond between two organic groups R^1 and R^2. This is facilitated by the presence of the catalyst, which is regenerated at the end of the reaction.
It corresponds to a generic reaction of the type: $R^1X + R^2M \xrightarrow{[Pd]} R^1{-}R^2 + MX$, where R^1X is generally a halide or pseudo-halide (triflate $R^1SO_3CF_3$, tosylate $R^1SO_2\mathit{Tol}$), while R^2M has no fixed nature, it bears the second organic group and its chemical nature depends on the type of reaction carried out.
The commonly accepted steps composing the catalytic cycle are: oxidative addition, transmetallation, reductive elimination. The oxidative addition consists of the coordination of R^1X onto the metal catalyst, from the form $Pd(0)L_n$ to $Pd(II)R^1L_{n\text{-}2}X$. Then, due to the approach of the second substrate, the halide ion X^- decoordinates to leave the place to R^2. This is the transmetallation step. Finally, the decoordination of both the organic groups gives birth to the final product R^1–R^2 and regenerates the catalyst. This whole cycle is depicted in Figure 1.

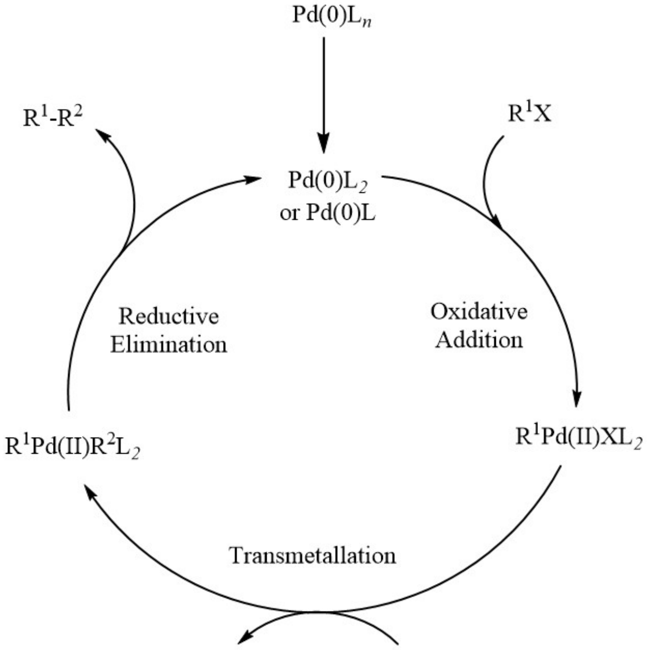

Figure 1: General cross-coupling mechanism found in textbooks and including oxidative addition, transmetallation and reductive elimination steps.

In a comprehensive review by Xue and Lin, some features about each step of the catalytic cycle were reported [1]:

- **Oxidative addition (OA)**. Being the first step a nucleophilic attack of the metallic center on R^1X, it is generally promoted by Pd complexes bearing strong electron-donor ligands L and halides consisting of an electron-poor R–X bond. That is why Cl-bearing halides are less reactive than bromides and iodides. Thereby, organochlorides must be activated by substitution of electron-withdrawing groups (EWGs) to R^1, which loosen the R–Cl bonding and make them

prone to a nucleophilic attack [1]. In addition, C(sp^3) hybridization leads to less strongly-bonded halides than C(sp^2), namely $R^1 = Me < Benzyl < Ph < Vynil$. In the case of aryl halides, the availability of Ar-X π^* orbitals promotes the reactivity [1].
Less reactive organochlorides are problematic substrates still nowadays, even with new catalytic systems and technologies [13, 37], even though they are the most cheap commercially available solutions.

Two mechanisms are often used to describe oxidative addition: S$_N$C and S$_N$2. They are represented by the scheme in Figure 2.

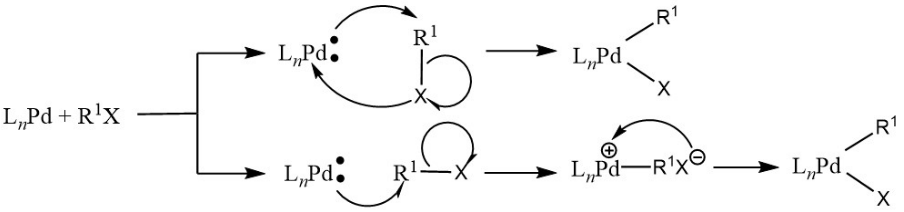

Figure 2: S$_N$C-type (*above*) and S$_N$2-type (*beneath*) mechanisms of oxidative addition. Adapted from [1].

During the concerted mechanism, the nucleophilic attack on R^1 and the halide coordination are simultaneous and the product complex will be in the *cis*-form. On the other hand, the S$_N$2-type mechanism undergoes two steps, where firstly the organic group coordinates to palladium giving anionic halide species in solution, which than attack the metallic center. Some researchers highlighted the effect of polar solvents on the regioselectivity of the whole reaction. This suggests that a S$_N$2 mechanism is more likely, leading to charged intermediates, stabilized in solution by the solvation process [40, 41]. This evidence also led Amatore and Jutand, in 2000, to hypothesize $[Pd(0)L_2X]^-$ species to be the actual catalyst form initiating the cycle, rather than $Pd(0)L_2$.
The problem about which Pd species is the most likely to start the catalytic cycle, is still open. Concerning this issue, one should notice that the Pd-ligand bond is generally weak. Indeed, depending on the geometry of the precursor complex the Pd d electrons have anti-bonding (σ^*) or non bonding character, and only the M-L σ^* anti-bonding d electrons are involved in the halide attack. Moreover, before a $Pd(0)L_2$ linear complex is ready to participate to the nucleophilic attack, the geometry must turn to bent, causing a change in the energy scheme of the MO Pd orbitals [1]. Bending energy and ligand decoordination, prior to oxidative addition, are both endoergonic contributions which must be balanced. Depending on the system, some authors advocated a most likely decoordination mechanism rather than bending.
On the whole, step-by-step decoordination of at least two ligands from a starting four-coordinate ligand-Pd complexes was theorized, happening prior to OA, since the halide electrons suffer from more intense repulsion from d electrons of Pd(0) than Pd(II). Thus, before oxidative addition, and following the reduction of the Pd(II) precursor, weakly coordinated ligands are decoordinated to obtain a $Pd(0)L_2$ (d^8) or Pd(0)L (d^6) complex and leave the place to the halide.
For instance, the use of sterically hindered phosphines has a great impact on the energy barrier which has to be overtaken for ligand decoordination. This may explain why density functional theory (DFT) calculations involving such ligands, are more oriented towards a starting Pd(0)L (d^6) catalytic complex: an easier dissociation can take place in the case of bulky phopshines and may lead to one-coordinate complexes which appeared to perform better for reluctant chlorides and bromides [42]. Besides, more strongly bonded phosphines are more suitable for more reactive iodides bearing EWGs [43, 44, 45].

***Cis-trans* isomerization** It is a commonly added step to catalytic cycles which accounts for the stabilization of OA *cis*-isomer products.

Figure 3 shows the three pathways that are likely for such step [1]. The former is ligand-assisted, where L may be a solvent molecule, and lead to a five-coordinate square-pyramid complex prior to phosphine dissociation. The second consists of a direct rearrangement *via* a tetrahedral intermediate. The latter goes through a series of 14e$^-$ T- and Y-shaped intermediates, and finally, a ligand fills the vacant place left in the Pd coordination sphere [1]. The ligand-assisted pathway was pointed out as the most favored under the majority of the conditions, however energy profiles depend on solvent, ligand and temperature conditions.

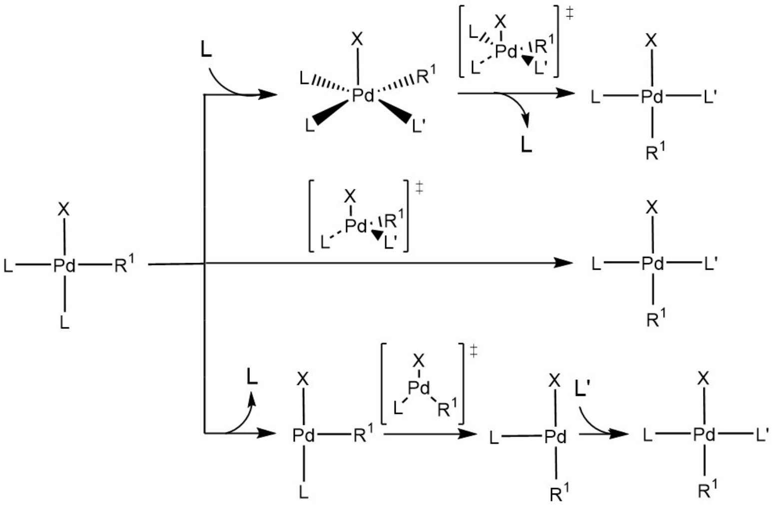

Figure 3: Three pathways likely to describe *cis-trans* isomerization. Adapted from [1].

- **Transmetallation**. Reaction mechanisms are supposed to vary for different couplings since different molecules carry the organic group R^2 [46, 47, 48, 49]. For instance, when organostannanes are exploited (Stille reaction), two mechanisms, namely cyclic and open, were proposed and are now accepted. Polar solvents appeared to favor the open mechanism because of the cationic complex species stabilization. In addition, the coordination energy of halide and phosphines play a key role in the choice of the pathway. More easily decoordinated electron-poor phosphines favor the cyclic mechanism, while the open one otherwise. Furthermore, strongly bonded highly electron-donor phosphines hinder the transmetallation process by increasing the energy necessary to decoordinate the halide X^-.

  Despite the lower coordination energy of iodides compared to chlorides, the energy barriers for the different halide decoordinations appeared to follow the order $Cl < Br < I$. This is explained by the balance between decoordination from Pd and subsequent capture by Sn. The Sn–X bond strength decreases down the halogens' group faster than the Pd–X, resulting in a more favorable effect for Cl rather than I. Therefore, in the case of coordinated chlorides, the open mechanism will be more likely.

  Figure 4 depicts Stille's transmetallation mechanisms, where two open pathways are proposed for the competitive isomer forms of the intermediate product.

  Hiyama transmetallation activation energy barriers appeared to decrease in the presence of fluoride ions, in the medium. It was explained by the authors that strong bonding between F^- and hypervalent Si stabilized the intermediate complex [50, 51]. Similarly, under Suzuki conditions, the presence of OH^- ions favored the transmetallation step, whatever the base [51].

- **Reductive elimination** While oxidative addition and transmetallation contend the nature of RDS, reductive elimination has always been reported to be very facile. Álvarez, Maseras and Es-

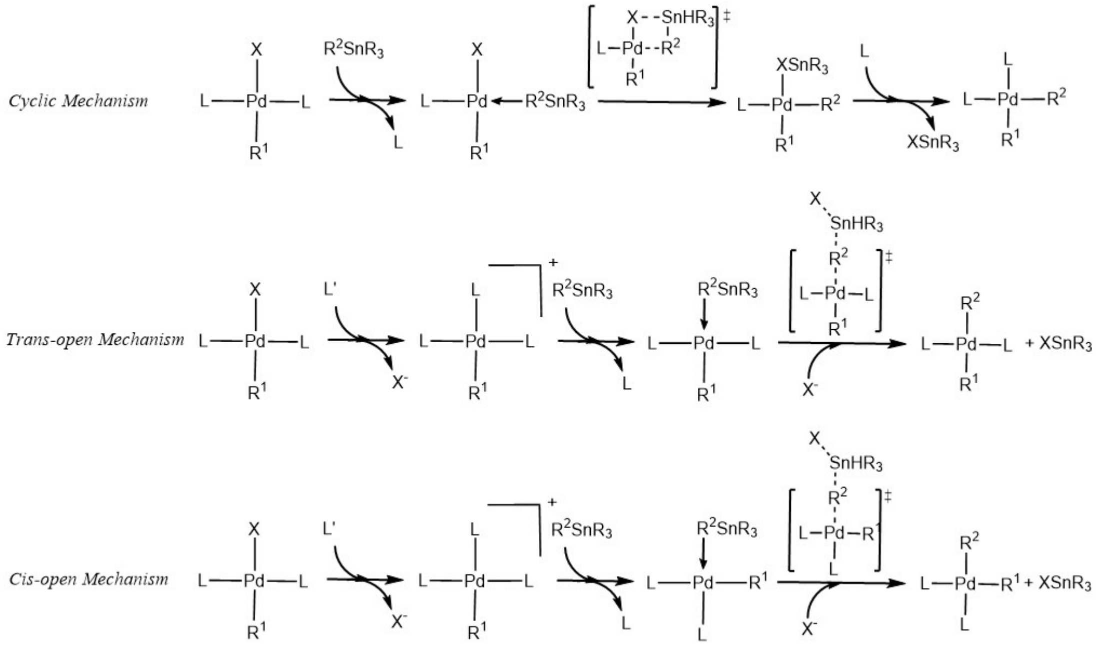

Figure 4: Open and cyclic mechanisms describing Stille's transmetallation. Adapted from [1].

pinet proved that aryl C(sp^2) undergoing reductive elimination, give highly exothermic reactions [52]. The involvement of π orbitals allows the Pd–C bond to be kept while C–C bond is forming. Thus, energy barriers for C(sp^3)–C(sp^3) couplings are higher [1].
Though, few more considerations should be done. First of all, decoordination of the product must be easy, that is why highly electron-donor ligands disfavor this step [53]. In addition, reductive elimination appeared to be performed only starting from *cis*-complex configurations. This is the reason why the aforementioned first isomerization was so much questioned. Due to reductive elimination affinity to *cis*-isomers, a second and highly endoergonic isomerization should take place after transmetallation, in order to recover the suitable configuration.

2.1 Chemistry of cross-couplings

Suzuki-Miyaura reaction Commonly studied, Suzuki-Miyaura coupling involves organic aryl or alkyl halides (or triflates) and organoboranes. Though, some variants exist, too.
The use of heterocyclic precursors found enormous interest in pharmaceutical applications. Aryl amides were used, in a challenging variant of Suzuki couplings, for the formation of diarylketones through selective cleavage of the highly energetic C–N bond [54, 55, 56]. The common organic biarylketone synthesis reaction consists of Fiedel-Crafts acylation [57]. Alternatively, Negishi coupling of primary amides, oxidative cleavage of C–C double bond in N-sulfonyl enamides or carbonylative Suzuki coupling under high-pressure CO atmosphere are viable solutions, improved by the adoption of chloroform as a soluble CO source [58]. The carbonylative Suzuki reaction gave no side reactions, namely homocoupling or common Suzuki coupling when using NHC carbenes as Pd ligands [57].
The generic SM reaction scheme consists of the three aforementioned basic steps. Seldom, isomerization is added in literature [48]. Figure 5 depicts the scheme which can be found in textbooks, and contains both theorized isomerizations even though their addition depends on the authors. Whether isomerizations happen or not has been sometimes clarified through DFT modeling and appears to depend on the chemical nature of precursors and intermediates, which fixes the activation barriers of each step.

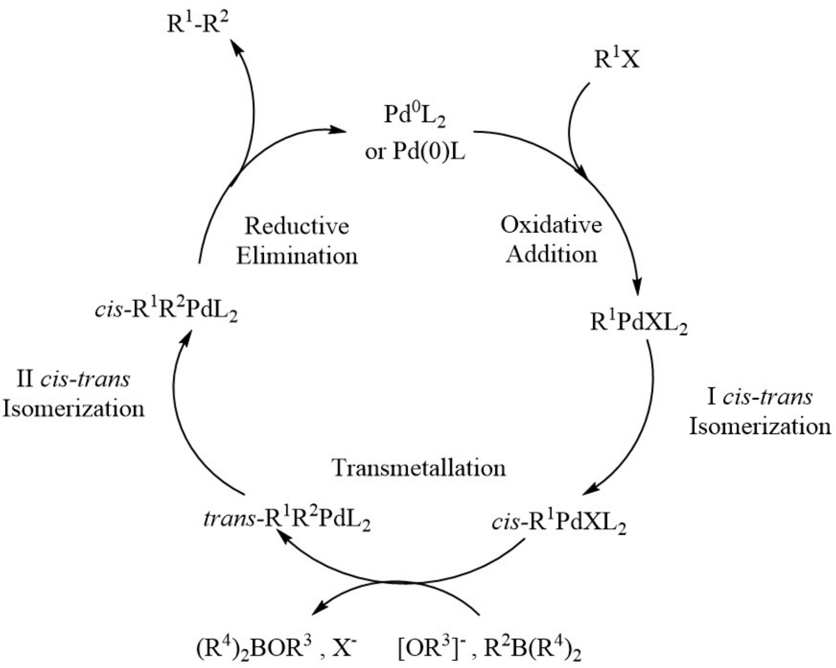

Figure 5: Homogeneous SMC mechanism found in textbook involving two isomerization steps (the presence or not of these two, depends on the authors and the experimental evidence of their works).

Amatore and Jutand first invoked the involvement of charged species in the cycle because of the apparent conflict linked to back and forth isomerization of *cis* oxidative addition products. According to their hypothesis no *trans*-isomer seemed to be necessary for the transmetallation to take place. They actually proposed the formation of five-coordinate complexes in order to avoid this problem [3]. Though, no anionic five-coordinate Pd(II) intermediate was ever detected in solution. Only up to four-coordinate complexes were found by Gooßen's group [42].
Gooßen and co-workers led a Density Functional Theory (DFT) calculation based on the comparison between "Jutand-type" anionic Pd complexes, namely $[Pd(0)(PMe_3)_2X]^-$ where PMe_3 was employed in order to reduce the computational effort [42]. The study's purpose was to investigate the counterions' effect on the charge of Pd complexes put forward by Amatore and Jutand [3].
As stated before, the presence of anionic intermediates in solution had also been reported by de Vries, while studying the reaction between acetic anhydride and phenylboronic acid [35]. After several investigations, both neutral and anionic pathways appeared viable, with the latter being slightly more energetically favored.
Later on, some benchmark reactions were studied with DFT techniques in order to draw the free-energy profile and to study the nature of each reaction-step. One study consisted of the reaction between vynilbromide and vynilboronic acid, in the presence of excess base, catalyzed by homogeneous $Pd(PH_3)_2$ [59]. The authors interestingly found that different competitive pathways fitted well the energy results, while the most energetically favored was the one involving the *cis*-isomer going through transmetallation directly after halide addition, ruling out the isomerization involvement. Though, oxidative addition appeared the rate-determining step (RDS).
As for chemical insights on organoboranes, electron-donating substituents (CF_3, F) showed faster reaction and better yields, than electron-withdrawing groups (OCH_3) in the work of Mohammadnia and Sun of 2020 [60, 61]. *Ortho*-substituted aryl bromides showed lower conversion compared to *meta* and *para* analogues, probably due to the related steric hindrance [61].

Heck reaction The Heck reaction allows to form Csp^2–Csp^2 bonds between aryl groups and terminal olefins. Several studies have been conducted on the popular Heck reaction mechanism, and some variants have been described [62, 63, 64, 65, 66]. Reaction with nitroarenes [67] or Catellani condi-

tions where norbornene helps Pd catalysis [68], were used as alternative Heck couplings. Otherwise, one variant which permitted to arylate itaconimide moieties is the Heck-Matsuda reaction [69]. As a whole, Heck-Matsuda reaction envisages the substitutions of halides or triflates with arenediazonium, characterized by the reacting group -N_2BF_4. Intramolecular Narasaka-Heck cyclization is well-known, too [70].
In 1998, a general homogeneous Heck reaction mechanism was proposed and is depicted in Figure 6 [2].

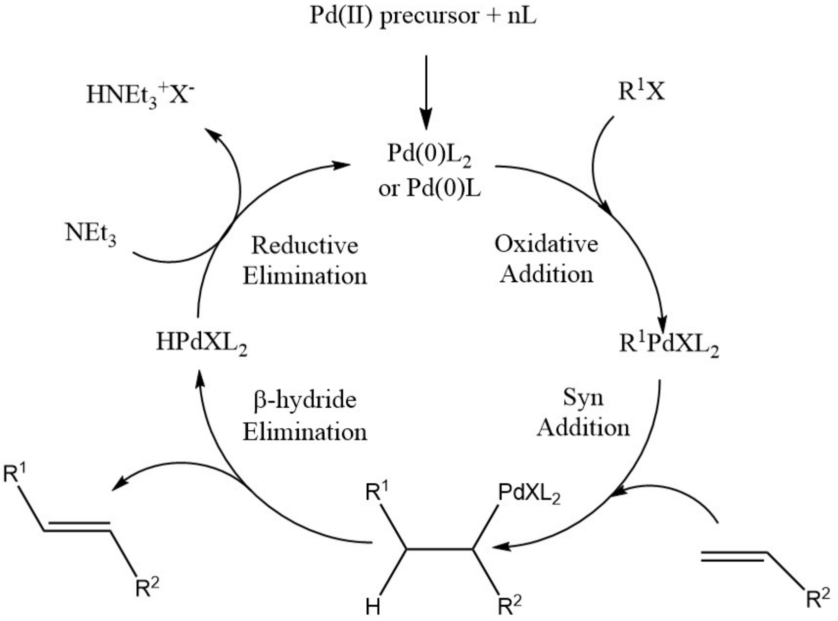

Figure 6: Homogeneous Heck reaction mechanism proposed in 1998 by T. Crisp [2].

As Figure 6 shows, Heck coupling's mechanism is slightly different from the aforementioned Suzuki's, due to different chemical properties of the substrates, namely of olefins, compared to organoboranes. The Pd precursor enters the cycle in the reduced Pd(0) molecular form and oxidative addition of the aryl halide follows, which brings Pd back to an oxidized state. Subsequently, the olefin inserts into the aryl-Pd bond creating a new C–C bond. A π-complex intermediate is likely for this reaction step.
Noteworthy, regioselectivity of the whole reaction almost entirely depends on the migration step. Many researchers have been spending energies on finding the most suitable catalytic system and conditions to optimize regioselectivity. The product is then, removed by β-hydride elimination leaving a L_2PdHX species. The added base finally helps to reductively eliminate HX and to restore $Pd(0)L_2$ [18].
Two pathways were proposed for the olefin migration step, namely neutral and cationic. In both cases the olefin coordinates to a three-coordinate T-shaped complex obtained from ligand dissociation. In the former, one L ligand decoordinates while in the latter is the halide X^- which leaves [71].
In the case of the neutral pathway the Pd-complex appears to attack the β carbon of the mono-substituted alkene, leading to a sterically controlled process. Besides, during cationic insertion electronic effects play the major role: EDGs direct the attack towards the α carbon giving birth to internal olefin, while EWGs favor the formation of terminal olefins. Deeth et al. studied Heck reactive systems with DFT calculations, accounting for electrostatic effects and orbital interactions, supposed to explain the regioselectivity of the olefin insertion step [72].
Similarly to the SMC, many studies were performed in order to clarify the nature of the cycle-starting Pd complex. DFT calculations advocate that phosphine dissociation is likely to happen prior to beginning the catalytic cycle, due to lower resulting activation barriers [65]. While for a common diphosphine-precursor system, oxidative addition is the RDS and the reaction is more likely to follow a neutral pathway [64, 65]. In addition, the role of the base during reductive elimination was debated, advocating that the equilibrium $L_2PdHX \rightleftharpoons PdL_2 + HX$is so fast that no base is needed to catalyze it.

Amatore and Jutand proposed an anionic version of the scheme in Figure 6 which is schematized in Figure 7 [3].

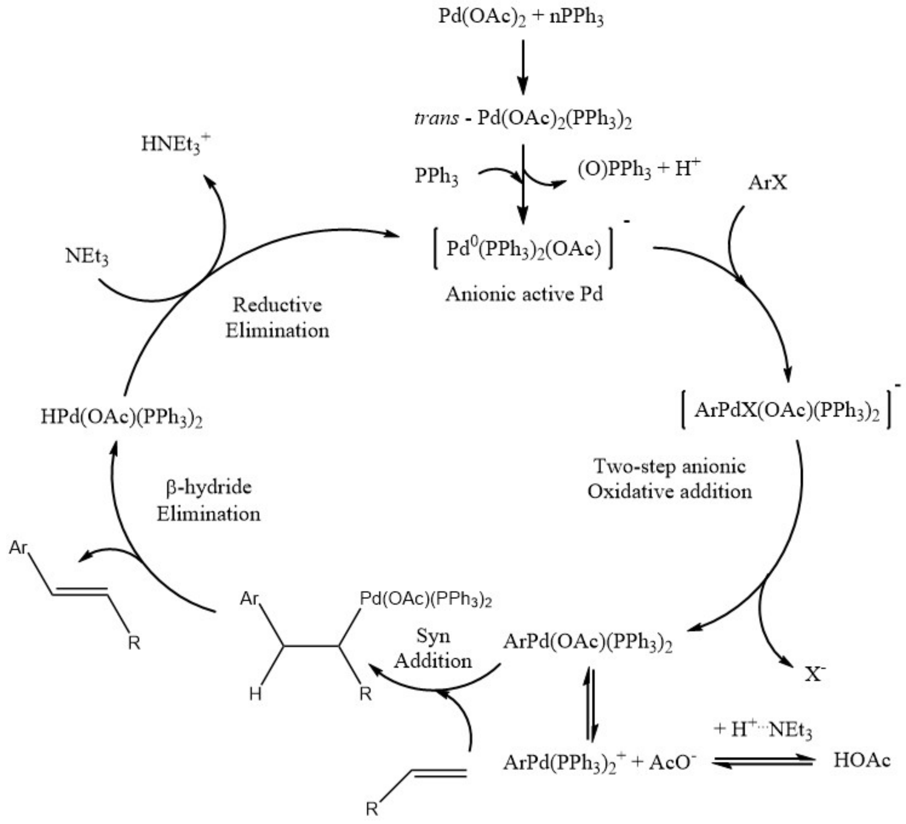

Figure 7: Anionic Heck reaction mechanism proposed by Amatore and Jutand [3].

The mechanism is similar to the one proposed by Crisp but involves the aforementioned pentacoordinated anionic Pd-complexes and is more likely for high temperature Heck reactions [18]. As stated above, pentacoordinated Pd is very unlikely and the hypothesis was soon discarded [42].
Some authors also hypothesized a Heck reaction mechanism involving Pd(II) and Pd(IV) species [4, 5]. The mechanism, involving palladacycles as catalytic systems, is represented by the scheme in Figure 8, yet the hypothesis of it representing the major catalytic contribution, as some evidences on palladacycles' activity suggested, was quickly ruled out [72].

One of the major concerns about Heck couplings is the harsh conditions under which it is performed, that are often necessary to be reached in order to obtain satisfying yields. While Suzuki coupling does not normally need high temperatures to be carried out, because of the reactivity of boron derivatives, this is not the case of olefins.
Due to the high temperatures reached, some other parasitic reactions become non-negligible. One out of all is the olefin coordination to Pd(0) prior to oxidative addition, causing waste of useful active sites. In addition, harsh thermal conditions are known to destabilize heterogeneous catalysts which are actually the target of this study. No truly heterogeneous catalyst has been supposed to exist under such conditions for years, which means sintering, leaching phenomena and aggregation of Pd in the liquid medium, are more likely to happen than under other coupling reaction conditions [32]. The issue will be thoroughly faced in Section 6.
Briefly, already in 2000, the coexistence of Pd nanoparticles dispersed in the reaction medium, formed by aggregation of leached Pd species, and supported Pd moieties, was hypothesized [73, 74, 75]. Further studies recalled the issue and highlighted the importance of this coexistence [76, 77, 78].

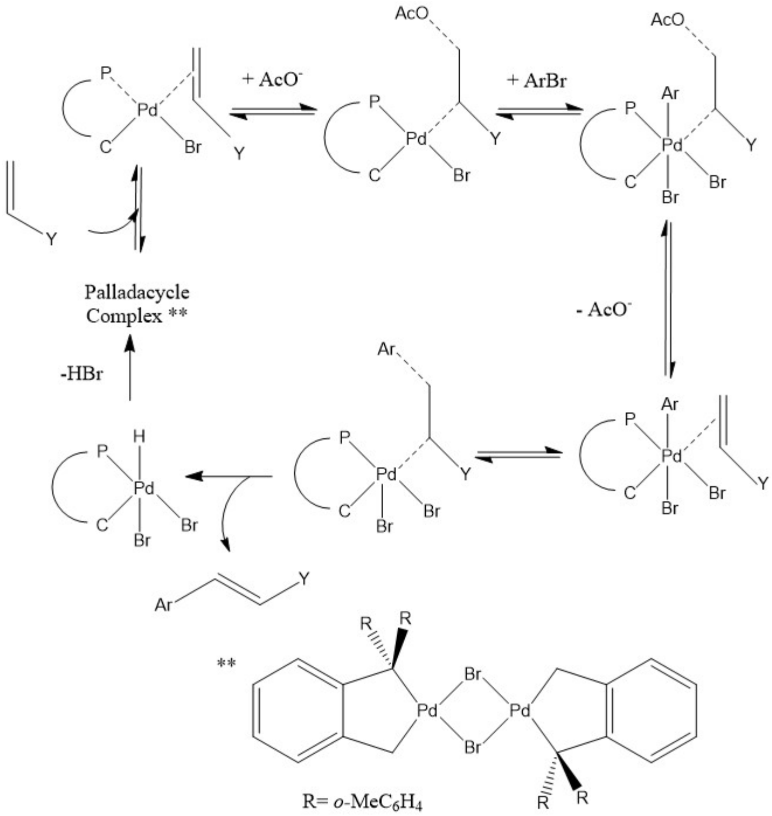

Figure 8: Heck reaction mechanism involving Pd(II)/Pd(IV) palladacycles [4, 5].

Sonogashira reaction The Sonogashira coupling consists of the reaction between organic halides and terminal alkynes which yields internal alkynes, through C–C bond formation [32]. It can be conducted in the presence of a copper co-catalyst, whose role is to form a copper(I) acetylide intermediate active towards the transmetallation step, or without. The intermediate formation facilitates the deprotonation of the alkyne before transmetallation. Besides ,the substrate becomes air sensitive and is more likely to suffer from homocoupling reactions such as the Glaser-Hay coupling which form a diyne. In 1997, it was first reported a ligand- and copper-free Sonogashira reaction.
Carbonylative Sonogashira variants with carbon monoxide (CO) [79, 80] or formic acid as a source of CO, in solution [81] were studied and applied, too.

The reaction mechanism of homogeneous copper-facilitated Sonogashira coupling is well-established and depicted in Figure 9(a) [6]. Copper-free Sonogashira, is instead, supposed to form a π-coordinated alkyne which σ-coordinates to Pd after deprotonation thanks to the added base. Its mechanism according to [6] is represented in Figure 9(b).

Others Other Pd-catalyzed C–C coupling reactions are known albeit less studied, namely the aforementioned Stille reaction, but also Negishi, Kumada, Murahashi, Hiyama, Fukuyama and Liebeskind-Srogl couplings. Table 1 sums up the main features of these couplings and the chemical nature of the reacting substrates involved.

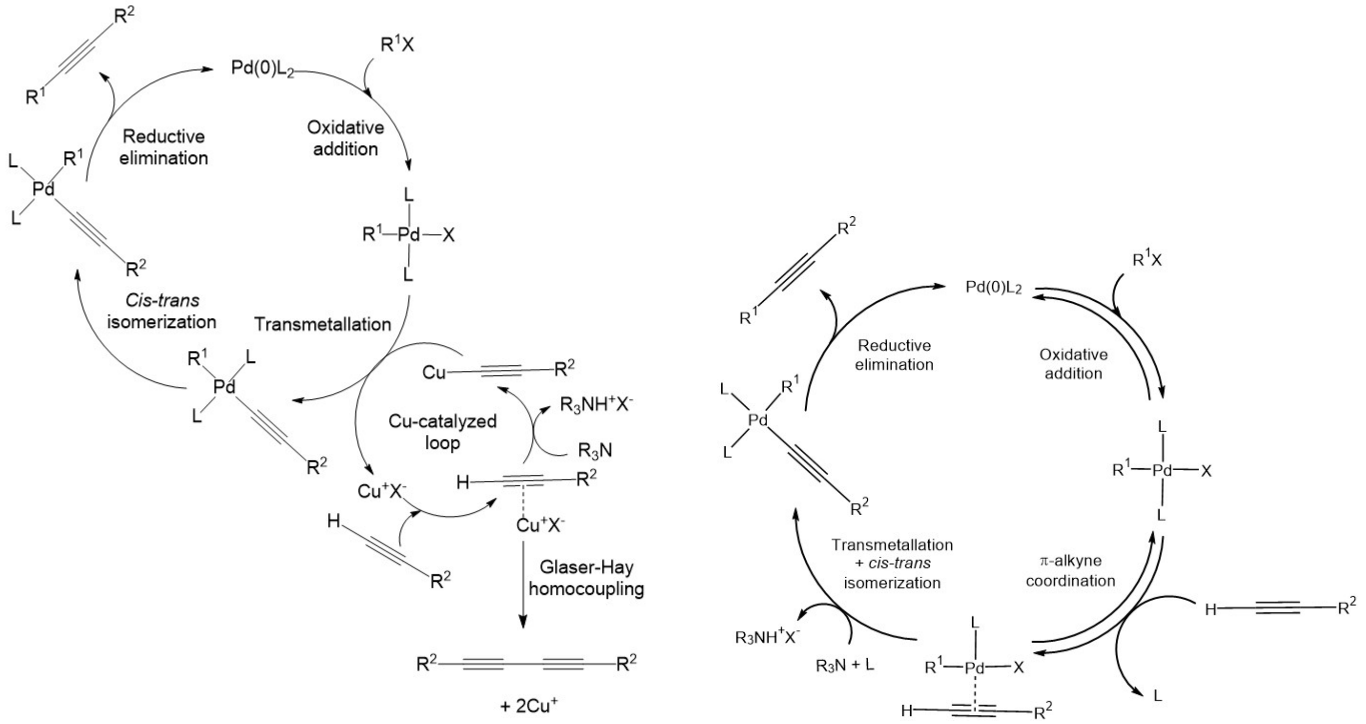

(a) (b)

Figure 9: Reaction mechanism of homogeneous Sonogashira cross-coupling **(a)** in the presence of copper-based co-catalyst with detail on Glaser-Hay homocoupling and **(b)** copper-free, according to [6].

Table 1: Pd-catalyzed C–C couplings in brief.

Reaction	**Substrate 1**	**C hybridization**	**Substrate 2**	**C hybridization**
Heck	Aryl halide/pseudo-halide	Csp^2	Alkene	Csp^2
Suzuki	Halide/pseudo-halide	Csp^3/Csp^2	Organoborane	Csp^3/Csp^2
Sonogashira	Halide/pseudo-halide	Csp^3/Csp^2	Alkyne	Csp
Stille[82, 83]	Halide/pseudo-halide	Csp^3/Csp^2	Organostannane	$Csp^3/Csp^2/Csp$
Negishi[84]	Halide/pseudo-halide	Csp^3/Csp^2	Organozinc halide	$Csp^3/Csp^2/Csp$
Kumada	Aryl halide/pseudo-halide	Csp^2	Arylzinc halide	Csp^3/Csp^2
Fukuyama	Thioester	Csp^2	Organozinc iodide	Csp^3
Murahashi	Halide/pseudo-halide	Csp^2	Organolithium	Csp^3/Csp^2
Hiyama[82, 83]	Halide/pseudo-halide	Csp^2/Csp^3	Organolithium	Csp^2
Liebeskind-Srogl	Thioester	Csp^3/Csp^2	Organoborane	Csp^2

2.2 Applications

Nowadays, cross-coupling reactions are widely used at the industrial scale for the production of useful molecules in several fields. These organometallic reactions satisfy the high need for new pharmaceuticals (i.e. naproxen anti-inflammatory drugs etc) and agrochemicals (i.e. herbicides) in recent years.

Though, they are also extensively employed in conductive polymers, molecular wires and liquid crystals syntheses [60]. Moreover, they allow to substitute common organic synthesis pathways with greener and easier processes.

A comprehensive work containing lots of patented drugs obtained through C–C and C–heteroatom couplings was published in 2012 [85]. While, few examples of cross-coupling integration in some famous drug syntheses schemes are presented below.
Early applications of cross-coupling were performed with homogeneous well-known and phosphine-based precatalysts. For instance, the widely used fungicide boscalid introduced by BASF in 1997 [86] and patented in 1999 [87], was produced on large scale exploiting homogeneously-catalyzed Suzuki reaction, as shown in Figure 10.

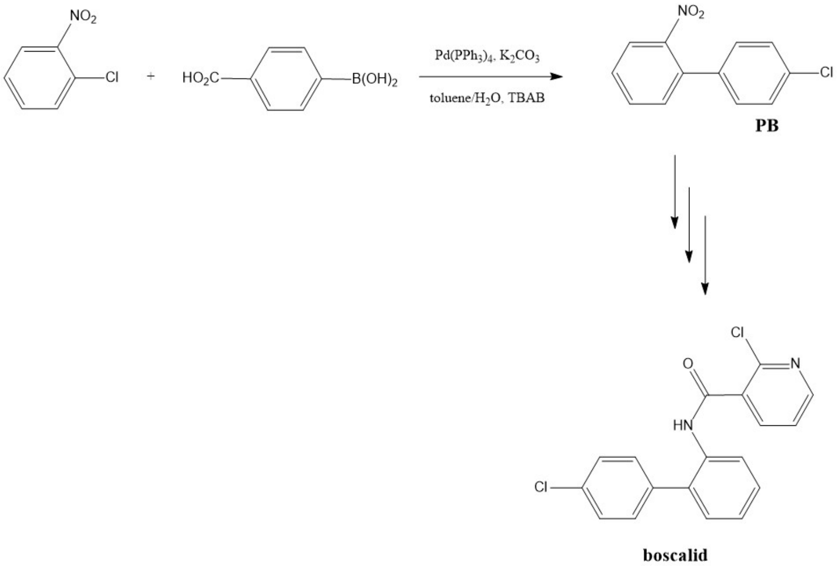

Figure 10: Simplified synthesis scheme by BASF, of boscalid, through Suzuki coupling.

At the same time, during the last years of the XX*th* century, the first large-scale heterogeneously-catalyzed processes appeared.
A division of GlaxoSmithKline plc (GSK), namely SmithKline Beecham Pharmaceuticals, launched the production of a potential antidepressant drug, compound **1** (Figure 11). The precursor, compound **P1** was obtained through Suzuki coupling catalyzed by 1.2% palladium on carbon (Pd/C) supplied by Johnson Matthey. The reaction conditions included heating at 78°C for 5 h, with a ratio base:substrate of 2:1, where Na_2CO_3 is the base and bromoaryl the substrate. Reflux conditions of the mixture MeOH:H_2O provided high yields (91%), while no product was obtained with DME:H_2O and EtOH:H_2O. Homogeneous catalysis by triphenylphosphine-ligated Pd performed worse than Pd/C [32, 88].

In 2005, Merck Research Laboratories and Merck Frosst Center for Therapeutic Research introduced a PDE4 inhibitor, compound **2** in Figure 12, displaying promising properties against asthma and chronic obstructive pulmonary diseases [89, 90]. The synthesis process undergoes a Suzuki coupling step, carried out with 2.6% Pd/C in 10:1 DMF:water at 80°C and in the presence of K_2CO_3. The highest obtained yield amounted to 92%. A similar anti-asthma drug, Montelukast, was proposed by Merck and the reaction scheme involved one Heck coupling step [91].

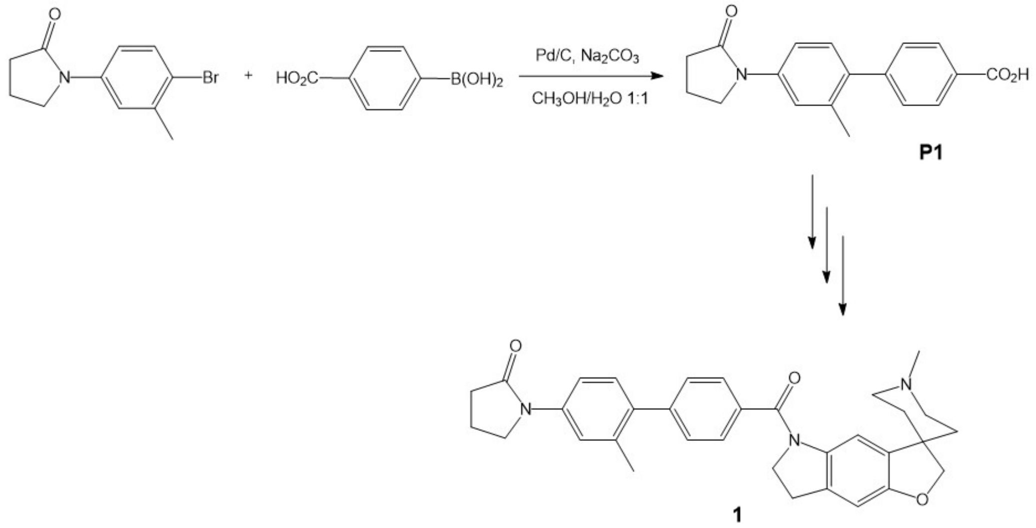

Figure 11: Simplified synthesis scheme by GSK plc, of compound's **1** precursor **P1**, through Suzuki coupling.

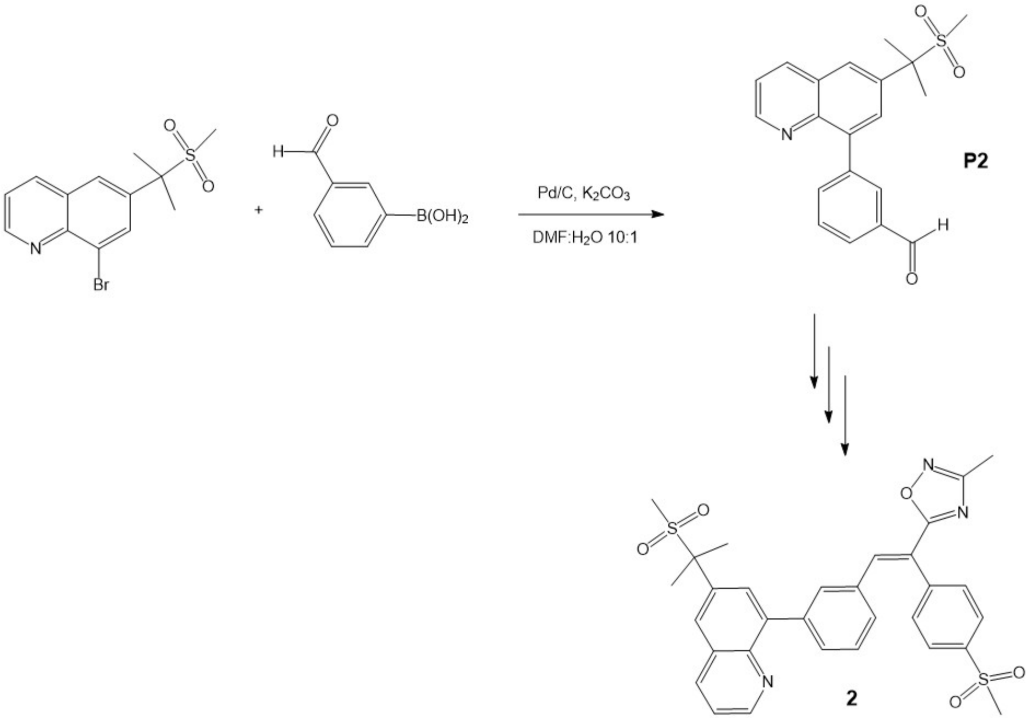

Figure 12: Simplified synthesis scheme by Merck Group, of compound's **2** precursor **P2**, through Suzuki coupling.

Eli Lilly and Company studied the Suzuki coupling for synthesizing an against-Parkinson drug (LY503430), compound **3** in Figure 13, through steps involving a Suzuki coupling catalyzed by Pd/C. The researchers noticed extremely low amounts of Pd-contaminants in the final product [85].

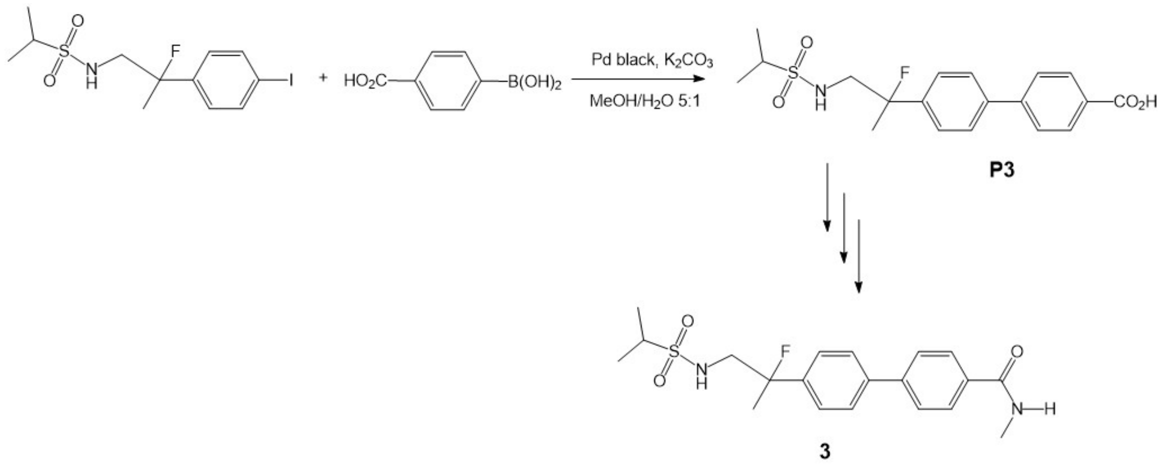

Figure 13: Simplified synthesis scheme by Eli Lilly, of compound's **3** precursor **P3**, through Suzuki coupling.

Furthermore, the non nucleoside reverse transcriptase inhibitor rilpivirine, **4** in Figure 14, contained in drugs TMC 278 and Edurant and approved for the treatment of HIV was obtained by Johnson & Johnson through Heck coupling of 4-iodo-2,6-dimethylaniline and acrylonitrile at 140°C [91]. Once again, Pd/C gave yields comparable to homogeneous catalysts but lower amounts of contamination.

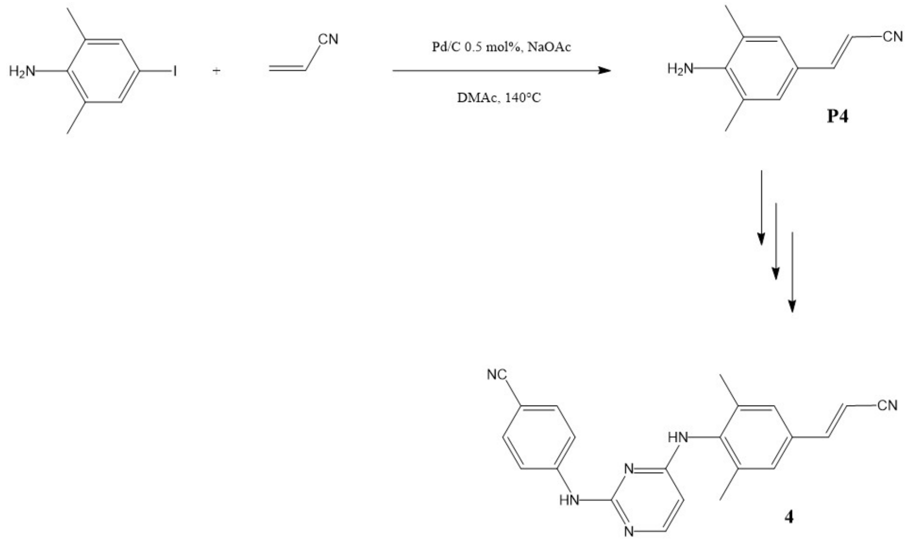

Figure 14: Simplified synthesis scheme by Johnson & Johnson, of compound's **4** precursor **P4**, through Heck coupling.

Recently, Gruber-Woelfler et al. proposed a continuous-flow synthesis scheme of valsartan's precursor [7]. Valsartan is the active component of Diovan, by Novartis, an against-high-pressure drug used to treat heart failure and improving living chances after heart attack. Gruber-Woefler's group modified a batch synthesis of precursor **PV** patented in 1991. For the Suzuki step a precursor functionalized with pinacolatoboron was reacted with two different cyanophenyl halides $(X = Br, I)$ with $Ce_{0.20}Sn_{0.79}Pd_{0.01}O_{2-\delta}$ as the catalyst, at 80°C in the presence of K_2CO_3 within a dioxane:H_2O mixture 1:1. Almost complete conversion was achieved after 50 minutes. The continuous process scheme is depicted in Figure 15.

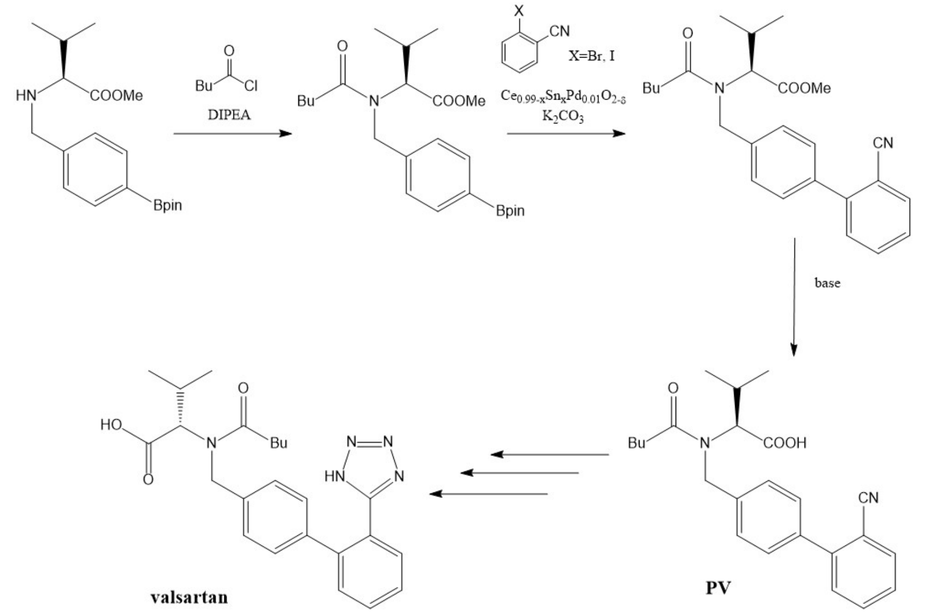

Figure 15: Continuous-flow synthesis scheme of precursor **PV** of valsartan, involving one step of Suzuki coupling with boronic pinacolatoboron, proposed by Gruber-Woelfler et al. [7].

Other examples of cross-coupling-involving syntheses can be done, namely production of elitriptan by Pfizer and anti-inflammatory naproxen by Albemarle.

2.3 Chemical properties of the main substrates

Aryl halides often need to be activated in order to efficiently undergo nucleophile S_N substitution reactions. Many of these substrates are electronically disfavored by high bond strengths, namely the C–Cl bond of aryl chlorides, and sometimes C–Br of bromoarenes [92]. The activation consists of ortho-, meta- or para- substitutions of highly electron-attracting groups, such as -NO_2, which direct a electronic density deficiency on the X-substitution position. Though, in most cases both EWG and EDG groups appeared to well perform for aryl iodides [13] while *ortho*-substitution gave higher steric hindrance and lower performances than *meta*- and *para*- [61]. Otherwise, harsh conditions are needed, namely high temperatures and high catalyst loading, in order to activate the reactions and obtain satisfying conversions [13]. As a whole, the reactivity order of halides appears to be: $X = I > Br > Cl$ [93].
Some examples of how substituents' nature impacts the reaction performance, can be found in Table 2, adapted from [37]. The table is interesting because of the definition of a parameter ΔV_c, accounting for the whole donating/withdrawing power of each group.

Table 2 shows the reactivity of differently substituted aryl halides, towards common SMC reaction catalyzed by three different systems, **1**, **2** and **3**. The electron-withdrawing and -donating power is represented by the values of the ΔV_c parameter, which assumes positive values for electron-attracting groups and negative otherwise [37]. The parameter was calculated as the molecular electrostatic potential at the nucleus difference between the *para*-carbon of bromobenzene and benzene.
The model reaction was taken to be between 4-bromobenzene and phenylboronic acid at 80°C, in a 1:1 MeOH:H_2O mixture, with sodium carbonate as the base and a Pd loading of 0.01 mol%.

Similar speculations can be done for the substrate bearing the R^2 organic group. For instance, electron-donating substituents (CF_3, F) substituted to boronic acid showed faster reaction and better yields, than electron-withdrawing groups (OCH_3) [60, 61]. Moreover, some boronic moieties are sensitive to protodeboronation and oxidation. Nucleophilic substituents were found to tune the stability of such moieties [94].

Table 2: Assessment on the performance improving properties of several EW and ED aryl bromide substituent groups. Adapted from [37].

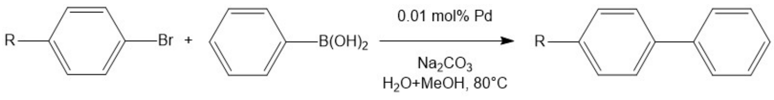

R	ΔV_c	Catalyst **1**	Catalyst **2**	Catalyst **3**
$4-CHO$	13.8	94.6	82.9	91.1
$4-COCH_3$	9.7	98.6	93.8	95.8
H	0.0	95.0	83.8	77.6
$4-OH$	-2.0	93.1	93.0	74.6
$4-CH_3$	-3.3	86.2	41.6	65.8
$4-OCH_3$	-5.0	91.2	89.6	75.0
$4-NH_2$	-9.0	90.1	53.3	78.2
$2-Bromothiophene$	–	95.7	75.0	90.4

2.4 Roles of compounds on the reaction kinetics

Solvent Different solvents have been tested through the years to better suit the needs of heterogeneously catalyzed cross-couplings. Two early and more rarely reported in literature are fluorinated solvents [124, 125, 126] and supercritical carbon dioxide [127]. Sinou performed Heck couplings of iodoarenes and methyl acrylate in perfluorinated solvents catalyzed by soluble fluorine-tagged triarylphosphines, family of compounds **11** (Figure 18, *vide infra*) [124]. Others employed fluorous dialkyl sulfides as ligands [125]. Furthermore, in [126] fluorous silica was used as catalyst sequestration phase in fluorous biphasic media.
Tumas and colleagues [128] and Holmes and Carroll [129] studied fluorinated phosphines as ligands for Pd in supercritical CO_2 (scCO_2). In [127], this solvent was used in the Heck olefination catalyzed by "heterogeneous" Pd/C.
Among the common solvents DMF is the most widely exploited. Though, DMF is highly reprotoxic and a substance of very high concern (SVHC) [1] [130]. DMF was replaced by NMP which has similar polarity properties, likewise it may free some toxic metabolites like formaldehyde oxidated derivatives. Thus, the release of toxic by-products for different alkyl/aryl-substituted forms of NMP was tested, namely for N-butylpyrrolidone (NBP) or N-octylpyrrolidone (NOP), N-benzylpyrrolidone (NBnP), N-cyclohexylpyrrolidone (NCP) and N-hydroxyethylpyrrolidone (HEP).
A screening of the most important properties of the solvents mentioned herein, is reported in Table 3. The dielectric constant accounts for the polarity of the solvent and the solvation power on dissolved/dispersed moieties, while part of their toxicity and harmful characteristics are summed up by the chemical hazard pictograms.

The polarity of the solvent appeared to impact the stereoselectivity of cross-couplings as well as

---

[1] Substances of Very High Concern (SVHC) are substances for which the use within the European Union is subject to REACH regulation

Table 3: Some properties of the solvents mentioned in this study. The dielectric constant accounts for the polarity and solvation power of the solvent (* calculated at 293K **Temperature non-specified).

Solvent	Formula	MW [g/mol]	Density [g/cm^3]	Boiling point [K]	ϵ (@298K)	Hazard Pictograms
Water	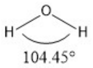	18.02	1	373	80*	–
Propylene carbonate	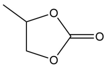	102.10	1.21	515	67.42 [95]	❗ [96]
DMSO	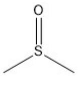	78.13	1.10	462	47* [97]	–
DMAc	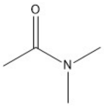	87.12	0.94	438	37.8** [98]	❗ ⚕ [99]
DMF	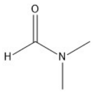	73.10	0.95	427	37.51 [100]	❗ ⚕ 🔥 [101]
Cyrene^{TM}	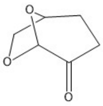	128.13	1.25	499	37.3** [102]	❗ [103]
Ethylene glycol	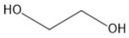	62.07	1.11	470	37* [104]	❗ ⚕ [105]
Acetonitrile	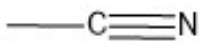	41.05	0.79	355	36.64* [106]	☠ 🔥 [107]
GVL	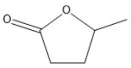	100.12	1.05	478	36.47 [108]	❗ 🔥 [109]
NMP	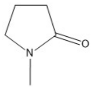	99.13	1.03	476	33 [110]	❗ ⚕ [111]
Methanol	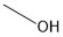	32.04	0.79	338	33* [104]	🔥 ⚕ ☠ [112]
Ethanol		46.07	0.79	351	25.3* [104]	–
Acetone		58.08	0.78	329	20.7 [104]	❗ 🔥 [113]
IPA	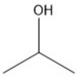	60.10	0.79	356	19.92 [114]	❗ 🔥 [115]
Ethyl lactate	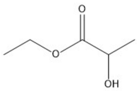	118.13	1.03	426	13.1* [116]	❗ 🧪 🔥 [117]
THF		72.11	0.89	339	7.9 [118]	❗ 🔥 ⚕ [119]
DME		90.12	0.87	358	7.3* [97]	❗ 🔥 ⚕ [120]
2-MeTHF		86.13	0.85	353	6.97** [121]	❗ 🔥 🧪 [122]
Toluene	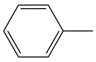	92.14	0.87	384	2.38 [97]	❗ 🔥 ⚕ [123]
DMI	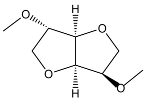	174.19	1.15	508	–	–

the activity of catalytic intermediates and the reaction rate (i.e. the RDS) [131]. Polarity causes, in most cases weak adsorption onto the heterogeneous catalyst surface and/or solvation processes around homogeneous species. The adsorption is a highly effective selectivity-controller process. Otherwise, strong adsorption could lead to inactivation because of the elevated concentrations of such species in the liquid phase, and deactivation.

Grivani and Nehzat studied the influence of various solvents, namely methanol, ethanol, acetonitrile, acetone, THF:H_2O mixture and carbon tetrachloride, for a benchmark Suzuki coupling at room temperature. MeOH was the best choice, lower yields were obtained with other polar solvents [13]. Yet, Sherwood worked on three different case studies, involving plenty of reaction conditions, and found no correlation between the chemical nature of the solvents and the obtained conversions in SM couplings. According to the author, SM could not be taken as a benchmark reaction for polarity effect assessment [131].

On the other hand, Mizoroki-Heck reaction has been demonstrated to be highly dependent on the polarity of the reaction medium, which allows to control the RDS [131]. Thus, experimental screening tests for each studied system are extremely important.

New generation solvents are now object of thorough tests, namely Cyrene^{TM} (unstable in the presence of inorganic bases), dimethyl isosorbide (DMI), ethyl lactate, 2-methyltetrahydrofuran (2-MeTHF), propylene carbonate, iPrOH (IPA) and γ-valerolactone (GVL), a polar aprotic and non-toxic solvent with good solubilization properties, studied in 2008 by Horv$\acute{a}$th [91, 130, 132, 131]. iPrOH was identified as a well-performing solvent for Suzuki-Miyaura couplings, while Cyrene^{TM}, GVL, DMI and propylene carbonate are known to have a high boiling point which makes recovery problematic.

Nowadays, water is preferred to organic polar solvents (e.g. MeOH, DMSO, NMP etc) due the environmental concern, in addition to its extremely low cost. Though, to maximize the catalyst activity, the solvent hydrophilicity properties must be appropriately tuned. Aqueous PEG400 media are usually used nowadays for environmentally-friendly applications [133]. In addition, PEG can be used as a solvent as well as a phase transfer agent [2], which increases the basicity of inorganic carbonate bases and the solubility of various coupling substrates [134].

Hence, water is extensively used as a co-solvent in liquid blends, due to its power to increase the hydrophilicity of the medium and solve some solubility problems. Water as co-solvent increased the yields of Suzuki-Miyaura cross-couplings when coupled to DMF with a ratio of 1:10 (H_2O:DMF) [135]. The catalyst consisted of thiol-functionalized amorphous silica-supported Pd. Though, the addition of water did not improve the reaction efficiency when using toluene as a solvent.

PdNPs/ZnO showed low affinity with aprotic polar solvents like DMF and CH_3CN while higher efficiency turned out with protic solvents like EtOH and H_2O, where the latter used as co-catalyst profoundly increased the conversion of various aryl halides [136].

Otherwise, the use of ionic liquids is environmentally-friendly and appeared to provide a good stabilization of supported PdNPs by preventing particle migration (PM). TBAB can be used in the form of ionic liquid (IL). This technique was used by Herrmann and co-workers [137, 138]. The system was recovered by distillation under vacuum at 130°C and gave excellent results in catalyst separation. Ionic liquids were also used as stabilizers of polar Pd species and sometimes acted as Pd ligand [139]. In [140] the Pd-IL phase coupled to homogeneous Pd complexes, was recycled up to 14 times without complete deactivation. Besides, Yokoama and co-workers used Pd(II)-exchanged oxide carriers coupled with ionic liquids, but great amounts of palladium dissolved in the ionic liquid phase [141].

Arai and co-workers remarkably advocated that Pd solubilization (i.e. leaching) could be controlled at some extent by the choice of the solvent [142], which also appeared to be crucial for the prevention of homocoupling parasitic reactions [143]. During studies on Pd/C catalyzing Heck coupling between iodobenzene and methyl acrylate at RT assisted by an ultrasound system, Samant et al. noticed that NMP and DMAc as solvents resulted in low leaching of Pd. Nonetheless, a recycling test showed significant lowering of the efficiency from one run another [144].

In the case of PdNPs supported on single-wall nanotubes [15], the use of non-polar solvents, like xylenes

---

[2] A Phase transfer agent (PTA) is a stabilizer for species leaving the solid surface to the liquid medium

and toluene, led to suppression of leaching [145, 146, 147, 148]. Besides, polar solvents appeared to increase activity of some catalysts while causing extensive leaching, evidence that can be explained by the effect of solvation onto Pd species.

The use of tridentate NNO Pd(II) complexes immobilized on mesoporous silica coupled to NMP as a solvent, in [149], resulted in large amounts of leached species, while no leaching was detected when using a biphasic system ethylene glycol/toluene.

Choline hydroxide (ChOH) is one of the recently studied ionic liquids (ILs) [150]. It consists of a cationic part (tertiary amine) and an anionic one (hydroxide). It was used for the SMC reaction of 3-methoxyboronic acid and 3-iodophenol. Its peculiar properties made it unnecessary the addition of the base and of water as co-solvent, under aerobic conditions [150].

Other ionic liquids like cetylpyridinium bromide have been studied, as amphiphylic solvents with self-assembling properties [151]. ILs facilitate the purification of the final product favoring a good recyclability of the system. Alternatively, deep eutectic solvents (DESs) are liquid blend of hydrogen bond acceptors (e.g. choline-chloride ChCl and K_2CO_3l) HBAs and hydrogen bond donors HBDs, namely amines, amides, carboxylic acids and alcohols, and a valuable alternative to ILs. These solvents are non-toxic, volatile and highly bio-compatible.

In a study of Khan and Thiyagamurthy a DES composed of potassium carbonate and ethylene glycol was studied in the Suzuki-Miyaura coupling of several substrates [152].

Base Inorganic bases, especially sodium and potassium carbonates, showed the highest affinity to a wide spectra of Suzuki couplings [37], while organic bases like triethylamine (TEA) or Et_3N worked better for Heck reactions [153, 154]. Apparently, the role of the base in the Heck reaction is to neutralize the aryl acid formed by hydrogen exchange during the reaction [155].

On the other hand, in the case of SMC reactions, the "textbook" mechanism was slightly changed through the years to add the effect of the base. Figure 16 shows a heterogeneous application of SM coupling and underlines the role of the inorganic base [8].

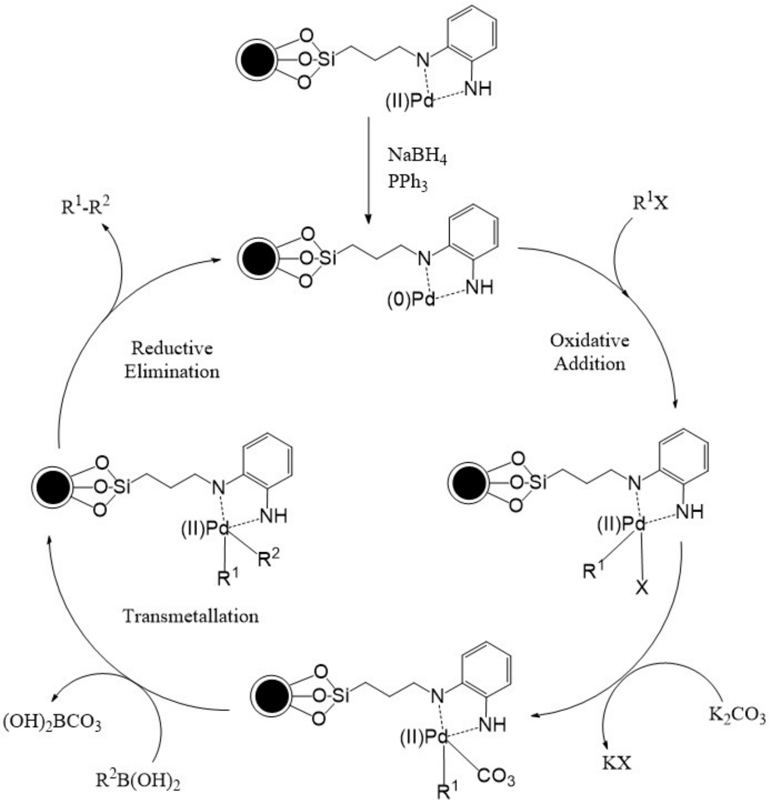

Figure 16: Heterogeneous mechanism for Suzuki-Miyaura coupling on the $Pd/SiO_2@Fe_3O_4$ magnetically recyclable catalytic system [8]

Before transmetallation, it induces the coordination of a carbonate ion on Pd, which represents a better leaving group for transmetallation, compared to the halide. This hypothesis may explain the great performances of inorganic bases like carbonates and phosphates. Moreover, the nature and concentration of the base appears to be essential for the transmetallation step in Suzuki couplings [61].

Jutand and Amatore tested SMC substrates coupled to the base and excluding one at a time, in the presence of the solid-supported core-shell Pd@Au nanoparticles, in order to assess their influence on Pd leaching. Anisole and acid alone showed low amounts of leaching, while the base was more efficient. The synergistic effect of the base/acid couple provided high amounts of Pd leached [156].
Moreover, use of strong bases like tBuOK in the Suzuki coupling of bromotoluene with phenylboronic acid, in DMF/water 4:1 at 100°C, caused high amounts of parasitic dehalogenation reaction [157].

Atmosphere In several studies inert atmosphere gave lower conversions compared to aerobic conditions [154, 158]. Oxygen was then supposed to trigger the formation of PdO. This oxide is more likely to dissolve in solution and can directly undergo transmetallation with arylboronic acid.
Activity was improved under aerobic conditions in [159], using Pd-PVPy. The authors hypothesized the formation of oxidized species onto PdNPs surface which are more easily leached and stabilized by the formation of peroxo-complexes.

3 Homogeneous Catalysis

Palladium is one of the most valuable source of activity for cross-coupling reactions. In theory, all forms of palladium are able to catalyze these reactions, for instance Pd complexes, supported Pd nanoparticles (NPs), free PdNPs. Though, practice is far from being that easy.
Firstly, most of times, catalysts must be tailored in terms of ligands and Pd loading, in order to activate less reactive substrates such as chloroarenes. Furthermore, all catalysts suffer from some forms of inactivation, because of the metal instability, especially in the Pd(0) form. Finally, in the case of supported catalysts, it is often difficult to tell whether the activity is expressed on the surface or in solution, due to solubilization and transformation of active species in the liquid medium.

Cross-coupling reactions catalyzed by palladium moieties have been extensively studied through the years, beginning in the late 20^{th} century. Historically, catalysts are divided into homogeneous and heterogeneous. This demarcation line, is not anymore valid due to the aforementioned hurdles, especially under Pd-catalyzed cross-coupling reaction conditions. For this reason, the present study briefly deals with some homogeneous systems and the problems encountered during catalysis. The purpose is to gain a better knowledge of these systems before the immobilization onto solid surfaces.
Homogeneous precatalysts consist of molecular species soluble in the reaction medium, e.g. "naked" Pd coming from salt-like precursors, namely $Pd(OAc)_2$ and $PdCl_2$, or Pd complexes. In this latter case, electron-rich ligands are ligated to Pd and fill its valence sphere up to 16 or 18 valence electrons, enhancing its stability and activity due to raised electron density. Phosphine-based ligands, of general formula $-PX_3$, where X is an organic substituent group, have been widely employed in recent years by the industry, especially for palladium applications.
Nonetheless, as stated above, species added to the reacting system are not necessarily the competent catalysts. The actual nature of homogeneous active species is still debated. Atomic Pd, molecular moieties or nanostructures (e.g. nanclusters, nanoparticles), formed through Pd(0) aggregation, contended this role.
One more factor of complexity is added by evidence of ligand–C bond cleavage, followed by aggregation of unstable Pd species into nanostructures and inactive Pd black.

Though, complexity appears to be more hard to handle in the case of heterogeneous catalysis. The researchers have been working on supported metal catalysts in order to fulfill product purity standards (e.g. pharmaceutical products) and facilitate flow chemistry applications, getting rid of complicated and highly consuming separation operations. Indeed, contamination, supposed more important for homogeneous catalysts, of heavy metals and/or toxic ligands, like phosphines, is considered not acceptable in many applications and extremely regulated. Heterogeneous catalysis would theoretically overcome this risk. Though, leaching of putative or true active species often occurs during cross-couplings catalyzed by supported Pd, caused by the harsh reaction conditions imposed (i.e. high temperatures, extremely alkaline media, high metal loading), invalidating this assumption.
The aforementioned ligands are not only toxic but also expensive [160], e.g. N-heterocyclic carbenes and other tailored ligands, as well as thermolabile [161]. Their production operations, instability and separation contribute to raise the cost and complexity of the whole catalytic process, even though they have the property of accelerating the reaction.
Dowstream separation operations are one example of what makes the process more expensive. Firstly, high temperatures, are attained during evaporation and distillation processes, which means risk of deactivation and loss of thermolabile molecules. Unfortunately, these molecules, namely ligated metal catalysts, represent a large portion of the whole cost of the process. Furthermore, energy consumption while running such operations is significant and raises the cost of the process. Ligand-free or "naked" palladium might solve some of these issues, albeit it suffers from lack of reactivity towards inactivated substrates and stability problems. Thus, heterogeneous catalysis could be a way to circumvent all these drawbacks. Supported catalysts are easily separated from the reaction medium, through simple operations, like filtration, decantation or magnetic separation [162].

The authors used to quantify the catalysts efficiency according to different parameters, e.g. yield, selectivity, conversion, turnover frequency (TOF), turnover number (TON), recyclability etc. However, a standardization is sometimes needed to be able to compare results, that are already deeply differentiated by the nature of the coupling system (i.e. base, solvent etc).

Reaction rates of cross-couplings of activated aryl halides could be significantly high, leading to the whole conversion in few minutes, namely for iodides. In this conditions of completed reaction, aggregation and re-deposition processes become more important. Thus, sometimes it is not clear if the conversion is attained totally thanks to leached homogeneous species or to heterogeneous sites or both. This happens even if valuable tests are conducted, due to lack of knowledge and "lightness" in drawing conclusions. A wide spectra of techniques apt to understand Pd catalysis are thoroughly described in Section 8.2.

Wrong assumptions have a major impact on interpretation of recyclability of supported catalysts.

In terms of recyclability, almost all authors just took into considerations the number of times for which one heterogeneous catalyst gave good activity, comparable to the first run. Whereby, this could be useful if only truly heterogeneous catalysts were used. Though, solid heterogeneous Pd precatalysts often showed characters of soluble Pd species reservoirs. In this case, if no reaction parameter is changed from one run to another, which is true only in theory, catalysts would be likely to show the same activity as soon as the accessibility to leachable Pd species is kept unvaried. Then, loss in accessibility due to catalyst concentration diminishing on the surface, would affect the results. Yet, given the high starting loading imposed compared to the necessary amounts of active species, this would occur after several recovers [163].

In order to avoid some of the misinterpretations, two parameters are presented which are used to cover both the definition of activity and recyclability:

- **Turnover frequency (TOF) [h^{-1}].** It represents the instantaneous efficiency, in terms of number of catalytic cycles per catalytic site and unit time. It is calculated as the derivative of the number of cycles per unit time and catalytic site [164]. One may theoretically calculate an average TOF, but any starting induction period has to be excluded. Beletskaya underlined the risk represented by such calculation when induction periods have not been precisely detected [165]. Induction periods may come from Pd leaching and aggregation and are common phenomena related to cross-coupling catalysis.

  In the case of first-order kinetics in S:

$$\begin{aligned} TOF(t) &= \frac{dN}{dt} && (1) \\ &= TOF^{\circ}\frac{[S]}{c^{\circ}} && (2) \end{aligned}$$

  Where $\overset{\circ}{c}$ the standard concentration ($1M$) which permits to the TOF to be expressed in frequency units, and $\overset{\circ}{TOF}$ is a "standard" TOF measured at standard concentration of substrate S. It can be computed at different conversions depending on the chosen contact time.

- **Turnover number (TON).** It defines the maximum yield reachable before one catalytic center loses its whole activity. It addresses the stability of the catalyst under fixed reaction conditions. Hence, it is not an instantaneous quantity: it stands for the lifetime of the catalyst. Martin and Kozuch defined it as a quantity which "specifies the maximum use that can be made of a catalyst for a special reaction under defined reaction conditions, by the number of molecular reactions or reaction cycles occurring at the reactive center until the decay of activity. Hence, it is dimensionless" [164].

$$TON = \frac{N^{\circ}cycles}{N^{\circ}sites} = \int_0^T TOF(t)dt \qquad (3)$$

  where T is the theoretical durability of the catalyst, while practically represents the catalyst exploiting time.

3.1 "Naked" palladium

Among the most exploited precatalysts there are Pd(OAc)$_2$ and PdCl$_2$ salts. These are known to be cheap choices, especially considering that low amounts of Pd are known to efficiently catalyze coupling reactions, but suffer from poor selectivity compared to Pd complexes [13, 166].
In addition, ligand-free palladium can be used in cross-coupling reactions, but one should consider that Pd species, especially reduced Pd(0), are unstable and suffer from aggregation and deactivation. Despite their toxicity and possible instability, ligands are particularly useful for tuning electronic and steric properties of catalysts and improving their activity, especially towards inactivated aryl halides.
A valuable solution to stability problems of "naked" palladium, seemed to consist of capping with tetra-*n*-butylammonium bromide (TBAB) and derivatives. These working conditions are known as "Jeffery's conditions" [167].
Ammonium salts cover the role of capping agents and work like shields against metallic species aggregation. They exploit electrostatic repulsion, steric hindrance or both. Dendrimers belong to this category of molecules, too.

In a study on Pd(OAc)$_2$ as precatalyst Reetz and Westermann detected amounts of Pd nanoparticles, which were identified as the competent species [168]. Colloids were also detected by TEM during the Heck reaction of bromobenzene and styrene within NMP, after an induction period characterized by no conversion. The authors inferred that before the reaction could take place, nanoparticles had to be formed during this measured induction period. Hence, they concluded that colloids necessarily played a role in the catalytic activity, also thanks to TBAB, which stabilized colloids from further aggregation.
In other studies, the activity of PdNPs formed *in situ*, was assessed. Colloids were hypothesized to act as reservoirs of active palladium species released during oxidative addition [25, 169, 170]. Therefore, molecular active Pd species are etched from the surface of Pd nanostructures and act as anionic species because of the halide ion attack during oxidative addition. A thorough explanation of the role of nanoparticles is provided in Section 5.5.

Nanoparticle contamination of molecular catalysts, linked to Pd ease to coalesce, is a major concern for "naked" palladium applications. The quality of the same commercial catalyst was found to vary up to 40% depending on the company and production process. Pd$_2$dba$_3$ [171, 172] and Pd(OAc)$_2$ [173] are two examples reported in literature. Nanoparticle contamination may be particularly affecting towards standardization of industrial processes, namely those involving enantioselectivity.
Pd$_2$dba$_3$ was used for the synthesis of (*S*)-(–)-2-allylcyclohexanone and authors highlighted the negative effect of supplier change, on conversion and yield [174]. The reproduceability of such processes is, thus, affected either when nanoparticles act as active-catalyst reservoirs or as sources of parasitic reactions [31]. The impact of catalyst contamination has been reported in different studies about Negishi and Suzuki couplings [175, 176] as well as in Stille polymerization reactions [177].
The purification of the precatalyst could be envisaged to correct the contamination problem, as reported in different studies [178, 179, 180, 181, 182]. After de Vries' group described the involvement of anionic Pd(II) complexes in cross-couplings [35], as stated in Section 2.1, one recycling process for "naked" palladium catalysts, exploiting charge properties of *in situ*-formed Pd complexes [183]. Otherwise, Chandrasekhar's group used poly(ethylene glycol) (PEG) as a scavenger for polar palladium species.

3.2 Phosphorous complexes

Pd-phosphine complexes have been widely employed as homogeneous precatalysts through the years. Some of them are commercially available (Figure 17), namely HandaPhos, EvanPhos, SPhos etc, while others have been studied starting from such commercial compounds, like WK-Phos [9] and N2Phos [10].

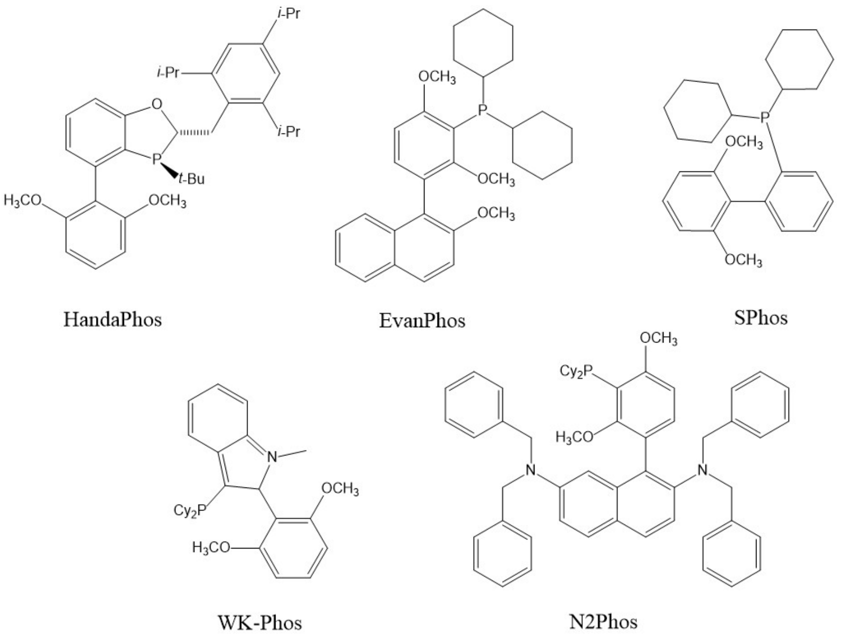

Figure 17: Molecular formula of three commercially available and bulky phosphine ligands (*Above*): HandaPhos, EvanPhos and SPhos; two other synthesized options reported in literature WK-Phos [9] and N2Phos [10] (*Below*).

Buchwald and Wolfe inferred that the complexation of Pd through phosphines enhanced the stability of those complexes and prevented deactivation through aggregation and Pd black precipitation [3] [184]. Whereby, Richards disagreed. His group studied the bulky and commercially available TomPhos **7** (Figure 18) ligand, i.e. triferrocenylphosphine. The resulting sterically hindered and electron-rich complex showed extremely high catalytic activity when $Pd_2(dba)_3$ was the precursor, but low stability, leading to coalescence into Pd black species after 5 hours [185, 186].

Several studies on phosphine's stability and efficiency have been conducted, namely on Pd:P ratios and thermal stability.

The Pd:P ratio was studied by Fu's group, who highlighted that the parameter had an impact on *in situ* transformed precatalysts [38]. The authors aimed to yield a monophopshine-ligated Pd compound in solution during Suzuki coupling, since they inferred it to be the actual species entering the cycle, rather than "naked" Pd or $[Pd(P(t\text{-Bu})_3)_2]$. Indeed, extremely high ratios such as 5:1 appeared to allow the activation and reaction of poorly reactive aryl chlorides. On the whole, Pd:P ratios of 2:1 seemed to be suitable for Suzuki couplings at room temperature, more than 5:1, at same Pd loading, as showed in Table 4. Noteworthy, the results were not easily comparable due to different substrates being involved in couplings.

A similar study by Herrmann and co-workers found that Pd:P ratio-related efficiency appeared in the order $1:1 > 1:2 > 1:4 > 1:6$, during the Heck coupling of 4-bromobenzaldehyde and n-butyl acrylate. This supported the evidence of high Pd:P ratios favoring C–C couplings [187].

Recently, Polynski and Ananikov mentioned the role of the Pd:P in a comprehensive DFT study on the mechanisms of leaching from PdNPs. The authors found that low ratios as 1:2 led to $PR_3[PhPdX]PR_3$ formation and drove successfully the reaction towards a Pd(0)/Pd(II) due to the complex's high stability towards re-deposition. In the case of 1:1 and 2:3 ratios, dimers and trimers $PR_3[PhPdX]_nPR_3$ ($n = 2, 3$) could be formed and being more unstable may lead to *in situ* decomposition, with the resulting species being stabilized by the base or the halides [34].

In addition, sensitivity of precatalysts to high temperatures turned out to be problematic, especially during high-temperature Heck reactions. Herrmann's group showed non-negligible catalyst decomposi-

---

[3] Pd blck is a "vulgar" term which refers to precipitated inactive clusters of elemental Pd obtained from deactivation of active Pd forms and agregation.

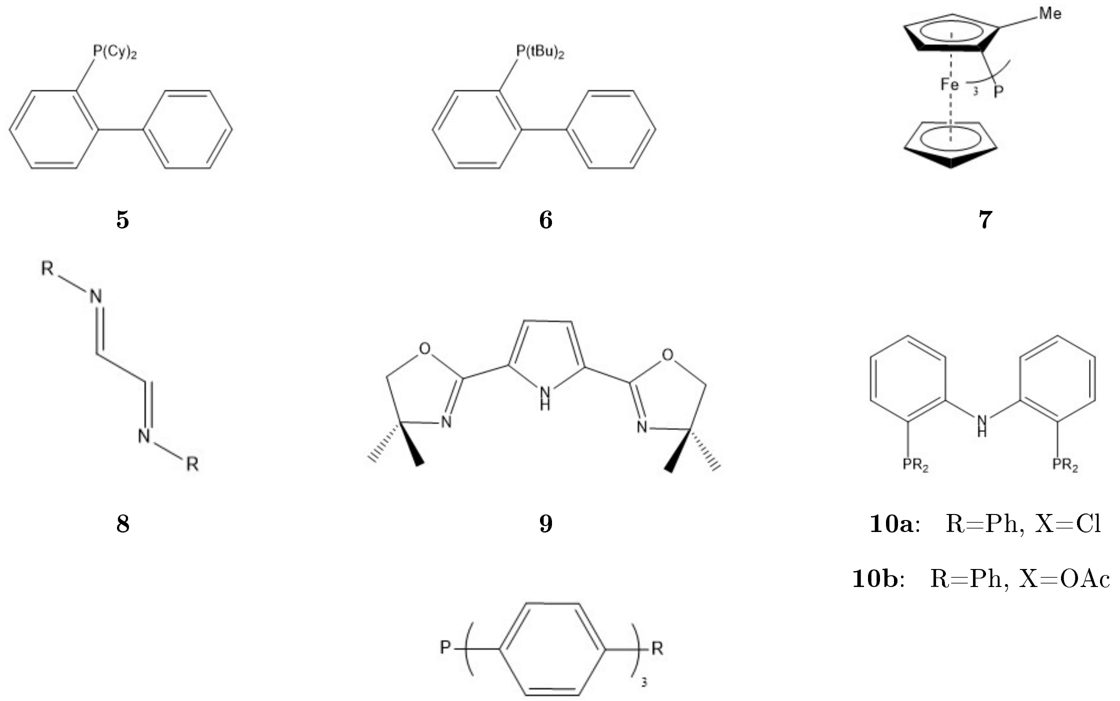

5 **6** **7**

8 **9** **10a**: R=Ph, X=Cl

10b: R=Ph, X=OAc

11a: $R = OCH_2C_7F_{15}$ (%F=58.7)
11b: $R = C_6F_{13}$ (%F=60.9)
11c: $R = O(CH_2)_2OCH_2CF_2[OCF(CF_3)CF_2]_p(OCF_2)_qOCF_3$
$\bar{p}$=3.38, $\bar{q}$=0.11, (%F=56.1)

Figure 18: Several phosphorous and non-phosphorous ligands reported in literature.

tion during the Heck reaction catalyzed by Pd(OAc)$_2$-phosphine complexes, due to P–C bond cleavage [187]. Similarly, other phosphines suffered from the same fate in specific conditions. The authors tested the catalyst, ligated to different phosphines under different conditions, with aryl chlorides and activated/deactivated bromides as substrates [187]. The only valuable solution appeared to be performing couplings of reactive activated aryl bromides in order to lower temperatures beneath 120°C, thanks to their higher reactivity. In the other cases, too high temperatures were necessary to obtain satisfactory conversions, which meant high rate of P–C bond cleavage and related side product formation such as Pd precipitation.

After Herrmann's studies, other Pd-phosphine complexes were efficiently applied to activated chloroarenes catalysis, yet researchers are still struggling with poor yields obtained from such cheap albeit reluctant moieties. Shen found trycyclohexylphosphin P(Cy)$_3$ and (diphenylphosphino)butane (dppp) to be efficient for this scope [92]. This was not the case of tricyclopentylphosphine and triisopropylphosphine even though electronically similar to $P(Cy)_3$ [188]. The same group addressed the high reactivity of [PdP(tBu)$_3$], the compound widely studied by Herrmann's group, to its bulky and electron-rich character.
Excellent efficiency, for a wide scope of substrates, was observed by Hartwig in [189] when substituting one Cy/*t*-Bu group, with a biphenyl (compounds **5-6** in Figure 18). These complexes had the property of balancing steric and electronic effects favoring both oxidative addition and reductive elimination, which was considered the key character of well-performing complexes. Indeed, the authors inferred that electron-rich phosphines favored oxidative addition, while steric hindrance facilitated reductive elimination.

Phosphines are known to be toxic, expensive and air-sensitive. Alternatives are discussed below, with studies on other electron-donor groups than phosphorous-based. It is note-worth that in recent

Table 4: Results of Fu's study about the correlation between Pd:P and yield. Adapted from [38].

Aryl chloride	Boronic acid	Product	Conditions	*Pd:P*	Yield
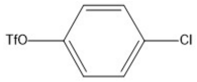	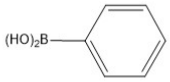	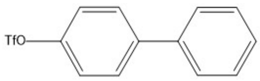	$1.5\%Pd_2(dba)_3$ $1.5\%P(t-Bu)_3$ 24 h, RT	2:1	97%
			$1.5\%Pd_2(dba)_3$ $0.6\%P(t-Bu)_3$ 32 h, RT	5:1	93%
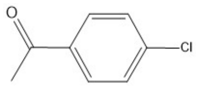	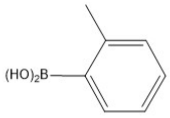	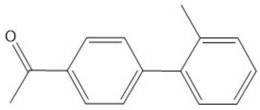	$0.5\%Pd_2(dba)_3$ $0.2\%P(t-Bu)_3$ 8 h, RT	5:1	99%
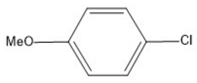	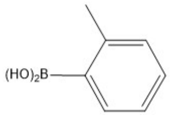	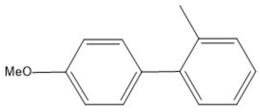	$1.5\%Pd_2(dba)_3$ $1.5\%P(t-Bu)_3$ 10 h, 70°C	2:1	75%

studies, chelating agents coming from natural plant extracts have been used sometimes as variants, namely curcumin [134].

3.3 Non-phosphorous and hybrid ligands

Since, well-performing phosphines still suffered from stability issues under harsh conditions, some other ways to ligate Pd were proposed. Pringle's group studied the coupling of aryl bromides and *n*-butylacrylate catalyzed by triarylarsines-Pd. These complexes showed higher activity than their phosphine "relatives", albeit involving the use of extremely toxic arsines [190]. Besides, easily synthesized nitrogen-based ligands have been more widely studied.

Nolan achieved some good results by catalyzing Suzuki and Heck couplings exploiting diazabutadiene-based (DAB) bidentate ligands **8**, with R= alkyl or aryl (Figure 18) [191, 192]. The authors reported that the presence of these ligands favored Heck couplings, giving higher conversions compared to "naked" palladium, under the same conditions. Pd/DAB-Cy (1,4-dicyclohexyl-diazabutadiene) showed high efficiency in activating Heck olefinations of electron-deficient bromoarenes, in the presence of Cs_2CO_3 as the base, at 100°C.

Gade and Mazet made a step forward in the investigation and described the NNN tridentate ligands based on bis(oxazolinyl)pyrrole **9** (Figure 18) observing no Pd black formation, whatever the conditions, for both Heck and Suzuki couplings. The authors studied the performance of two slightly different helical dipalladium compounds in the Heck coupling of bromobenzene and styrene, in N-methylpyrrolidone (NMP) with K_2CO_3 as the base. The results are summarized in Table 5. Lower loading of palladium seemed to enhance the TON of both catalysts but not necessarily the conversion (i.e. activity). They concluded by comparing the activity of these N-based complexes with commonly used phosphines and N-heterocyclic carbenes. Their activities appeared slightly lower than the others, albeit still valuable [39].

Liang performed the Heck reaction catalyzed by PNP pincer complexes, family of compounds **10** in Figure 18. No Pd black was detected after heating at 200°C for 100 h [193].

Other families of hybrid PNP pincer compounds were studied by the group of Beletskaya, e.g. compounds **12** and **13** (Figure 19). The authors highlighted the negative impact of the bulky character of

Table 5: Stability and efficiency study conducted by Gade and Mazet on NNN tridentate bis(oxazolinyl)pyrrole-ligated palladium. The two catalysts **9a** and **9b** are shown above the Table. Adapted from [39]

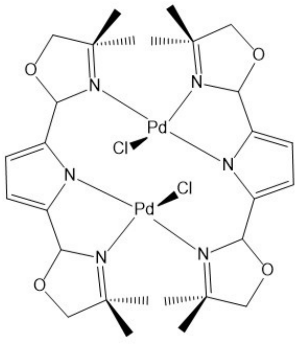

9a

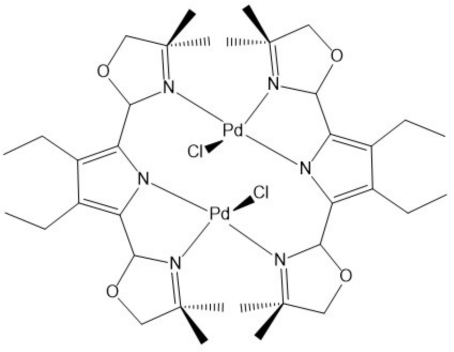

9b

Catalyst	Cat./Sub.	Time [d]	Conversion [%]	TON
9a	10^{-3}	3	97.1	971
9b	10^{-3}	3	96.6	966
9a	10^{-4}	3	87.3	8730
9b	10^{-4}	3	85.4	8540
9a	$5 \cdot 10^{-5}$	4	47.4	9480
9b	$5 \cdot 10^{-5}$	4	43.2	8640

pincers on resulting TOFs, due to the slowdown of Pd(0)-species release in solution [194].

Indeed, many phosphine-free complexes appeared to behave like "naked" palladium during Heck reactions [195]. It remains unclear whether all type of ligands are cleaved from the complexation sphere of palladium or if some are conserved. Though, it is evident the importance of the Pd–ligand bond stability to prevent decomposition and really exploit ligand properties.

In 2020, Pd–PNO complexes were investigated by Morales-Morales et al. in DMF:H_2O 1:2 mixture as a solvent for Suzuki reactions. No decomposition of the homogeneous catalyst into PdNPs and Pd black was detected. Furthermore, a mercury-drop test was conducted and showed no decrease in the yields, demonstrating that no heterogeneous species is whenever present in solution [196].

3.4 Palladacycles

Palladacycles are Pd complexes characterized by at least one Pd atom in a heterocyclic ring, which may contain several electron-donor groups (N, P, Si, Se etc). These compounds were firstly studied by Herrmann and Beller in 1995 as catalysts for Suzuki and Heck reactions. Beller, Riermeier et al. tested palladacycle **14** (Figure 19) in Heck olefinations of bromoarenes. The authors sustained that Pd(II)-species were reduced *in situ* to give active Pd(0)-moieties [197, 198]. Later on, in [199], Bergbreiter et al. evidenced some complex decomposition releasing Pd(0), starting from SCS Pd(II) palladacycles. Similarly, Eberhard showed that PCP-Pd(II) pincers decomposed under reaction conditions and formed active Pd(0) colloids [200].

Bedford and co-workers compared the activities of phosphinite-based palladacycles and phosphorous Pd complexes and demonstrated that the former better activated chloroarenes [201].

In [202] Indolese, Studer and coworkers added bulky secondary phosphines to help NC palladacycles catalyzing the Heck and Suzuki reactions and compared the results to common "naked" Pd salts such as $Pd(OAc)_2$ and $PdCl_2$. The authors observed activities comparable to Fu's $Pd_2(dba)_3/P(t\text{-Bu})_3$ [38].

Later on, Nolan advocated better synergistic activity of N-heterocyclic carbenes (NHC) with NC palladacycles during a RT Suzuki-Miyaura reaction of aryl chlorides [203].

Nowadays, more solid evidences allowed to describe these precatalysts as reservoirs of Pd active species, that are released in solution. Decomposition was recently, detected at different temperatures depending on the synthetic pathway and substituents, though, really close to common Heck reaction temperatures (around 160°C) [204]. Pd black precipitation was observed at the end of the reaction. Indeed, already in 2003, De Vries and colleagues showed that homeopathic $Pd(OAc)_2$ and palladacycle **14** behaved in the same way [25]. The same kinetics should mean same active species involved.

In 2000, Nowotny et al. dealt with NC palladacycles and registered appreciable induction periods likely to consist of production of soluble active species, enough to start the Heck coupling of iodobenzene and styrene [205]. PdNPs were supposed to be produced during induction periods and to be the active species [125, 205, 206, 207]. The same hypothesis was supported by de Vries [26] and Reetz [168].

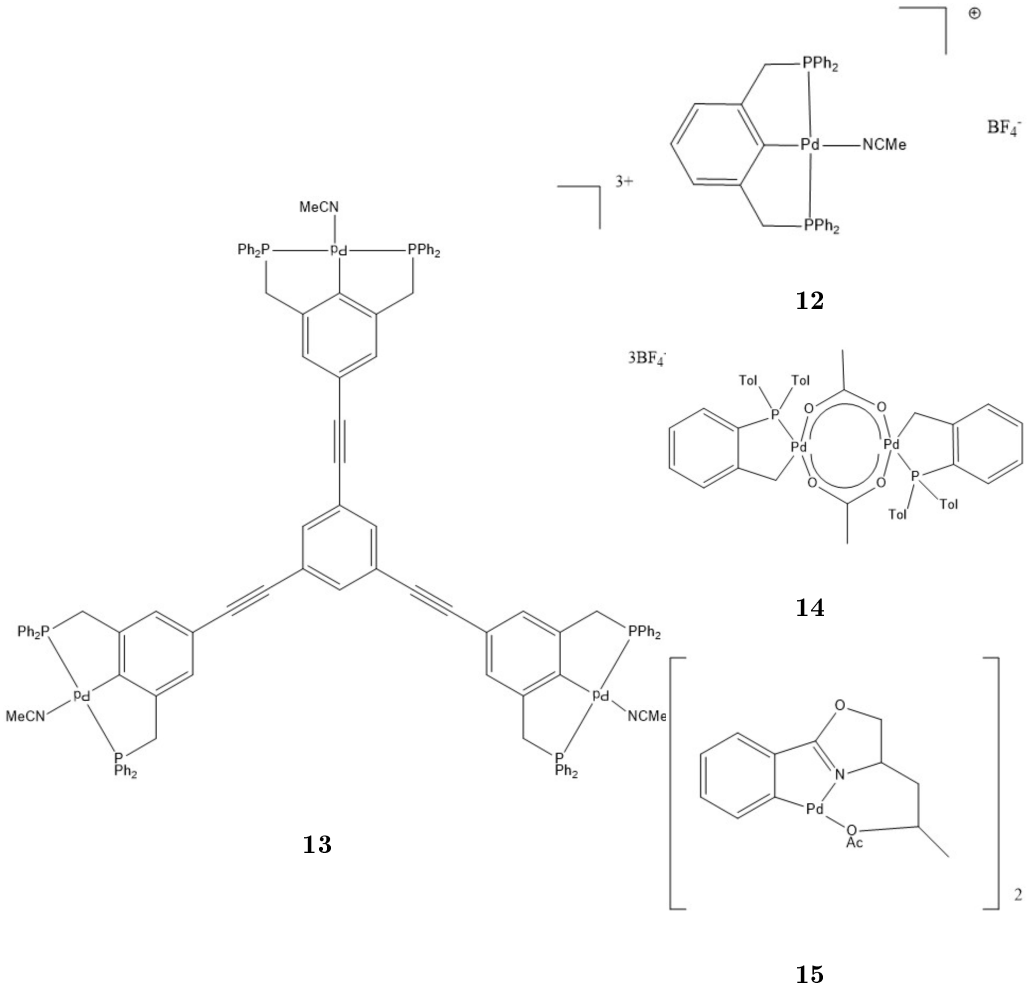

Figure 19: Detail on some PCP pincer ligands and palladacycles found in literature

DuPont witnessed the colloid formation process, as well. He highlighted the possibility of PdNPs to be the true active species in Heck reaction media, produced by palladacycle decomposition [208]. This hypothesis was supported by positive results to the poisoning Hg(0)-drop test, yet no evidence was reported about visible nanoparticles by TEM. In [11] the team provided a good explanation of palladacycles activation through release of molecular Pd(0)-species. Figure 20 reports the activation-deactivation scheme of Pd species proposed by DuPont et al. and occurring in solution [11]. A thorough study was conducted playing on the two Heck's substrate concentrations. In the presence of exceeding iodoarenes, iodo-Pd(II) species were mostly detected, proving a higher rate of oxidative addition compared to olefin insertion. Hence, an equilibrium correlation was proposed for the olefin insertion step, strongly underlining its disfavored character. On the other hand, excess of olefins resulted in high concentration of Pd(0) species which are really sensitive to aggregation, hence to deactivation. Indeed, the authors complained about some complications encountered, hindering the proper finalization of mechanistic studies. These were related to doubtful initial measurements, caused by the complex decomposition paths followed by the different intermediates. Though, they stated that Pd colloids might actually be the competent species in the liquid medium.

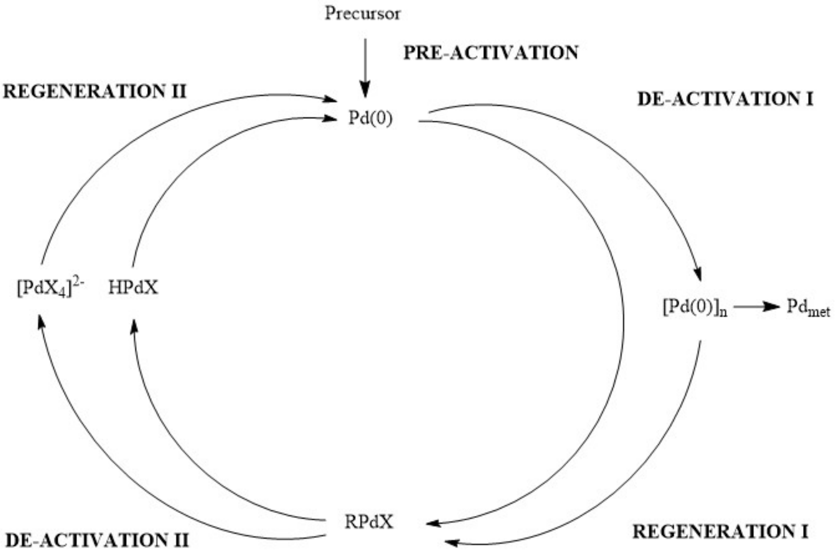

Figure 20: Pd-catalyst precursors activation-deactivation process scheme proposed by DuPont et al. Adapted from [11].

Around 2012, Schiff-base Pd complexes were studied as catalysts for the Suzuki-Miyaura reaction [209, 210, 211, 212]. Schiff bases are compounds containing imine-groups and coming from the condensation of carbonyl and amino groups. This class of compounds is generally tailored in order to satisfy coordination chemistry necessities, through a wide spectra of different possible functionalizations. Indeed, they are often used as multidentate ligands for palladacycles synthesis.

In 2012, the aim of Kumar's group was to tailor new pincer ligands for metal catalysts, based on the assumption that different chelating groups are able to change the activity of the final catalyst. They focused on selenated Schiff bases containing both "soft" and "hard" donor groups. The molecules were used to stabilize PdNPs, too [210].

The mechanism of Schiff-base complexation of Pd was re-explored by Singh and co-workers by designing tailored homogeneous palladacycles for Suzuki-Miyaura coupling [12]. Thiophene-containing palladacycles, **16**-**20** (Figure 21) were supposed, by the authors, to protect reduced Pd(0) species from aggregation into isolated NPs, thanks to sulfur TM-scavenging properties [12]. Between compounds **16** and **18**, the latter showed the highest activity, albeit both produced Pd black during the reaction. On the contrary, during catalysis by compounds **17**, **19** and **20** no Pd black was detected. The authors hypothesized pure homogeneous catalysis in this second case.

It is note-worth that both reactions were conducted at 70°C, while TGA analyses of compounds **16** and **18** showed decomposition before 90°C, which is the most likely explanation of such extensive decomposition. In case of decomposition, any stabilization by thienyl groups is not possible, and activity was supposed to be purely homogeneous coming from leached Pd(0) species [12].

Recently Grivani and Nehzat investigated the activity of two ligands, compound **21** with varying R, imidazole- or sulfate-based (Figure 21). The two systems performed well in the reaction of phenylboronic acid and 4-bromotoluene in MeOH at 65°C and appeared to play an indispensable role in raising the yield in product. The imidazolium-containing ligand resulted in lower yield, probably because of the presence of the chloride counterion which competes with 4-bromotoluene for oxidative addition.

Other bis-NO-Pd complexes were studied in 2020 with similar good to excellent results [213, 214, 215]. Some were studied in an interesting application of SMC reaction involving micellar chemistry. PEG400 and DMF were added to water in the presence of sodium dodecyl sulfate (SDS) [216].

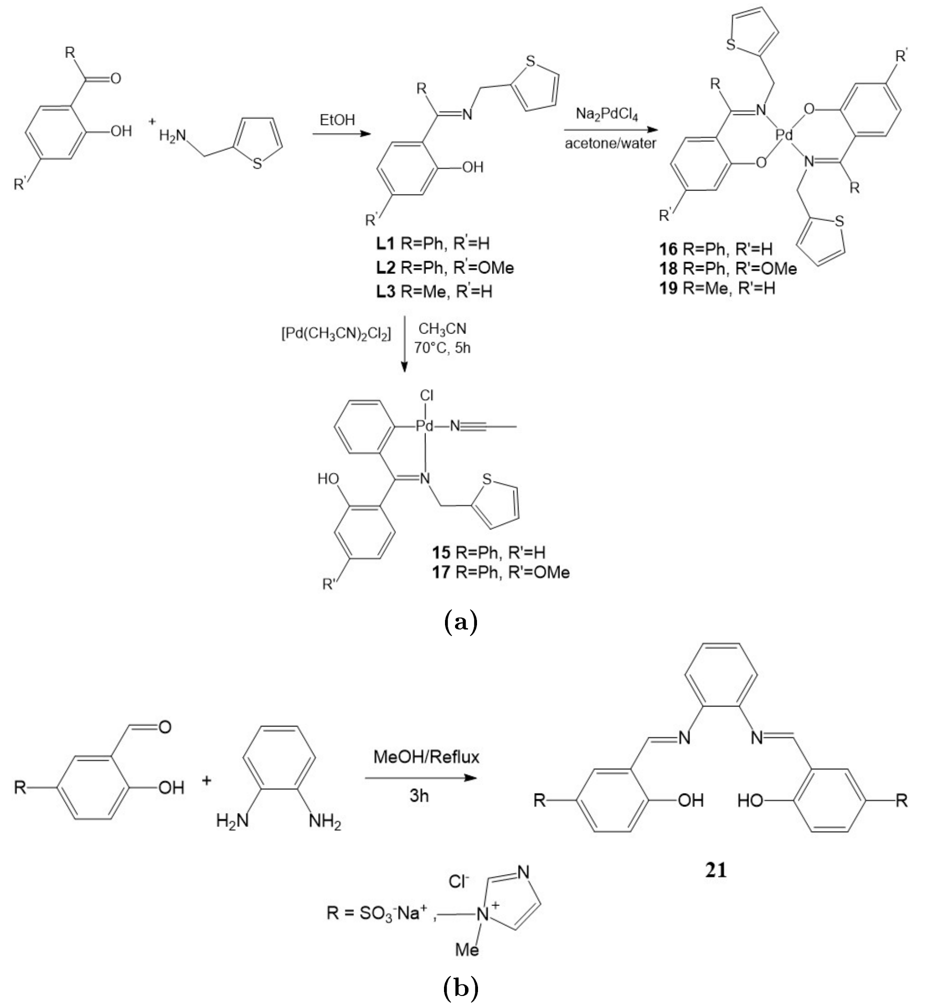

(a)

(b)

Figure 21: **(a)** Thiophene-functionalized palladacycles (**16**-**20**) synthesized by Singh and co-workers [12]. **(b)** Schiff base ONNO-Pd complexes **21**, with varying substituents *R*, synthesized by Grivani and Nehzat [13].

3.5 The Pd(II)-P(IV) cycle

Palladacycles were firstly studied by Herrmann and Beller in 1995 as catalysts for Suzuki and Heck reactions. The authors hypothesized these catalysts to undergo transformations following a P(II)-Pd(IV) catalytic cycle, under cross-coupling conditions [217, 218, 219]. Indeed, it was because of the lack of Pd black deposition, consistent with Pd(0) species absence, to lead authors think that palladacycles were actually the competent species being activated by an oxidative step from Pd(II) form, to Pd(IV) [219]. Though, Herrmann's group was not the only one to guess so. In 2000, Pd(IV)-species were detected in solution, when palladium was complexated with a chiral aminophosphine ligand [220]. The authors were able to isolate a Pd(IV) intermediate in solution and to characterize it with X-ray structure analysis.

In [221], Shibasaki and co-workers supported the behavior of palladacycles as precursors for active species going through a Pd(II)/Pd(IV) cycle. More studies about SC and SCS palladacycles supported this theory since they were recycled several times, without structure changes, evidence that is not consistent with the formation of Pd(0)-species [222]. Later on, NC palladacycles such as **15** (Figure 19), used for Suzuki couplings, showed efficient recyclability and presence of Pd(IV)-species, while Chung and co-workers highlighted the low stability of NCN-P(II) complexes under Heck conditions, giving early birth to Pd black [223]. Yao studied ligand-free precatalysts [224]. His group invoked the existence of palladacycle-like intermediates taking part to a Pd(II)/Pd(IV) cycle. Though, in the case of palladacycle **15** depicted in Figure 19 of Section 3.4, it was finally stated the characteristic cycle involved Pd(0)/Pd(II) species with possible small amounts being oxidized into Pd(IV) species. Nowadays the hypothesis of Pd(II)/Pd(IV) being the competent catalytic cycle for C–C cross-coupling reaction, has been completely ruled out. Besides, Pd(IV) species appeared to be responsible for parasitic reactions, namely homocouplings. Recently, a study by Polynski and Ananikov clarified the role of Pd(IV) species in cross-coupling reaction media [34]. Actually, Pd(II)-complexes can be further oxidized by the presence of excess organohalide compared to the second substrate (R^2M). This double oxidative addition would cause homocoupling reactions and biphenyl formation. Though, the presence in the system of R^2M normally prevents this process. Another way to, bypass the process is to coordinate X^- or L to Pd and cause oligomerization, into $L[PhPdI]_nL$. Thereby, homocoupling proportion compared to heterocoupling depends on halides and R^2M activity and concentration, as well as on the presence of stabilizers (i.e. X^- and L) and on the reaction conditions, in general. On the whole, one must take care of not working with excess halide in order to prevent and/or control homocoupling rates [34].

3.6 NHC-ligands

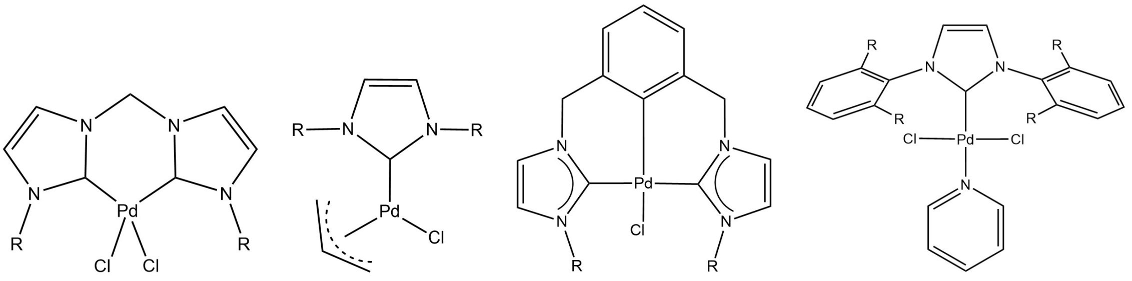

22 **23** **24** **25**

Figure 22: Families of NHC-based complexes according to Özdemir et al. [14]. Examples of bis-Pd-NHCs (**22**), allyl-type Pd-NHCs (**23**), pincer-type Pd-NHCs (**24**) and PEPPSI-type Pd-NHCs (**25**).

This family of compounds, involving at least one Pd–C bond, is grouped into: bis-Pd-NHCs (**22**), allyl-type Pd-NHCs (**23**), Pincer-type Pd-NHCs (**24**) and PEPPSI-type (Pyridine Enhanced Pre-catalyst Preparation Stabilization and Initiation) Pd-NHCs (**25**). This latter group facilitates the OA step thanks to the low-coordination power of pyridine group. Moreover they are stable against aerobic conditions and polar solvents, namely water [14]. They also act similarly to phosphines as strong σ-donors and weak π-acceptors, thus increasing the electron density of Pd and accelerating the OA step [225]. N-heterocyclic carbene (NHC) complexes of Pd(II) salts, namely compound **26** in Figure 23, were reported by Herrmann and co-workers to be capable of activating chloro- and bromoarenes under Heck and Suzuki conditions [226]. This kind of ligands, especially compound **27** (Figure 23), were also reported to prevent Pd black formation, when coupled with bis-triarylphosphine complexes [227]. Though, coalescence happened at long reaction times [228].

Pd(0) species are known to be easily cleaved from complexated precatalysts and to form new complexes during oxidative addition, with halides. In some early studies, induction periods explained by the reduction of ligated Pd(II) to solubilized Pd(0), were observed, but no loss of Pd(0) in solution was detected [62, 229]. Whereby, precatalysts based on P(II) ligated to two monodentate N-heterocyclic carbenes, compound **28** (Figure 23), showed high stability at 120°C. No palladium metal deposition was detected and 90% of the starting precatalyst was efficiently recovered, evidence that triggered the interest on these ligands. Recovery was obtained by crystallization and subsequent recycling appeared to be possible. Though, such compounds showed lower efficiency at lower temperatures (e.g. 80°C) due to too long induction periods.

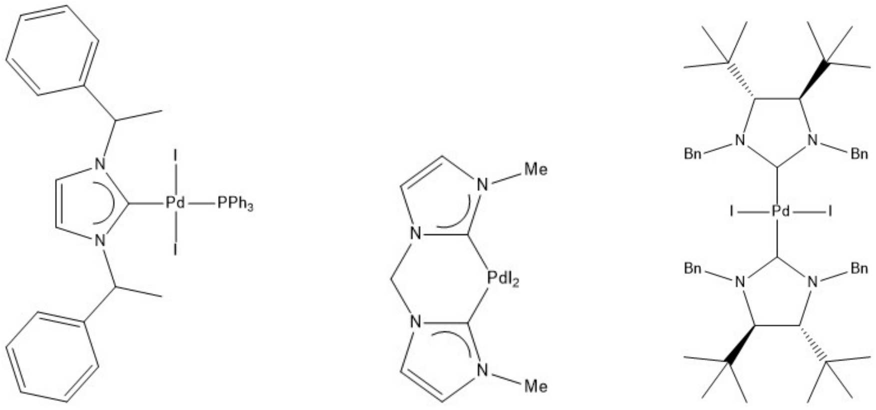

26 **27** **28**

Figure 23: N-heterocyclic carbene-based Pd complexes

The fact that using NHC-based precatalysts, palladium was hindered from separating, gave hope for further heterogeneous supported-catalyst applications. Unfortunately, not all the authors agree about the strength of the Pd–C bond in NHC-based complexes.
Other NHC-based tailored systems have been studied in the last years showing excellent activities [14, 230, 231, 232]. The tailoring of these systems is often carried out thanks to DFT calculations [230].

4 Solid supports for the heterogeneous catalysis

Supporting of TM catalysts, namely palladium, is a technique which allows better and easier recyclability of the catalyst at the end of the reaction. Besides, it has high impact on the catalyst activity.
Transition metals are adsorbed on many surfaces thanks to several techniques. The results of such deposition methods are normally differentiated between physisorption and chemisorption. The former is characterized by catalysts anchored to the surface, thanks to weak electrostatic interactions. Hence, those species suffer from easy detachment during simple flushing of solvents or of the reaction medium, under conditions of high flow-rate or presence of phase transfer agents, for instance.
Besides, chemisorption involves a chemical reaction between catalyst and carrier, resulting in strong covalent or ionic bonding. Though, this causes significant change in the chemical properties of the catalyst, namely modification of the Pd electron density, which are known to control the kinetics of the whole catalytic cycle. Heterogeneous catalyst often showed lower activities compared to homogeneous species. If one does not account for leaching and more complex reaction mechanisms, this evidence can be easily explained by introducing the concept of "apparent kinetics".
Biphasic systems are characterized by hindrance for the substrates to reach the solid catalytic surface. This fact adds complexity in tuning catalyst's properties. Not only, the reaction kinetics must be controlled by well-performing chemical species, but also, the supports need to optimize the accessibility of the active sites and the fluidodynamic conditions. Indeed, according to the film theory, a stagnant film of thickness $\delta \lll L$, where L is the characteristic dimension of the system, is formed around the phase-separating interface, the solid catalytic surface in this case. Due to its null motion velocity at the interface, the matter transport phenomena in the film are limited to diffusion, without convective mixing which maintains macroscopic homogeneity of concentrations within the reaction medium. Hence, a substrates concentration gradient is established within the film, and the amount of reactive molecules reaching the surface is linked to the reaction kinetics and the substrate concentration in the liquid bulk. Moreover, a fluidodynamic turbulent regime reduces the thickness of the stagnant film accelerating the supply of substrates to the solid surface.
The kinetics consists now of the actual reaction parameters added to a resistance to mass transfer characterized by the aforementioned film properties and parameters. In addition, the catalytic surface often can not be considered as a smooth layer of catalytic active species like in Figure 24, instead it is uneven and characterized by porosity and hindrances in reaching the actual active sites. By simply considering a porous catalytic particle, the solubilized substrates have to follow a complex pathway before reacting on the Pd active sites, as showed in Figure 24. The substrates are carried by the liquid motion towards the catalytic particle external surface. There, their motion is slowed down by the vicinity with the solid phase and a diffusive transport is established (1). Then, the molecule has to cross the particle porosity and diffuse towards the active internal sites (2) where it will be adsorbed (3) and allowed to react(4). The inverse process is supposed for the leaving products (5-7) [233].

The new kinetic constant accounts for both transport phenomena and reaction kinetics according to the formula:

$$\frac{1}{K_0} = \frac{1}{k_s a} + \frac{1}{\eta k'(1-\epsilon)} \tag{4}$$

where K_0 is the new kinetic constant accounting for both reaction rate and mass transport resistances, k_s is the mass transfer coefficient between liquid and solid phase, equal to D_e/δ (D_e=equivalent diffusion coefficient, δ=film thickness), a is the volumic surface accounting for the accessible surface area created by the porosity, η is the effectiveness factor which is a function of the Thiele modulus (ψ), thereby of the shape of the catalytic system, k' is the kinetic constant and $1-\epsilon$ the porosity of the catalytic particle.

Some examples of widely employed carriers are provided below, in order to provide few information regarding these materials and their usage in C–C couplings.

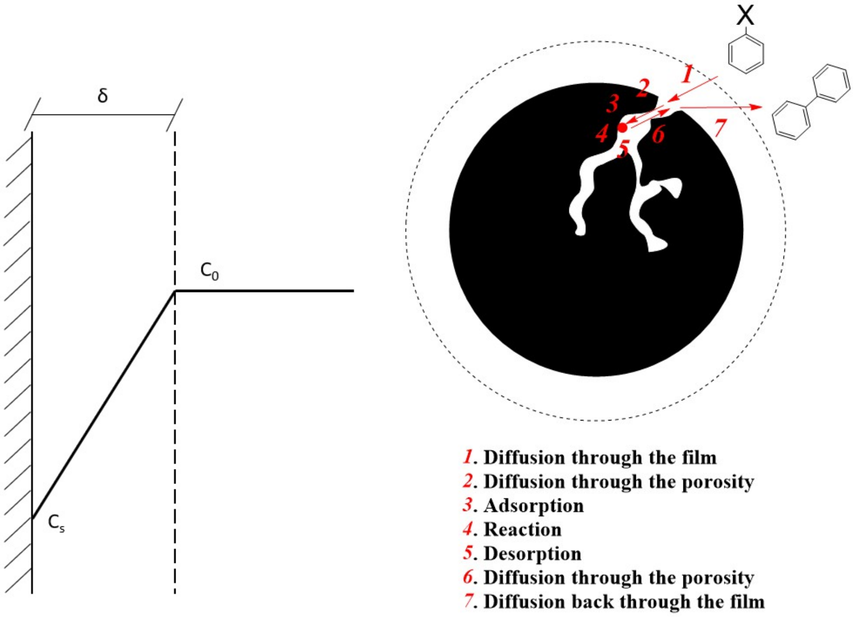

(a) **(b)**

Figure 24: **(a)** Scheme representing the film theory, portion of space which is stagnant next to the solid surface. **(b)** Scheme of the apparent kinetics involving transport phenomena and reaction on the active site.

4.1 Carbonaceous supports

The earliest exploited carbonaceous carrier was activated carbon, consisting of a graphitic-like structure. Carbon- and oxide-based supports are among the most exploited solid matrices for any kind of heterogeneous catalysis application. They are cheap and highly standardized commercially-available solutions for heterogeneous cross-coupling reactions. The main properties of this carrier are significant and controlled porosity for improved transport of molecules, controlled chemical surface properties and high surface area, inertness and high stability towards alkaline and acid environments and harsh thermal conditions [234]. Though, one of the most likely to suffer from leaching and sintering, because of the absence of stabilizing groups on the solid surface [235].

After the discovery of nano-sized materials, extensive studies have been conducted on them. Carbon-based nanostructures are characterized by several allotropic forms and tunable oxygen content. This two properties make them extremely ductile supports and efficient for a wide spectrum of applications. Graphite oxide is often used as a precursor of such nanostructures. Reduced graphene oxide (RGO) can be obtained by exfoliation and stabilization of graphite foils. Interestingly, distancing between layers of GO can be tuned by the concentration of water in the medium, which is an extensively used solvent [236]. Hence, the inter-layer spaces are perfect sites for intercalation of molecules and nanostructures, from polymeric chains to transition metal nanoparticles.

Mastalir and co-workers showed good-to-excellent yields in the reaction between bromobenzene and styrene after impregnating GO frameworks with N-based Pd/complexes, where the precursor cations underwent ion-exchange onto the GO framework [236]. Other studies were led on GO frameworks, consisting of functionalizing groups for layers separation and trapping of PdNPs [237]. Bending of these 2D RGO structures gives birth to carbon nano-tubes (CNTs), which can be single- or multi-wall (SWNTs, MWNTs).

Other structures are known, like carbon nano-fibers, nano-globules, fullerens etc. These carriers have unique chemical and excellent mechanical properties, different from macroscopic graphitic carbon, due to their size. For instance, Likholobov and co-workers found that similar preparation processes of both nano-tubes and nano-globules gave different oxygen contents. The amount of surfacial oxygenated groups gave a different pH, more acidic for CNGs compared to CNTs. In addition, the reduction of deposited TMNPs appeared more facile in the case of lower oxygen amounts, resulting in more homogeneously-dispersed and smaller nanoparticles. Thus, CNTs appeared more suitable for TMNPs deposition and C–C coupling applications [238].

PdNPs are particularly apt for deposition onto such carbonaceous structures due to the strong interaction with the support, enabled by the presence of defects and oxygenated groups (e.g. hydroxide, carbonyl, carboxyl) [225]. Oxygen functionalization is the easiest obtainable modification of carbon surfaces, thanks to GO precursors.
Corma and co-workers studied the activity of PdNPs supported on single-wall carbon nanotubes (SWNT). This nanostructured catalyst showed promoted activity compared to the classical and commercial Pd/C, during Heck coupling of iodo- and bromobenzene with styrene, while using DMF as a solvent the authors detected some leached species that they described as Pd(0) NPs [15]. The preparation process is showed in Figure 25.

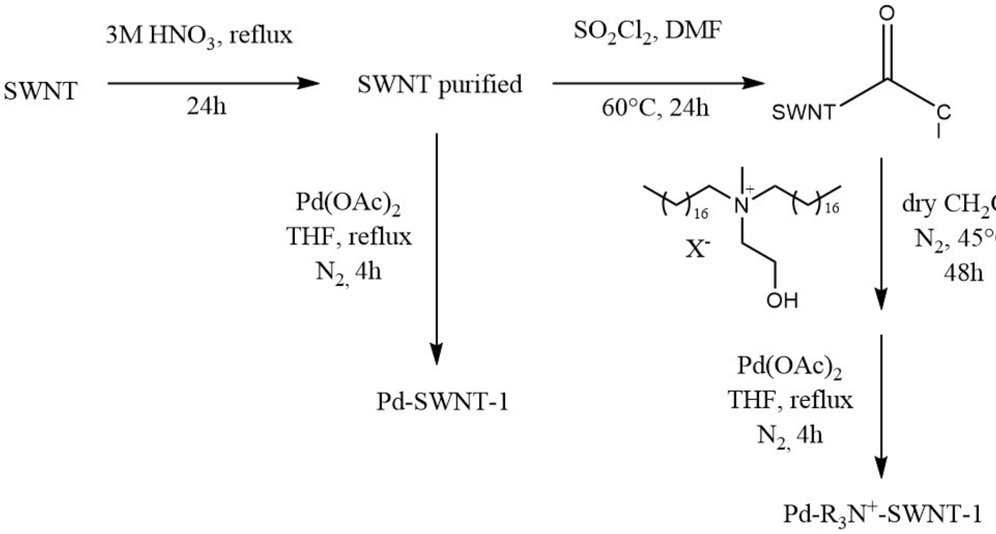

Figure 25: Preparation process scheme of single-wall nanotube-supported palladium by Leyva et al. [15]

Later on, Namboothiri, Doris and colleagues studied Pd-CNT in the Suzuki coupling of chloroarenes at RT. The catalyst was made of multi-wall carbon nanotubes (CNT) where the most external layer consisted of Pd spherical nanoparticles of around 2 nm [239]. XPS analysis resulted in coexistence of Pd metal and PdO. Really good yields were obtained in the coupling of several aryl chlorides, in water/EtOH at RT, with K_2CO_3 as the base, under air atmosphere. Besides, N-doping and the correlation between CN structures and catalyst activity were investigated, as well. NCNT were used in [240] to promote the dispersion of Pd nanoparticles onto the carriers. Doping and coordination into the carbon lattice are among some of the utilized functionalization methods [240].
Nitrogen introduction in the lattice is easy because of the vicinity of nitrogen and carbon into the periodic table of elements and their similar size. Doping also allows to increase the spin density of the Pd catalyst, by introducing defects bearing one electron more per site, in the carbon lattice. The positive effect of N-doping was already proved on mesoporous carbon (MC).
Manufacturing of NCNT is obtained by chemical vapor deposition, impregnation or plasma techniques, resulting in three main types of NC species: graphitic-N, pyridinic-N and pyrrolic-N. The second form performed better in Heck couplings according to DFT studies [240].

4.2 Inorganic oxides

Inorganic oxides are involved in a large part of catalytic processes. They can be used either as supports or as catalysts themselves, depending on the application. Moreover, they are characterized by high surface area and oxidized functional groups ready for chemical transformation of their surface. Most of them are extremely porous materials, namely mesoporous silica and zeolites.

This category of materials contains CeO_2, MgO, TiO_2, ZnO, ZrO_2, clays, perovskites, alumina, bohemite etc.

The extremely different sizes of metal cations and oxygen at the surface causes a loss in the symmetry of coordination, and together with other defects contributes to the catalytic activity of such materials [241]. For instance, electronic defects impact their conduction properties (i.e. semi-conductors). Thus, introduction of palladium in the lattice of their crystalline structure, by ion exchange, changes their conductivity and affects the catalytic activity.

Several groups supported palladium on different carriers such as Al_2O_3, TiO_2, ZrO_2, ZnO, CeO_2, Nb-MCM-41, mesoporous silica MCM-41 and agarose-alumina [81, 242, 243, 244, 245, 246]. Djakovitch and co-workers advocated that the catalytic activity of these systems is influenced by the nature of the support as well as by the Pd dispersion on the surface [245]. In the case of Titania, weak interactions between the support and active palladium were found [243]. Besides, MgO is characterized by strong interactions metal-support and by hydrophilicity and surfacial acid sites which are able to activate the substrates [247].

Bohemite is an aluminum oxide-hydroxide commonly found in nature in the form of crystals. It was used in [134] as a supporting solid matrix for Pd complexes.

Periodic mesoporous organosilica (PMO) has been employed by Lόpez and co-workers [248]. This carrier consists of an organic-inorganic structure, obtained through grafting or co-condensation, which shows interesting properties of unblocked mesoporosity and tunable loading of organic units. The co-condensation technique allows to tailor the supporting material and endowing it with the desired porosity. Their organic synthons (monomers) are easily functionalized for coordination chemistry necessities, either by direct synthesis of group-containing units or by post-functionalization.

4.3 Polymers

Polymers are probably the most exploited matrices for metal catalysts supporting, and offer high surface area and tunable properties. Indeed, a wide scope of monomers are suitable for polymerization reactions, allowing porosity-size control and grafting of reactive functional groups, making them perfect for transition metal complexes/nanoparticles deposition.

A widely used deposition technique is ion-exchange on polymeric resins, like Merrifield resins. Those materials consist of cross-linked polystyrene bearing a chloromethyl functional group [249, 250].

Polystyrene was used by Takata et al. for chemoselective aqueous Suzuki-Miyaura coupling as a support for Pd(II)-macrocylic complex [251]. Then, polyacrilonitrile (PAN) was used by Saitalavi et al. as an easy functionalizable carrier [154]. It was functionalized with amidoxime groups.

Some other, N-containing systems were studied, namely urea-based porous polymers, obtained by condensation of amine and isocyanate groups [252], thermosensitive polydopamine, poly(vynilpyridine) [159] etc.

Cross-linked polymers and interpenetrating polymer networks (IPN) hydrogels were used by Dong et al. [253, 254]. Swelling of hydrogels thanks to water action, theoretically imposes leaching of Pd only in the hydrogel porosity and allows the use of extremely low amounts of palladium. In this case deposition of PdNPs during supporting hydrogel synthesis appeared to give a less polydispersed PSD. The catalyst resulted in a TOF of 1800 [h^{-1}]. Decrease in catalytic activity after several cycles was suggested to be caused by Ostwald ripening. Indeed, porous matrices are nowadays, extremely used in order to increase the surface area and try to confine leaching into the pores.

Porous organic polymer (POP) poly(1,4-diazacyclo [2.2.2]octane) (DABCO) was used as carrier for Pd nanoparticles in aqueous Suzuki reaction. The hydrophobicity of such polymers normally hinders applications in water, yet this catalyst worked well [255]. The porosity was partially filled with PdNPs.

Other systems, namely nanoporous phenantroline [256] and microporous organic polymers (Hypercross-linked polymers HCPs) [257] were recently studied. In the latter case, the cross-linking process gave birth to extensive porosity dug into a rigid structure. One example of this kind of polymers is the Davankov resins firstly synthesized in 1970 [257]. This catalyst prepared with HCPs functionalized with triazole NHC carbenes showed high thermal stability and varied porosity (meso- and macroporosity). The activity of the catalyst resulted in elevated TONs around 16000 in aqueous media.

Metal Organic Frameworks (MOFs) characterized by inorganic joints linked through organic bridges, are commonly utilized porous materials for heterogeneous catalyst's supporting. Though, the adsorbed substrates suffer from lack of diffusivity. Metal Organic Polyhedra (MOPs), similar to MOFs, are rigid porous structures where each cell is independent from the others. They were used by Shin et al. as a support for Pd catalyst in Suzuki C–C couplings. Their surface is highly hydrophylic due to the metal oxide groups. This property makes them particularly suitable for aqueous media [37].

Other polymeric structures are used more than for supporting applications, as entrapping frameworks, protecting nanoparticles from aggregation, mainly through steric hindrance. This is the case of dendrimers. Dendrimers gained importance over the years, since they appeared recyclable entrapping structures for both heterogeneous and homogeneous active species, but maintaining activity during consecutive runs.

Firstly studied in 1999 by Crooks et al., the group encapsulated PdNPs into polyamidoamine (PAMAM) dendrimers [258]. These molecules are neutral macromolecular systems containing coordinating groups for metal catalysts. They are characterized by a spherical symmetry and their size can be controlled by tuning the generation number Gn [4] [161]. According to Crooks' group they act as nanofilters for cross-coupling substrates. They used these systems to encapsulate PdNPs in Heck reaction catalysis and showed 100% selectivity in the coupling between iodobenzene and *n*-butylacrilate at 90°C [258]. Whereby, G2 dendrimers showed better reactivity than G4 dendrimers, while stability behaved inversely. Though, the synthesis of dendrimers is sometimes inefficient, giving poor yields and some other problems. The group of Gao investigated the substitution of dendrimers with triazole-based hyper-branched polymers (HBPs) [259].

4.4 Biopolymers and natural supports

Recently, researchers have shown an increasing interest towards natural products, namely carriers. Their bio-compatibility and, most of times, biodegradability are particularly suitable for improving the "green" properties of industrial processes. Some are abundant natural polymers which often come from industrial scrap. Hence, industrial waste may be up-cycled, undergo treatments for standardization of catalytic processes and be employed as support. This is the case of some biopolymers such as cellulose, starch, lignin, chitosan, agarose, alginate etc.

Cellulose is the most abundant biopolymer on earth. It has been thoroughly studied and successfully exploited in the last years as a green alternative to common solid carriers. Among all advantages this biopolymer resulted particularly interesting due to several properties, namely hydrophobicity, biodegradability and compatibility, low cost and wide functionalization capacity [60]. It has been recently extensively used as a coating bio-layer for magnetically recoverable nanoparticle-based Pd catalysts (*vide infra*). Lignin was employed as magnetic ferrite nanoparticles coating, too [260]. Similarly, Sargin and co-workers improved the mechanical properties of chitosan by creating a composite structure of CS and multi-wall nanotubes (MWNT) [261].

A comprehensive review on green biopolymers was written this year by Wolfson and Levy-Ontman [262]. Natural inorganic materials were studied. It is the case of montmorillonite and sepiolite clays [5], diatomite [6], volcanic pumice etc.

Foroumadi et al. supported PdNPs on volcanic pumice magnetic micro-plates textured by cellulose.

---

[4] The generation number refers to the number of cycle necessary for dendrimers synthesis through branching

[5] Montmorillonite clays consist of phyllosilicate crystals precipitated from water in form of clay, while sepiolites are cheap clay minerals of ideal formula $Mg_8Si_{12}O_{30}(OH)_4{\cdot}4H_2O{\cdot}nH_2O$, with a structure characterized by talc-based ribbons

[6] Siliceous material obtained as a fossil residue of diatomae's family of algae

The pumice is characterized by ease of functionalization as well as biocompatibility and a mesoporous morphology. It appeared particularly suitable for greener magnetic-recycling cross-coupling applications [263]. The catalyst was efficiently recycled 10 times after working in DMSO.
One last and note-worth application is that of biomimetic supports. Beyzavi immobilized Pd nanoparticles on peptides constituted by a green fluorescent protein (GFPuv) body functionalized by a linear-chain Pd4 peptide, produced by transformed *E. Coli* recombinant plasmides. The Pd4 chain acted as a source of nucleation sites for PdNPs [264]. The recyclability test resulted in significantly lowered activity after the fifth cycle.

5 Heterogeneous catalysis

As seen before, the catalysts can be prepared at the same time of the support [265]. According to the moment of preparation one can distinguish among: bulk catalysts prepared through co-precipitation, sol-gel techniques or hydrothermal synthesis, supported catalysts on preformed supports and mixed-agglomerated catalysts. For instance, sol-gel techniques are used for the preparation of common Pd/SiO_2 catalyst while hydrothermal synthesis is utilized in zeolites or porous materials preparation (e.g. MCM-41).
Supported catalysts consist of a metal deposition subsequent to the carrier synthesis, exploiting impregnation techniques (i.e. simple impregnation and co-impregnation), vapor deposition (CVD), grafting etc [265]. Then, according to the type of interaction between metal and support one can distinguish between covalent bonding, encapsulation, entrapment and ion-bond formation [266].

5.1 Supported complexes

Several commercial heterogeneous Pd-phosphine catalysts exist, e.g. FibreCat by Johnson Matthey, PdEnCat^{TM} by Reaxa. For instance, FibreCat consists of poly(ethylene)-supported phosphines, and it was successfully used in Suzuki couplings by Sauer et al. [267].
Indeed, polymers are among the most studied carriers for Pd-phosphine complexes [268]. Polystyrene, functionalized with triarylphosphines was used in [269]. Later on, Miyaura and Inada functionalized polymer resins with triphenylphosphine for Suzuki-coupling applications [270]. The best results were achieved in three-phase systems including toluene and water as solvents.
Li and colleagues worked with SO, SN and thiols supported on both polymers and silica. After loading with Pd(II), the solid catalyzed the Heck olefination of iodobenzene [271]. Leaching was detected in some extent and a XPS analysis showed that palladium was still in the oxidized form after reaction, while sulfur was oxidized, probably by iodine, in solution. The catalytic activity was addressed to unknown Pd(0) complexes.
In [272] random copolymers containing Pd-alkyl(triaryl)phosphines monomers and trialkylammonium salt-based co-catalyst were prepared. The proximity of catalyst and co-catalyst was supposed to favor the Heck vinylation reaction tested. The catalyst was obtained through free radical polymerization of 3- and 4-vinylbenzyl-diphenylphosphine (VBBP) or 3,4-bis(diphenylphosphine)-1-butene (BDPB), in solution with excess vinylbenzyl tributyl ammonium chloride (VBAC). Palladium was then, complexated to phosphine-groups and supported onto the solid matrix. The results were significantly superior to classic homogeneous catalysts. The authors inferred that the substrate was likely to adsorb at the ammonium-sites giving best performances. Later on, the same group developed cross-linked polystyrene nanoparticles obtained through emulsion polymerization and coated with tetralkylammonium groups and Pd-phosphine complexes [273].
In 1999, Bergbreiter and co-workers worked on SCS palladacycles immobilized on thermomorphic polymers, the two main compounds are depicted in Figure 26 [274]. These catalysts showed good stability during high-temperature Heck reactions. Though, compound **29**, containing an ether linkage between the aromatic ring and the polymer, showed Pd black formation, whereas, the amide bond of compound **30** enhanced the stability of the catalyst.

Herrmann and colleagues studied N-heterocyclic carbene-Pd(II), compound **31** in Figure 26, as polymer-supported catalyst for the Heck reaction [17]. The precatalyst was supposed to be a more stable and valuable choice than phosphine-functionalized ones because of the higher bond energy of the C–Pd bond compared to the P–Pd. The catalyst appeared to be reactive even at extremely low Pd loading, however, the resulting *TOF*s were lower than in the homogeneous case. Furthermore, no activity towards aryl chlorides was detected despite the addition of TBAB, which was known for aiding homogeneous counterparts activating those reluctant substrates. Nonetheless, the Pd loading compared to the available sites was low, probably due to some hindrance in reaching the active sites [275].

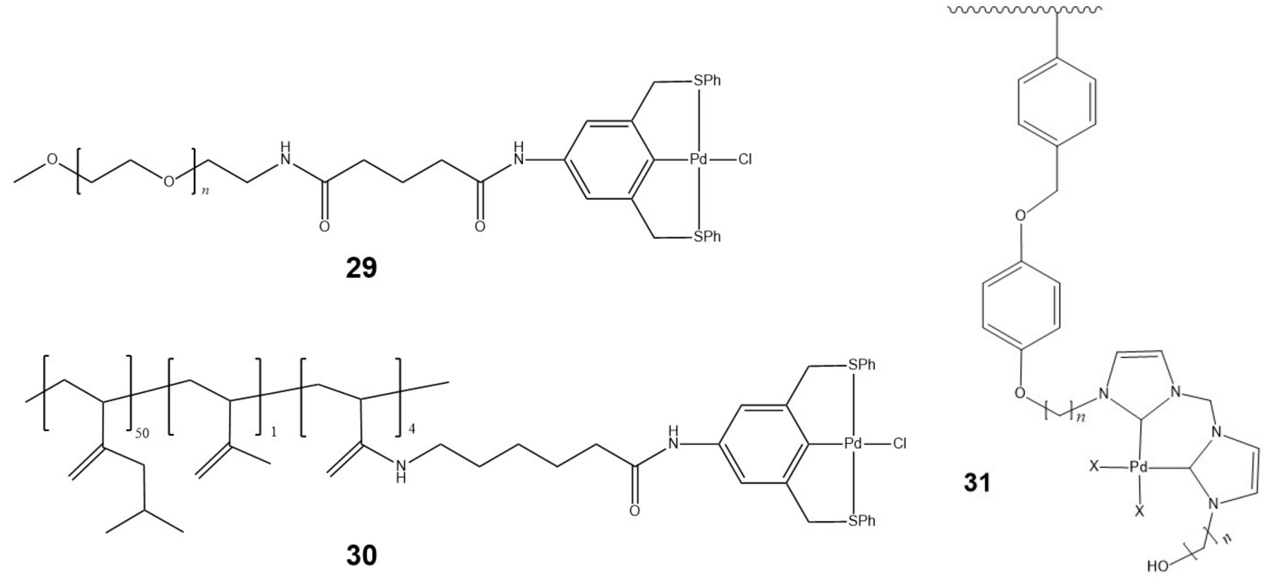

Figure 26: SCS palladacycle **29** and **30** synthesized by Sink et al. [16] and N-heterocyclic carbine-Pd **31** from [17].

Recently, NHC-Pd complexes loaded on Calixarene polymeric frameworks were used in the aqueous SMC reaction at 37°C [94]. Its structure, presenting defects coming from the reduction process, is suitable for PdNPs nucleation and growth. Those Pd nanoparticles were activated by complexation by N-containing ligands, namely *p*-phenylenediamine and benzidine. The SM reaction of bromobenzene reached excellent yields in 15 minutes under MW irradiation, with TOFs of 408000 [h^{-1}] and 373700 [h^{-1}] for the two catalysts, respectively Pd-PPD and Pd-BZD. These are among the highest results in heterogeneous catalysis ever reached. Furthermore, no conversion was measured after catalyst removal and low leaching was detected. The catalyst was reused up to 6 times.

Bedford immobilized PC and NC palladacycles on a commercial dicyclohexyl(phenyl)phosphine-functionalized poly(styrene), following the synthesis scheme depicted in Figure 27, and yielding compounds **32** and **33** [276]. The authors reported that 25-45% of phosphine-sites remained unexploited. Noteworthy, the immobilization changed significantly the reactivity of the palladacycles and the final solid precatalyst showed some Pd black formation, evident from the solution color turning from yellow to black. The authors inferred that the Pd(0) species produced before oxidative addition were likely to coalesce into clusters, because of the low stabilizing character of phosphine-ligands [25, 36].
In [19], Pd(II) species were supported on PEG-immobilized phosphines as catalyst for Suzuki couplings. The three studied compounds, **34**, **35** and **36** are represented in Figure 28, as well as the synthesis scheme of **34** and **35**. The results were showed to be highly dependent on the Pd:P ratio. Recycling was also good with no plummeting of TOFs after 5 consecutive runs.

Buchwald and Parrish worked with Merrifield resin-supported dialkylphosphinodiphenyl ligands, i.e. immobilized **5** and **6** (Figure 18), and used them to catalyze Suzuki couplings [92]. The synthesis reaction scheme is depicted in Figure 29, producing the two alternatives **i5** and **i6**. The catalyst was easily separated from the liquid phase thanks to the absence of by-products. Nonetheless, considerable amounts of Pd and phosphine leaching were detected during the $2\%_{wt}$ palladium-catalyzed Suzuki-coupling of aryl halides with arylboronic acid, while no solubilized-phosphine was detected when cesium carbonate was the base and $Pd_2(dba)_3$ the Pd precursor [20].

Styring et al. worked with a Merrifield resin-supported tetradentate ONNO-Pd(II) complex. The synthesis pathway, leading to compound **37**, is represented in Figure 30. A study around reaction conditions optimization was conducted. Different bases and temperatures were tested, resulting in best conversion for the couples 90°C/$Ba(OH)_2$ and 90°C/K_2CO_3.

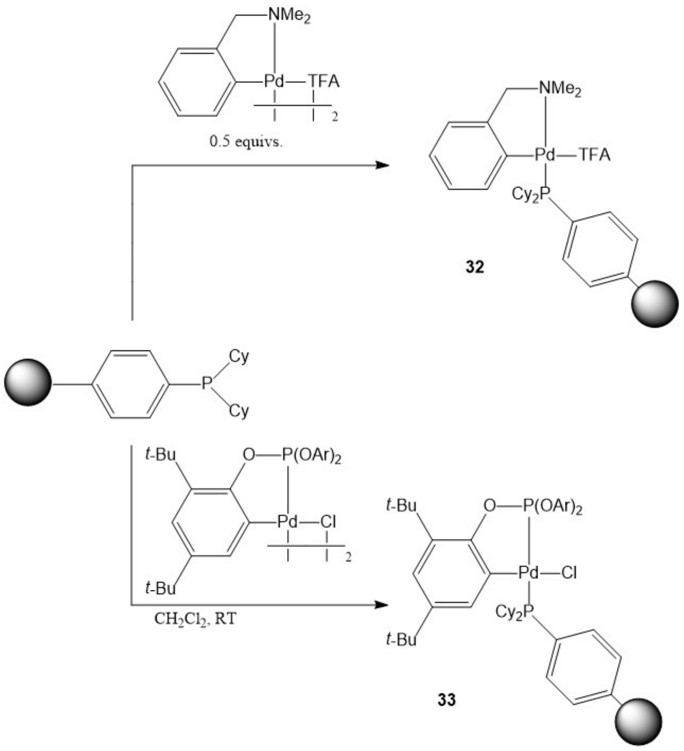

Figure 27: Immobilization reaction of PC and NC palladacycles on phosphine-functionalized poly(styrene). Adapted from [18].

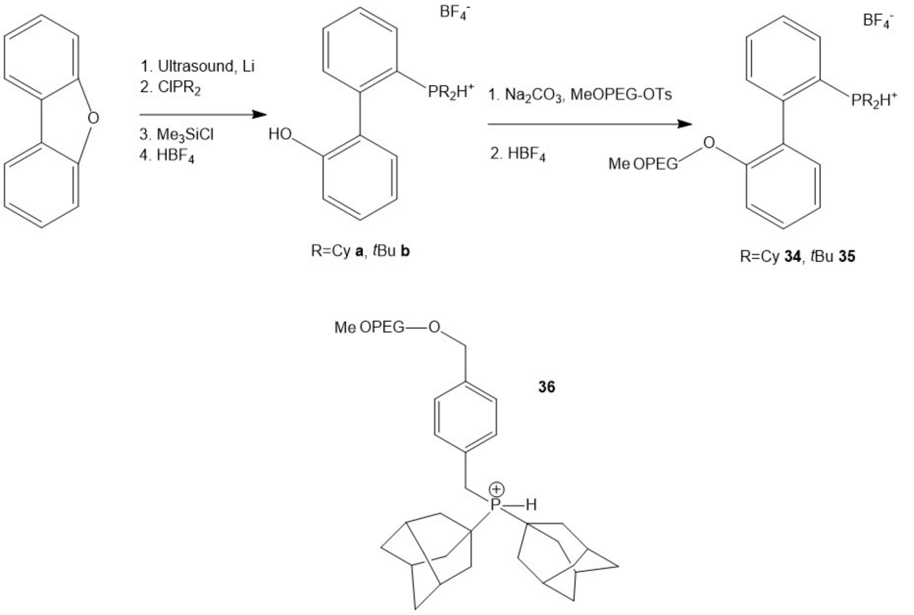

Figure 28: Compounds **34**, **35** and **36**, PEG-supported phosphine ligands studied by and der Heiden and Plenio in [19]. The synthesis reaction scheme is reported for compounds **34** and **35**.

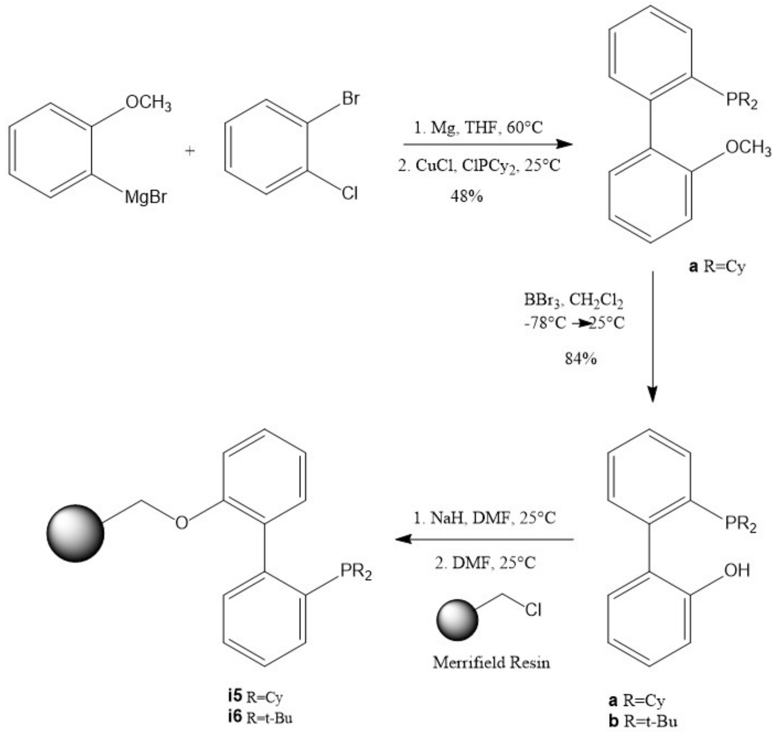

Figure 29: Synthesis scheme of Merrifield resins functionalized dialkylphosphinodiphenyl ligands, according to [20].

The catalyst showed better activity compared to homogeneous analogues, an evidence that was explained by better stabilizing properties of the couple carrier-catalyst compared to soluble species [21].

Some studies dealt with the encapsulation of palladium complexes into dendrimers. These supramolecular structures were supposed to protect Pd from aggregation, though, they were shown to slow down reaction kinetics due to high hindrance to substrate diffusion.
Kaneda et al. immobilized Pd-phosphine complexes within a protonated poly(propylene imine) dendrimer *via* ionic interactions between the positively charged polymer and the negative charges of acetate incorporated into the phosphines [277]. The authors inferred that the reaction was actually catalyzed by Pd-complexes within the dendrimer core. Other dendrimers functionalized with terminal triphenylphosphine moieties were used by Dahan and Portnoy in the Heck reaction [278]. In this case the presence of the homocoupling product was detected and explained by the involvement of solid-Pd species. Nowadays, it is the oxidation of Pd species on solid surfaces, to PdO species, under aerobic conditions, which is supposed to cause leaching of peroxo-complexes, likely to favor the parasitic reaction [61].
Later on, Janssen and co-workers functionalized "click" [7] dendrimers with different phosphines and used the precatalyst in Suzuki coupling of 4-bromotoluene with phenylboronic acid, at 60°C for 16h. A flow reactor was used and a nanofiltration membrane was put at the outlet for catalyst recovery [279]. No consideration about the TON of the reaction was provided.
Some further studies were conducted by Mapolie on iminopyridine-ligated Pd(II) on poly(propyleneimine) dendrimers, like in Figure 31 compound **38** [22]. The catalyst showed faster reaction compared to homogeneous $PdCl_2$ but also evidence of parasitic reactions such as styrene polymerization, during Heck coupling of styrene and iodobenzene. No Pd black formation was detected while this was the case for non-dendritic systems. Similar iminopyridine groups were immobilized on silica-based supports in [280]. Around the 20% of the nitrogen sites were effectively metallated.

---

[7] "Click" chemistry groups different reactions which are known to be efficient, produce only easy-removable by-products akin to easy-recoverable solvents and stereospecific

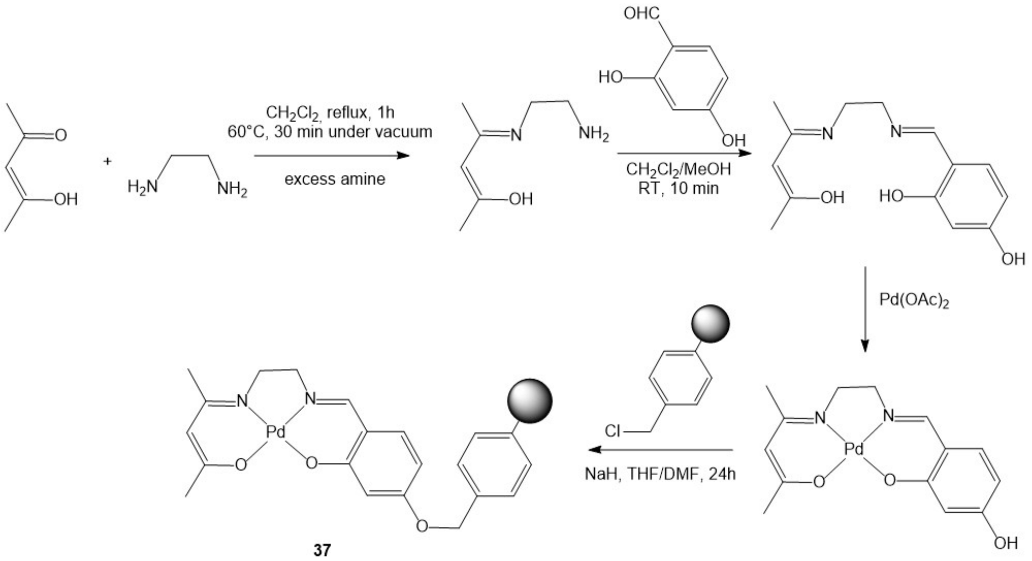

37

Figure 30: Resin-supported tetradentate ONNO-Pd(II) complex synthesis exploited by Styring et al. in [21].

Sugar-based matrices were also exploited for supporting Pd-ligated species. In particular, iminopyridine ligands, similar to compound **38**'s extremities, were used in [281] to functionalize chitosan and loaded with Pd(OAc)$_2$. The precatalyst was treated with ethanol, toluene and acetonitrile in order to remove any physisorbed Pd species. Only 35% of the nitrogen sites were occupied after Pd-loading. 25% of the sites maintained the Pd complexated after preconditioning. Nonetheless, it showed good activities towards Suzuki and Heck couplings but problems of long-term deactivation through clustering. A washing operation was performed in order to recover the activity of the catalyst after reaction at high temperatures around 140°C. Conversion turned from 57% to 86% whether washing after the first run of Heck reactions, was applied.
Besides, cellulose appeared as a green substitute of polymeric structures. Mohammadnia and Sun functionalized nano cellulose with [2,2-bipyridine]-4-amine for palladium-catalyzed Suzuki couplings [60]. The catalyst gave good yields and was recycled up to 4 times without loss of activity.
In 2020, Boztepe et al. supported PEPPSI-NHC-Pd complexes on hydrogels [253]. Neither EWGs or EDGs substituted to bromobenzene (i.e. model halide) worsened the Suzuki and Heck reaction efficiency. The authors supposed the catalyst to be heterogeneous and no precipitation of Pd black was detected.
Pore and co-workers investigated the activity of Pd(II)-AMP-Cell@Al$_2$O$_3$ systems were alumina-cellulose composite nanoparticles were functionalized with 2-aminopyridine (AMP) and coordinated to Pd. The precatalyst showed high thermal stability up to 263°C. Moreover, a wide scope of halides efficiently reacted under SMC conditions, in DMF at 80°C [153]. K$_2$CO$_3$ was selected as the best base for SM couplings while triethylamine (TEA) performed better under Heck conditions and the catalyst could be reused five times with no significant activity drop and resulted in low percentage of leaching [153].

Nowadays, carbonaceous nanostructures are widely employed, too. The concentration in oxidized carbon sites (i.e. hydroxy, carbonyl and carboxyl groups) of graphene oxide (GO) and reduced graphene oxide (RGO) allows the easy functionalization with molecular Pd complexes.
Heravi and co-workers investigated Pd-NHC deposited onto GO (GO-PEG-Imidazole) as catalysts for Suzuki couplings. The catalyst was extremely efficient towards phenyl bromide, even at extremely low amounts [225]. Liang and co-workers studied bulky imine-Pd complexes supported on graphene oxide (GO) as catalyst for SM couplings, at 60°C in the presence of K$_2$CO$_3$ within a mixture EtOH:water 1:1. The catalyst was compared to other previously reported catalysts, with slightly better efficiency. No leaching was detected by ICP-AES after six reuses, and the resulting TOF was calculated (10778

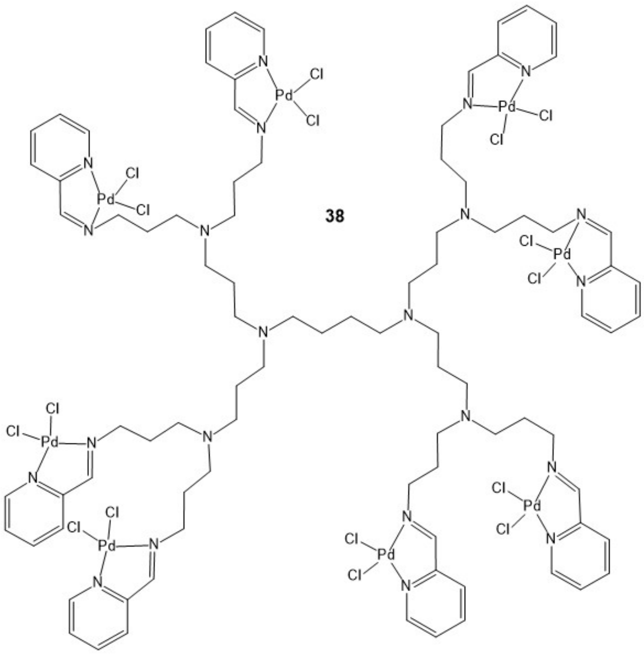

Figure 31: "Second-generation" poly(propyleneimine)-supported Pd-iminopyridine metallodendrimer **38** synthesized by Wu and co-workers [22].

$[h^{-1}]$) [282]. Then, El-Shall and colleagues worked on the deposition of Pd complexes onto reduced graphene oxide (RGO) [283].

As for other carriers, MOF- and inorganic oxide-based systems were employed. Silica-supported mercapto-hydroxyl-containing macromolecular bidentate Pd chelates were investigated by Liu and Wang during Heck reaction [16]. The synthesis was performed in sealed autoclave during 26h according to the scheme presented in Figure 32. The optimum S:Pd ratio was found to be between 3 and 6.

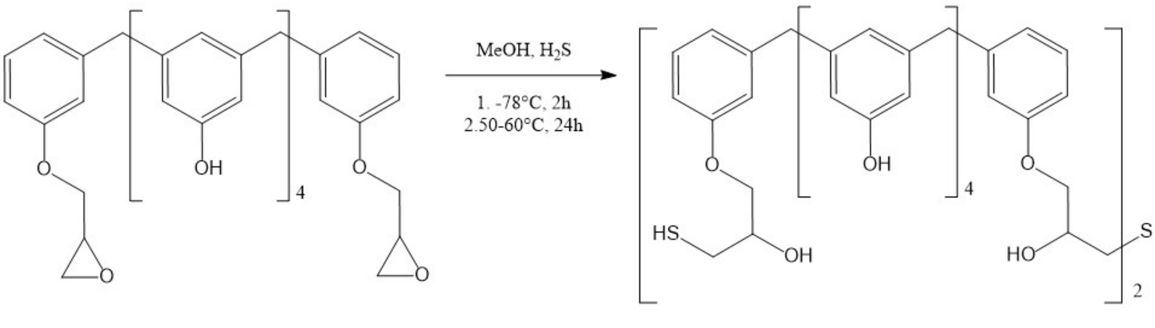

Figure 32: Synthesis scheme of silica-supported mercapto-hydroxyl-containing macromolecular bidentate Pd chelates [23].

Some studies dealt with the synergistic effect of Pd/MgO coupled to PPh_3 ligand. The addition promoted the conversion. Moreover, the authors noted that the catalyst behaved like "homeopathic" $Pd(OAc)_2$ [246]. Some leaching was detected, albeit this was not the main source of deactivation. Hydrocarbon deposition onto the precatalyst surface prevented it from being recycled with good conversion.

Later on, Ying's group used Pd/Nb-MCM-41 for the Heck reaction. The material was composed of a mesoporous MCM-41 matrix onto which the active Pd is attached, in a way that a discrete and uniform distribution of active sites is formed. The authors advocated that the vapor phase deposition of the sublimated under-vaccum Pd-precursor $[Pd(\eta\text{-}C_5H_5)(\eta^3C_3H_5)]$ gave good results in terms of dispersion of Pd, on the mesoporous surface and inner-porosity walls. Furthermore, this technique ensured the

maintaining of high surface area and accessibility of the pores by preventing cluster growth [284, 285]. The catalyst appeared to reach good conversions in Heck couplings [286].
Panahi et al. functionalized the metal organic framework MIL-101(Cr) with Pd-NHC complexes and tested the precatalyst on Suzuki-Miyaura coupling of several halides, in aqueous medium containing K_2CO_3 as the base at 85°C [287]. The high porosity of the MOF's structure allowed an efficient diffusion of substrates towards the metal active sites, activated by the NHC ligands. Low amounts of Pd leached in the liquid medium resulting in low conversion after removal of the solid matrix. The authors concluded that the catalyst was mainly heterogeneous.

5.2 Supported "naked" palladium and single-atom supported transition metals

All along this section we will mean supported "naked" palladium mainly as ion-exchanged bulk heterogeneous catalysts, where Pd is incorporated in a crystalline lattice. Otherwise, Pd salts used in the absence of ligands and PdNPs formation through reduction, have been considered as precursors of supported "naked" palladium, in few examples. Unfortunately, instability of Pd towards aggregation and *in situ* reduction of Pd(II) species, thanks to the action of molecules carried within the liquid phase, would eventually produce nanoparticles. A solution to this borderline application will be provided. One recent technology for atom-by-atom deposition and manufacturing of supported single-atom Pd catalysts is reported at the end of the section.

Early in the study of cross-coupling reactions, putative heterogeneous precatalysts were studied: Pd/C by Julia and co-workers, which was believed capable of activating aryl chlorides [288, 289], Pd supported on porous glass under Heck conditions [290] and Pd encapsulated between layers of graphite which was apparently unable to catalyze the Heck coupling of aryl chlorides [291]. One main problem about these former studies was the role of Pd black, produced through Pd aggregation, since some groups hypothesized it to be catalytically active towards cross-couplings [292, 293]. Later on, Mizoroki showed that the reaction rate was not correlated to the amount of Pd black added to the reaction medium.
Augustine et al. concentrated on the surface of heterogeneous catalysts and described the active sites as "coordinatively unsaturated corner atoms and adatoms [8] on the Pd surface" [242, 294]. The authors described the variety of active sites present on the surface of a crystal in order to distinguish from the "one-active-species" nature of homogeneous catalysts. A fcc crystalline cell was taken as an example. In this case {111} and {100} are the only orientations of face atoms, while four in the case of edge atoms and seven for corner atoms. Hence, surface adatoms have {111} and {100} orientations. The reactivity of each site depends on the concentration and geometry of the atomic neighborhood. Starting from all these considerations, they pointed out that the Pd black produced from $Pd(OAc)_2$ aggregation was likely to be the true catalytic species rather, because of the results of the mercury-drop test, later explained in Section 8.2. Though, they based the conclusion on the assumption that Hg(0) is only able to poison heterogeneous sites. Since they measured no activity after the test, they were brought to believe some form of Pd black to be the true active species [242].
The synthesis of anysotropic nanostructures recently found large application, especially in electrochemical processes [295]. Patil and Samal synthesized CTAB-protected nanocubes for cross-coupling applications. The growth of nanocrystallites was controlled and happened mainly in the {100} direction. This significantly promoted the SM coupling product yield, resulting in wide reaction scope.

Okumara's group studied the effect of different Pd deposition/exchange processes on zeolites, mordenite, Y and ZSM-5. Ion-exchanging of zeolites gave different results, with the proton-form showing more Pd stabilization and retention of nanoclusters [296].
In [146] ion-exchanged zeolites Y are shown to better perform when oxidized Pd(II) is present, rather than in the presence of reduced palladium. Nonetheless, both catalysts gave leaching of Pd in solution, resulting in Pd species aggregation and giving birth to a leaching/re-deposition cycle.

---

[8] An adatom is the opposite of a crystal surface vacancy: it consists of a single atom lying on the surface of a crystallite

Pd-exchange montmorillonite clays were studied in [297], for the Heck reaction of aryl halides with styrene and acrylates. The clay was prepared by exchanging in a diluted solution of $PdCl_2$, at room temperature (RT) for 24h. The catalyst was recycled up to three times without loss of activity. Shimizu also worked on Pd(II)-exchanged sepiolites during the Suzuki coupling of aryl bromides and phenylboronic acid [298]. The clay was exchanged at 25°C for 48h in a diluted solution of $[Pd(NH_3)_4]Cl_2$. Similar procedures were exploited for the exchange of NaY-zeolites. TEM analyses at the end of the reaction-cycles highlighted the oxydation of some Pd(II) into Pd(0) nanoclusters.

García used alkali-exchanged sepiolites as catalyst for base-free Heck and Suzuki couplings, obtaining interesting results and a clear, inert, hot filtrate, when utilizing *o*-xylene as a solvent [299].

Pd(II)-exchanged perovskites, minerals of ideal formula $LaFe_{0.57}Co_{0.38}Pd_{0.05}O_3$, synthesized by Ley, leached some active Pd in the Suzuki coupling of bromoarenes and arylboronic acids [300]. Similarly, Yokoama and co-workers used Pd(II)-exchanged oxide supports coupled with ionic liquids [141]. Great amounts of palladium dissolved in the ionic liquid phase, too.

On the whole, discordant opinions were given about the nature of true catalytic species, in the case of ion-exchanged precatalysts. Buchecker and co-workers supported "pure" heterogeneous catalysis [301], while Köhler and some other groups completely ruled out this hypothesis [302, 303]. Nowadays the concept of "cocktail" catalysis is embraced by researchers and explains some of the aforementioned discordant theories. It will be better explained in Section 5.5

Recently, López and co-workers studied the Suzuki coupling of bromobenzene and phenylboronic acid as a model, for further scope broadening, at 80°C under aerobic conditions, in dodecane:EtOH with K_2CO_3 as the base [248]. The investigated precatalysts contained sulfur, covering the role of Pd scavenger. The amount of sulfur was tuned in order to study its impact on the activity. The authors hypothesized that the actual reaction was carried out in solution by competent leached species and explained the lack of activity of the highly S-charged Pd-SH-E-PMO and Pd-SH-E-PMO(H_2), with the scavenger properties of sulfur, which hinders leaching, and thus, conversion [248]. A treatment with hydrogen appeared to enhance activity, possibly due to the formation of surfacial defects which favor leaching.

$PdCl_2$ was deposited on MOF structures by Zheng et al. [304]. The heterogeneous catalyst worked well for several organoboronic acids, even when sterically hindered by *ortho*-substitution. It was efficiently recycled up to five times with negligible loss of Pd in solution, but during the fifth cycle a brownish medium was recovered because of Pd black deposition.

Other studies by Costano et al. investigated the activity of Pd supported onto GO monoliths in flow-synthesis. The solid monolithic matrix avoided channeling phenomena and pressure drops [305]. Use of PdTA as precursor showed higher activity and longevity compared to $PdCl_2$. Though, after a certain time disruption of the structure by collapsing was detected and the efficiency plummeted. This was explained by the presence of structural defects produced by MW irradiation. Besides, leaching was lowered from GO sheets to the monolith.

Recently, Zhang et al. investigated the activity of Pd-ZnO-ZrO_2 for ligand-free SMC reactions at room temperature. In alcohol:water mixtures with carbonates as bases, the catalyst reached a TON of 62500 for the reaction of bromobenzene and *p*-tolylboronic acid. The catalyst was directly reused five times before activity losses, and the structure appeared unchanged [306].

Finally, Shin et al. succeeded in supporting single atoms of Pd, from $PdCl_2$ precursor, on metal organic polyhedra (MOPs) [37].Metal single-atom catalysts (SACs) supported on solid matrices has been employed and studied with outstanding results. The application allows near-to monodispersion of active sites and their complete usability. Thus, ligand-free couplings can be carried out with such catalysts. In general, single-atom palladium coordinates into inorganic oxides lattice thanks to the coordinating power of oxygen sites. This coordination by neighboring sites allows to tune Pd catalytic properties. Though, up-scaling of their fabrication is still a challenge due to the low production efficiency.

5.3 Supported nanoparticles (NPs)

Shape and size of PdNPs was shown to be important for catalytic activity in the catalyzed Suzuki-Miyaura coupling of phenylboronic acid and iodobenzene [307]. The phenomenon was explained by the concentration in low-coordinated vertex and edge atoms compared to the face, which was supposed to change and enhance the activity of such sites, and was taken as a proof of heterogeneous catalytic activity.

Nowadays it is clear that this type of catalytic sites are more prone to leaching, due to their lower coordination numbers, and to trigger catalytic cycles in solution. A comprehensive DFT study by Polynski and Ananikov will be introduced in Section 5.5, and explains this evidence.

In the studies of Holmes, McGlaken and colleagues, different crystalline structures of PdNPs were studied: cubic, cuboctahedral and octahedral [158]. The size of the particles was around 20 nm. Hence, the best conversions were reached with cubic systems, while octahedral particles showed induction periods of 5 h. The authors advocated that the shape of the particles was more important than the size. Cubic nanoparticles appeared subjected to shrinking giving leaching species, from well-defined sites, namely more from {100} facets than {111} ones. Moreover, leaching was found to be triggered and favored by the presence of molecular oxygen, because of the oxidation of Pd to more soluble PdO. In some other cases smaller PdNPs were found to be less active because of stronger adsorption of substrates onto the nanoparticle surface. For instance, biphenyl moieties produced by Suzuki couplings are particularly likely to poison NP's surface because of their affinity for metal surfaces [30].

Measurement of particle-size distribution (PSD) before and after reaction is often very useful to understand the causes of catalytic-activity changes. Immobilization of PdNPs reduces the importance of particle migration (PM) and coalescence and should enhance the catalyst reusability. Though, during the reaction, processes such as Ostwald ripening (OR) may occur and modify the shape of the PSD as well as the reactivity of the nanoparticles. Thorough studies of these curves may give lots of hints on the importance and nature of the aggregation process.

Beller utilized preformed PdNPs to catalyze the Heck reaction. The harsh conditions, i.e. high temperatures, typical of Heck couplings made colloids being unstable and causing Pd black formation by coalescence.

In 1996, some studies about colloid stabilization by TBAB or poly(vynilpyrrolidone) (PVP) capping, were conducted [308]. The authors also inferred that catalysis occurred at the surface of the NPs. For instance, in [309], a study by the same group, no Pd black was detected when coupling Pd nanoclusters with stabilizing tetraphenylphosphonium salts.

El-Sayed and co-workers studied the aforementioned means of stabilization of PdNPs during the Suzuki reaction [307]. Stabilization with capping agents appeared to disfavor both OR and reactivity. In a successive study El-Sayed et al. hypothesized the dissolution of shrinked adatoms during cross-couplings. The movement of such atomic species through a liquid medium may mean for them to be captured by other species, e.g. solvent molecules or carrier-functionalizing scavengers [310].

Hu and Liu proposed a reaction mechanism for polymer-supported Pd nanoparticle composites as precatalysts for Suzuki couplings of aryl bromides and iodides with phenylboronic acid [24, 311]. The mechanism takes into account the importance of NPs' polydispersion, measured during the reaction and the lack of of homocoupling. The authors inferred that the responsible species for catalytic activity were leached Pd(II) species. The mechanism is depicted in Figure 33. It is similar to those described by DuPont [169] (Section 8.2) for PdNPs in ionic liquids and by de Vries [25] for "naked" palladium (Section 5.4).

In 2007, Astruc and co-workers designed some "click" ferrocenyldendrimers which were able to stabilize Pd(II) cationic species [312]. The authors calculated the coordination number of Pd species for G1 and G2 dendrimers. 27 ferrocenyltriazole termini surrounded NPs of 1.3±0.2 nm diameter, and 81 for 1.6±0.3 nm respectively. The use of G0 dendrimer resulted in larger nanoparticles due to the fact that they were encapsulated between several dendrimers rather than being complexated by one.

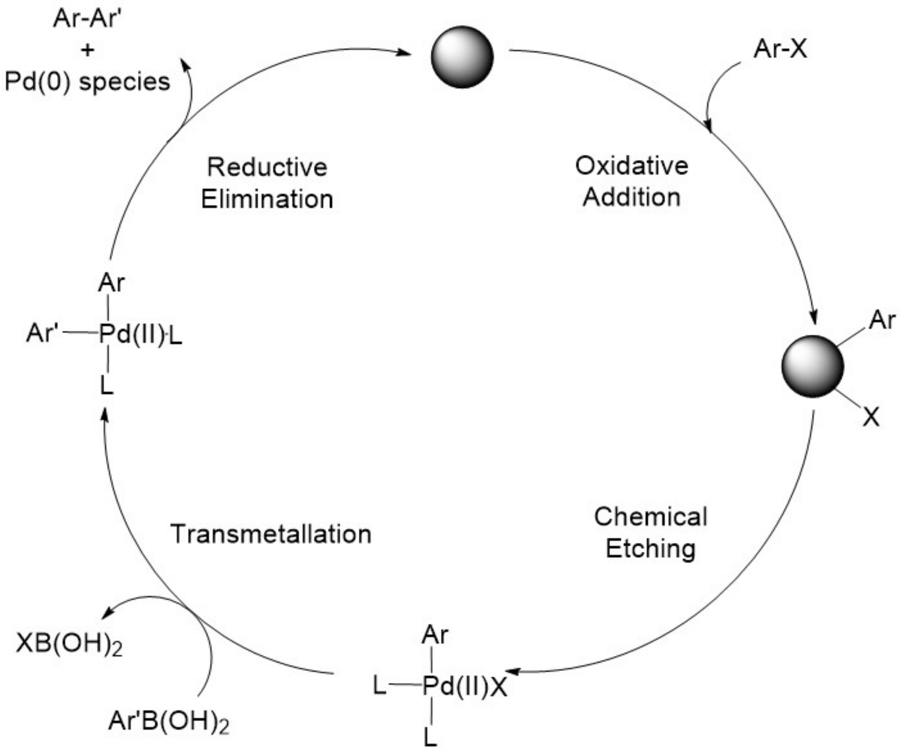

Figure 33: Suzuki reaction mechanism proposed by Christiansen and involving polymer-supported palladium nanoparticles as precatalysts [24]

In [313] another generation of dendrimers containing both triazoly- and triethylene glycol (TEG)-termini were tested in aqueous cross-coupling media. They were able to stabilize both molecular species [314] and nanoparticles [315]. This new generation of catalysts efficiently catalyzed Suzuki couplings of inactivated bromoarenes and phenylboronic acid at 80°C. It was also observed that these bio-compatible capping dendrimers were likely to interpenetrate thanks to the TEG-termini. Unfortunately, these new moieties showed reduced stability at high temperatures compared to common capping agents, but were used at really lower concentrations.

Choudary and co-workers anchored palladium onto layered double hydroxides (LDH), catalyzing Suzuki couplings of aryl chlorides in dioxane:water at 100°C and KF as the base. The yields were good albeit reaction rates significantly slow, with $TOFs$ around 6-9 [h^{-1}] [316]. Good yields were also obtained in the Sonogashira reaction of aryl chlorides in THF:water at 80°C, but with low resulting $TOFs$ of 1-3 [h^{-1}] [317]. Interestingly the catalyst was declared truly heterogeneous after detecting, with XPS, Pd(II) species bounded to fluoride, halide and hydroxide, onto the surface. Though, it is unclear if these species came from a re-deposition process or if they were adsorbed *in situ* on defects of NPs.

Sastry et al. worked on aminopropyl-functionalized NaY zeolites as support for PdNPs during Heck couplings [318]. The nanoparticles were supposed to remain bonded to the surface of the precatalysts without significant changes in dimension, but explanations are still dubious because of the lack of some information. Eventually, based on a negative hot filtration test and on the evidence that no NP-size change occurred during the reaction, the authors supported the theory for which zeolites were efficient catalysts for Heck coupling and PdNPs stabilizers.

One well-performing catalyst was proposed in 2007 by Diaconescu et al. [319]. It consisted of PdNPs immobilized on nanosized polyaniline (PANI) fibers. Suzuki couplings of several aryl chlorides were performed in water, under air atmosphere, with NaOH as the base, at 80-100°C for 2-6 h. The catalyst gave high $TOFs$ of 300-500 [h^{-1}] for all the chlorides tested. Outstandingly, it was found to be also an aryl fluorides activator, without the phenylboronic acid partner. Though, the size of the particles

on the surface of the nanofibers appeared to be significantly polydispersed.
In 2008, a ligand-free system consisting of PdNPs anchored on PEG-400 was studied by Liu et al. Both electron-rich and -poor chloroarenes were efficiently converted into coupling products. The reactions were performed at low temperature (RT or 45°C) with resulting best $TOFs$ of 200 [h^{-1}]. Moreover, nanoparticles generated *in situ* showed higher activity than preformed ones [320, 321].
In 2010, Li, Jiang and co-workers studied Pd nanoparticles supported on the metal organic framework MIL-101. This catalyst showed prevalent presence of reduced Pd(0). Contrarily to the study of Liu et al. [321], it appeared to be more reactive under inert atmosphere, while it was able to activate chloroarenes towards SMC reactions [322].

Innovative structures, namely metalloenzyme-like (MEPI-Pd) catalysts, were studied in 2012 by Uozumi et al. [28]. They consisted of deposited PdNPs onto a [(N-vynilimidazole)-*co*-(N-isopropylacrylamide)] copolymer. The catalyst showed excellent results towards Suzuki couplings. Though, it is also insoluble in the majority of common solvents. The reaction was performed in water at 100°C in the presence of the phase transfer agent tetrabutylammonium fluoride (TBAF) and K_2CO_3 as the base. Very low loadings of Pd were showed to be highly reactive towards a wide spectra of substrates. Interestingly, the production of 4-methylbiphenyil gave around 100% yield and TON and TOF of 3.5710^6 and 1.1910^5 respectively, among the highest value of TOF for heterogeneous catalysts.
In 2014, Schüth's group worked on PdNPs supported on solid polyphenylene with excellent results in Suzuki-Miyaura cross-couplings of inactivated and sterically hindered substrates [323]. The support itself was produced by a Suzuki coupling. No Pd(II) on the surface of the carrier and few ppm of leached species were detected.
Taniike and co-workers developed, in 2018, a method to encapsulate PdNPs into graphene oxide frameworks (Pd@GOF) [235]. The authors compared the new precatalyst to simple Pd@GO and Pd/C, in three different solvents (i.e. EtOH, DMF, Toluene). They obtained better yields with Pd@GOF but similar $TOFs$ (of the order of few [h^{-1}]) to the others. The best performances were reached in toluene. Though, the authors stated that the retention power of new Pd@GOF was higher than the other carbon-like supported palladium precatalysts.
Recently, Pd nanoparticles protected by cyclodextrin supramolecular structures were deposited onto ceria [243]. Palladium atoms may coordinate within the CeO_2 by forming a square-planar morphology with oxygen anions and expanding the lattice. However, high-temperature processes led to deactivation through loss of Pd active sites and incorporation in the lattice. The authors underlined that the precatalyst appeared to play the role of reservoir of homogeneous active species.
Li's group investigated a scavenger-based system consisting of mercapto-propyl functionalized amorphous silica-supported PdNPs. Thiol groups were used in order to sequestrate Pd in solution, reducing loss and metal loading needed. Little nanoparticles ($\sim 2-5nm$) were detected on the surface together together with discrete single atoms. After subsequent runs of cross-couplings, losses were lower than 3 ppb and no NP-aggregation were detected [135].
Otherwise, electrospinning manufacturing of chitosan (CS) and sodium polyacrylate (PAAS) nanofibers, functionalized with palladium for *in situ* formation of PdNPs, gave more then good activities, it gave outstanding recyclability power [324]. The catalyst was recovered up to 18 times without significant loss of activity. High diffusion into the fiber's channels and nanoparticle's stabilization were ensured. Similarly, Pd(II)/CS nanofibers were exploited for Sonogashira coupling catalysis [325].
PdNPs were also deposited onto RGO and hybrid chitosan-RGO materials with good activities and recyclabilities [326, 327, 328].

One note-worth technology which is still studied nowadays is the synthesis of core-shell Pd@Au nanoparticles, firstly investigated by Jutand and Amatore [156]. Palladium was deposited in several layers around an Au core. The catalyst was employed in aqueous Suzuki couplings. It performed well in the coupling of 4-bromoanisole and phenylboronic acid at RT within 4h. No induction period was detected for 2-to-5 monolayers, but leaching unequivocally occurred. Different precatalyst shape were investigated. The cubic precursors showed higher activities towards phenyl iodide coupled to phenylboronic acid, in 4:1 water/EtOH, at 80°C, with $K_3PO_4 \cdot H_2O$. No significant structure change was reported.

In 2011, Wiley et al. worked on flower-shaped Pd@Au core-shell nanostructures of size ∼40 nm [329]. This precatalyst, named Au_cPd_s, catalyzed the Suzuki coupling of iodobenzene and phenylboronic acid. Leaching was detected and the authors assigned all the activity to soluble Pd species.

Sun, Wang and Yan reported similar core-shell structures synthesized through heteroepitaxial growth of Pd shells on high-index-faceted tetrahexahedral (THH) and trisoctahedral (TOH) Au cores [330]. These structures achieved good conversions in the Suzuki coupling of phenyl iodide and phenylboronic acid.

These new nanostructures appeared suitable for another important application: photoactivation.

Movahed and co-workers studied the activity of photocatalytically activated Mott-Schottky-type Pd@Au nanoparticles supported onto graphitic carbon nitride [331]. Some SMC reactions were conducted in $EtOH:H_2O$ 1:1 mixture in the presence of K_3PO_4 as the base under MW irradiation in 25°C water bath. Protic solvents worked better than aprotic due to their oxydation potential.

Sun et al. studied a system based on Pd@Au core-shell nanorods for laser-promoted Suzuki couplings [332]. On the hemispherical extremities of the rods, Pd nanoparticles were deposited, too. The reaction between bromobenzene and *m*-tolylboronic acid was performed in water, in the presence of NaOH and CTAB and activated by an 809 nm laser at 1.68 W. No activity was measured in the absence of photo-activation. The catalyst reached around 100% yield in 1 h with a TOF of 160 $[h^{-1}]$ with respect to the whole metal content, while it amounted to 1000 $[h^{-1}]$ whether only palladium was counted. Interestingly, nanorods-supported Pd nanocrystals did not reach the same excellent yield, and Pd nanocrystals alone, did not show any activity, at all.

Then, the same nanostructures were used in solar light-activated benchmark reactions. Again, excellent yields were reached. Pd leaching was also investigated resulting in high amounts of active metal dissolved in the reaction media, albeit independently on the laser power.

Zhou's group investigated Pd@Au core-shell nanosystems supported on zirconia (ZrO_2) and compared the reactivity results with Pd/ZrO_2 and Au/ZrO_2 [333, 334]. The authors showed the activity- enhancing power of visible light on the catalytic system, towards Suzuki couplings. For instance, the coupling between iodobenzene and 4-methoxyphenylboronic acid, at 30°C for 2 h in 3:1 DMF:water reached 99% yield under light and only 58% in the dark. The catalytic activity appeared to be linearly dependent on light intensity. The range of wavelength that showed the best results was 490–600 nm, comprising the 530 nm wavelength corresponding to the localized surface plasmon resonance of the system Au/ZrO_2. This explained how the synergistic effect of the contemporary presence of plasmonic and catalytic systems was effective in this kind of systems. The authors hypothesized a truly heterogeneous catalysis mechanism, even though without any direct proof, suggesting that interactions between Pd and the halide substrates took place on the surface due to the high superficial charge heterogeneity combined with the presence of energetic conduction electrons at the reactive Pd sites, under irradiation.

Different photocatalytically activated Pd precatalysts were reported by Chen and Wang. The system consisted of PdNPs deposited on 8-hydroxyquinoline-based polymers [61]. The recyclability of the catalyst was excellent, with little activity loss after 10 runs.

Photoactivation allows a change in the reaction pathway giving peculiar selectivities and conversion. Weiss' group reported the activation of inactivated Csp^3 alkyl halides [335]. This happens through reaction of radical complex intermediates. The mechanism involves one photoexcitation of the starting Pd(0) complex to a Pd(I) radical form. This is caused by an electron transfer to the alkyl halide which is then coordinated to palladium and promotes its relaxation to Pd(II), in order to subsequently follow an ordinary Heck mechanism [335]. The addition of a photosensitizer helps to promote, in some cases, the selectivity of the reaction by preventing undesired β-hydride eliminations.

5.4 Few parameters influencing heterogeneous catalysts

Metal loading and Pd precursor The nature of the support and Pd precursor, the deposition method and the Pd loading, are known factors impacting the efficiency of Pd-catalyzed couplings. Though, few studies about those parameters were reported. The one of metal catalyst loading is,

maybe the most studied influence on cross-coupling catalysis.
In 2003, de Vries' group was studying the impact of Pd loading on conversion and proved that increasing in this parameter led to less efficient catalysis, as already noticed by other researchers [187]. Hence, they suggested that the active monomeric species were in equilibrium with inactive Pd nanoclusters and that higher amounts of loaded Pd resulted in faster inactivation [25]. The scheme depicted in Figure 34 explains the correlation between active and inactive species, showing that Pd black is actually the most likely product of palladium deactivation.

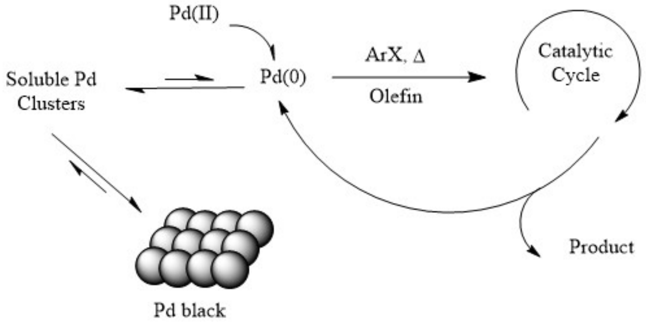

Figure 34: Mechanism of production and coexistence of active and inactive catalytic Pd species in solution. Adapted from [25].

Hence, de Vries finally proposed a general Pd(0)-Pd(II)-like Heck reaction mechanism in 2006, involving both colloids and molecular anionic species which could be stabilized by cationic ILs [26]. This inverse proportional correlation between Pd loading and conversion, as well as mass spectroscopy [35] and EXAFS analyses [336] supported, according to de Vries, the involvement of anionic Pd species in C–C couplings [26]. The scheme is depicted in Figure 35 and involves the inactivation equilibrium proposed in 2003.

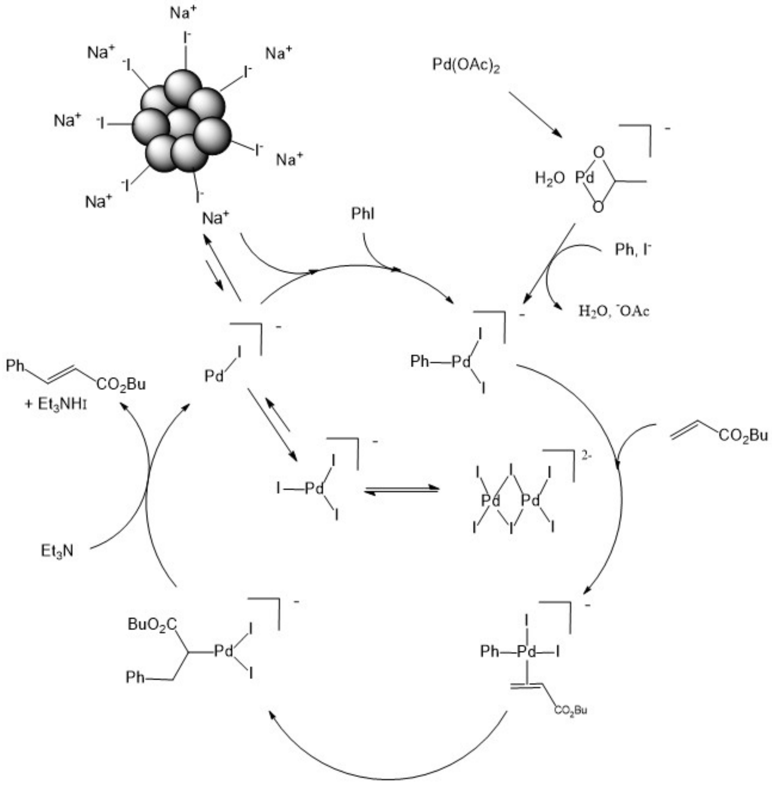

Figure 35: Heck reaction mechanism proposed by de Vries in 2006. Adapted from [26].

Recently, Grivani and Nehzat found that an increasing amount of catalyst from 0.1mol% and 0.5mol%, increased the yield of *p*-phenyltoluene at 65°C in MeOH [13]. Thus, the role of the Pd loading is still dubious. Low loading appeared sometimes to be as reactive as higher ones [37, 154, 159, 247, 255]. Other studies reported that increase in Pd loading meant better yields [204, 331].

Phase transfer agents Phase transfer agents are molecules aiding the motion of substrates from one phase to another, where the reaction is supposed to take place. Tetraalkylammonium salts are the most known and employed, often under IL form. In our particular case, of Pd-catalyzed reactions, they are commonly studied as Pd(0)-species stabilizers, preventing their aggregation and favoring both oxidative addition and reductive elimination, even if a non-optimal use could make the work-up of the process more complex [13]. ILs are considered perfect solvents and capping agents for *in situ* formation of PdNPs, which slow down OR and enable to control nanoparticle growth [155].
Noteworthy, the group of Umadevi studied tetralkylammonium salts' efficiency towards formation and activity of PdNPs in w/o H_2O/CTAB in *n*-butanol/isooctane microemulsions, for Heck reactions [155]. In addition, tetralkylammonium salts are known in the literature to increase the polarity of commonly used solvents. Since their role of phase transfer agents is expressed in reactions involving anionic species, the evidence seemed to support de Vries' hypothesis about anionic species involvement in coupling reaction mechanisms [35]. All these observations were proposed by Herrmann et al. to explain enhanced catalytic activity and thermal stability due to tetralkylammonium introduction [137].
Solvation processes causes the covering of nanoparticle's surface with charged layers of ions or polarized species and give birth to an electric double layer, which electronically stabilizes the particle. The inner shell, known as Stern layer, has been found to be made of cations, for which the stabilizing character increases proportionally to the size of the ions [161]. However, electronic stabilization is not the only possible way. Steric stabilization has been exploited, and is part of the stabilization power of many ammonium salts. Some capping agents, from literature, are depicted in Figure 36, showing both electronic and steric protection character.

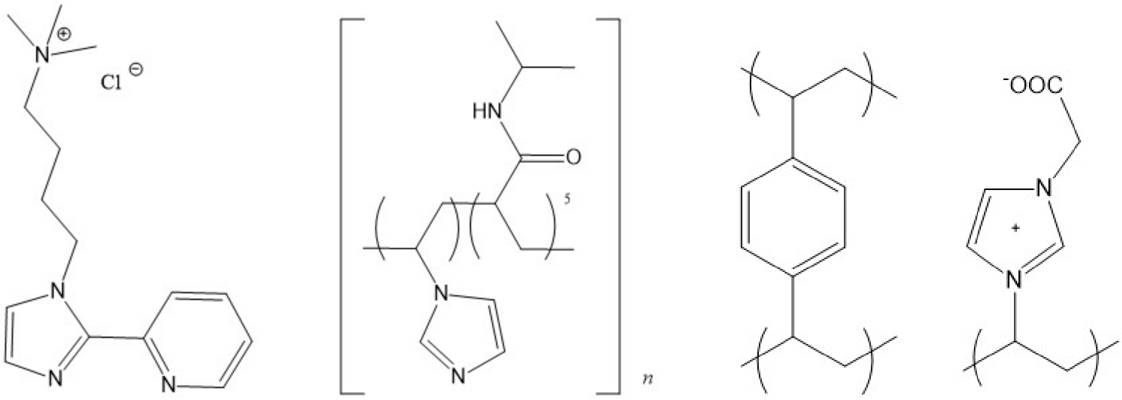

1 **2** **3**

Figure 36: Some capping agents employed in literature to substitute the commonly used tetra-*n*-butylammonium bromide (TBAB). **1**: Imidazolium ammonium chloride synthesized by Zhou et al. [27] **2**: Enzyme-like polymeric imidazole synthesized by Yamada et al. [28] **3**: Porous ionic copolymer synthesized by Yu et al. [29]

Noteworthy, at the temperatures attained during some coupling reactions, such as the Heck reaction, no reducing agent (e.g. $NaBH_4$ most often) is needed for *in situ* production of PdNPs. At such temperatures, the anions coming from the Pd salt precursor and surrounding the particle surface, act as reductants [161]. This observation seems to support the hypothesis of nanoparticles formation theory in ordinary coupling reaction media.

Some studies showed that stabilization of the colloids formed in the medium by ammonium and phosphonium salts gave good results in terms of prevention of Pd black formation [337, 338] even though it was also found to vary according to reaction conditions, namely the base used, pH etc. Nonetheless, according to de Vries, PdNPs are probably not the true active species, while they only act as reservoirs of molecular Pd(0) [170].

In [339] Zhou et al. used TBAB to stabilize PdNPs reaching a respectable TON of 66,000 corresponding to a TOF of 22,000 [h^{-1}] in the Suzuki-Miyaura reaction between 4-chloronitrobenzene and phenylboronic acid at 120°C in water, while in [340], the reaction between iodobenzene and phenylboronic acid at RT gave TONs of 540,000 albeit poor TOF of 6,000 [h^{-1}]. The stabilizing method appeared to impact the catalysis efficiency.

The group of Soomro and Köhler pointed out that the use of TBAB in the Suzuki reaction of chloroarenes led to no evidence of re-deposition. This was explained either because of the lower conversions of less reactive chloroarenes and of stabilization through ammonium solvation process [341, 342]. The TOF_{leach} of the reaction of 4-chloroacetophenone and phenylboronic at 65°C amounted to 1070 [h^{-1}], in the presence of stabilizing TBAB. Besides, the addition of TBAB, to Sugi's reaction medium [280], was found to induce Pd leaching, according to the results of a filtration test. These conclusion appeared to be particularly interesting since during hot filtration tests, independently from the amounts of homeopathic soluble Pd, these active species may have a so short lifetime that they won't be detected by hot filtration. Thus, leached species appeared more stable in solution than usual, probably due to the TBAB capping action. Moreover, leaching was found to be more significant in the presence of polar solvents.

In addition, the effect of capping agents was found to be dubious as for its impact on catalytic activity. Together with stabilization of PdNPs, some authors found that they caused reduction of reaction rates. Perhaps capping action reduced the availability of NPs defects for leaching of active species in solution, which caused a decrease in the whole activity. For instance, PVP was found to decrease both reaction efficiency and Ostwald ripening. The authors hypothesized it acting as a poison for leached Pd species or as a hindrance for reaction on particular surface sites [343, 344].

El Sayed and co-workers worked with PVP-capped and PAMAM-OH G4 dendrimer-encapsulated PdNPs. In the former case, large particles are produced during the first catalytic cycle; the same particles precipitated during the second one. The encapsulation efficiency of dendrimers prevented the occurring of precipitation in the second scenario. Though, the NPs continued to grow larger. Furthermore, the group observed that PVP stabilization hindered both OR and reactivity. Evidences about capping were reported in some later studies advocating that PAMAM dendrimers had an effect on activity higher than PVP [343]. Furthermore, in some Suzuki couplings, phenylboronic acid appeared, to the group, to strongly adsorb on the NPs surface, so that an Eley Rideal reaction mechanism was proposed [343, 344, 345, 346]. Though, later, PAMAM dendrimers appeared to hinder the most the catalytic activity because of tight encapsulation of PdNPs [254]. Dendrimers were used as stabilizers of PdNPs in cross-coupling reactions. In [347, 348] some Pd black formation at high temperatures was observed, while at lower temperatures the system appeared to be stable. Furthermore, in [349], Christensen and co-workers measured significant Pd leaching when nanoparticles were encapsulated in dendrimers, during Heck reaction, using DMF as a solvent.

Sometimes, solvents may cover the role of phase transfer agents. Recently, Obora's group studied the influence on catalytic activity of the DMF-protection method of PdNPs [350]. The role of the protecting capping agent was proven by a screening test involving DMF, NMP, MeOH, H_2O and some mixtures as solvents. In MeOH the catalyst reached significantly higher yields than in DMF. The capping action seemed to lower catalytic activity while hindering NPs coalescence.

5.5 Heterogeneous cross-coupling kinetics: "cocktail catalysis"

Reduced Pd(0) forms of palladium are known to be highly unstable and to aggregate in solution forming nanoparticles (NPs). Many papers have been published arguing about the catalytic role of PdNPs, as stated before. Some sustained that they were completely inactive, leading through coalescence, to precipitation of exhaust Pd black; some others supported the theory about their activity; some even

advocated Pd black itself being the true catalytic species, a role which was mentioned before.
In 2012, a cross-coupling reaction mechanism involving both heterogeneous (nanoparticles) and homogeneous (soluble metallic Pd) catalysis, was drawn [30]. The proposed mechanism, where solid clusters and soluble Pd concur for the coupling efficiency, can be seen in Figure 37.

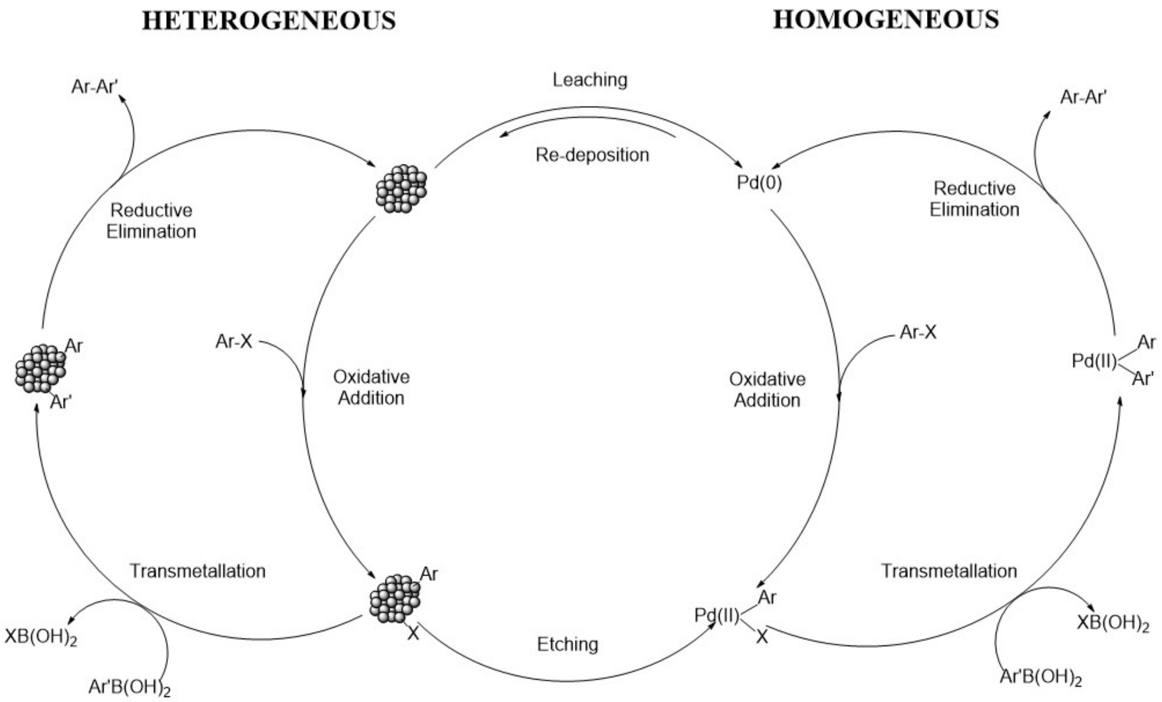

Figure 37: Hybrid scheme of both homogeneous and heterogeneous Suzuki-Miyaura reaction mechanism. Adapted from [30].

In the last years, it has been highlighted that the competent species could be several and all cooperate in a "cocktail" catalysis mechanism, with different reaction rates and yields, prone to giving birth to different competing reactions [31, 351]. Dynamic evolution of the nature of the Pd species [352], from metal to molecular to clusters, is the representative concept of this hypothesis. Indeed, Ananikov and Eremin underlined the importance of not focusing on only one catalytic system at a time. They meant that, molecular Pd, complexes, nanoparticles, nanoclusters, solid surfaces are not fixed systems which either are active or not. One system may be suitable for certain reactions, while less for others and during the reaction it might turn into another by simple aggregation or re-deposition processes. Thus, "cocktail" catalysis is due to several processes occurring in the reaction medium, such as leaching, clustering, aggregation, sintering [31]. Such catalytic systems are dynamic systems often involving multiple active species at a time.
On the whole, two scenarios describe "cocktail" catalysis depending on reaction conditions:

- "Cocktail" catalysis is present in the reaction medium but only one species is active at a time.
- "Cocktail" catalysis is present in the reaction medium and multiple pathways are followed depending on the activity of different Pd species

In [266], all possible active species in solution or deposited onto the solid matrix are treated differently in terms of efficiency and kinetic constant. The resulting activity is a sum of the single activities:

$$-\frac{d[A]}{dt} = (\sum k_i x_i(t))[Pd]_T[A][B] = k(t)[Pd]_T[A][B]. \tag{5}$$

Figure 38 describes the possible coexistence and/or co-activity of different Pd supported or in-solution species in "cocktail" catalysis, namely atomic Pd (**M**), Pd complexes (**ML**$_n$) and PdNPs (**M NPs**).

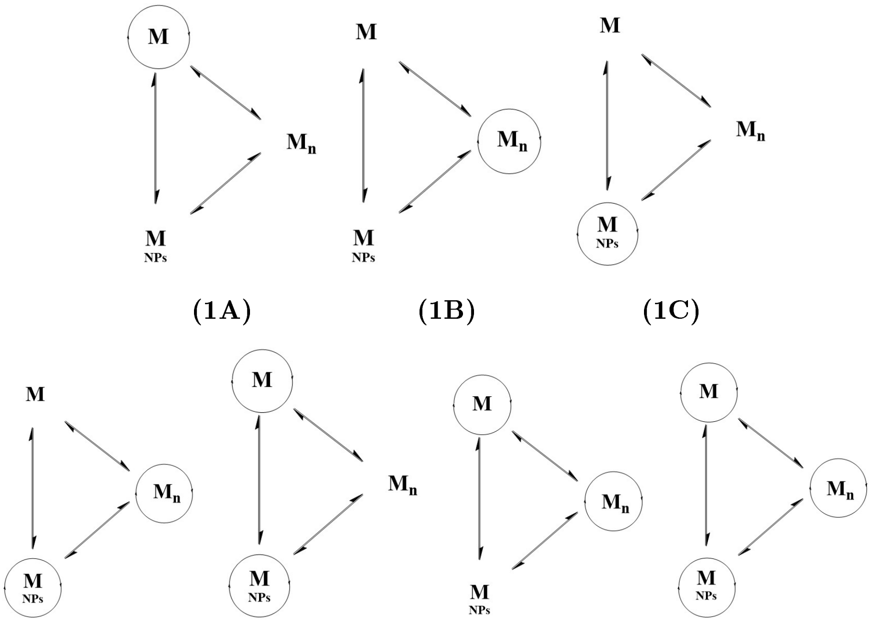

(1A) (1B) (1C)

(MA) (MB) (MC) (MD)

Figure 38: Scenarios occurring in "cocktail" catalysis according to [31]. **(1A)-(1C)** "Cocktail" catalysis with ONE active species at a time. **(MA)-(MD)** "Cocktail" catalysis with MULTIPLE active species at a time. Note: each of the three species **M**, $\mathbf{ML}_n$ and **M NPs** can be supported or in-solution.

Figure 39 represents the location and nature of different sources of active Pd species pointed out through the years in literature, during cross-coupling catalytic reactions [32]. Namely, supported metal species suffer from *in situ* reduction, sintering and particle migration. They are also supposed to leach because of oxidative addition of aryl halides and to trigger the catalytic cycle. Moreover, Pd(0) and Pd(II) moieties may be involved in re-deposition processes, leading to nanoparticle formation through crystallization. The process is particularly favored at the end of the reaction Though, these same species might remain in solution, and in particular in the reduced form, and aggregate into clusters and Pd black.

Köhler and co-workers advocated that during the Heck reaction, induction periods correspond to Pd accumulation in solution [302]. At its maximum concentration palladium species begin catalyzing the

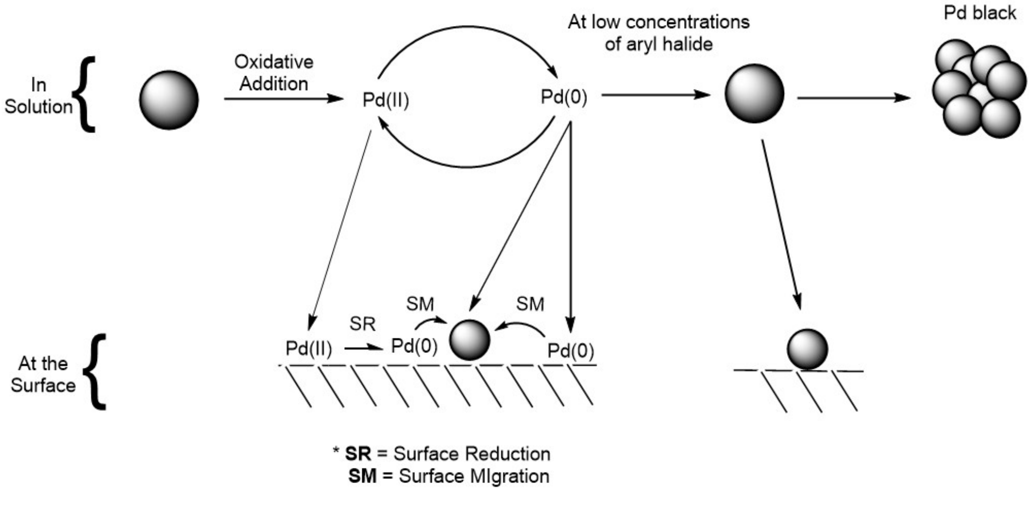

Figure 39: Scheme of coexisting active/inactive supported/in-solution species of Pd and "location" with respect to the catalytic cycle and to conversion [32].

reaction and once exhausted a re-deposition process was observed, decreasing the concentration of Pd in solution.

During these last years more sophisticated hybrid mechanisms have been proposed, based on these evidences [31, 351]. Eremin summed up all the possible ways Pd species may enter the common "cocktail" catalysis scheme, represented by the scenarios of Figure 38. This improved scheme is depicted in Figure 40 [33]. The possible active species are considered to be nanoparticles, nanoclusters, "naked" (e.g. ionic or metallic) palladium and Pd complexes, sometimes in form of oligomers. On the whole Pd(II) on the solid surface may be reduced or suffer from leaching, through salt solubilization and ionization, in solution. As for supported metallic palladium, it undergoes coalescence through OR or PM, but is also sensitive to leaching through attacks from the liquid medium, mainly by halides and/or solvent molecules. Nanoparticles and nanoclusters can be added to the medium by contaminated metallic palladium catalysts, formed *in situ* by reduction and aggregation of Pd(II) species, thanks to the action of organic molecules or reducing agents, or detached from preformed surfaces. Moreover, nanoparticles may give life to clusters or metallic atomic palladium through leaching or detachment. Hence, atomic Pd species are often solubilized and attacked by in-solution molecules, which can coordinate onto it and form Pd complexes or form a solvation layer. Finally, all solubilized species are prone to coalescence, deactivation and/or re-deposition processes. This represents an almost exhaustive scheme which describes "cocktail" catalysis and its complexity.

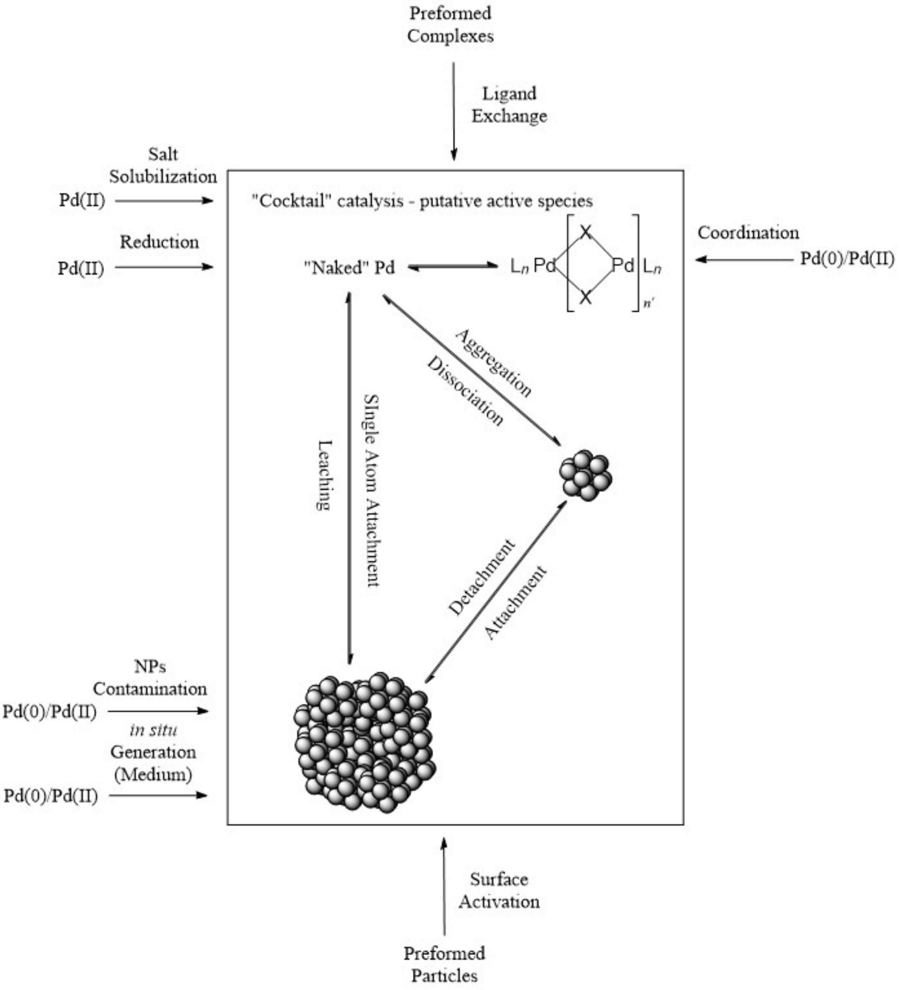

Figure 40: Scheme explaining the concept of "Cocktail" catalysis: putative active species and sources. Adapted from [33]

Among the transformation mechanisms representing "cocktail" catalysis, leaching and re-deposition processes are the ones establishing a connection between solid and liquid phases. Leaching has been categorized into 4 typologies, the four mechanisms are depicted in Figure 41 [31]. Local leaching occurs in case of solvation, adsorption or oxidative addition processes. A single atom of metal is leached from the surface into the solvation sphere of the supported or dispersed nanoparticle. At the end of its task the atom will be re-adsorbed onto the surface at the same position. The catalytic cycle probably occurs in this solvation sphere [351]. Hence, the bulk solution will not contain high amounts of leached Pd, so that it could result undetectable, and nanoparticles will show retention of morphology. Complete leaching of monometallic species, on the other hand, forces changes in nanoparticle's morphology. The metallic species leached will act as a single active species. This does not exclude on-the-surface heterogeneous catalysis, albeit the extent of homogeneous contribution may raise significantly. One main effect of the process is the slow (depending on the rate of solubilization) broadening of the PSD, which may cause extensive Ostwald ripening and more rapid leaching as well as re-deposition processes. In general this mechanism induces higher cristallinity ratios of nanoparticles after the reaction.

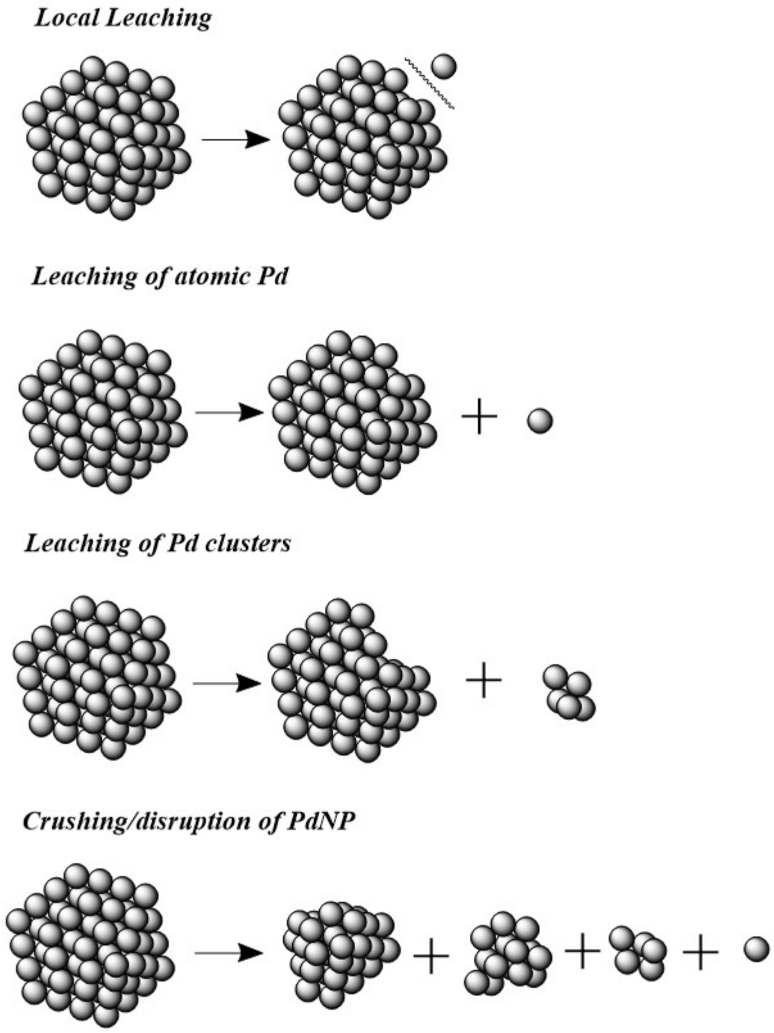

Figure 41: Leaching mechanisms described by Eremin and Ananikov. Adapted from [31].

Furthermore, small clusters may also be solubilized. Most of times, cluster's solubilization make this species gain completely original electronic properties and could cause the switch in the trend of catalytic activity. For instance, Alexandrov et al. led a study on solvation processes of Pd_6 and Pd_{19} nanoclusters [353] The authors observed a high number of stabilizing molecules gathered around the clusters' surface, compared to atomic leached Pd. Finally, the nanoparticles may, mainly mechanically, lose its morphology giving birth to new smaller particles and clusters.

All these mechanisms contribute to draw a scenario in which morphologically different and potentially active species coexist and exchange matter and energy.

Charges may be formed and exchanged, as well. They can be originated through leaching of Pd(0) species from PdNPs. These latter species may undergo oxidative addition, producing a positively charged complex; ligand exchange, leaving their neutrality unchanged or solvation/capping by solvents/capping agents, providing a temporary stabilization of reduced Pd(0) species; finally, complexation by anionic species, like halide anions (X^-). Alternatively, such complexes may undergo decoordination, producing charge modifications, too [31].

Detachment and solubilization are not the only processes which Pd species may undergo. Aggregation and re-deposition are important, as well. Figure 42 underlines the different putative aggregation mechanisms involving leached Pd species (i.e. clusters and/or atoms). Clustering and Pd precipitation has been pointed out to be due to exhausted catalyst coalescence and led to catalyst deactivation, but this is not completely true. Nanoparticle formation in solution could be particularly useful for the promotion of catalytic activity and/or favoring of certain reaction pathways [31].

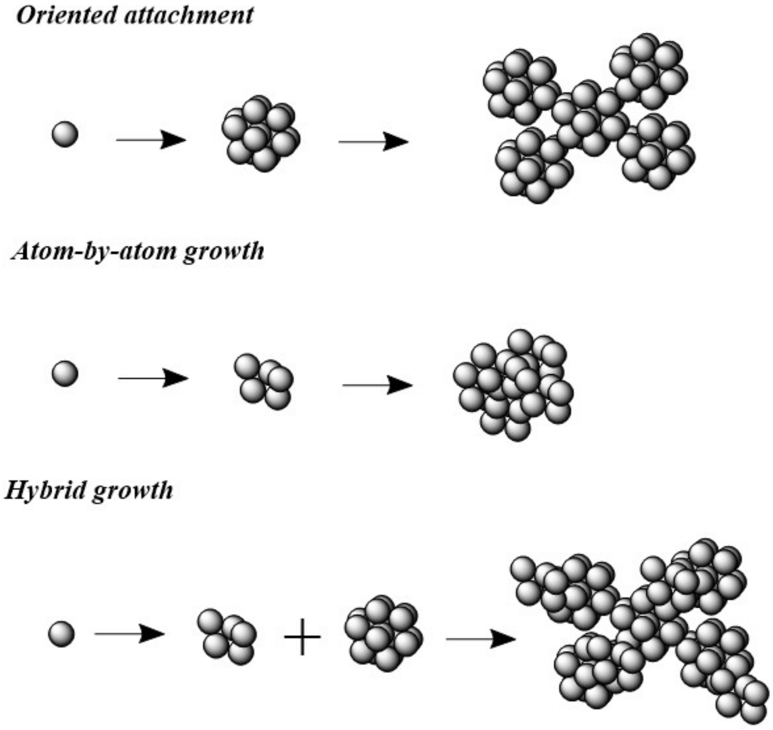

Figure 42: Aggregation mechanisms described by Eremin and Ananikov. Adapted from [31].

In the case of oriented growth, good cristallinity and low-dispersed PSD are normally obtained. On the other hand, "chaotic" atom-by-atom growth may occur, too. The resulting nanoparticles are extremely polydispersed with low-cristallinity ratios. The process is influenced by several parameters [354].

"Cocktail"-like catalysis was reported by Alabugin et al., in a study on the conversion of propargyl vynil ethers into *(E,Z)*-dienals catalyzed by rhodium precatalysts [355]. The reaction mechanism was observed to occur in steps where certain active species converted the substrates into intermediates, and these one were then transformed into the final products. DFT-calculations were conducted in order to clarify the nature of the mechanism.

In a comprehensive DFT study by Polynski and Ananikov, the leaching and stabilization processes were well explained, in 2019 [34]. The whole study aims to calculate by means of quantum mechanics modeling a bunch of energy values linked to the leaching process, and assess its spontaneity.

If one considers that the molecules may adsorb on the surface palladium nanoparticles, in particular haloarenes, starting oxidative addition and leaching, or Pd may simply detach and be attacked later, the whole energy barrier contributions will appear as follows:

$$\Delta E = \Delta E_{det} + \Delta E_{stab} = \Delta E_{det} + \Delta E_{bind} + \Delta E_{OA} + \Delta E_{oligo} \tag{6}$$

where palladium detaches from the surface (ΔE_{det}), the haloarene binds to the metallic site (ΔE_{bind}), starts the oxidative addition (ΔE_{bind}) and finally causes the oligomerization of Pd complexes (ΔE_{oligo}). Figure 43 depicts the two pathways of leaching which were supposed interesting for this study [34].

On the whole, the leaching and stabilization processes were found to be exothermic in DMF as the solvent and with model ligands for Palladium, namely NMe_3, PMe_3, Br^- and I^-. In order to study the process, Pd nanoparticles were taken as Pd sources, namely cuboctahedral Pd_m ($m = 79, 116, 140$) particles. No cue is provided whether PdNPs are considered supported or dispersed in the liquid phase. Though, it is not of prior importance for such a DFT study.

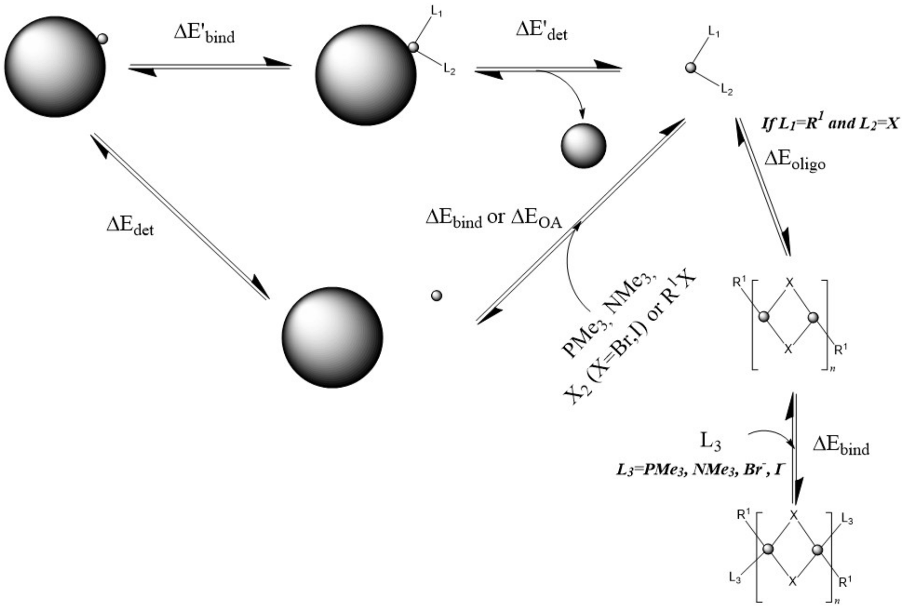

Figure 43: Scheme of "cocktail" catalysis according to Polynski and Ananikov's DFT study. Adapted from [34].

Firstly, Detachment of clusters from {111} and {100} facets was taken into account and one parameter (N_{broken}) was defined, accounting for the number of bonds broken during the separation process of Pd atoms/clusters from colloids. The aforementioned types of Pd atoms forming the nanoparticles were defined according to N_{broken}. Vertex atoms are the least coordinated with $N_{broken} = 6$, compared to edge ($N_{broken} = 7$) and facet ($N_{broken} = 9$) atoms. Certain n-fixed clusters (Pd_n) were investigated for assessing the extent of endothermicity as a function of the number of Pd atoms consituting the clusters and of the cleaved bonds. Indeed, the values of the energy barriers were approximated by the empiric law:

$$\Delta E_{det} = 44.68n + 6.62N_{broken} \tag{7}$$

where the considered detachment reaction is $\mathrm{Pd}_m \longrightarrow \mathrm{Pd}_{m-n} + \mathrm{Pd}_n$.

Once the energy of detachment is calculated, the maximum number of bonds that can be broken (N_{max}), while keeping the whole process exothermic can be calculated, when the other contributions are obtained. Moreover, in order to account for the stability against the re-deposition process, one parameter was evaluated: N_{max}/n. Low absolute values of ΔE would gave cluster's sizes near to the maximum number of atoms allowed, thereby, low values of N_{max}/n. For instance, Pd species leaching from {111} and {100} facets, were found to be not easily recaptured due to a $N_{max}/n \geq 9$. Once the Pd cluster is leached, those facets are so stable that arecapturing process is highly improbable.

It was stated before that highly directional growth of Pd nanoparticles may increase their activity. The authors reported the same evidence, advocating doubled activity for high-index facets-containing nanoparticles, namely {730} and {221} ($N_{broken} = 4, 5$ respectively), due to easier leaching of Pd adatoms and atoms coming from surface defects. Moreover, anionic mono- and dipalladium moieties were found to be catalytically active and coming from other types of low-coordination facets, giving $4.5 \leq N_{max}/n < 8$. Indeed, already prior to this study, some ligandless and base-free Suzuki reactions

were reported to be well-catalyzed by nanoparticles containing Pd atoms with coordination numbers of 4-5 [330, 356].
The detachment follows the scheme NP $\longrightarrow$ NP*+Pd$_n$, giving an equilibrium constant of $K_{eq} = [NP^*][Pd_n]/[NP]$, where [ ] values are activities, ore concentrations under ideal solution hypothesis. Since the structure of the nanoparticle does not change too much before and after the detachment, $[NP]$ can be considered almost equal to $[NP^*]$, which means one may calculate the concentration of Pd clusters in solution according to:

$$\Delta G_{leach} = -RTlog(\omega_{Pd}\frac{\rho_{medium}}{M_{Pd}}). \tag{8}$$

Actually, palladium can be, experimentally, found in the liquid phase in amounts comprised between 0.5 and 300 ppm. Since ΔG_{leach} values are extremely sensitive to N_{broken}, the Pd concentrations will firstly raise thanks to leaching of adatoms and then, of vertex and edge atoms. Stability of {111} and {100} facets appeared to significantly lower the leaching extent.
Then, the binding energy contribution, E_{bind}, was considered. NMe$_3$ showed low binding properties, with a maximum of 4 ligands coordinated onto Pd$_2$ and Pd$_4$ clusters, and only in the μ_1 bridging configuration, leading sometimes to Pd-Pd bond cleavage. Besides, PMe$_3$ stabilized also μ_2 and μ_3 configurations with higher binding power.
Stabilization from recapture appeared null for the NMe$_3$ case, while the Pd species did not readsorb onto particles's edge when PMe$_3$ was used. For instance, $[Pd_4(PMe_3)_8]$ ($N_{max}/n = 6.5$) complexes were formed when the phosphine stabilized Pd$_4$ species.
The oxidative addition was modeled, as well, accounting for an important cause of leaching. PhBr and PhI were taken as model aryl halides. The affinities of these molecules for Pd centers are similar to those of phosphine and amine ligands. Though, the only appreciable stabilization was found when two molecules of PhI were coordinated, per Pd atom ($N_{max}/n = 3$), but this was not enough for preventing re-deposition. Stronger stabilization is provided by X$^-$ coordination, which could be produced during the coupling reaction or introduced in form of salts. Ligands like NR$_3$ (base in most coupling media) and PR$_3$ may undergo the binding process, as well. The proportion of binding depends on the environment conditions. Though, halide ions and NMe$_3$ have great affinity to [PhPdX]$_n$. Together with some cases of phosphine coordination, these cases produce a N$_{max}$, high enough to stabilize the Pd species from being re-captured on the surface ($N_{max} > 4.5$). Halides can particularly stabilize palladium halide species [Pd$_n$X$_{2n}$] by coordination, to X[Pd$_n$X$_{2n}$]X^{2-}. This coordination stabilizes really well the Pd oligomers towards re-capture (N$_{max}$ $\sim$ 9) but also lowers the reactivity, which can be restored thanks to a further reduction of halides. This high stability explains the detection and involvement of anionic species in coupling reactions [3, 26].
Leaching appeared extremely easy also from detached nanoclusters, in an atom-by-atom way, which is endoergonic and compensated by up-to-four ligands complexation.

Moreover, oligomerization was considered. Oligomerization with [PhPdX] or [PhPdX$_2$]$^-$ allows the stabilization of [PhPdX] species. Species like [PhPdX]$_n$ and [PhPdX$_2$]$^-$ were often detected in experimental Heck reaction media. In this study, bridging through phenyl groups appeared to give stronger bonds than with an halogen. Besides, [PdX$_2$] species can oligomerize as well, into [Pd$_n$X$_{2n}$]$^-$. Some ligand associations, i.e. NMe$_3$, caused oligomerization through Pd(I) species formation [357, 358]. The authors finally advocated that the use of PdX$_2$ salts as precursors may give life in solution to too highly stable oligomers [Pd$_2$X$_6$]$^{2-}$ which increase the homocoupling rate and the Pd(IV) species formation.

Anyway, although the theory about unavoidable leaching of Pd species in solution is still supported, in the last years, some catalysts showed hopeful nearly pure heterogeneous catalytic character, under certain conditions [32, 359].

5.6 Heterogeneous cross-coupling kinetics: homeopathic catalysis

Pd moieties are now known for their high specific activity. Extremely low amounts of metal may drive activated-substrate couplings to complete conversion in few hours, or even minutes.
Deraedt and Astruc sustained the theory about "homeopathic" amounts of Pd leached from PdNPs surfaces catalyzing cross-coupling reactions [161]. Evidence of reaction rates increasing when decreasing catalyst loading is consistent with the hypothesis. The authors also reported that "homeopathic" catalysts had been observed when using heterogeneous catalysts coupled to stoichiometric amounts of surfactants, e.g. TBAB or imidazolium salts [161]. This can be explained by the anionic salts attacking the neutral immobilized Pd speciesand causing their leaching and stabilization in solution.
De Vries and colleagues worked on Heck couplings catalyzed by "homeopathic" $Pd(OAc)_2$. They proposed an efficient way to recycle the catalyst *via* filtration on celite or silica and reoxidation of Pd(0) species, mostly Pd black, to Pd(II) precatalyst form, by iodine. Figure 44 represents this recycling process scheme.

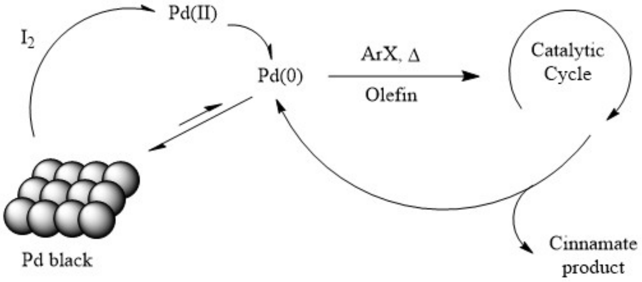

Figure 44: Catalyst recycling process scheme proposed by de Vries and co-workers in 2002. Adapted from [35].

It is note-worth the fact that "homeopathic" amounts of palladium in solution are able to catalyze the whole reaction leading to 100% conversion in a little time, in the presence of highly activated substrates like aryl iodides. This is the major cause of leaching tests misinterpretations, a topic that will be addressed in Section 8.2.

6 Deactivation mechanisms and recyclability

6.1 Recycling generalities

As stated above, homogeneous palladium complexes have been extensively employed in industrial processes, namely drugs' production. Though, their difficult separation from the reaction medium could cause contamination, which is strictly regulated, especially in the pharmaceutical domain. The European Medicines Agency and the Australian Therapeutic Goods Administration both refer to a common guideline on "Impurities in Drug Products" (CPMP/ICH/2378/99) [360, 361]. When the catalyst is solubilized, common purification methods cause bearing of solvent molecules with the product, containing traces of Pd, and contamination is unavoidable. Moreover, due to the instability of Pd complexes, namely phosphines, the process becomes uncontrollable and risky, because of the release of these highly toxic molecules.
Evaporation, distillation and membranous processes are commonly used for purification purposes. But these operations, involving high temperatures, decomposition pathways may also add toxic decomposition by-products to this already complex scenario. Moreover, purification increases the cost of the whole process. A "simple" evaporation-based product-purification process may cost to a pharmaceutical industry several thousands of Euros every year.
The choice of handling cross-couplings heterogeneously is, as said in Section 3, a question of satisfying the purity standards of chemical products as well as simplifying the downstream handling of the medium and the treatment of the exhausted catalyst if not supported. Nonetheless, by simplifying the downstream one is theoretically, substituting the expensive purification set-ups with expensive research and production processes of supported catalysts, e.g. the catalyst preparation and deposition takes much more effort compared to the homogeneous "relative". It obviously follows the fact that in-solution active species leached from a heterogeneous catalyst make it lose its inner meaning. Similarly, deactivation of the catalyst surface after several runs must be controllable, in a way that the substitution is economically favorable and amortized in the least time possible.

During lab-scale tests, common recovery protocols consist of rinsing with various solvents, namely water and acetone, in order to remove all impurities adsorbed/deposited onto the surface, and drying under vacuum. Though, all these operations could cause leaching, too. This is an aspect that is hardly ever taken into account. In addition, palladium leaching in solution is often characterized by extremely low amounts of soluble and dispersed moieties, of the order of few ppm or even ppb. This made it a challenge to efficiently detect Pd species in cross-coupling media, since those amounts may be lower than the sensitivity of the measuring devices. Some authors believed and still believe, the reaction mechanism to be "truly heterogeneous" owing to the detection limits. Though, it is now known that the majority of the putative heterogeneous catalysts follow a "quasi-homogeneous" path, involving leached species, according to the mechanisms of "cocktail" catalysis (*vide supra*). For instance, Wu et al. loaded $PdCl_2$ on poly(acrylonitrile)-supported imidazolinyl ligands [362]. The authors inferred that the catalyst was reused up to 20 times, yet no discussion about activity losses was provided.
Other considerations on recycling were made by Bedford et al. who synthesized NC imine palladacycles and functionalized a silica-based carrier. Two different systems, **39** and **40**(Figure 45), were studied, one containing PPh_3 and the other without. Both systems showed decomposition under the reaction conditions, forming soluble species. Furthermore, the reaction medium underwent a significant change in color, during the reaction, from pale yellow to brownish red, meaning Pd(0) NPs formation [36]. The authors advocated that silca-based supports without PPh_3 were able to stabilize PdNPs, acting as reservoirs of these catalytic species and working through a release-and-catch mechanism [74, 73], but they could be recycled just few times with no significant decrease in yield. As for, the phosphine-based system recycling appeared more difficult. The authors inferred that the low coordination of Pd typical of phosphine complexes facilitated the Pd-species leaching.

Some new technological advances in recycling techniques were proposed by Gao et al., who worked on magnetic nanoparticle-immobilized Pd-NHC. The magnetic properties of NPs helped the recycling

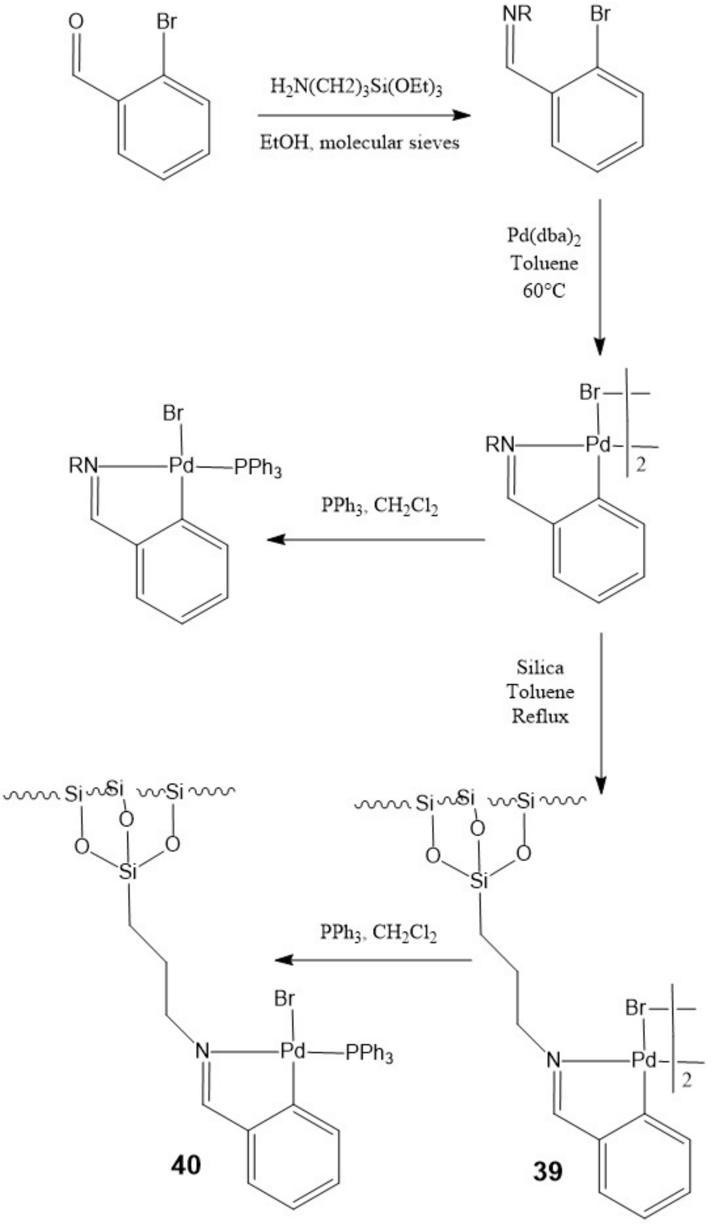

Figure 45: NC palladacycles supported by Bedford et al. on a silica support. Compounds **40** and **39**, including or not triphenylphosphine ligand [36].

of the catalyst [363, 364]. The efficient recover of the solid, though, did not mean that any leaching occurred, and the authors neither proved this, nor the contrary.

The magnetic properties of magnetite (Fe_3O_4) are still exploited in 2020, providing an easy way for heterogeneous catalyst recycling. Heravi and co-workers prepared Fe_3O_4 nanoparticles, functionalized with an acetic acid derivative as an OO-bidentate ligand for palladium. The catalyst was magnetically recovered and showed high yields both in Suzuki and copper-free Sonogashira couplings under similar conditions. Pd loss from leaching was said to be negligible [365].

Afsharpour and colleagues used magnetically recyclable magnetite nanoparticles functionalized with Pd-fuberidazole complexes to catalyze the Suzuki and Stille couplings in green PEG400 [366]. Good to excellent yields of different aryl halides were obtained. The recyclability was good up to 8 consecutive runs.

Bronstein and Shfrina immobilized PdNPs on polypyridilphenylene-functionalized magnetic mesoporous silica (Fe_3O_4-SiO_2). The catalyst performed really well, giving total conversions and selectivities with minimum TOF of 23000 [h^{-1}].

Other magnetic systems have been studied recently, most of them exploiting the ease of functionalization property of magnetite to obtain Fe_3O_4-SiO_2 systems [8]. These systems often showed recyclability up to around 10 consecutive cycles. They were used for functionalization with selenated complexing ligands, in a greener and efficient coupling process [367].
Hasan recently studied a similar system were a layer of chitosan is deposed on magnetite nanoparticles for ligand functionalization [368], while a hybrid system containing both silica and chitosan was developed by Veisi and co-workers [369]. Also Lignin has been used for coating in Heck applications [93]. Coating is, in general, useful to avoid magnetite NPs aggregation and chemical modifications (e.g. oxydation) while keeping their magnetic properties.

6.2 Deactivation mechanisms

One main problem of heterogeneous catalysis is the catalysts deactivation. It is triggered by different phenomena, namely thermal, physical and chemical. Moreover, deactivation processes can be grouped into: thermal particle sintering, metal and support leaching, deposition of inactive metal layers or polymeric species onto the surface (fouling or cocking), chemical poisoning by adsorbed chemicals, and mechanical deactivation [370, 371].

Sintering of particles and colloids coalescence Sintering is a thermal process favored by high temperatures.
On a long time-scale, supported metal particles are likely to aggregate. This happens thanks to atom exchange process among nanoparticles, likely even at RT, known as Ostwald ripening (OR) or through the entire particle migration (PM) [371]. The phenomenon is favored by the presence in solution of capping molecules such as polyhydroxylic molecules which can carry the atoms from one particle to another. It leads to loss of surface area and collapse of the porous structure of the solid [372].
Good dispersion of the metal, sometimes thanks to promoters added during catalyst's synthesis, can avoid or slow down such phenomenon [373]. Besides, homogeneous species in solution are likely to coalesce at low temperatures, due to the instability of "naked" Pd(0), and deactivate through precipitation carbon black-like clusters.

Leaching of active species and support The process implies the formation of a phase which is soluble in the reaction medium, different from detachment which implies dispersion of larger structures [372]. Nonetheless, in this study, detachment and leaching are put together in order to simplify, since entire unsoluble nanostructures may detach and contribute to the catalysis of cross-couplings, from the liquid phase. Even strongly bonded species, like encapsulated particles, grafted species in mesoporous materials or scavenger molecules-containing systems are prone to leaching, under certain conditions. Indeed, the process is highly environment-dependent, i.e. on pH, oxidation potential, capping properties of molecules, upon bulk and surface catalyst conditions and oxidative atmosphere [372]. For instance, aluminas which are widely exploited as heterogeneous catalyst carriers, suffer from significant leaching in acidic and chelating conditions [371]. Leaching can occur following different mechanisms:

- Direct solubilization of slightly soluble phases like metal oxides, hydroxides and carbonates [372].
- Chemical reaction of solvent or acids/bases with the active metal species present on the surface, producing soluble phases [372]. The oxidative addition appears to be another main cause of leaching in the liquid phase.
- Detachment of clusters from the solid surface, and subsequent solubilization of adatoms.

Zhang and Liu exemplified the influence of the oxidation potential on leaching of Pd from solid supports, and how different species present in solution could affect this phenomenon [374]. They showed how complexation by chloride ions could lower the high oxidation potential of palladium and allow oxidants like Fe^{3+} to oxidize Pd species and facilitate their leaching.

Poisoning by adsorbed species and deposition of inactive metals Sulfur-based moieties are known to be strong adsorbing species onto supported metal-particles surfaces. This can lead to metal inactivation [371].

Organic moieties are likely to poison heterogeneous catalysts, too. They could consist of solvent molecules or be produced during the reaction, as by-products. It is note-worth the affinity between biphenyl molecules which are products of cross couplings and the catalyst surface.

Another source of poisoning is constituted by acidic species which are, if not reacted, more easily desorbed by washing with alkaline solutions [371].

All these species may undergo, physical deposition (fouling/cocking) and block the accessibility of the pores of the solid carrier structure as well as of the active catalytic sites or by chemical reaction with the catalyst. Moreover, adsorbed chemical species like molecules, adatoms and ions can act as selectivity modulator and enhance or direct it. Deactivation through deposition of less active metal layers can occur, too. It consists of covering the active sites (e.g. metal particles) with layers of inactive or less active metal species.

Metal oxidation and ligands degradation Under certain reaction conditions, transition metals can be oxidized. This property also depends on the reducing potential of substrates. For instance, Pd/C suffers from over-oxidation under aerobic conditions, losing part of its activity with time. This over-oxidation and transformation of leached species into peroxo-moieties have been hypothesized to be at the base of homocoupling reactions.

In addition, ligands may degrade under oxidative or harsh thermal conditions, giving birth to toxic by-products or simply reduce the catalytic activity of complexes [160].

Mechanical alterations Attrition phenomena can cause particle-size reduction and even breakage of the catalyst support. Firstly, as stated before, change in the particles' size affects the PSD and increases the probability of OR to occur. Then, the dispersion of small particles in the liquid phase could represent an activity loss or at least lead to easier Pd leaching. Moreover, in continuous operations free solid particles dispersed within the liquid phase, could cause clogging of membranes and porous systems, leading to uncontrolled raise of the pressure in the reactor.

7 Sintering

The sintering is the phenomenon which causes metal particle-size growth, in order to minimize their free energy. The surface's free energy is always higher compared to the bulk, and unevenness in the particle/size distribution promotes it . Sintering happens through particle migration (PM) or Ostwald ripening (OR), i.e. atoms migration from smaller to bigger particles.
Particle migration often occurs in the presence of weakly-bonded small ($l < 6nm$) particles, moving according to Brownian-like motions, while Ostwald ripening is a thermal process characterized by atom migration. Besides, both cause the increase in size of metal particles and the change in the particle-size distribution (PSD). The PSD generally shows longer tails to the right, in both cases, which represent the particles growing bigger than the initial average size [375]. Nonetheless, the shape of these tails changes between OR and PM.
Some microscopic analyses performed during cross-couplings showed that particles remained immobile, decreasing in size. Actually, larger particle's difference in size is often undetectable, but one can follow the shrinking of the smaller ones by TEM [376]. Ostwald ripening, which is the most important process in this case, has been supposed to be linked to vapor pressure of transition metal atoms: lower vapor pressures cause ripening at higher extents.
The decrease in size, of smaller particles, was computed first by Langmuir [377]. Two mean-field models were then, employed to describe surface ripening: interface-controlled and diffusion-controlled ripening, where different processes, such as the diffusion of atoms through the particle-substrate, since substrates were supposed to adsorb onto the surfaces, were considered as process' RDS. The model employed in [376] appears as a corrected exponential law, where the pre-exponential factor depends on the contact angle between particle and surface (θ), the frequency of thermal vibration of an atom in a crystal lattice (ν) and the interatomic distance (l); the exponential contains the term E_{tot} which is obtained by summing the contributions of sublimation, adsorption and adatoms diffusion activation energy.
The sintering process was considered temperature-dependent and enhanced by the presence of adatoms as surface defects.

Uncontrolled growth of metal particles in industrial processes is a major economic concern, since large particles are catalyst consumers and provide very low accessibility to active sites. In some studies the abnormal growth was actually detected at the last stages of the process [378, 379]. The resulting big particles showed strongly directed growth, giving highly faceted shapes (e.g. hexagonal, triangular). Some authors supported the theory for which PM and OR occurred simultaneously. Though, abnormal directed growth and lack of depletion zones appeared not to support the influence of PM [375]. The sintering process has been actually divided into three phases: during the first one the activity loss is fast and significant, secondly this loss slows down, up to the third phase where the catalyst finally reaches a stable condition, even if sintering does not stop [380]. In this scenario, the little starting particles are surprisingly, and in opposition to previous literature findings [381], not concerned by PM during Phase I, whereas OR is the most observed mechanism of disappearance of such small particles. Then, shrinking slows down and leaves the place to more important migration (PM). At the end, other parasitic processes, like surface restructuring take place, especially at high temperatures.
In order to distinguish between the two processes, two approaches have been widely employed. The first one is the observation of the PSDs, since PM gives a more important tail towards large sizes, while OR the opposite, and appears to have impact up to a cut-off size value around 1.3-1.5 times the initial diameter [380]. The second technique is to study the shape of the growth kinetic curves: different mechanisms would mean different slopes.

Datye et al. performed a series of Monte Carlo-based [9] simulations and found that, the disappearance of particles by ripening is characterized by an almost constant slope of size loss at the beginning of the process, followed by fast plummeting towards the end. Indeed, when particles get smaller than a critical size, they undergo fast sublimation due to the Gibbs-Thompson effect: too small particles change their vapor pressure and sublimation gets easier. Ostwald ripening is responsible for the dynamics of catalyst surfaces involving atomic species migration through the liquid or gas phase (volatile carbonyls in the case of Pd/C) [380, 382, 383].

Substantial transformation of the surface of solid precatalyst was reported in the presence of microwave (MW) irradiation, which has been recently, widely explored as efficient heating mean for cross-coupling reactions [384]. This transformations involved, growth of nanotubes, etching and pitting of the surface of Pd on carbon materials.

The atmosphere under which the reaction occurs appeared to play a role in sintering mechanism: hydrogenated and oxygenated atmospheres showed enhanced sintering compared to inert nitrogen, for metal/C catalysts. Bartholomew explained the evidence by gasification of the carbon carrier into methane and carbon dioxide [385]. This gasified carbon layer would help crystallites migrating. The effect of other molecules, belonging to a liquid medium, for instance, may be the one of creating a protective layer around atoms/particles which undergo sintering, and facilitating their leaching into the medium.

Indeed, in addition to atmosphere's role, water appeared to favor sintering in reducing environments. Adsorbed water molecules or hydroxyl groups increased the mobility of metal atoms. Bartholomew designed a scale of thermal stability of metal catalysts, i.e. $Ru > Ir > Rh > Pt > Pd > Ni > Cu > Ag$, which is another parameter supposed to affect the sintering phenomenon.

The influence of coordination number of metal atoms has been studied, similarly to Polynski and Ananikov's study [34]. Indeed, the coordination number of metal atoms, linked to the bond strength with the metal cluster, decreases with decreasing crystallite size [385]. Due to this parameter, at temperatures near to the Tamman point [10], the crystallites acquire liquid-like properties which favor atom migration, especially in the presence of hydrogen.

Migration of metal atoms is more likely in the case of low metal-metal bond strength, but significant metal-support linkage, since the whole particle is supposed to remain anchored to the surface and shrinking little by little. Furthermore, surface defects and change in curvature may cause atom migration toward a valley where it gets stuck.

Conclusively, porous materials may hinder sintering by limiting the crystallite size and accessibility to the carrier's surface by gas species, and some impurities, such as Ca, Ba, Ce and Ge may reduce mobility, too.

---

[9] Monte Carlo simulations consist of risk analysis assigning to each uncertain parameter a probability distribution. Random values of the probability function are taken, and risk is calculated several times in order to assess its importance.

[10] The Tamman temperature represents the half of the melting point, and determines the beginning of the solid-liquid transition. By definition, it is the temperature at which the mobility of atoms and molecules on a solid surface becomes appreciable

8 Leaching

8.1 Leaching tests

Being able to detect leached species from solid matrices is a major concern for researchers. According to [18], the best choice in order to well characterize new catalysts, is to use deactivated aryl bromides or chlorides as substrates in order to slow down the reaction rate and give time to measure interesting quantities.
A bunch of detecting/measuring techniques are reported, which have been performed through the years but also misinterpreted because of detection limits and theoretical flaws:

1. Direct methods

    - **Inductively Coupled Plasma (ICP)**. It allows the detection of traces of molecular moieties in liquid phases. Though, since re-deposition processes can happen and very little "homeopathic" amounts of leached species are now known to be active towards coupling reactions, some authors misinterpreted ICP results allocating all activity to heterogeneous catalysis when encountering false-negatives. Indeed, the detection limits of these analyses depend on the sample composition [372].
    Measures at different conversions must be performed, keeping in mind not to cool down the medium, since low temperatures favor re-deposition. The team of Köhler, Soomro et al. found that the amount of Pd leached correlates to the reaction rate and conversion, this made them state that even using a solid matrix, the reaction mechanism is to be considered purely homogeneous [341, 342].

    - **Microscopy**. Transmission Electron Microscopy (TEM) and Atomic Force Microscopy (AFM) used by Hanyu and Davis in [386], are valuable techniques which allow to follow the evolution of the solid surface of the catalyst.
    - **X-ray Adsorption Spectroscopy (XAS)**. It can be used to follow the evolution of the catalytic species through the reaction. Lee et al. used it to map the evolution of PdNPs catalyzing the reaction between 4-iodoanisole and phenylboronic acid [387, 388]. Variants like Extended X-Ray Adsorption Fine Structure (EXAFS) and X-Ray Adsorption Near Edge Structure (XANES) are used. EXAFS gives information about interatomic distances and lattice dynamics. Besides, XANES elucidates about, valence state, energy bandwidth and bond angles.
    On a graph Adsorption *vs* Energy [eV], the outputs of the two measures represent two different sections of the resulting curve. EXAFS consists of an interference effect between inner core electrons , and the backscattered electrons from the near neighbor atoms. It can be obtained by *transmission, fluorescence, dispersion* and *reflectance* experiments.
    XANES is the result of the excitation of an inner level electron to higher energy levels by an incident photon. The Group of Hii used the EXAFS in [389] to correlate dynamic structural rearrangement of NPs and oxidation state changes to parameters like the type of support and presence/absence of substrates. NPs were supported on a packed bed subjected to continuous flow of protic solvents.
    - **MALDI-MS and UV-Vis**. Matrix-assisted laser desorption/ionisation mass spectroscopy and UV-visible spectroscopy are commonly exploited techniques to access the observation of aggregation processes [31].

2. Indirect methods

    - **Hot-filtration**. It is a qualitative test which helps appreciating catalytic activity of leached species by keeping reaction conditions unaltered and removing the solid supported catalyst. The aforementioned re-deposition processes appeared to affect this kind of tests, especially at high conversions. Hence, one should be careful to deduce any theoretical statements from such experiment. Coupling with other measures would give more solidity to conclusions. Furthermore, a source of re-deposition is the temperature decrease, and keeping the same reaction conditions while removing the solid catalyst is not always simple. Hence, positive responses always mean somewhat homogeneous contribution, this is not the same for negative results, though [162].

The test has been used in the cross-coupling of 4-iodoanisole and phenylboronic acid. The catalyst was removed 10 minutes after the beginning of the reaction. Eventually, no further activity was detected, hypothesizing a pure heterogeneous mechanism [390].

- **Reusability test**. It simply consists of recycling the solid catalyst for further batch reactions. It is now known that a "release-and-catch" process may happen at full conversions. Thus, with these premises no conclusion can be drawn around leaching and related activity. Nonetheless, the test could still be useful to calculate the real TON of the catalyst under certain conditions. This misinterpretation has been source of some mistakes through the years: reusability does not state anything about the reaction mechanism. Moreover, solid supported catalysts showed potential as highly charged reservoirs of leachable species, since "homeopathic" amounts of palladium are able to reach outstanding TOFs.

  Coupling this test with hot-filtration, before reaching 100% conversion or to ICP-MS could be a valuable source of information.
- **Compartmented reactor with membrane**. It consists of two batch reactors connected by exchange of molecules and ions through a nanoporous membrane ($l \sim 5nm$). The initial condition is characterized by the presence of the reactants in both the compartments, the solid catalyst in the former and the base in the latter. Since, leached molecular species are allowed to cross the porous septum, measured activity in the second chamber actually proves the homogeneous contribution to catalytic activity. It is not the same in case of lack of conversion. Rothenberg's group applied the test in Suzuki coupling [391].
- **Continuous compartmented operation or Split-test**. Two reactors are fed continuously with fresh reactants and base. The former is a packed bed reactor containing the solid catalyst; the latter an empty plug-flow reactor. Measuring the conversion at both outlets enables to distinguish the importance of homogeneous catalysis from heterogeneous one. Again, no negative result ensures the absence of activity from leached species. Moreover, one should take into account that the contribution of the first reactor may be both heterogeneous and homogeneous.

  The advantage of separating the two reactors consists of the possibility to vary the external conditions (e.g. temperature, pressure, etc) in order to assess the influence of some other parameters (e.g. effect of the base/reactants) on the leaching process [392].
- **3 Phase-test**. During this test, in addition to the supported catalyst, one substrate is supported, (e.g. linked through amide bonds to a resin). Under these conditions only leached species are theoretically available to catalyze the reaction, since one of the substrates is prevented from moving towards the catalyst surface and reacting.

  The test was introduced in 2001 by Davies et al. in [393] and used by Budroni et al. in [394]. Interestingly the team highlighted the fact that leached species were present and active but mostly towards dehalogenation, rather than cross-coupling.

  Crudden and co-workers, underlined the necessity of setting a three-phase test through both tethering the halide on the carrier and solubilizing part of it in the medium, in order to well mimic the conditions of leaching caused by oxidative addition [395]. Since the authors worked with Pd/C, which appeared to leach the majority of the species because of oxidative addition, the suggestion is actually sensible. It might not be the case for other precatalysts which follow other kinds of leaching mechanism. Results obtained in case of immobilization of halides, instead of other substrates, could be misleading when halides themselves are thought to cause leaching.
- **Mercury-drop test**. It exploits the poisoning properties of Hg(0) towards Pd(0).

  Mercury forms an amalgam with atomic Pd(0) or adsorbs on the surface of the catalyst.

Though, it is even reactive towards some Pd complexes, e.g. palladacycles [396]. Since the interest of the test was mainly based on the hypothetical impossibility of Hg(0) to react with Pd complexes, some results became doubtful. Indeed, it appeared to be able to react even with some forms of palladacycles. One can find valuable information about the limits of this techniques at [397]. One major problem of this test is the putative reactivity of Hg(0) towards PdNPs. If nanoparticles are really reservoirs of molecular and effectively competent species, the prevention of leaching provided by the alloy formed, could hinder both heterogeneous and homogeneous catalysis, resulting in no activity, at all [32].
In [398] and [399], cross-coupling's catalysis is ensured by Pd dendrimer-based complexes. The authors wanted to prove the molecular nature of those catalysts and that the Pd black formed during the reaction was not active. They used the mercury-drop test.
Scrivanti et al. studied iminophosphine ligated to Pd(0) and demonstrated that addition of Hg(0) completely freezed the reaction. Though, they gave no final structure to the putative active species [400].

- **Other poisoning methods**. Similarly to the mercury-drop test, some other Pd-scavenging properties have been studied [18, 298, 401]. Thiols were proven to be particularly suitable [402]. Though, one must consider the slow rate of scavenging kinetics and that efficiency hardly-ever reaches 100%. This could leave some active Pd species in solution acting as highly effective "homeopathic" catalytic species [403]. Furthermore, leaching of thiols in solution could cause poisoning of Pd-supported species rather than scavenging and false all results.
  Another scavenger system, namely Quadrupure TU was used by Pe´rez-Pla et al. [266].
- **Differential selectivity phase-portraits (SADS)**. Interestingly, Schmidt and co-workers recently went out with an approach to evaluate the so-called differential selectivity (S_{dif}). The parameter allows the assessment of the selectivity between two competitive coupling products (P_1 and P_2) coming from different halides and one second substrate, or the opposite [404].
  If r_1 and r_2 are the production rates of P_1 and P_2, S_{dif} can be defined as:

$$\frac{d[P_1]}{dt} = r_1, \frac{d[P_2]}{dt} = r_2 \tag{9}$$

$$S_{dif} = \frac{r_1}{r_1 + r_2} = \frac{d[P_1]}{d[P_1] + d[P_2]} \tag{10}$$

and with a rearrangement:

$$\frac{d[P_1]}{d[P_2]} = \frac{S_{dif}}{1 - S_{dif}}. \tag{11}$$

Thanks to this method a trajectory can be built in the phase space $[P_1] vs. [P_2]$. If one assumes that three possible active species (i.e. species in solution, supported and in-solution nanoparticles) are the same and in similar proportions whatever the precatalyst, equal trajectories would mean same active species involved and same proportions.
Competitive couplings of iodobenzene and 4-bromoacetophenone with styrene were studied and catalyzed by three different systems: Pd/SiO_2, Pd/Al_2O_3 and $PdCl_2$ [405]. The same data-fitting curve was obtained, showing that the same active species were involved in the catalysis of these competing couplings. While, when using benzoyl chloride at the place of the halide, the curve diverged for $PdCl_2$ and Pd/C systems. This showed that in this case, the two catalysis mechanisms were somehow different.
Differential selectivity studies were performed by Wan et al. after Heck and Ullmann reactions of chloroarenes in aqueous media [406]. The reactions were catalyzed by Pd supported on mesoporous silica (Pd/MSC) in the presence of a soluble phenolic resin. The outcoming curve showed several changes of slope all along the reaction time, especially after 8 h. The

evidence suggests that a shift between molecular Pd and nanoparticles occurred in terms of activity, according to Schmidt's interpretation.

Schmidt's studies, provided a proof that palladium is never truly heterogeneous during high-temperature Heck couplings, in the presence of common aryl iodides and bromides [32]. Nonetheless, during Suzuki couplings, slight differences were detected in differential selectivity studies. The evidence gave hope about the possibility for Suzuki-Miyaura reactions to undergo true heterogeneous catalysis [407].

- **Centrifugation test**. Centrifugation allows to force the deposition of heterogeneous particles dispersed in solution and obtained through erosion of the solid surface or aggregation of atomic Pd species leached.

Few other considerations can be done without performing difficult tests and measures. At first glance, it is always important to calculate a general TON for the new catalyst, which will be more interesting than the recyclability parameter. Moreover, TOF is more meaningful than the yield parameter, since it accounts for the kinetics, too. Between average and instantaneous TOF, it is always better to pick the latter, since significant induction periods could affect the averaging calculation.

Reaction selectivity may also be an easy way to tell whether a catalyst is heterogeneous or not, and between two different catalysts. Hence, similar catalysts, such as $Pd(OAc)_2$, $Pd_2(dba)_3$ and palladacycles, give similar product distributions, especially when product isomers are considered.

An interesting example of how to exploit the available leaching tests was recently published by Pérez-Pla and colleagues. They immobilized the Pd complex $[Pd\mu\text{-}(C_6H_4)PPh_{22}\mu\text{-}_2C(C_6H_5)_2]$ on carboxy-polystyrene and studied its heterogeneous/homogeneous nature. For this purpose, they performed hot filtration, centrifugation, 3-phase and poisoning tests as well as a differential selectivity analysis.

PdNPs formation in reaction media is commonly accepted to be an autocatalytic process which shows characteristic sigmoidal reaction kinetic curves, with initial induction periods. Recognizing such shape of the kinetic curves, could help to conclude that whatever the precatalyst, PdNPs are formed in solution and are likely to act as Pd(0) reservoirs. Detected induction periods made the authors infer that 0 is the actual oxidation state of active species rather than +II. The same Pd(0) species are subjected to aggregation into NPs, followed by activity loss. Indeed, the activity loss is measurable if the aggregation process is faster than the reaction. The porous polymer matrix appeared to release Pd(0) atoms and NPs all along the reaction, till exhaustion, while non-porous silica materials leached all species at the beginning of the reaction.

The catalyst was reused up to the fifth cycle and followed by a plummet in the reaction efficiency, consistent with the matrix Pd-reservoir nature. Precipitation of Pd black was also visible during the 6th cycle. The authors stated that the recover process between one run and the other caused the re-deposition of Pd(0) ("boomerang system") which is more likely to coalesce, worsening the catalyst efficiency as time went by. This invalidated every hot filtration test envisaged.

The reaction appeared to go on till Pd(II) exhaustion through reduction and subsequent aggregation, which meant contemporary Pd–P bond cleavage. This also rules out the possibility of the adsrobed Pd(0) clusters to be the competent species, since activity would be present after the 6th cycle. Finally, at the 6th cycle, clusters were significantly larger than at the beginning, since uncontrolled crystallization and re-deposition occurred.

Hence, the SADS assay supported the theory about Pd(II) reduction and leaching from PdNPs surface.

8.2 Evidences of leaching

Among the deactivation mechanisms, leaching covers an important role in cross-coupling chemistry. Many authors have pointed out the presence of leached species in solution during cross-couplings under a wide spectra of conditions, and Pd species are particularly sensible to this phenomenon. Some other authors, even hypothesized that no true heterogeneous catalyst existed.

Pd/C has been employed as a putative heterogeneous catalyst for Sonogashira cross-couplings. In

these conditions the precatalyst actually acts only as a reservoir of competent and soluble Pd(0) species [408]. In the presence of ligands, which was the most employed condition and pretty unavoidable in the presence of alkyne substrates, these species are likely to form complexes in solution. Interestingly, some studies advocated that the addition of the copper-based co-catalyst was harmful to the activity of the catalytic Pd/C system, since the conversion was lowered [409, 410, 411].
In 1996, Schmidt and Mametova assessed that only leached soluble Pd-species were responsible for catalyzing Heck couplings when using supported Pd-catalysts like Pd/C and Pd/SiO_2 [412]. The authors explained that this process occurred mainly because of the oxidative addition of aryl halides on Pd(0)-species, releasing P(II) moieties. In a opposite manner to Augustine, they supported the catalytic importance of soluble species [242, 294].
In [301], Buchecker et al. deduced from mercury-drop test and hot filtration that the Suzuki coupling of haloarenes with phenylboronic acid catalyzed by Pd/C occurred at the surface of the precatalyst. On the contrary, Köhler supported the theory about leaching and re-deposition processes occurring in cross-coupling reactions, when using Pd/C-like precatalysts. Though, the re-deposition process, caused a significant loss of the catalytic activity [302, 303]. Köhler finally reported that leaching occurred for a series of precatalysts under Heck reaction conditions: Pd/C, Pd/SiO_2, Pd/MgO, Pd/Al_2O_3 and Pd trapped in zeolites. Besides, parasitic reactions like aryl dehalogenation appeared to occur at the precatalyst's surface [413, 414]. In the case of Heck couplings, a heterogeneous contribution cannot be completely ruled out, albeit due to harsh thermal conditions homogeneous catalysis by leached species had a major importance [415]. A study was performed on the leaching mechanism by measuring halides conversion and in-solution palladium concentration, at the same time. The reaction started when the peak of palladium leaching was reached, while at its end, a re-deposition process took place. The solubilized species were stabilized by TBAB. The cause for palladium leaching was found to be the oxidative addition while a pre-reduction to Pd(0), was performed by organic molecules like olefins onto the surface of the catalyst. Interestingly, the leaching process was favored by the presence of additional bromide ions which lowered the activation barriers for Pd–Pd bond cleavage of Pd deposited clusters, similarly to Ananikov's studies [34]. Though, this effect does not change the onset temperature of the reaction. Besides, the addition of PPh_3 causes a complete leaching and makes it start at lower temperatures (around 90°C), which reaches 140°C in phosphine-free systems. In the case of Pd(tmeda) deposition on silica support, leaching started even at 40°C with a peak of 98% around 100°C and a little drop at 120°C. At 120°C the reaction started. Again, the addition of bromide ions favored the leaching process of Pd which was not part of any lattice and for which smaller energy barriers had to be crossed. At high temperatures, Pd(II) species were reduced and the oxidative addition took place. When the substrate concentration decreased, Pd was re-deposited. Though, the re-deposited catalyst appeared to provide less likely-to-leaching Pd. In the case of PdO supported on silica, the reduction took place prior to dissolution, because the lattice energy had to be overtaken and it was possible only at high temperatures (120°C). Interestingly, the presence of aryl bromides shifted the dissolved/supported palladium equilibrium towards dissolved, contrarily to aryl chlorides [415].
Yet, researchers are still persuaded that, even though leaching at some extent is unavoidable, suitable quasi-heterogeneous catalysts can be found under certain conditions and with tuned properties.

In this context, the main problem through the years has been telling "where" the reaction actually took place: whether on the surface of the solid catalyst or in solution. The problem has been widely addressed in Section 5.5. To sum up, Pd moieties can be found in solution both as molecular solubilized organometallic complexes, "naked" atomic species and as colloids (i. e. nanoparticles or nanoclusters, depending on their dimensions).
In [161] PdNPs are considered effective active species, resulting from ligated or "naked" precatalyst decomposition. Though, they are told to be less reactive than molecular Pd species. Huang and coworkers found that PdNPs were formed in the reaction medium, growing up as the reaction time went by. Interestingly, these same nanoparticles were found to be smaller in the absence of the solid carrier, during hot filtration tests, than in its presence. Yet, the authors inferred the PdNPs to be the only active species in the medium. Though, the presence of nanoparticles in the medium, especially under

autocatalytic growth conditions, could lead to Pd black formation and inactivation. This is avoided only if the reaction rate is fast, which means the concentration of the halide must always be high, so that the base is the limiting reagent. Nonetheless, re-deposition of large clusters onto the surface of the solid precatalyst (Pd/SiO_2) was detected.

Schimdt et al. dealt with the autocatalytic process of NPs growth. They found that deposition and leaching of Pd(0) species onto nanoparticles was in equilibrium under certain condition [416].

In Reimann's study, soluble Pd species appeared undetectable by EXAFS, even though the authors accepted their presence in the medium. Since no proof about effective activity of nanoparticles was provided, it was still dubious whether to entitle them with the catalytic role or molecular Pd(0) [32].

Hence, the engineering aspect gains some importance, once the "location" of the real reaction has been pointed out: a flow reactor necessarily varies its set up between a reaction taking place in solution or onto a surface [162]. In particular, a pure heterogeneous catalyst, in a different phase from the reaction medium, would help facilitating the recovery and the continuous-flow handling [392].

Nanoparticles are capable of leaching molecular Pd-moieties, acting as Pd reservoirs. It was reported as an example that, in the presence of nanocrystals leaching has been demonstrated to be geometrically-directed. For instance, Pd appeared more easily leached from {100} facets than from {111} ones. Similar mechanisms have to be hypothesized in case of re-deposition processes [158].

Bradley et al. studied the Heck coupling of *p*-bromobenzaldehyde and butyl acrylate catalyzed by PVP-stabilized PdNPs [417]. The authors found that the reaction rate correlated with the amount of surface defects of colloids more than to the availability of active sites, and that it raised when decreasing colloids dimension. They interpreted the evidence as if PdNPs were the only active species in solution and the reaction occurred at the surface. Otherwise, surface defects might be seen as preferential leaching sites for solubilization of true active molecular species [18, 286].

Superficial disorder of nanoparticle's surface was addressed as a source of more significant leaching [418]. Small clusters are more likely to leach from disordered nanosurfaces and act as reservoirs of molecular Pd. These species were found to be more reactive than the ordered cores.

It is note-worth that the NPs' PSD changed during some reactions, due to leaching and sintering. In general, it is now assumed that even without detecting actual dimension change of nanoparticles, however catalysis may easily occur in solution due to the enormous activity of homeopathic Pd [419].

Some further studies about PVP-capped PdNPs' influence of size on activity, revealed that the real correlation was between reaction rate and low coordination edge and vertex atoms rather than with the nanoparticle size [420]. Some other researchers studied the effect of treatments on nanoparticle size, e.g. flushing with solvent, or solvent/reagent or reactive medium [345]. They found that whatever the treatment, the PSD broadened and a higher mean size was found. Hence, they explained the evidence with Ostwald ripening occurring. During further subsequent runs, the average size appeared to decrease, and this was explained by aggregation and precipitation of Pd black.

Several mechanistic studies have been performed in order to better understand the leaching process. Hii et al. used a set of different ODEs to represent the leaching mechanisms and six PDEs to solve the cascade-reactor problem linked to their study, in order to fit a series of experimental data [392]. Methyl acrylate and iodobenzene reacted on a packed-bed reactor in DMF, in the presence of triethylamine, at different temperatures, and subsequently flowed in a plug-flow reactor.

Leaching was modeled using two different approaches: surface erosion of PdNPs or particle loss. The former represents actual leaching, based on atoms/particles solubilization, species that may establish a release-and-catch equilibrium. The latter consists of detachment of particles by cleavage of particle-support bonds. The two were mathematically introduced into the model, respectively, through equations:

$$\frac{dW_{Pd}}{dt} = -k_{leach} W_{Pd}^{\frac{2}{3}} C_1 \tag{12}$$

$$\frac{dW_{Pd}}{dt} = -k_{leach} W_{Pd} \tag{13}$$

where W_{Pd} is the weight of heterogeneous Pd; k_{leach} is the rate constant of leaching depending on the

PSD, since for spherical particles, the rate of leaching is supposed to diminish following the decrease in diameter; C_1 is the concentration of electrophylic reactant in the first reactor.
The former experiments showed that a major part of conversion was attained by the sole PFR working with leached Pd species at temperatures around 100°C, while in the PBR at room temperature no activity was detected. Besides, fixing the temperature of the PBR at 90 °C gave product-detection at the PBR's outlet, resulting in a k_{het} consistently smaller than k_{homo}. Eventually, the resulting activity did not seem to be influenced by heterogeneous catalytic activity [392].

Seldom, measures of leaching have been misinterpreted not taking into account the re-deposition process. However, some Pd species in solution have been proved to be likely to deposit back onto the carrier, especially at high conversions, as stated in [162].
In [421] the leaching process was supposed to be coupled to re-deposition, and seen as a good opportunity to perform multiple runs especially in continuous processing, thanks to low amounts of losses. Leaching and re-deposition processes are reaction-condition dependent and might be quite accelerated [422], so that further tests such as the hot filtration are faked (*vide infra*). Actually, re-deposition appeared to be highly favored, only at total conversions, thus, at the end of the reaction, and rapidly completed in the case of highly reactive aryl iodides. In addition, the re-deposition may consist of an uncontrolled process likely to form clusters on the surface which could lead to loss of active surface area. It is still open the challenge for understanding whether this loss of activity is due to surface rearrangement or Pd depletion [162].
Then, one must pay attention to the important role of "homeopathic" catalysis (*vide supra*): few ppm of leached Pd may catalyze the whole reaction in a little time reaching an excellent conversion and selectivity. Hence, the only way to assess the catalytic importance of the liquid phase is, sometimes, to calculate the resulting TOF (turn-over frequency) $[h^{-1}]$ of the sole reaction medium after removing the solid phase. Indeed, in some cases, the solid phase only acts as a reservoir of soluble and hyperactive species [423].
When hybrid reaction mechanism is supposed to happen, a cumulative TOF (TOF_{tot}) accounts for the whole catalytic activity consisting of two contributions: one from leaching and one purely heterogeneous. One should note that this value is not the simple addition of the two contributions since they refer to different quantities of catalytic sites. Thus, it often happens to find $TOF_{tot} < TOF_{leach}$. Finally, the heterogeneous contribution, if existent, has often been pointed out as negligible in term of TOFs since it was not comparable to the several hundreds of $[h^{-1}]$ of homogeneous catalysts.
Finding a way to separately measure the two and eventually rule out the minor contribution has been the subject of study of the past years.

Li et al. reported some leaching during studies on SO, SN and thiols supported on polymers and silica [271]. Similar silica-supported mercapto-hydroxyl-containing macromolecular bidentate Pd chelates showed leaching. The leaching mechanism was explained by oxidative addition of halides [424], and Pd(II) was found to re-adsorb in the absence of thiol-functionalization onto fresh polymeric supports. During Heck reactions, palladium leaching in solution appeared to be problematic only in contemporary presence of all three substrates: Iodobenzene, ethylacrylate and tributyl amine. The authors were brought to hypothesize that the cooperation of the three substrates was necessary to activate the Pd solubilization, rather than a simple equilibrium between the chelated and leached metal species. The proposed leaching scheme is depicted in Figure 46. The palladium precursor is reduced in the first step giving the common induction period measured in most couplings. Then, the three substrates aid Pd(0) leaching, thanks to the lower affinity of this reduced form to mercapto-chelating agents.

Pd(II)-exchanged perovskites leached some active Pd in the Suzuki coupling of bromoarenes and arylboronic acids [300]. This was proven by a 3-phase test and a poisoning study based on the use of a polymeric poison [425].
Srinivas, Ratnasamy and colleagues detected leached species coming from Pd-silicoaluminophosphate SAPO-31 used in Heck couplings [426]. These species redeposited at total conversion.
Studies on mordenite, Y and ZSM-5 zeolites showed really low amounts of Pd leached even in the

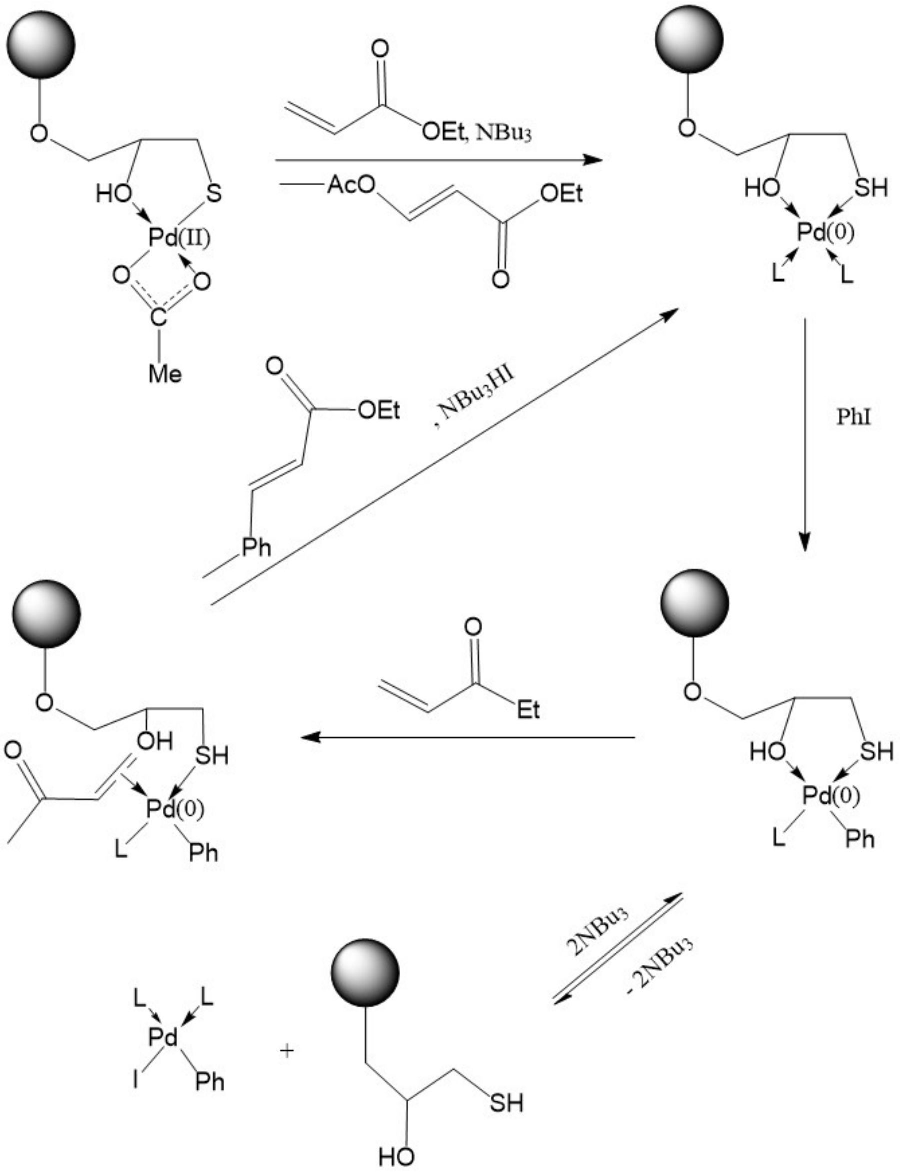

Figure 46: Thiol-based macromolecular bidentate Pd-chelating agent leaching scheme according to [16].

presence of polar solvents [296]. In [147], zeolites were tested, too. The reactions resulted in non-negligible amounts of Pd leached in polar solvents. Though, working with toluene and tributylamine was a good way to access true heterogeneous zeolites, but leading to lower reaction rates. Other studies on zeolites remarkably reported that calcination led to catalysts more likely to leach Pd species, while precatalysts containing Pd(0) nanoparticles coupled to tetrabutylammonium compounds seemed to work heterogeneously due to NPs stabilization [167, 168, 170].
Djakovitch and Rollet dealt with Pd-NH_4-Y zeolites catalyzing some Sonogashira couplings. The hot filtration test reported the evidence of leaching related to slow reaction rates [427]. In an opposite trend were the studies of Davis and co-workers who exploited ICP analyses, poisoning studies and split-test to assess the influence of leached species from Pd(II)-exchanged Y zeolites on the conversion of iodobenzene, under Heck conditions [163]. The authors stated that the great majority of the conversion was obtained thanks to the activity of soluble species. Finally, a release-and-catch process was theorized for zeolite-based catalysts and is mechanistically consistent with the general cycle proposed de Vries in [26]. "Homeopathic" palladium is leached in solution under reaction conditions and re-deposited onto the precatalyst surface depending on the progress in the reaction conversion . Thus, TOFs increase when the Pd loading onto the carrier decreases[18, 26].

Then, the group of Vaccaro studied a $10\%_{wt}$ palladium supported on highly cross-linked imidazolium-based catalyst for the Suzuki-coupling of 4-bromotoluene at 50°C. Four consecutive tests were performed, leading to a final yield in product of 95%, $TON = 3800$ and $TOF_{tot} = 26[h^{-1}]$. Actually, $0,015\%_{wt}$ of the precatalyst was detected in solution, corresponding to a calculated TOF_{leach} of $176,000[h^{-1}]$ [342]. The same group studied PdNPs supported on zirconium phosphate glycine diphosphonate nanosheets (Pd/ZPGly-15) for the reaction of 4-bromoanisole for 3 catalytic cycles. The two experiments were discussed on the base of an efficient "release-and-catch" mechanism, in order to explain the lack of active Pd detection in solution [428, 429].
An interesting evidence of leaching was provided by the group of Crudden. They catalyzed the reaction of 4-iodo-nitrobenzene and phenylboronic acid at 100°C with a Pd foil without stirring. The conversion reached was 45% and the mean TOF_{leach} amounted to 2000 $[h^{-1}]$. The absence of stirring causing a not-negligible mass transfer resistance, the conversion was low. The catalyst showed pitting when analyzed with SEM and EDXS, which was explained by leaching, and by the presence of iodine, nitrogen and oxides on the foil surface [430]. The group also proved the release-and-catch mechanism of Pd onto solid supports.
Felpin and colleagues prepared Au/Pd alloys in order to protect nanoparticles from leaching [431]. The authors found amounts of leached Pd four times lower than common catalysts. Later on, Pd@Au core-shell nanostructures were studied and used for catalysis in only-water solvent [156]. The authors hypothesized a true heterogeneous catalytic process. Several others authors worked on Pd@Au core-shell NPs showing that leaching could be tuned depending on the number of layers covering the Au-nanoparticle core [430].
However, the issue whether it does exist a consistent heterogeneous contribution in running such reactions and above all if it is possible to separate from the homogeneous contribution, is still open. Many studies on putative pure heterogeneous catalysts were misled by detection limits and lack of knowledge about re-deposition processes, and sometimes the authors themselves chose to neglect consistent amounts of catalyst leached and giving raising value of TOF and TON, as reported in [162].

In the case of the NHC-Pd(II) complexes studied by Herrmann et al. [275], the differences between solid catalysts and homogeneous counterparts seem to support a truly heterogeneous reaction mechanism, based on a negative filtration test, too. Though, Pd-losses were evident after several consecutive runs. Moreover, in similar studies on NHC ligands induction periods were measured and were explained by the reduction of immobilized Pd(II) to active Pd(0).
Some groups interestingly, found that thiol-groups were able to capture Pd(0) labile species leaching in solution and to prevent this phenomenon. In particular, the studies concentrated on the Pd-scavenging properties of thiols after decomposition of palladacycles and subsequent heterogeneous cross-couplings of aryl chlorides [395, 432]. The discussion is still open, since evidence of decomposition of palladacycles was reported but no significant change in the Pd loading were proven.
In [433], no clue was found about heterogeneous-site activity, even though thiols appeared to work well as scavengers. Later on, a comprehensive study by Shimizu et al. was published. The authors tested a variety of metallated solid carriers such as mercaptopropryl-functionalized mesoporous and amorphous silica, unfunctionalized mesoporous silica and NaY zeolites and compared them to commercial Pd/C. The samples were characterized both before and after reaction thanks to different microscopy techniques. The reaction kinetics and recyclability of the catalysts were also studied. The thiol-containing system was synthesized in order to ensure a sulfur-site excess on the surface (S:Pd=1:0.36). This system was analyzed by X-ray absorption spectroscopy (EXAFS and XANES), UV-vis spectroscopy and X-ray diffraction, showing that Pd(II) species covered almost uniformly the surface and were ligated to two or more thiol groups, similarly to the sample of Pd(II) on thiol-functionalized amorphous silica. $Pd(OAc)_2$ on silica had a similar structure to its homogeneous counterpart, while Pd/C was mostly covered by Pd(II) in form of palladium oxide. The systems catalyzed the Suzuki coupling of 4-bromoanisole and phenylboronic acid and were re-characterized. The zeolites and Pd/C were almost fully reduced to Pd(0) species, while the silica samples contained a majority of Pd(II) with formation of some nanoparticles. Furthermore, Pd on zeolites leached the most of Pd in solution (6%), while mesoporous Pd-silica the least (0.05%). The Pd precatalyst on mesoporous silica gave good TONs and

TOFs of 73000 and 36000 [h^{-1}], corresponding to five consecutive runs of the Heck reaction.
The role of thiol groups was explained by the authors as a hindrance to Pd(0) nanoclusters leaching. Crudden's group supported the hypotheses of Shimizu [395, 432] regarding the pure heterogeneous catalysis related to thiol-functionalized mesoporous silica Pd, while Davis et al. led similar studies concluding that all conversion took place in solution [163]. Supporting continuous-flow chemistry, filtration test and ICP analyses were performed before formulating such a theory.
The group also effectuated a control experiment on each catalyst by flushing the solid with DMF at 353 K for a certain time. No Pd leaching was detected in this condition, so that the authors concluded that leaching was not caused by weakly-bonded physisorbed Pd. Finally, the effect of the solvent was assessed. Conversion in non-polar toluene appeared to plummet dramatically and the solvent gave more significant induction periods, whatever the catalyst. Leaching was lower in toluene than in DMF, as well.

Leaching can be controlled by tuning the properties of the reaction medium (e.g. pH, solvent, pressure, temperature), by changing the catalytic material and technology, by pre-treatments, washing and surface modifications, but also leaching is less likely when the reaction is performed in gas phase [372]. For instance, pre-treatments of pristine PdEnCat and Pd/Al_2O_3 made conversion more reproducible, since in the former case, not all the Pd(II) was reduced, and this gave little peaks of conversion followed by decay. Furthermore, ultrasounds appeared to favor leaching [372].
In 2006-2007 Rothenberg and co-workers studied a reacting system containing a nanofiltration membrane and conducting Heck couplings. Substrates were present in both the compartments while the base and the Pd precatalyst were separated. The authors found that some molecular Pd species were able to cross the membrane and underwent reaction in the non-containing Pd compartment. They assumed that two leaching mechanisms took place: one, the most known and described due to oxidative addition, causing leaching of complexated Pd(II) species; the second one involving unstable Pd(0) species which were likely to coalesce into nanoclusters [391, 434]. This latter mechanism occurred in non-oxidizing conditions, and Pd(0) species formed were undetectable with TEM before coalescence. The choice of the solvent appeared to influence the extent of leaching coming from one or the other mechanism.
In 2013, Leyva-Pérez published a comprehensive study explaining the correlation between these two mechanisms and the catalytic activity [435]. They supported the theory for which during reaction Pd(II) NPs are formed and act as reservoirs of active Pd species, whatever the precatalyst (namely Pd complexes, salts, nanoparticles or Pd/C). They also noted that the presence of hard bases increased significantly the reactivity of the precatalysts, causing higher amounts of leaching and formation of 3-4 atoms nanoclusters. In the presence of these hard Lewis bases, it is evident that they are Pd(0) species to be leached, while Pd(II) moieties are solubilized during a process linked to oxidative addition.
Reimann et al. studied the Heck coupling of bromobenzene and styrene in NMP at 150°C, with NaOAc·$3H_2O$ as the base and Pd/SiO_2 as precatalyst. The authors divided the process in three phase, namely heating of the system, reaction and inactive phase. During the first phase leaching was detected only starting from 140°C and was almost stopped at 150°C. The active phase started at 150°C and stopped after .ca 50 *min* due to the consumption of the base. The products were mainly *trans*- and *cis*-stylbene with traces of biphenyl and α-phenylstyrene. The authors finally stated the reaction was effectively catalyzed by soluble Pd species [78]. In addition, the heating phase was effective in the reduction of PdO to metal Pd and nanoparticles formation (2 nm), while the final phase caused the growth of the nanoparticles (5 nm). EXAFS, XANES and STEM analyses were conducted to draw such conclusions. Eventually, the authors inferred the PdNPs to be the only active species in the medium . They acted like good scavengers of Pd(0) species leached from the solid support.

9 Density Functional Theory (DFT)

We mentioned before several works exploiting DFT calculations for molecular properties assessment. These type of studies concentrate on the relativistic and non-relativistic effects of electrons interaction, in order to obtain energy values which explain the reaction mechanisms, and much more. Indeed, molecules, complexes in our case, are studied from geometrical and energetic point of views, in order to point out the most likely association-dissociation pathways which lead to the cross-coupling product. For this purpose, a large spectrum of softwares have been developed, namely *Gaussian* and *Turbomole*. Implemented within the software, numerical methods allow to approximate quantum mechanics laws and to calculate ground and excited states of molecules involved in micro- and macroscopic transformations.
Herein, we aim to give a brief mathematical explanation of what a DFT study consists of and is based on.

An electron moving around a nucleus is named a *quantum state* ($|\Psi\rangle$), which is a mathematical entity, namely an abstract Hilbert space, connected to a probability distribution of some key quantities, changing at each measurement. Indeed, according to the Heisenberg's uncertainty principle, position and momentum, which are key variables describing the electron motion around a nucleus, can not be unequivocally determined, at the same time. When trying to describe the dynamical state of such particles, the uncertainty about the measurements of one quantity raises proportionally to the assessment precision of the other. The principle is expressed by the law [436]:

$$\sigma_x \sigma_p \geq \frac{\hbar}{2} \tag{9.14}$$

where σ_x and σ_p are standard deviations of position (x) and momentum (p), and $\hbar$ the reduced Planck's constant ($h/2\pi$).
A wave function (ψ) is always associated to a quantum state for the description of its dynamics, which is governed by the Hamilton operator ($\hat{\mathbf{H}}$). In addition, this wave function can be either symmetric (i.e. bosons) or antisymmetric (i.e. fermions) for particles of the same nature. As for the electrons, a switch in their coordinates (j and i) makes their wave function change in sign, because of its antisymmetry. Therefore, the time-evolution of a quantum state is given by the time-dependent Schrödinger's equation [437]:

$$-\frac{\hbar}{i}\frac{\partial}{\partial t}|\Psi\rangle = \hat{\mathbf{H}}|\Psi\rangle \tag{9.15}$$

[11] and its stationary state can be obtained by solving the eigenvalue problem:

$$\hat{\mathbf{H}}|\Psi\rangle = |\Psi\rangle E, \qquad \langle\Psi|\Psi\rangle = 1. \tag{9.16}$$

The strategy to computationally face the Schrödinger's equation for fermions is to adopt the variational principle, which delivers the ground stationary state, or state of minimum energy E_0. Hence, the principle states that for any arbitrary wave function of guess (Ψ_{trial}), the expectation value of $\hat{\mathbf{H}}$ will be an upper bound of the ground state:

$$\langle\Psi_{trial}|\hat{\mathbf{H}}|\Psi_{trial}\rangle = E_{trial} \geq E_0 = \langle\Psi_0|\hat{\mathbf{H}}|\Psi_0\rangle\,. \tag{9.17}$$

This notation introduces the definition of functional, which associates a number, e.g. E_{trial}, with a function, e.g. Ψ_{trial}. Thereby, the expectation value, e.g. $\langle\Psi_{trial}|\hat{\mathbf{H}}|\Psi_{trial}\rangle$, is a functional.
The aim of the variational principle is to find among all acceptable N-electron wave functions, the one that minimizes the quantum state's energy and describe its stationary ground state:

$$E_0 = \min_{\Psi\to N} H[\Psi] = \min_{\Psi\to N} \langle\Psi_0|\hat{\mathbf{H}}|\Psi_0\rangle\,. \tag{9.18}$$

---

[11] The Dirac's Bra-ket notation makes use of angle brackets and vertical bar to simplify the notation for the description of quantum states, in quantum mechanics. The $\langle f|$ notation denotes a linear functional $f : V \to \mathbb{C}$ which associates a generic vector of the space $\mathbf{V}$ to a value in the complex plane $\mathbb{C}$. Besides, the $|v\rangle$ denotes the generic vector of the space $\mathbf{V}$

Though, this research among all suitable functions carries too much mathematical effort. Some simplifications must be done. Most of times, a subset of eligible functions is chosen to simplify the problem, but one should consider that the solution is going to be approximated, if the subset does not contain the real solution. This is the case of the Hartree-Fock approximation (*vide infra*).

For a many-body system, constituted of M nuclei and N electrons, the Hamiltonian operator is a differential operator, representing the energy of the quantum state, of the type [438]:

$$\hat{\mathbf{H}} = -\frac{1}{2}\sum_{i=1}^{N}\boldsymbol{\nabla}_i^2 - \frac{1}{2}\sum_{A=1}^{M}\frac{1}{M_A}\boldsymbol{\nabla}_A^2 - \sum_{i=1}^{N}\sum_{A=1}^{M}\frac{Z_A}{r_{iA}} + \sum_{i=1}^{N}\sum_{j>i}^{N}\frac{1}{r_{ij}} + \sum_{A=1}^{M}\sum_{B>A}^{M}\frac{Z_A Z_B}{R_{AB}}. \tag{9.19}$$

If no external magnetic or electric field is applied. The first two terms represent the kinetic energy of electrons and nuclei, while the remaining three, the interaction potentials.
The operator can be simplified if one considers the electrons moving in a structure of fixed nuclei, whose kinetic energy is thus, null, and potential energy almost constant:

$$\hat{\mathbf{H}}_e = -\frac{1}{2}\sum_{i=1}^{N}\boldsymbol{\nabla}_i^2 - \sum_{i=1}^{N}\sum_{A=1}^{M}\frac{Z_A}{r_{iA}} + \sum_{i=1}^{N}\sum_{j>i}^{N}\frac{1}{r_{ij}} = \hat{\mathbf{T}} + \hat{\mathbf{V}}_{Ne} + \hat{\mathbf{V}}_{ee} \tag{9.20}$$

where $\hat{\mathbf{T}}$ is the kinetic energy operator, $\hat{\mathbf{V}}_{Ne}$ is the external potential imposed by the nuclei position and charge and depends upon the considered molecule, and $\hat{\mathbf{V}}_{ee}$ is the interaction potential among electrons.
Once obtained the expression of the Hamiltonian operator, the path to follow in order to find the ground state, is to iteratively calculate $\hat{\mathbf{H}}$ given {N, Z_A, R_A}, guess a Ψ_{trial}, calculate E as the eigenvalue of $\hat{\mathbf{H}}\,|\Psi\rangle$ and finally find the new Ψ_{trial}, till E reaches the ground state.

9.1 Hartree-Fock Approximation

In order to find an appropriate solution to the problem, testing all N-electron wave functions is not feasible. For this reason, the Hartree-Fock approximation was introduced. It consists of taking a series of antisymmetric one-electron wave functions ($\chi_i(\vec{\mathbf{x}}_i)$) and constructing a suitable N-electron wave function-approximating product, known as Slater determinant (Φ_{SD}):

$$\Psi_0 \approx \Phi_{SD} = \frac{1}{\sqrt{N!}}\begin{vmatrix} \chi_1(\vec{\mathbf{x}}_1) & \chi_2(\vec{\mathbf{x}}_1) & \cdots & \chi_N(\vec{\mathbf{x}}_1) \\ \chi_1(\vec{\mathbf{x}}_2) & \chi_2(\vec{\mathbf{x}}_2) & \cdots & \chi_N(\vec{\mathbf{x}}_2) \\ \vdots & \vdots & & \vdots \\ \chi_1(\vec{\mathbf{x}}_N) & \chi_2(\vec{\mathbf{x}}_N) & \cdots & \chi_N(\vec{\mathbf{x}}_N) \end{vmatrix}. \tag{9.21}$$

The one-electron wave functions $\chi_i(\vec{\mathbf{x}}_i)$ are known as *spin orbitals* and composed by a spatial function $\phi_i(\vec{\mathbf{r}})$ and a spin one, $\sigma(s) = \alpha(s), \beta(s)$ [438], where:

$$\chi(\vec{\mathbf{x}}) = \phi(\vec{\mathbf{r}})\sigma(s). \tag{9.22}$$

Indeed, according to Schrödinger's formalism, by definition [437]:

$$\vec{\mathbf{x}} = f(\vec{\mathbf{r}}, s)\bigg|\int dx = \sum_s \int d^3r. \tag{9.23}$$

In addition the spin functions α and β are orthonormal ($\langle\alpha|\alpha\rangle = 1$, $\langle\beta|\beta\rangle = 1$ and $\langle\alpha|\beta\rangle = \langle\beta|\alpha\rangle = 0$) that is why the pre-factor $\frac{1}{\sqrt{N!}}$ is present in the determinants expression.

Now, the Hamiltonian expectation value assumes the form [438]:

$$E_{HF} = \langle \Phi_{SD} | \hat{\mathbf{H}} | \Phi_{SD} \rangle = \sum_{i}^{N} (i|\hat{\mathbf{h}}|i) + \frac{1}{2} \sum_{i}^{N} \sum_{j}^{N} (ii|jj) - (ij|ji) \tag{9.24}$$

where

$$(i|\hat{\mathbf{h}}|i) = \int \chi_i^*(\vec{\mathbf{x}}_1) \left\{ -\frac{1}{2}\boldsymbol{\nabla}^2 - \sum_{A}^{M} \frac{Z_A}{r_{1A}} \right\} \chi_i(\vec{\mathbf{x}}_1) d\vec{\mathbf{x}}_1 \tag{9.25}$$

represents the kinetic energy and electron-nucleus attractive interaction and:

$$(ii|jj) = \int\int |\chi_i(\vec{\mathbf{x}}_1)|^2 \frac{1}{r_{12}} |\chi_j(\vec{\mathbf{x}}_2)|^2 d\vec{\mathbf{x}}_1 d\vec{\mathbf{x}}_2 \tag{9.26}$$

$$(ij|ji) = \int\int \chi_i(\vec{\mathbf{x}}_1)\chi_j^*(\vec{\mathbf{x}}_1) \frac{1}{r_{12}} \chi_j(\vec{\mathbf{x}}_2)\chi_i^*(\vec{\mathbf{x}}_2) d\vec{\mathbf{x}}_1 d\vec{\mathbf{x}}_2 \tag{9.27}$$

represent the interaction between two electrons and are called *Coulomb* and *exchange* integrals. These last two terms can be simplified by taking an average value of them, and transforming into one-electron terms, complex two-electron functions. The *i-th* electron is now subject to an average value of the repulsion contribution given by the remaining N-1 electrons.
Then, the electron-electron interaction term is, on the whole:

$$V_{HF}(\vec{\mathbf{x}}_1) = \sum_{j}^{N} (\int |\chi_j(\vec{\mathbf{x}}_2)|^2 \frac{1}{r_{12}} d\vec{\mathbf{x}}_2 - \hat{\mathbf{K}}_j(\vec{\mathbf{x}}_1)) \tag{9.28}$$

where the exchange operator ($\hat{\mathbf{K}}$) has no classical interpretation and is defined only on the base of its effect on a spin orbital $\chi_i(\vec{\mathbf{x}}_1)$:

$$K_j(\vec{\mathbf{x}}_1) = \int \chi_j^*(\vec{\mathbf{x}}_2) \frac{1}{r_{12}} \chi_i(\vec{\mathbf{x}}_2) d\vec{\mathbf{x}}_2 \chi_j(\vec{\mathbf{x}}_1). \tag{9.29}$$

It represents the repulsion between electrons due to their spin, which hinders them from collapsing into an inner shell and accounts for the Pauli exclusion principle. The integration over $\vec{\mathbf{x}}_2$ makes it depend upon all the position of the N-1 electrons at each instant. Thus, the operator is *non-local.* In addition it exists only for electrons of equal spin and is due to the antisymmetry of fermions, a family of subatomic particles to which electrons belong.
On last important property is that the exchange term gets rid of the electrostatic self-interaction contribution allowed in the Coulomb term (for i=j), which is physically non-sense.
The whole Hartree-Fock theory gives a *pseudo-eigenvalue* problem, since the equivalent of the Hamilton operator is spin orbital-dependent, which can be solved with a *self-consistency field* (SCF) technique (*vide infra*).

Noteworthy, one Slater determinant never represents exactly a N-electron wave function. A precise linear combination of Slater determinants does. This fact introduces an error in the calculation of the ground state, through the Hartree-Fock approximation. The difference between the two energies, exact ground state E_0 and Hartree-Fock energy E_{HF}, is called *correlation energy* [438]:

$$E_C^{HF} = E_0 - E_{HF} \tag{9.30}$$

This term mainly accounts for the instantaneous interaction among electrons which is not counted in the HF theory. Indeed, the theory allows the electrons to approach too much, more than physically allowed.
In addition, the resulting ground Slater determinant sometimes is not the only possible solution, because other determinants have similar energies and might well approximate the ground state energy.

It is now important to introduce the key DFT quantity: the electron density ($\rho(\vec{\mathbf{r}})$). It is defined as:

$$\rho(\vec{\mathbf{r}}) = N \int \cdots \int |\Psi(\vec{\mathbf{x}}_1, \vec{\mathbf{x}}_2, \cdots, \vec{\mathbf{x}}_N)|^2 ds_1 d\vec{\mathbf{x}}_2 \cdots d\vec{\mathbf{x}}_N \tag{9.31}$$

and represents the probability of finding one of the N electrons within the volume element $d\vec{\mathbf{r}}_1$ with arbitrary spin, while the other N-1 electrons are dispersed arbitrarily in the space, with arbitrary spin. This electron density will have discontinuities, due to the Coulomb term $-Z_A/r_{1A}$, at the nuclei positions. It also decays at infinite distances from the nuclei.

In order to account for all electron interactions, a two-electron density can be defined:

$$\rho_2(\vec{\mathbf{x}}_1, \vec{\mathbf{x}}_2) = N(N-1) \int \cdots \int |\Psi(\vec{\mathbf{x}}_1, \vec{\mathbf{x}}_2, \cdots, \vec{\mathbf{x}}_N)|^2 d\vec{\mathbf{x}}_3 \cdots d\vec{\mathbf{x}}_N = \frac{N-1}{N} \rho(\vec{\mathbf{x}}_1)\rho(\vec{\mathbf{x}}_2). \tag{9.32}$$

One may also define a *reduced density matrix*, of which ρ represents the diagonal:

$$\gamma_2(\vec{\mathbf{x}}_1, \vec{\mathbf{x}}_2, \vec{\mathbf{x}}_1', \vec{\mathbf{x}}_2) = N(N-1) \int \cdots \int \Psi(\vec{\mathbf{x}}_1, \vec{\mathbf{x}}_2, \vec{\mathbf{x}}_3, \cdots, \vec{\mathbf{x}}_N)\Psi^*(\vec{\mathbf{x}}_1', \vec{\mathbf{x}}_2', \vec{\mathbf{x}}_3, \cdots, \vec{\mathbf{x}}_N) d\vec{\mathbf{x}}_3 \cdots \vec{\mathbf{x}}_N. \tag{9.33}$$

This quantity allows to more easily account for the antisymmetry of the wave functions, since an inversion of coordinates $\vec{\mathbf{x}}_1$ and $\vec{\mathbf{x}}_2$ (or $\vec{\mathbf{x}}_1'$ and $\vec{\mathbf{x}}_2'$) changes the sign of the term of the γ_2 matrix.

The density matrices allow to reduce the computational effort while solving the Shrödinger's equation, which passes from a dependence on 4N variables (3 spatial and one spin for each electron) to eight (3+1 for two electrons).

For instance, Thomas and Fermi drew a very simple model for the energy functional which exploits the density, and is based on the uniform electron gas model [438].

9.2 Exchange-correlation energy

Electrons are charged particles which are hindered from approaching due to this property. This effect is independent from their spin. We define this electrostatic effect, *Coulomb correlation*, and the one produced by electron's spin *Fermi correlation.*

According to the Hartree-Fock approximation, the two-electron density will be [438]:

$$\rho_2^{HF}(\vec{\mathbf{x}}_1, \vec{\mathbf{x}}_2) = [det\{\phi_1(\vec{\mathbf{r}}_1)\sigma_1(s_1)\phi_2(\vec{\mathbf{r}}_2)\sigma_2(s_2)\}]^2. \tag{9.34}$$

This yields an uncorrelated expression of the density in the case $\sigma_1 \neq \sigma_2$, which should though, draw some form of correlation, and a different value in the opposite case, which should be uncorrelated. Indeed, the electrostatic repulsion effect is not taken into account by the Hartree-Fock approximation. On the whole, the density should show an uncorrelated prefactor and a correlation contribution, containing both antiparallel-spin electrons correlation and electrostatic repulsion:

$$\rho_2(\vec{\mathbf{x}}_1, \vec{\mathbf{x}}_2) = \rho(\vec{\mathbf{x}}_1)\rho(\vec{\mathbf{x}}_2)[1 + f(\vec{\mathbf{x}}_1, \vec{\mathbf{x}}_2)] \tag{9.35}$$

where $f(\vec{\mathbf{x}}_1, \vec{\mathbf{x}}_2)$ is the *correlation factor.*

One can define a new quantity, named *exchange-correlation hole*:

$$h_{XC}(\vec{\mathbf{x}}_1, \vec{\mathbf{x}}_2) = \frac{\rho(\vec{\mathbf{x}}_1, \vec{\mathbf{x}}_2)}{\rho(\vec{\mathbf{x}}_1)} - \rho(\vec{\mathbf{x}}_2) = \rho(\vec{\mathbf{x}}_2) f(\vec{\mathbf{x}}_1, \vec{\mathbf{x}}_2), \qquad \int h_{XC}(\vec{\mathbf{x}}_1, \vec{\mathbf{x}}_2) d\vec{\mathbf{x}}_2 = -1. \tag{9.36}$$

The exchange-correlation hole interestingly integrates exactly the charge of one electron. It practically consists of a depletion of probability of finding other electrons around the considered one, especially if with parallel spin.

The exchange-correlation hole can be divided into two terms: *Fermi* and *Coulomb hole.* The first contribution accounts for the Pauli principle, coming from the antisymmetry of the wave function and is valid only for antiparallel electrons. The latter accounts for the electrostatic repulsion among electrons, and is not considered in the definition of the Slater determinants.

As for, the exchange term of the Hartree-Fock approximation, Slater provided an approximation, consisting of:

$$E_X = \int\int \frac{\rho(\vec{\mathbf{r}}) h_X(\vec{\mathbf{r}}_1, \vec{\mathbf{r}}_2)}{r_{12}} \tag{9.37}$$

where $h_X(\vec{\mathbf{r}}_1, \vec{\mathbf{r}}_2)$ represents the Fermi contribution to the exchange-correlation hole.
The approximation provides an expression for the exchange Fermi hole, starting from its symmetry, which is assumed spherical. If one considers a constant density within the hole, equal to the opposite of $\rho(\vec{\mathbf{r}}_1)$, and null outside, the radius of the sphere (*Wigner-Seitz radius*) will be:

$$r_S = (\frac{3}{4\pi})^{1/3} \rho(\vec{\mathbf{r}}_1)^{1/3}. \tag{9.38}$$

Hence, the exchange energy function will assume the form:

$$E_X[\rho] \simeq C_X \int \rho(\vec{\mathbf{r}}_1)^{4/3} d\vec{\mathbf{r}}_1 \tag{9.39}$$

and will only depend on the local (at $\vec{\mathbf{r}}_1$) values of the electron density.
A further, slight modification of the functional led to the definition of the Hartree-Fock-Slater (HFS) exchange energy functional, widely used in DFT calculations:

$$E_{X\alpha}[\rho] = -\frac{9}{8} (\frac{3}{\pi})^{1/3} \alpha \int \rho(\vec{\mathbf{r}}_1)^{4/3} d\vec{\mathbf{r}}_1 \tag{9.40}$$

with $2/3 \leq \alpha \leq 1$.

9.3 The Kohn-Sham Theory and Variational Principle

Hohenberg and Khon demonstrated with their first theorem, that the electron density giving a certain energy of the quantum state is unique. As a consequence, the ground state density will allow to find out all the energetic properties related to the ground state.
One can now reformulate the variational principle in terms of the Hohenberg-Kohn's notation (*Second Hohenberg-Kohn theorem* [438]:

$$E_0 \leq E[\rho_{trial}] = T[\rho_{trial}] + E_{Ne}[\rho_{trial}] + E_{ee}[\rho_{trial}], \qquad \rho_{trial}(\vec{\mathbf{r}}) \geq 0, \int \rho_{trial}(\vec{\mathbf{r}}) d\vec{\mathbf{r}} = N. \tag{9.41}$$

Thus, accoring to the Levy constrained-search, one can split the new whole ground state energy contribution into a universal term, i.e. not depending on N, Z$_A$ and R$_A$, and one functional depending on only the electron density:

$$E_0 = \min_{\rho \to N} \Big(\min_{\Psi \to \rho} \langle \Psi | \hat{\mathbf{T}} + \hat{\mathbf{V}}_{ee} | \Psi \rangle + \int \rho(\vec{\mathbf{r}}) \hat{\mathbf{V}}_{Ne} d\vec{\mathbf{r}} \Big). \tag{9.42}$$

Later on, Kohn and Sham realized that some problems of orbital-based theories, like Hartree-Fock approximation, resided in the calculation of the kinetic energy. Therefore, they introduced the concept of absolutely non-interacting one-electron set of orbitals in order to compute the non-interacting contribution to the kinetic energy, with high precision.
In the Hohenberg-Kohn expression of the variational principle:

$$E_0 = \min_{\rho \to N} \Big(F[\rho(\vec{\mathbf{r}})] + \int \rho(\vec{\mathbf{r}}) \hat{\mathbf{V}}_{Ne} d\vec{\mathbf{r}} \Big), \qquad F[\rho(\vec{\mathbf{r}})] = T[\rho(\vec{\mathbf{r}})] + J[\rho(\vec{\mathbf{r}})] + E_{si}[\rho(\vec{\mathbf{r}})] \tag{9.43}$$

where $T[\rho]$ is the universal kinetic energy of the electron, $J[\rho]$ is the Coulomb interaction between electrons and $E_{si}[\rho]$ is the Coulomb contribution accounting for the self-interaction, only $J[\rho]$ is actually

known. Contrarily, in the case of the Thomas-Fermi model, all functionals are explicit functions of the electron density, but its simplicity gave lots of problem. In particular, the simple expression for the kinetic term often resulted in molecular systems being less stable than their fragments.
Kohn and Sham took the interpretation of the Hartree-Fock approximation, from a non-interacting point of view, to solve this problem. In particular, since the Slater determinants do not account for the Coulomb interaction, they can be considered as the true wave functions of a system of uncharged electrons which are only interacting through their spins, according to a Fermi point of view, like fermions. For this system, the kinetic contribution can be exactly calculated by:

$$T_{HF} = \sum_{i}^{N} \langle \chi_i | \boldsymbol{\nabla}^2 | \chi_i \rangle \, . \tag{9.44}$$

Similarly, Kohn and Sham introduced a non-interacting reference system which, at the ground state, has the exact wave function represented by a Slater determinant (Θ_S). The new Hamilton operator may be split into the kinetic energy of the non-interacting system and an effective potential, partly accounting for the many-electron interactions:

$$\hat{\mathbf{H}}_S = -\frac{1}{2}\sum_{i}^{N} \boldsymbol{\nabla}^2 + \sum_{i}^{N} V_s(\vec{\mathbf{r}}_i). \tag{9.45}$$

This operator has its one-electron form, called Kohn-Sham operator ($\hat{\mathbf{f}}^{KS}$) and appears in the new version of the Schödinger's eigenvalue problem for the calculation of the new spin orbitals (ϕ_i):

$$\hat{\mathbf{f}}^{KS}\phi_i = \epsilon_i \phi_i, \qquad \hat{\mathbf{f}}^{KS} = -\frac{1}{2}\boldsymbol{\nabla}^2 + V_s(\vec{\mathbf{r}}). \tag{9.46}$$

Actually, the new spin orbitals are chosen in order to obtain a density which exactly equals the ground state energy of the target interacting system:

$$\rho_S(\vec{\mathbf{r}}) = \sum_{i}^{N} \sum_{s} |\phi_i(\vec{\mathbf{r}}, s)|^2 = \rho_0(\vec{\mathbf{r}}). \tag{9.47}$$

The authors also defined the new universal functional ($F[\rho]$):

$$F[\rho(\vec{\mathbf{r}})] = T_s[\rho(\vec{\mathbf{r}})] + J[\rho(\vec{\mathbf{r}})] + E_{XC}[\rho(\vec{\mathbf{r}})], \qquad E_{XC}[\rho(\vec{\mathbf{r}})] = T_C[\rho(\vec{\mathbf{r}})] + E_{si}[\rho(\vec{\mathbf{r}})]. \tag{9.48}$$

The functional E_{XC} now contains all the unknown contributions coming from the interaction, namely the kinetic energy of the interacting system, as well as, the self-interaction and the exchange and correlation terms of potential energy.
We now can provide the explicit form of the Kohn-Sham energy functional:

$$\begin{aligned} E[\rho(\vec{\mathbf{r}})] &= F[\rho(\vec{\mathbf{r}})] + E_{Ne}[\rho(\vec{\mathbf{r}})] \\ &= T_S[\rho(\vec{\mathbf{r}})] + J[\rho(\vec{\mathbf{r}})] + E_{XC}[\rho(\vec{\mathbf{r}})] + E_{Ne}[\rho(\vec{\mathbf{r}})] \\ &= T_S[\rho(\vec{\mathbf{r}})] + \frac{1}{2}\int\int \frac{\rho(\vec{\mathbf{r}}_1)\rho(\vec{\mathbf{r}}_2)}{r_{12}} d\vec{\mathbf{r}}_1 d\vec{\mathbf{r}}_2 + E_{XC}[\rho(\vec{\mathbf{r}})] + \int \rho(\vec{\mathbf{r}}) V_{Ne} d\vec{\mathbf{r}} \\ &= -\frac{1}{2}\sum_{i}^{N} \langle \phi_i | \boldsymbol{\nabla}^2 | \phi_i \rangle + \frac{1}{2}\sum_{i}^{N}\sum_{j}^{N} \int\int |\phi_i(\vec{\mathbf{r}}_1)|^2 \frac{1}{r_{12}} |\phi_j(\vec{\mathbf{r}}_2)|^2 d\vec{\mathbf{r}}_1 d\vec{\mathbf{r}}_2 \\ &+ E_{XC}[\rho(\vec{\mathbf{r}})] - \sum_{i}^{N} \int \sum_{A}^{M} |\phi_i(\vec{\mathbf{r}}_1)|^2 d\vec{\mathbf{r}}_1. \end{aligned} \tag{9.49}$$

One may use this functional to solve the variational principle together with the orthonormalization condition $\langle \phi_i | \phi_i \rangle = \delta_{ij}$.
The approach is exact and in principle, yields the exact ground state density and energy. The error appears when the unknown E_{XC} is approximated.

9.4 Exchange-correlation functionals

Before talking about the exchange-correlation energy (E_{XC}), one needs to understand the role and expression of the correlation kinetic term (T_C). To do this, the so-called adiabatic connection has been introduced. It consists of connecting the non-interacting and interacting systems through a parameter $0 \leq \lambda \leq 1$, where the latter also accounts for the neglected Coulomb interaction, proportional to $1/r_{ij}$. Accordingly [438]:

$$\hat{\mathbf{H}}_\lambda = \hat{\mathbf{T}} + V^\lambda_{ext} + \lambda \sum_i^N \sum_{j>i}^N \frac{1}{r_{ij}}. \tag{9.50}$$

One can compute the energy of the interacting system as:

$$E_{\lambda=1} - E_{\lambda=0} = \int_0^1 dE_\lambda \tag{9.51}$$

The differential energy is actually the expectation value of the differential of the Hamilton operator:

$$\begin{aligned} dE_\lambda &= \langle \phi_i | d\hat{\mathbf{H}} | \phi_i \rangle \\ &= \langle \phi_i | dV^\lambda_{ext} + d\lambda \sum_i^N \sum_{j>i}^N \frac{1}{r_{ij}} | \phi_i \rangle \\ &= \int \rho(\vec{\mathbf{r}}) dV^\lambda_{ext} d\vec{\mathbf{r}} + \frac{1}{2} d\lambda \int\int \frac{\rho(\vec{\mathbf{r}}_1)\rho(\vec{\mathbf{r}}_2)}{r_{12}} d\vec{\mathbf{r}}_1 d\vec{\mathbf{r}}_2 \\ &+ \frac{1}{2} \int\int\int_0^1 \frac{\rho(\vec{\mathbf{r}}_1) h^\lambda_{XC}(\vec{\mathbf{x}}_1, \vec{\mathbf{x}}_2)}{r_{12}} d\vec{\mathbf{x}}_1 d\vec{\mathbf{x}}_2 d\lambda. \end{aligned} \tag{9.52}$$

After applying some considerations, one obtains:

$$E_{\lambda=1} = T_S + \int \rho(\vec{\mathbf{r}}) V_{eff} d(\vec{\mathbf{r}}) + \frac{1}{2} \int\int \frac{\rho(\vec{\mathbf{r}}_1)\rho(\vec{\mathbf{r}}_2)}{r_{12}} d\vec{\mathbf{r}}_1 d\vec{\mathbf{r}}_2 + \frac{1}{2} \int\int \frac{\rho(\vec{\mathbf{r}}_1) \bar{h}^\lambda_{XC}(\vec{\mathbf{x}}_1, \vec{\mathbf{x}}_2)}{r_{12}} d\vec{\mathbf{x}}_1 d\vec{\mathbf{x}}_2. \tag{9.53}$$

What happens is that $\bar{h}_{XC}(\vec{\mathbf{x}}_1, \vec{\mathbf{x}}_2)$ now contains the kinetic correlation term T_C.

The earliest and most exploited approximations of the exchange-correlation functional is the Local Density Approximation (LDA). This is not the most accurate but represents the departure for many further exchange-correlation functional approximation. It is based on the uniform electron gas model [12], mostly employed for metals. According to this model, the electron density is finite and constant everywhere, a scenario which is not suitable for molecular systems, for which density instantaneously varies significantly. Though, for this model, the exchange and correlation functional is often known exactly.

Firstly, the functional is written in the following form:

$$E^{LDA}_{XC} = \int \rho(\vec{\mathbf{r}}) \epsilon_{XC}(\rho(\vec{\mathbf{r}})) d\vec{\mathbf{r}} \tag{9.54}$$

where ϵ_{XC} is the exchange-correlation energy per particle within a uniform gas of density $\rho(\vec{\mathbf{r}})$. Furthermore, the term can be split into two: exchange ($\epsilon_X(\rho(\vec{\mathbf{r}}))$) and correlation ($\epsilon_C(\rho(\vec{\mathbf{r}}))$) contributions. According to the LDA, the former is similar to the one found by Slater and discussed above, and gives the $\rho^{4/3}$ dependence. More precisely:

$$\epsilon_X = -\frac{3}{4}(\frac{3\rho(\vec{\mathbf{r}})}{\pi})^{1/3}. \tag{9.55}$$

As for the correlation term, no exact analytical expression is known, but several interpolation studies gave accurate results.

---

[12] Electrons are supposed to move within a uniform and repetitive framework of positively-charged nuclei, where the ensemble is neutral

The works from Vosko et al. [439] and Perdew et al. [440] are the most known and contributed to the definition of Gaussian's VWN implemented correlation functional.
One main shortcoming of the LDA approximation is the overestimation of the atom binding energy, giving higher atomization energy barriers [438].

Later on, local approximations were introduced in order to account for local density fluctuations. The earliest idea was to introduce information about the gradient of the electron density ($\boldsymbol{\nabla}\rho(\vec{\mathbf{r}})$) to the expression of the approximation. This new model is known as *Generalized Gradient Approximation* (GGA). The structure of the expression consists of a Taylor expansion at the first order, of the uniform electron density.
Unfortunately, the first version of the GGA, the *Gradient Expansion Approximation* (GEA), often underperformed due to the loss of meaning of the exchange-correlation hole. In particular, the exchange hole appeared sometimes non-negative.
In order to correct these non-sense, all these positive components were set to zero. The following equations represent the GGA expression:

$$\begin{aligned} E_{XC}^{GGA} &= E_X^{GGA} + E_C^{GGA} \\ &= \Big(E_X^{LDA} - \sum_{\sigma=\alpha,\beta} \int F(s_\sigma)\rho_\sigma^{4/3}(\vec{\mathbf{r}})d\vec{\mathbf{r}}\Big) + E_C^{GGA} \end{aligned} \tag{9.56}$$

where s_σ is the reduced density gradient, defined as:

$$\frac{|\boldsymbol{\nabla}\rho_\sigma(\vec{\mathbf{r}})|}{\rho_\sigma^{4/3}(\vec{\mathbf{r}})} \tag{9.57}$$

and accounts for the density fluctuations.
One expression for the $F(s_\sigma)$ term of the GGA approximation, was proposed by Becke et al. [441]:

$$F^{B88} = \frac{\beta s_\sigma^2}{1 + 6\beta s_\sigma sinh^{-1} s_\sigma}, \qquad \beta = 0.0042 \tag{9.58}$$

Among all functionals containing this approach, one important Gaussian's exchange functional is noteworth: PW91, by Perdew [442] and Wang [23].
In theory, all exchange functionals can be combined with correlation ones to obtain a valid approximation of the exchange-correlation energy functional. For instance, one extremely used functional was the Gaussian's BLYP composed by the exchange functional proposed by Becke [441] and a correlation contribution by Lee, Yang and Parr [443]. Alternatively, one interesting application, is that of hybrid functionals, which exploit both exact Hartree-Fock calculation of part of the exchange energy contribution and approximate the remaining part and the correlation terms. This is the case of the B3LYP functional, implemented in Gaussian, and used for a wide scope of experiments, still nowadays. This hybrid functional takes inspiration from the adiabatic connection. Indeed, in [444], Becke advocated that if one weighs the exchange-correlation (E_{XC}) term with the weighing parameter λ, the Hartree-Fock exact exchange energy is obtained when $\lambda = 0$, in a non-interacting system, while the other terms are completely considered in the case of $\lambda = 1$.
Therefore, he designed a hybrid functional containing both contributions and weighed by empirical coefficients, according to the expression:

$$E_{XC}^{B3} = E_{XC}^{LSDA} + a(E_{XC}^{\lambda=0} - E_{XC}^{LSDA}) + bE_X^{B88} + cE_C^{PW91} \tag{9.59}$$

where E_{XC}^{LSDA} is the unrestricted form of the LDA model, which includes the open-shell spin states like radicals:

$$E_{XC}^{LSDA}[\rho_\alpha, \rho_\beta] = \int \rho(\vec{\mathbf{r}})\epsilon_{XC}(\rho_\alpha(\vec{\mathbf{r}}), \rho_\beta(\vec{\mathbf{r}}))d\vec{\mathbf{r}} \tag{9.60}$$

and the coefficients were empirically found to be $a = 0.20, b = 0.72, c = 0.81$.
The final form of the B3LYP functional was proposed by Stephens et al. in 1994 [445]:

$$E_{XC}^{B3LYP} = (1-a)E_X^{LSDA} + aE_X^{\lambda=0} + bE_X^{B88} + cE_C^{LYP} + (1-c)E_C^{VWN} \tag{9.61}$$

where the coefficients a, b, and c are the same obtained by Becke [444].
With these new functionals the self-interaction is canceled by addition to the $J[\rho]$ term.

9.5 Self-consistency and basis sets

A brief explanation of how to computationally face a Kohn-Sham DFT calculation is now provided. The aim of the operations is to minimize the Kohn-Sham energy value according to the variational principle, by exploiting a density functional which is not known, but built by N one-electron normalisable spin orbitals (ϕ_i):

$$\begin{aligned} \hat{\mathbf{f}}^{KS}\phi_i = \epsilon_i\phi_i, \qquad \hat{\mathbf{f}}^{KS} &= -\frac{1}{2}\boldsymbol{\nabla}^2 + V_s(\vec{\mathbf{r}}) \\ \rho(\vec{\mathbf{r}}) &= \sum_i^N |\phi_i(\vec{\mathbf{r}})|^2. \end{aligned} \tag{9.62}$$

Thus, one needs to iteratively calculate the spin orbitals from the Kohn-Sham eigenvalue problem, where the Hamilton operator is obtained from a guessing electron density, then, these spin orbitals are used to calculate a new density, like in Equation 9.62. In order to satisfy the self-consistency condition of the algorithm, at the final iteration, the densities introduced in the Hamiltonian and got from the second equation must be the same [446], otherwise the last calculated density is taken as ρ_{trial} and the iterations are re-launched. In order to do this, the spin orbitals are always approximated by a sum of bases in the form of gaussian functions or more complicated entities. The operation is named linear-combination-of-atomic-orbitals (LCAO), but not in the case of plane waves, which are non-centered functions but can be used in certain applications, too.
During the application of such basis sets, the electrons can be treated all the same, or alternatively one may distinguish between core and valence electrons. In this scenario core electrons are all alike and described by a minimum number of bases, and represented by the so-called pseudopotentials, while valence electrons are more precisely described, because of their impact on the chemical and calculative properties.
In a general manner, spin orbitals are decomposed according the following linear combination of functions:

$$\phi_i(\vec{\mathbf{x}}) = \sum_{\mu=1}^{\infty} \alpha_{i\mu}\chi_\mu(\vec{\mathbf{x}}). \tag{9.63}$$

The series is always truncated to a N_b number of bases, thus, to a finite region of the Hilbert space. Moreover, N_b has generally the same order of magnitude of the electrons number N.
The non-linear eigenvalue problem is now linear, and the coefficients $\alpha_{i\mu}$ are the only variables.
The problem assumes the following form:

$$\hat{\mathbf{f}}^{KS}(\vec{\mathbf{r}}_1)\sum_{\mu=1}^{N_b} \alpha_{i\mu}\chi_\mu(\vec{\mathbf{r}}_1) = \epsilon_i \sum_{\mu=1}^{N_b} \alpha_{i\mu}\chi_\mu(\vec{\mathbf{r}}_1) \tag{9.64}$$

and after further handling, one obtains the matricial form:

$$F^{KS}C = SC\epsilon. \tag{9.65}$$

Just for general knowledge, in the case of plane waves, the functions have the form:

$$\chi^{PW} = \exp\Big\{i\vec{\mathbf{k}}\vec{\mathbf{r}}\Big\}. \tag{9.66}$$

As stated before, they are not centered at the nuclei but spread throughout the whole positive charged framework, that is why it is not a real LCAO approximation. For that reason, they are particularly suitable for the uniform electron gas model, and applied for metal calculations.
For further insights on numerical methods, their convergence and conditioning, see [446].

6-31G(d,p) basis set Basis sets are of different types, namely Gaussian- and Slater-orbitals. In addition, these sets can be characterized by a minimal set of functions, were only one contracted function represents one atomic orbital at a time, or by a double-zeta set where two functions stand for each orbital. This latter case, named split-valence type set, treats the core orbitals with a minimal set, while valence electrons are substituted by a double-zeta set. In some cases, the sets are augmented by polarization functions, with higher momentum, which account for the excited states of the atom, by introducing d-orbitals to a second-row element's electronic configuration, for instance.

The 6-31G(d,p) is a Gaussian basis set coupled to polarization functions which is widely exploited for the approximation of hydrogen, helium and first- [447, 448], second- [449] and third-row-element [450, 451, 452, 453]atomic orbitals.

The non-polarizable-system's set is formed by contracted and double-zeta Gaussian functions, approximating mainly s- and p- atomic orbitals, of the form:

$$\begin{aligned} g_s(\alpha, \vec{\mathbf{r}}) &= (\frac{2\alpha}{\pi})^{3/4} exp(-\alpha\vec{\mathbf{r}}^2) \\ g_{px,py,pz}(\alpha, \vec{\mathbf{r}}) &= (\frac{128\alpha^5}{\pi^3})^{1/4}\{x, y, z\} exp(-\alpha\vec{\mathbf{r}}^2). \end{aligned} \tag{9.67}$$

Considering an atom, like carbon, containing both s and p orbitals at its ground state [447, 448], the basis sets acquires the 9-function form:

$$\begin{aligned} \phi_{1s}(\vec{\mathbf{r}}) &= \sum_{k=1}^{N_1} d_{1s,k} g_s(\alpha_{1k}, \vec{\mathbf{r}}) \\ \phi_{2s'}(\vec{\mathbf{r}}) &= \sum_{k=1}^{N_{2'}} d_{2s,k'} g_s(\alpha_{2k'}, \vec{\mathbf{r}}) \\ \phi_{2p'}(\vec{\mathbf{r}}) &= \sum_{k=1}^{N_{2'}} d_{2p,k'} g_p(\alpha_{2k'}, \vec{\mathbf{r}}), p = \{p_x, p_y, p_z\} \\ \phi_{2s''}(\vec{\mathbf{r}}) &= \sum_{k=1}^{N_{2''}} d_{2s,k''} g_s(\alpha_{2k''}, \vec{\mathbf{r}}) \\ \phi_{2p''}(\vec{\mathbf{r}}) &= \sum_{k=1}^{N_{2''}} d_{2p,k''} g_p(\alpha_{2k''}, \vec{\mathbf{r}}), p = \{p_x, p_y, p_z\}. \end{aligned} \tag{9.68}$$

Indeed, the name of the basis set comes from the cut-off numbers taken for each type of function ($N_1 = 6, N_{2'} = 3, N_{2''} = 1$). $N_{1'} = 3$ and $N_{1''} = 1$ are taken for hydrogen and helium.

The functions have the form: $f(\vec{\mathbf{r}}) = d \exp\{-\alpha\vec{\mathbf{r}}^2\}$. This expression is the simplest, while in the case of spatially oriented orbitals (non-null angular momentum), the characteristic spatial coordinate is multiplied to the pre-exponential factor d. For instance, a p-orbital basis element will have the form: $f_p(\vec{\mathbf{r}}) = d_p(x, y, z) \exp\{-\alpha_p\vec{\mathbf{r}}^2\}$. Furthermore, the coefficients d and α, for each basis element can be found within some tables, in literature. Noteworthy, α_s and α_p of the valence shell are the same [454].

A set of uncontracted d-gaussian functions can be added to the 6-31G basis set, accounting for polarization of heavier atoms. These are unnormalized functions of the type:

$$(x^2, y^2, z^2, xy, yz, xz) exp(-\alpha_d\vec{\mathbf{r}}^2) \tag{9.69}$$

where α_d exponents are identical to the ones of the external s+p valence shell.

LanL2DZ basis-set and the Pseudopotentials The LanLDZ basis set is suitable for elements heavier than Krypton, thereby, palladium in our specific case. It is based on the definition of a (relativistic) effective core potential, or pseudopotential, for modeling the core electrons. Indeed, the effective potential accounts for the repulsive electrostatic and spin interaction, as stated above.

In principle, the core can be substituted by an effective Hartree-Fock-like potential. Though, this involves the exchange term, which connects the core to the valence electrons. Thus, no simple expression can be provided, without neglecting this interaction [455].

The solution of the eigenvalue problem with a Hartree-Fock Hamilton operator, containing the effective interaction potential, empirically provides the needed coefficients for the construction of the basis set [456, 457, 458].

10 Conclusions and perspectives

The present study has summed up the main features of Pd-catalyzed coupling chemistry and showed how this could get complicated. Indeed, evaluating the true heterogeneity of the precatalysts appeared to be difficult and sometimes, untrue results were reported, due to misleading interpretations/analysis results.

In addition to inner burdens, a light attitude towards the interpretation of recyclability results has been perceived while reading the papers. Most often only ICP analyses and/or hot filtration tests were conducted, even in most recent papers, before drawing rushed conclusions. It has been already explained why these tests are not sufficient to explain all the nuances of the results. Hence, this made it difficult to wisely organize and interpret the sources. Nonetheless, the goal of organizing the material and give a clearer overview of the topic has been accomplished.

Nowadays, the technological advances in material science allowed the synthesis of highly interesting catalytic systems, namely SACs, magnetically recyclable NPs, photocatalytically activated systems, and the results seemed promising towards the obtaining of heterogeneous catalysts. Though, one always must account for partial leaching and for large fraction of the reactions being catalyzed in solution, due to solubilized palladium's outstanding activity.

One question may rise: does it actually exist a pure heterogeneous catalyst under coupling conditions? Maybe. Though, at the moment the state of the art is still concentrating on how to tune leached amounts in a separate way from activity, i.e. decorrelating solubilization and efficiency and shutting down the former without affecting the latter. For instance, in some early studies, the use of non-polar solvents appeared to decrease leaching, but activity followed that trend, too, which is not satisfactory and rises some wonders about actual heterogeneous catalysis. Indeed, a catalyst hardly ever showed pure heterogeneous behavior, owing to the complexity related to its activity mechanisms. Yet, some authors advocated such behavior, often due to the aforementioned issues. Besides, really comprehensive and interesting studies have been read and reported. Some of them highlighted the necessity for a good and profound mathematical knowledge of the phenomena linked to heterogeneous catalysis, namely leaching. To this end, due to the complexity of experimental works, theoretical DFT calculations recently caught on. This quantum mechanical modeling of chemical systems (i.e. atoms, molecules etc) permits to assess free-energy barriers of reaction steps, ionization energies etc and draw a thorough scheme of the reaction with all side-phenomena taking part to it. These modeling techniques would allow to save time and chemicals by drawing a plausible scenario before carrying on whatever reaction. For this reason, DFT methods have been taken as a really useful tool for such heterogeneous catalysis applications.

The research group is now working on some continuous-flow experiments for testing CSMs' utility. It has been reported that some palladium leaching was detected during the reactions, whatever the support. Despite some good results, which helped drawing a scale of efficiency of the different supports, good conversion were detected without catalyst, too. This could be due to the deposition of palladium onto the walls of the reactor, which is hard to handle and flushed with efficient acid/alkaline solutions because of the harm those would cause to the equipments (e.g. pumps, reactor, pipelines etc).

In brief, further work needs to be done, both by the group and by authors in general, in order to optimize the reaction conditions, control leaching and subtly understand and explain cause-effect correlations, while performing C–C coupling reactions.

List of symbols

l, L	Characteristic microscopic/macroscopic length and interatomic distance
σ, π	Categories of covalent bond
π^*	Anti-bonding π-orbital
X°	Standard quantity X ($[]^{\circ} = 1M$, $p^{\circ} = 1atm$, $T^{\circ} = 25^{\circ}C$)
δ	Thickness of the stagnant film (Film Theory)
K_0	Apparent kinetic constant
k_s	Mass transfer coefficient between liquid and solid phase
a	Volumic surface
η	Effectiveness factor (apparent kinetics)
k	Generic kinetic constant
ϵ	Porosity of a solid system (one-electron Kohn-Sham eigenvalues of the energy, or derivative of the exchange-correlation energy with respect to the electron density in Section 9)
D_e	Equivalent diffusion coefficient
N	Number of coordinative bonds (Number of electrons in Section 9)
n	Number of atoms
NP^*	Resulting nanoparticle after detachment of Pd_n nanocluster
Pd_n	Nanocluster of n Pd atoms
ΔG	Gibbs energy difference
R	Ideal gas constant
T	Temperature
ω	Mass fraction
ρ	Macroscopic density (Electron density $\rho(\hat{\mathbf{r}})$ in Section 9)
M	Molecular weight [g/mol] (Mass of a nucleus in Section 9)
θ	Contact angle between particle and solid surface
ν	Frequency of thermal vibration of an atom in a crystal lattice
E	Generic expression of total energy value (*apices/pedices specify the nature)
S_{dif}	Differential selectivity (SADS technique)
r	Reaction rate
W	Weight [g]
σ_y	Standard deviation of quantity y
$\hbar$	Reduced Planck's constant
Ψ	Electron wave-function
$\langle f\|$	Functional f
$\|\Psi\rangle$	Vector or quantum state Ψ
$\langle \Psi\|\hat{\mathbf{H}}\|\Psi \rangle$	Expectation value of an operator (e.g. Hamiltonian $\vec{\mathbf{H}}$) calculated with respect to a vector (e.g. quantum state Ψ)
$\hat{\mathbf{H}}$	Hamiltonian operator
$\boldsymbol{\nabla}$	Gradient operator
r_{ij}	Distance between the subatomic particles i and j
Z	Charge
$\hat{\mathbf{T}}$	Kinetic energy operator
$\hat{\mathbf{V}}$	Generic potential operator
$\hat{\mathbf{K}}$	Exchange operator
$\hat{\mathbf{J}}$	Coulomb interaction operator according to the Kohn-Sham Theory
$\hat{\mathbf{f}}^{KS}$	One-electron Kohn-Sham operator
Φ_{SD}	Slater determinant
$\chi_i(\vec{\mathbf{x}}_i)$	One-electron wave function
$\phi(\vec{\mathbf{r}})$	Spatial component of a spin orbital
$\sigma(s)$	Spin component of a spin orbital, of values α or β

h_{XC}	Exchange-correlation hole
λ	Adiabatic connection parameter

List of abbreviations

AFM	Atomic-Force Microscopy
AMP	2-aminopyridine
BDPB	3,4-bis(diphenylphopshine)-1-butene
BZD	Benzidine
Cell	Cellulose
CNG	Carbon Nano-Globule
CNT/NCNT/ SWNT/MWNT	(N-doped/Single-Wall/ Multi-Wall) Carbon Nanotubes
CS	Chitosan
CSM	Catalytic static mixer
CTAB	Cetrimonium bromide
CVD	Chemical Vapor Deposition
DAB-Cy	Cyclohexyl-diazabutadiene
DES	Deep Eutectic Solvent
DFT	Density Functional Theory
DMAc	Dimethylacetamide
DME	Dimethoxyethane
DMF	N-N-dimethylformamide
DMI	Dimethyl isosorbide
EDG	Electron-Donating Group
EtOH	Ethanol
EWG	Electron-Withdrawing Group
EXAFS	Extended X-ray Absorption Fine Structure
GEA	Gradient Expansion Approximation
GGA	Generalized Gradient Approximation
GO	Graphene oxide
GOF	Graphene Oxide Framework
GVL	γ-Valerolactone
HBD/HBA	Hydrogen Bond Donor /Acceptor
HBP	Hyper-branched Polymers
HCP	Hypercross-linked Polymers
ICP-AES	Inductively Coupled Plasma-Atomic Emission Spectroscopy
ID	Internal Diameter
NBP/NOP/NBnP /NCP/HEP	N-butyl/octyl/benzyl/ cyclohexyl/hydroxyethylpyrrolidone
NHC	N-heterocyclic carbene
NMP	N-methyl-2-pyrrolidone
ODE/PDE	Ordinary/Partial Differential Equation
OR	Ostwald Ripening
Pd@Au	Core-shell Au-Pd nanostructures
Pd/C	Palladium on carbon
Pd-SH-E-PMO	Thiol-functionalized periodic porous organosilica-supported palladium
PAMAM	Polyamidoamine
PAN	Poly(acrylonitrile)
PANI	Polyaniline
Ph	Phenyl group
PDE4	Phosphodiesterase-4
PdNP(M NP)	Palladium/metal nanoparticle
PdTA	Palladium tetracetate
PEG	Poly(ethylenglycol)
PFR/PBR	Plug-flow/Packed-bed Reactor
PM	Particle Migration
PMO	Periodic Mesoporous Organosilica
POP	Porous Organic Polymer
PPD	*p*-Phenylenediamine
PEPPSI	Pyridine Enhanced Precatalyst Preparation, Stabilization and Initiation
PSD	Particle-size Distribution
PTA	Phase Transfer Agent
PVP	Poly(vynilpyrrolidone)
PVPy	Poly(vynilpyridine)
RDS	Rate-determining Step
RGO	Reduced Graphene Oxide
RT	Room Temperature
SAC	Single-atom Catalyst
SADS	Schmidt's Analysis of Differential Selectivity
SCF	Self-Consistent Field
SMC (SM)	Suzuki-Miyaura coupling (Suzuki-Miyaura)

IL	Ionic liquid
IPN	Interpenetrating Polymeric Networks
***i*PrOH**	*Iso*-propanol
LCAO	Linear Combination of Atomic Orbitals
L(S)DA	Local (Spin) Density Approximation
M	Atomic metal
MALDI-MS	Matrix-assisted Laser Desorption /Ionisation-Mass Spectroscopy
MC	Mesoporous carbon
MCM	Mobile Composition of Matter
Me	Methyl group
MeOH	Methanol
MEPI-Pd	Metalloenzyme-like Pd catalyst
MIL-101	Metal-organic framework by Material Institute Lavoisier
ML$_n$	Metal complex
MO	Molecular Orbital
MOF	Metal-organic Framework
MOP	Metal Organic Polyhedra
MW	Micro-wave
MW	Molecular Weight
S$_N$C/S$_N$2	Concerted/Bi-molecular nucleophilic substitution
SVHC	Substance of Very High Concern
TBAB/TBAF	Tetra-*n*-butylammonium bromide /fluoride
***t*BuOH**	*Tert*-butanol
TEA	Triethylamine
TEM/STEM	(Scanning) Transmission Electron Microscopy
TGA	Thermogravimetric analysis
THF	Tetrahydrofuran
THH	Tetraexahedral
TM	Transition Metal
tmeda	Tetramethylethylenediamine
TOF	Turnover Frequency
TOH	Trisoctahedral
TON	Turnover Number
VBAC	Vynilbenzyl Tributyl Ammonium Chloride
VBBP	4-Vynilbenzyldiphenylphosphine
w/o	Water in oil emulsion
XANES	X-ray Absorption Near Edge Structure

References

[1] Xue L. and Lin Z. Theoretical aspects of palladium-catalysed carbon-carbon cross-coupling reactions. *Chem. Soc. Rev.*, **39**(5):1692–1705, 2010.

[2] Crisp G.T. Variations on a theme - recent developments on the mechanism of the Heck reaction and their implications for synthesis. *Chem. Soc. Rev.*, **27**(6):427–436, 1998.

[3] Amatore C. and Jutand A. Anionic Pd(0) and Pd(II) intermediates in palladium-catalyzed Heck and cross-coupling reactions. *Acc. Chem. Res.*, **33**(5):314–321, 2000.

[4] Shaw B.L. Chelating diphosphine–palladium(II) dihalides; outstandingly good catalysts for Heck reactions of aryl halides. *Chem. Commun.*, (17):1863–1864, 1998.

[5] Shaw B.L. Speculations on new mechanisms for Heck reactions. *New J. Chem.*, **22**(2):77–79, 1998.

[6] Chinchilla R. and Nájera C. Recent advances in Sonogashira reactions. *Chem. Soc. Rev.*, **40**(10):5084–5121, 2011.

[7] Hiebler K., Soritz S., Gavric K., Birrer S., Maier M.C., Grabner B., and Gruber-Woelfler H. Multistep synthesis of a valsartan precursor in continuous flow. *J. Flow Chem.*, **10**(1):283–294, 2020.

[8] Maleki A., Taheri-Ledari R., Ghalavand R., and Firouzi-Haji R. Palladium-decorated o-phenylenediamine-functionalized Fe_3O_4/SiO_2 magnetic nanoparticles: a promising solid-state catalytic system used for Suzuki–Miyaura coupling reactions. *J. Phys. Chem. Sol.*, **136**:109200, 2020.

[9] Choy P.Y., Yuen O.Y., Leung M.P., Chow W.K., and Kwong F.Y. A highly efficient monophosphine ligand for parts per million levels Pd-catalyzed Suzuki–Miyaura coupling of (hetero)aryl chlorides. *Eur. J. Org. Chem.*, **2020**(19):2846–2853, 2020.

[10] Akporji N., Thakore R.R., Cortes-Clerget M., Andersen J., Landstrom E., Aue D.H., Gallou F., and Lipshutz B.H. N2Phos - an easily made, highly effective ligand designed for ppm level Pd-catalyzed Suzuki-Miyaura cross couplings in water. *Chem. Sci.*, **11**(20):5205–5212, 2020.

[11] Consorti C.S., Flores F.R., and Dupont J. Kinetics and mechanistic aspects of the Heck reaction promoted by a CN-palladacycle. *J. Am. Chem. Soc.*, **127**(34):12054–12065, 2005.

[12] Joshi H., Prakash O., Sharma A.K., Sharma K.N., and Singh A.K. Suzuki coupling reactions catalyzed with palladacycles and palladium(II) complexes of 2-thiophenemethylamine-based schiff bases: Examples of divergent pathways for the same ligand. *Eur. J. Inorg. Chem.*, **2015**(9):1542–1551, 2015.

[13] Nehzat F. and Grivani G. Two efficient ligand-assisted systems of two different ionic Schiff base ligands for palladium chloride catalyzed in Suzuki-Miyaura reaction. *J. Chem. Sci.*, **132**(1):33, 2020.

[14] Karataş M.O., Özdemir N., Alıcı B., and Özdemir İ. N-heterocyclic carbene palladium complexes with different N-coordinated ligands: comparison of their catalytic activities in Suzuki-Miyaura and Mizoroki-Heck reactions. *Polyhedron*, **176**:114271, 2020.

[15] Corma A., García H., and Leyva A. Catalytic activity of palladium supported on single wall carbon nanotubes compared to palladium supported on activated carbon: study of the Heck and Suzuki couplings, aerobic alcohol oxidation and selective hydrogenation. *J. Mol. Catal. A: Chemical*, **230**(1-2):97–105, 2005.

[16] Wang Y. and Liu H. Syntheses and characterization of mercapto-hydroxyl-palladium macromolecular chelates and their catalytic properties. *J. Mol. Catal.*, **45**(1):127–142, 1988.

[17] Schwarz J., Böhm V.P.W., Gardiner M.G., Grosche M., Herrmann W.A., Hieringer W., and Raudaschl-Sieber G. Polymer-supported carbene complexes of palladium: well-defined, air-stable, recyclable catalysts for the Heck reaction. *Eur. J. Chem.*, **6**(10):1773–1780, 2000.

[18] Phan N.T.S., Van Der Sluys M., and Jones C.W. On the nature of the active species in palladium catalyzed Mizoroki-Heck and Suzuki-Miyaura couplings - Homogeneous or heterogeneous catalysis, a critical review. *Adv. Synth. Catal.*, **348**(6):609–679, 2006.

[19] An Der Heiden M. and Plenio H. Homogeneous catalysts supported on soluble polymers: biphasic Suzuki-Miyaura coupling of aryl chlorides using phase-tagged palladium-phosphine catalysts. *Chem. Eur. J.*, **10**(7):1789–1797, 2004.

[20] Parrish. C.A. and Buchwald S.L. Use of polymer-supported dialkylphosphinobiphenyl ligands for palladium-catalyzed amination and Suzuki reactions. *J. Org. Chem.*, **66**(11):3820–3827, 2001.

[21] Phan N.T.S., Brown D.H., and Styring P. A polymer-supported salen-type palladium complex as a catalyst for the Suzuki-Miyaura cross-coupling reaction. *Tetrahedron Lett.*, **45**(42):7915–7919, 2004.

[22] Smith G.S. and Mapolie S.F. Iminopyridyl-palladium dendritic catalyst precursors: evaluation in Heck reactions. *J. Mol. Catal. A Chem.*, **213**(2):187–192, 2004.

[23] Burke K., Perdew J.P., and Wang Y. *Derivation of a Generalized Gradient Approximation: the PW91 Density Functional.* Dobson, J. F. and Vignale, G. and Das, M. P., Plenum Press, New York, 1998.

[24] Hu J. and Liu Y. Pd nanoparticle aging and its implications in the Suzuki cross-coupling reaction. *Langmuir*, **21**(6):2121–2123, 2005.

[25] de Vries A.H.M., Mulders J.M.C.A., Mommers J.H.M., Henderickx H.J.W., and de Vries J.G. Homeopathic ligand-free palladium as a catalyst in the Heck reaction. A comparison with a palladacycle. *Org. Lett.*, **5**(18):3285–3288, 2003.

[26] de Vries J.G. A unifying mechanism for all high-temperature Heck reactions. The role of palladium colloids and anionic species. *Dalton Trans.*, **2020**(3):421–429, 2006.

[27] Zhou C., Wang J., Li L., Wang R., and Hong M. A palladium chelating complex of ionic water-soluble nitrogen-containing ligand: the efficient precatalyst for Suzuki–Miyaura reaction in water. *Green Chem.*, **13**(8):2100–2106, 2011.

[28] Yamada Y.M.A., Sarkar S.M., and Uozumi Y. Self-assembled poly(imidazole-palladium): highly active, reusable catalyst at parts per million to parts per billion levels. *J. Am. Chem. Soc.*, **134**(6):3190–3198, 2012.

[29] Yu Y., Hu T., Chen X., Xu K., Zhang J., and Huang J. Pd nanoparticles on a porous ionic copolymer: a highly active and recyclable catalyst for suzuki–miyaura reaction under air in water. *Chem. Commun.*, **47**(12):3592–3594, 2011.

[30] Pérez-Lorenzo M. Palladium nanoparticles as efficient catalysts for Suzuki cross-coupling reactions. *J. Phys. Chem. Lett.*, **3**(2):167–174, 2012.

[31] Eremin D.B. and Ananikov V.P. Understanding active species in catalytic transformations: from molecular catalysis to nanoparticles, leaching, “cocktails” of catalysts and dynamic systems. *Coord. Chem. Rev.*, **346**:2–19, 2017.

[32] Biffis A., Centomo P., Del Zotto A., and Zecca M. Pd metal catalysts for cross-couplings and related reactions in the 21st century: a critical review. *Chem. Rev.*, **118**(4):2249–2295, 2018.

[33] Kashin A.S. and Ananikov V.P. Catalytic C-C and C-heteroatom bond formation reactions: in situ generated or preformed catalysts? Complicated mechanistic picture behind well-known experimental procedures. *J. Org. Chem.*, **78**(22):11117–11125, 2013.

[34] Polynski M.V. and Ananikov V.P. Modeling key pathways proposed for the formation and evolution of "cocktail"-type systems in Pd-catalyzed reactions involving ArX reagents. *ACS Catal.*, **9**(5):3991–4005, 2019.

[35] de Vries A.H.M., Parlevliet F.J., Schmieder-van De Vondervoort L., Mommers J.H.M., Henderickx H.J.W., Walet M.A.M., and de Vries J.G. A practical recycle of a ligand-free palladium catalyst for Heck reactions. *Adv. Synth. Catal.*, **344**(9):996–1002, 2002.

[36] Bedford R.B., Cazin C.S.J., Hursthouse M.B., Light M.E., Pike K.J., and Wimperis S. Silica-supported imine palladacycles - recyclable catalysts for the Suzuki reaction? *J. Organomet. Chem.*, **633**(1-2):173–181, 2001.

[37] Kim S., Jee S., Choi K.M., and Shin D.S. Single-atom Pd catalyst anchored on Zr-based metal-organic polyhedra for Suzuki-Miyaura cross coupling reactions in aqueous media. *Nano Res.*, pages 1–7, 2020.

[38] Littke A.F., Dai C., and Fu G.C. Versatile catalysts for the Suzuki cross-coupling of arylboronic acids with aryl and vinyl halides and triflates under mild conditions. *J. Am. Chem. Soc.*, **122**(17):4020–4028, 2000.

[39] Gade L.H. [bis(oxazolinyl)pyrrole]palladium complexes as catalysts in Heck- and Suzuki-type C-C coupling reactions. *Eur. J. Inorg. Chem.*, **2003**(6):1161–1168, 2003.

[40] Kurosawa H., Kajimaru H., Ogoshi S., Yoneda H., Miki K., Kasai N., Murai S., and Ikeda I. Novel syn oxidative addition of allylic halides to olefin complexes of palladium(0) and platinum(0). *J. Am. Chem. Soc.*, **114**(22):8417–8424, 1992.

[41] Kurosawa H., Ogoshi S., Kawasaki Y., Murai S., aki Miyoshi M., and Ikeda I. Novel dependency of stereochemistry upon metal, ligand, and solvent in oxidative addition of allylic chloride to Pd(0) and Pt(0) complexes. *J. Am. Chem. Soc.*, **112**(7):2813–2814, 1990.

[42] Goossen L.J., Koley D., Hermann H.L., and Thiel W. The palladium-catalyzed cross-coupling reaction of carboxylic anhydrides with arylboronic acids: a DFT study. *J. Am. Chem. Soc.*, **127**(31):11102–11114, 2005.

[43] Galardon E., Ramdeehul S., Brown J.M., Cowley A., Hii K.K., and Jutand A. Profound steric control of reactivity in aryl halide addition to bisphosphane palladium(0) complexes. *Angew. Chem. Int. Ed.*, **41**(10):1760–1763, 2002.

[44] Hartwig J.F. and Paul F. Oxidative addition of aryl bromide after dissociation of phosphine from a two-coordinate palladium(0) complex, bis(tri-o-tolylphosphine)palladium(0). *J. Am. Chem. Soc.*, **117**(19):5373–5374, 1995.

[45] Stambuli J.P., Bühl M., and Hartwig J.F. Synthesis, characterization, and reactivity of monomeric, arylpalladium halide complexes with a hindered phosphine as the only dative ligand. *J. Am. Chem. Soc.*, **124**(32):9346–9347, 2002.

[46] Casado A.L. and Espinet P. Mechanism of the Stille reaction. 1. The transmetalation step. Coupling of R^1I and R^2SnBu_3 catalyzed by trans-$[PdR^1IL_2]$ ($R^1 = C_6Cl_2F_3$; R^2 = vinyl, 4-methoxyphenyl; L = $AsPh_3$). *J. Am. Chem. Soc.*, **120**(35):8978–8985, 1998.

[47] Casado A.L., Espinet P., and Gallego A.M. Mechanism of the stille reaction. 2. Couplings of aryl triflates with vinyltributyltin. Observation of intermediates. A more comprehensive scheme. *J.Am. Chem. Soc.*, **122**(48):11771–11782, 2000.

[48] Casares J.A., Espinet P., and Salas G. 14-electron T-shaped [PdRXL] complexes: evidence or illusion? Mechanistic consequences for the Stille reaction and related processes. *Chem. Eur. J.*, **8**(21):4843–4853, 2002.

[49] Espinet P. and Echavarren A.M. The mechanisms of the Stille reaction. *Angew. Chem. Int. Ed.*, **43**(36):4704–4734, 2004.

[50] Shimizu M., Nakamaki C., Shimono K., Schelper M., Kurahashi T., and Hiyama T. Stereoselective cross-coupling reaction of 1,1-diboryl-1-alkenes with electrophiles: a highly stereocontrolled approach to 1,1,2-triaryl-1-alkenes. *J. Am. Chem. Soc.*, **127**(36):12506–12507, 2005.

[51] Sugiyama A., Ohnishi Y.Y., Nakaoka M., Nakao Y., Sato H., Sakaki S., Nakao Y., and Hiyama T. Why does fluoride anion accelerate transmetalation between vinylsilane and palladium(II)-vinyl complex? Theoretical study. *J. Am. Chem. Soc.*, **130**(39):12975–12985, 2008.

[52] Pérez-Rodríguez M., Braga A.A.C., Garcia-Melchor M., Pérez-Temprano M.H., Casares J.A., Ujaque G., De Lera A.R., Álvarez R., Maseras F., and Espinet P. C-C reductive elimination in palladium complexes, and the role of coupling additives. A DFT study supported by experiment. *J. Am. Chem. Soc.*, **131**(10):3650–3657, 2009.

[53] Tatsumi K., Hoffmann R., Yamamoto A., and Stille J.K. Reductive elimination of d 8-organotransition metal complexes . **54**(6):1857–1867, 1981.

[54] Jian J., He Z., Zhang Y., Liu T., Liu L., Wang Z., Wang H., Wang S., and Zeng Z. Palladium-catalyzed Suzuki coupling of N-acyloxazolidinones via selective cleavage of C–N bonds. *Eur. J. Org. Chem.*, **2020**(27):4176–4180, 2020.

[55] Liu J., Ling M., and Xie H. Mechanisms of chemoselectivity for acyl and decarbonylative Suzuki–Miyaura coupling of N-acetyl amide with arylboronic acid catalyzed by Pd and Ni catalysts: insights from DFT calculations. *Comput. Theor. Chem.*, **1185**:112889, 2020.

[56] Reina A., Krachko T., Onida K., Bouyssi D., Jeanneau E., Monteiro N., and Amgoune A. Development and mechanistic investigations of a base-free Suzuki-Miyaura cross-coupling of α,α-difluoroacetamides via C–N bond cleavage. *ACS Catal.*, **10**(3):2189–2197, 2020.

[57] Mansour W., Fettouhi M., and El Ali B. Novel and efficient bridged bis(N-heterocyclic carbene)palladium(II) catalysts for selective carbonylative Suzuki–Miyaura coupling reactions to biaryl ketones and biaryl diketones. *Appl. Organomet. Chem.*, **34**(6):1–20, 2020.

[58] Layek S., Agrahari B., Ganguly R., Das P., and Pathak D.D. Carbonylative Suzuki coupling reactions catalyzed by ONO pincer–type Pd(II) complexes using chloroform as a carbon monoxide surrogate. *Appl. Organomet. Chem.*, **34**(3):1–14, 2020.

[59] Braga A.A.C., Ujaque G., and Maseras F. A DFT study of the full catalytic cycle of the Suzuki-Miyaura cross-coupling on a model system. *Organometallics*, **25**(15):3647–3658, 2006.

[60] Sun Y. and Mohammadnia M. Synthesis and characterization of Pd based on [2,2'- bipyridin]-4-amine functionalized nano cellulose as a novel and recyclable nano catalyst for Suzuki reaction. *Inorg. Chem. Commun.*, **118**:107993, 2020.

[61] Zhang Y., Zhang X., Gao J., Du C., Xie M., Au C., Chen J., and Wan L. Photocatalytic Suzuki–Miyaura Coupling Reactions over Palladium Anchored on 8-Hydroxyquinoline-Based Polymers. *Macromol. Chem. Phys.*, **221**(14):1–9, 2020.

[62] Albert K., Gisdakis P., and Rösch N. On C-C coupling by carbene-stabilized palladium catalysts: a density functional study of the Heck reaction. *Organometallics*, **17**(8):1608–1616, 1998.

[63] Henriksen S.T., Norrby P.O., Kaukoranta P., and Andersson P.G. Combined experimental and theoretical study of the mechanism and enantioselectivity of palladium-catalyzed intermolecular Heck coupling. *J. Am. Chem. Soc.*, **130**(31):10414–10421, 2008.

[64] Lee M.T., Lee H.M., and Hu C.H. A theoretical study of the Heck reaction: N-heterocyclic carbene versus phosphine ligands. *Organometallics*, **26**(6):1317–1324, 2007.

[65] Surawatanawong P., Fan Y., and Hall M.B. Density functional study of the complete pathway for the Heck reaction with palladium diphosphines. *J. Organomet. Chem.*, **693**(8-9):1552–1563, 2008.

[66] Surawatanawong P. and Hall M.B. Theoretical study of alternative pathways for the Heck reaction through dipalladium and "ligand-free" palladium intermediates. *Organometallics*, **27**(23):6222–6232, 2008.

[67] Okita T., Asahara K.K., Muto K., and Yamaguchi J. Palladium-catalyzed Mizoroki-Heck reaction of nitroarenes and styrene derivatives. *Org. Lett.*, **22**:3205–3208, 2020.

[68] Rago A.J. and Dong G. Unexpected *ortho*-Heck reaction under the Catellani conditions. *Org. Lett.*, **22**:3770–3774, 2020.

[69] Matelienė L., Knaup J., Horsten F.V., and Gu X. Benign arylations of dimethyl itaconate via Heck–Matsuda reaction utilizing in-situ generated palladium on aluminum. *Eur. J. Org. Chem.*, **2020**:127–135, 2020.

[70] Feng L., Guo L., Yang C., Zhou J., and Xia W. Visible-light-induced palladium-catalyzed intermolecular Narasaka-Heck reaction at room temperature. *Org. Lett.*, **22**:3964–3968, 2020.

[71] Cabri W. and Candiani I. Recent developments and new perspectives in the Heck reaction. *Acc. Chem. Res.*, **28**(1):2–7, 1995.

[72] Deeth R.J., Smith A., and Brown J.M. Electronic control of the regiochemistry in palladium-phosphine catalyzed intermolecular Heck reactions. *J. Am. Chem. Soc.*, **126**(22):7144–7151, 2004.

[73] Zhao F., Bhanage B.M., Shirai M., and Arai M. Heck reactions of iodobenzene and methyl acrylate with conventional supported palladium catalysts in the presence of organic and/or inorganic bases without ligands. *Chem. Eur. J.*, **6**(5):843–848, 2000.

[74] Zhao F., Murakami K., Shirai M., and Arai M. Recyclable homogeneous/heterogeneous catalytic systems for Heck reaction through reversible transfer of palladium species between solvent and support. *J. Catal.*, **194**(2):479–483, 2000.

[75] Zhao F., Shirai M., and Arai M. Palladium-catalyzed homogeneous and heterogeneous Heck reactions in NMP and water-mixed solvents using organic , inorganic and mixed bases. *J. Mol. Catal. A: Chem.*, **154**(1):39–44, 2000.

[76] Huang L., Wong P.K., Tan J., Ang T.P., and Wang Z. Studies on the nature of catalysis: suppression of the catalytic activity of leached Pd by supported Pd particles during the Heck reaction. *J. Phys. Chem. C Nanomater. Interfaces*, **113**(23):10120–10130, 2009.

[77] Numbermska-Ray I., Gniewek A., Trzeciak A.M., Ziółkowski J.J., and Tylus W. Homogeneous/heterogeneous palladium based catalytic system for Heck reaction. The reversible transfer of palladium between solution and support. *Top. Catal.*, **40**(1-4):173–184, 2006.

[78] Reimann S., Stötzel J., Frahm R., Kleist W., Grunwaldt J.K., and Baiker A. Identification of the active species generated from supported Pd catalysts in heck reactions: an in situ quick scanning EXAFS investigation. *J. Am. Chem. Soc.*, **133**(11):3921–3930, 2011.

[79] Albano G. and Aronica L.A. Acyl Sonogashira cross-coupling: state of the art and application to the synthesis of heterocyclic compounds. *Catalysts*, **10**(1):25–61, 2020.

[80] Albano G., Interlandi S., Evangelisti C., and Aronica L.A. Polyvinylpyridine-supported palladium nanoparticles: a valuable catalyst for the synthesis of alkynyl ketones via acyl Sonogashira reactions. *Catal. Letters*, **150**(3):652–659, 2020.

[81] Zhou Z., Li J.X., Xu Z., and Cai M. Recyclable heterogeneous palladium-catalyzed carbonylative Sonogashira coupling under CO gas-free conditions. *Synth. Commun.*, **50**(13):2015–2025, 2020.

[82] Álvarez R., Faza O.N., De Lera A.R., and Cárdenas D.J. A density functional theory study of the Stille cross-coupling via associative transmetalation. The role of ligands and coordinating solvents. *Adv. Synth. Catal.*, **349**(6):887–906, 2007.

[83] Álvarez R., Faza O.N., López C.S., and De Lera Á.R. Computational characterization of a complete palladium-catalyzed cross-coupling process: the associative transmetalation in the Stille reaction. *Org. Lett.*, **8**(1):35–38, 2006.

[84] Chass G.A., O'Brien C.J., Hadei N., Kantchev E.A.B., Mu W.H., Fang D.C., Hopkinson A.C., Csizmadia I.G., and Organ M.G. Density functional theory investigation of the alkyl-alkyl negishi Cross-coupling reaction catalyzed by N-heterocyclic carbene (NHC)-Pd complexes. *Chem. Eur. J.*, **15**(17):4281–4288, 2009.

[85] Busacca C.A., Fandrick D.R., Song J.J., and Senanayake C.H. *Transition Metal Catalysis in the Pharmaceutical Industry*, chapter 1, pages 1–24. John Wiley & Sons, Ltd, 2012.

[86] Dey R., Sreedhar B., and Ranu B.C. Molecular sieves-supported palladium(II) catalyst: Suzuki coupling of chloroarenes and an easy access to useful intermediates for the synthesis of irbesartan, losartan and boscalid. *Tetrahedron*, **66**(13):2301–2305, 2010.

[87] Jingquan S., Xiangshan W., and Xianzhen Z. *Preparation method of Boscalid*. International Application CN201410298571.8A. International Publication of CN104016915A; China Patent, 2014.

[88] Ennis D.S., McManus J., Wood-Kaczmar W., Richardson J., Smith G.E., and Carstairs A. Multikilogram-scale synthesis of a biphenyl carboxylic acid derivative using a Pd/C-mediated suzuki coupling approach. *Org. Proc. Res. Dev.*, **3**(4):248–252, 1999.

[89] Conlon D.A., Drahus-Paone A., Ho G.J., Pipik B., Helmy R., McNamara J.M., Shi Y.J., Williams J.M., Macdonald D., Deschênes D., Gallant M., Mastracchio A., Roy B., and Scheigetz J. Process development and large-scale synthesis of a PDE4 inhibitor. *Org. Proc. Res. Dev.*, **10**(1):36–45, 2006.

[90] Macdonald D., Mastracchio A., Perrier H., Dubé D., Gallant M., Lacombe P., Deschênes D., Roy B., Scheigetz J., Bateman K., Li C., Trimble L.A., Day S., Chauret N., Nicoll-Griffith D.A., Silva J.M., Huang Z., Laliberté F., Liu S., Ethier D., Pon D., Muise E., Boulet L., Chi C.C., Styhler A., Charleson S., Mancini J., Masson P., Claveau D., Nicholson D., Turner M., Young R.N., and Girard Y. Discovery of a substituted 8-arylquinoline series of PDE4 inhibitors: Structure-activity relationship, optimization, and identification of a highly potent, well tolerated, PDE4 inhibitor. *Bioorg. Med. Chem. Lett.*, **15**(23):5241–5246, 2005.

[91] Fodor D., Kégl T., Tickas J.M., Horváth A.K., and Mika L.T. Homogeneous Pd-catalyzed Heck coupling in γ-valerolactone as a green reaction medium: a catalytic, kinetic, and computational study. *ACS Sustain. Chem. Eng.*, **8**:9926–9936, 2020.

[92] Shen W. Palladium catalyzed coupling of aryl chlorides with arylboronic acids. *Tetrahedron Lett.*, **38**(32):5575–5578, 1997.

[93] Bharamanagowda M.M. Fe_3O_4-Lignin@Pd-NPs : a highly efficient , magnetically recoverable and recyclable catalyst for Mizoroki-Heck reaction under solvent-free conditions. *Appl. Organomet. Chem.*, **2020**:1–18, 2020.

[94] Peramo A., Abdellah I., Pecnard S., Mougin J., Martini C., Couvreur P., Huc V., and Desmaële D. A self-assembling NHC-PD-loaded calixarene as a potent catalyst for the Suzuki-Miyaura cross-coupling reaction in water. *Molecules*, **25**(6), 2020.

[95] You X., Chaudhari M., Rempe S., and Pratt L.R. Dielectric properties of ethylene carbonate and propylene carbonate using molecular dynamics simulations. *ECS Trans.*, **69**(1):107–111, 2015.

[96] Fisher Scientific. Propylene Carbonate Safety Data Sheet. Available at https://www.fishersci.com/store/msds?partNumber=043314&productDescription=PROPYLENE+CARBONATE+R+4L&vendorId=VN00033897&countryCode=US&language=en, 2018.

[97] Common Solvents Used in Organic Chemistry: Table of Properties. Available at https://www.organicdivision.org/wp-content/uploads/2016/12/organic_solvents.html.

[98] Solvent Physical Properties. Available at https://people.chem.umass.edu/xray/solvent.html.

[99] Fisher Scientific. N,N-Dimethylacetamide Safety Data Sheet. Available at https://www.fishersci.com/store/msds?partNumber=D1601&productDescription=N%2CN-DIMETHYLACETAMIDE+GC+HS+1L&vendorId=VN00033897&countryCode=US&language=en, 2018.

[100] Corradini F., Marcheselli L., Tassi L., and Tosi G. Static dielectric constants of the N,N-dimethylformamide/2-methoxyethanol solvent system at various temperatures. *Can. J. Chem.*, **70**(12):2895–2899, 1992.

[101] Fisher Scientific. N,N-Dimethylformamide Safety Data Sheet. Available at https://www.fishersci.com/msdsproxy%3FproductName%3DD1314%26productDescription%3DDIMETHYLFORMAMIDE%2BSPECTRA%2B4L%26catNo%3DD131-4%26vendorId%3DVN00033897%26storeId%3D10652, 2018.

[102] Cseri L. and Szekely G. Towards cleaner PolarClean: efficient synthesis and extended applications of the polar aprotic solvent methyl 5-(dimethylamino)-2-methyl-5-oxopentanoate. *Green Chem.*, **21**(15):4178–4188, 2019.

[103] CYRENE^{TM} BioRenewable - Cyrene(TM) nan Sigma-Aldrich. Available at https://www.sigmaaldrich.com/catalog/product/sial/807796?lang=it&region=IT&gclid=Cj0KCQjws536BRDTARIsANeUZ5-DuZ2Pbf7iKjLlfDka_FJ9WKW0HaC0rsPNWEfjlSQB-Il7UIvNwFwaAk8hEALw_wcB.

[104] Dielectric Constants of Liquids - Engineering ToolBox. Available at https://www.engineeringtoolbox.com/liquid-dielectric-constants-d_1263.html.

[105] Fisher Scientific. Ethylene Glycol Safety Data Sheet. Available at https://www.fishersci.com/msdsproxy%3FproductName%3DE1774%26productDescription%3DETHYLENE%2BGLYCOL%2BLABORATORY%2B4L%26catNo%3DE177-4%2B%26vendorId%3DVN00033897%26storeId%3D10652, 2018.

[106] Acetonitrile - High Purity Solvents | Sigma-Aldrich. Available at https://www.sigmaaldrich.com/chemistry/solvents/acetonitrile-center.html.

[107] LabChem. Acetonitrile Safety Data Sheet. *Federal Register*, **77**(58):1–9, 2016.

[108] Nomura K. and Terwilliger P. Self-dual Leonard pairs a bio-based green solvent and ligand for iron-mediated AGET ATRP. *De Gruyter*, pages 323–329, 2019.

[109] Restek Corporation. γ-Valerolactone Safety Data Sheet. Available at `https://www.restek.com/documentation/msds/34080_useng.pdf`, 2017.

[110] N-Methyl-2-pyrrolidone. Available at `http://www.microkat.gr/msdspd90-99/N-Methyl-2-pyrrolidone.html`.

[111] Fisher Scientific. 1-Methyl-2-pyrrolidone Safety Data Sheet. Available at `https://www.fishersci.com/store/msds?partNumber=036884&productDescription=1-METHYL-2-PYRROLIDINONE+P+4L&vendorId=VN00033897&countryCode=US&language=en`, 2020.

[112] Global Safety Management. Methanol, Lab Grade, 4L. Available at `https://beta-static.fishersci.com/content/dam/fishersci/en_US/documents/programs/education/regulatory-documents/sds/chemicals/chemicals-m/S25426A.pdf`, 2015.

[113] LabChem. Acetone Safety Data Sheet. *Federal Register*, **77**(2):1–10, 2012.

[114] Dielectric Constant. Available at `https://macro.lsu.edu/HowTo/solvents/Dielectric%20Constant%20.htm`.

[115] LabChem. Isopropyl Alcohol (2-Propanol) Safety Data Sheet. *Federal Register*, **77**(58):1–10, 2020.

[116] Ethyl lactate | Search by name | Musashino Chemical Laboratory. Available at `https://www.musashino.com/english/product/name/ethyl_lactate/`.

[117] Fisher Scientific. Ethyl L(-)-lactate Safety Data Sheet. Available at `https://www.fishersci.com/store/msds?partNumber=AC118662500&productDescription=ETHYL+L%28-%29-LACTATE+97%25+250MLE&vendorId=VN00032119&countryCode=US&language=en`, 2018.

[118] Dielectric constant of tetrahydrofuran. Available at `http://www.ddbst.com/en/EED/PCP/DEC_C159.php`.

[119] Central Drug House (P) Ltd. Tetrahydrofuran Safety Data Sheet. pages 1–8, 2008.

[120] Sigma-Aldrich. 1,2-Dimethoxyethane Material Safety Data Sheet. pages 1–7, 2013.

[121] 2-methyltetrahydrofuran - Stenutz. Available at `http://www.stenutz.eu/chem/solv6.php?name=2-methyltetrahydrofuran`.

[122] Fisher Scientific. 2-Methyltetrahydrofuran Safety Data Sheet. Available at `https://www.fishersci.com/shop/msdsproxy?productName=NC0848706&productDescription=2-METHYLTETRAHYDROFURAN%2C+19L&catNo=NC0848706&vendorId=VN00033897&storeId=10652`, 2015.

[123] LabChem. Toluene Safety Data Sheet. *Federal Register*, **77**(58):1–10, 2018.

[124] Moineau J., Pozzi G., Quici S., and Sinou D. Palladium-catalyzed Heck reaction in perfluorinated solvents. *Tetrahedron Lett.*, **40**(43):7683–7686, 1999.

[125] Rocaboy C. and Gladysz J.A. Syntheses , oxidations , and palladium complexes of fluorous dialkyl sulfides : new precursors to highly active catalysts for the Suzuki coupling. *Tetrahedron*, **58**(20):4007–4014, 2002.

[126] Tzschucke C.C., Markert C., Glatz H., and Bannwarth W. Fluorous biphasic catalysis without perfluorinated solvents : application to Pd- mediated Suzuki and Sonogashira couplings. *Angew. Chem. Int. Ed.*, **41**(23):4500–4503, 2002.

[127] Bhanage B.M., Ikushima Y., Shirai M., and Arai M. Heck reactions in supercritical carbon dioxide using organometallic complex catalysts. *High Press. Res.*, **20**(1-6):131–142, 2001.

[128] Morita D.K., Pesiri D.R., David S.A., Glaze H., and Tumas W. Palladium-catalyzed cross-coupling reactions in supercritical carbon dioxide. *Chem. Commun.*, **1998**(13):1397–1398, 1998.

[129] Carroll M.A. and Holmes A.B. Palladium-catalysed carbon-carbon bond formation in supercritical carbon dioxide prepared and employed in the first examples of palladium. *Chem. Commun.*, pages 1395–1396, 1998.

[130] Ferrazzano L., Martelli G., Fantoni T., Daka A., Corbisiero D., Viola A., Ricci A., Cabri W., and Tolomelli A. Fast Heck-Cassar-Sonogashira (HCS) reactions in green solvents. *Org. Lett.*, **22**:3969–3973, 2020.

[131] Sherwood J. Suzuki-Miyaura cross coupling is not an informative reaction to demonstrate the performance of new solvents. *Beilstein J. Org. Chem.*, **16**:1001–1005, 2020.

[132] Horváth I.T., Mehdi H., Fábos V., Boda L., and Mika L.T. γ-valerolactone - a sustainable liquid for energy and carbon-based chemicals. *Green Chem.*, **10**:238–242, 2008.

[133] Fu L., Cao X., Wan J.P., and Liu Y. Synthesis of enaminone-Pd(II) complexes and their application in catalysing aqueous Suzuki-Miyaura cross coupling reaction. *Chin. J. Chem.*, **38**(3):254–258, 2020.

[134] Jani M.A. and Bahrami K. BNPs@Cur-Pd as a versatile and recyclable green nanocatalyst for Suzuki, Heck and Stille coupling reactions. *J. Exp. Nanosci.*, **15**(1):182–201, 2020.

[135] Li X., Huang Z.G., Zhang H., Zhang Y., Zhang C., Li H.Y.H., Martin D.C., and Ni C. Si-thiol supported atomic-scale palladium as efficient and recyclable catalyst for Suzuki coupling reaction. *Nanotechnology*, **31**(35):355704, 2020.

[136] Bankar D.B., Hawaldar R.R., Arbuj S.S., Shinde S.T., Gadde J.R., Rakshe D.S., Amalnerkar D.P., and Kanade K.G. Palladium loaded on ZnO nanoparticles: synthesis, characterization and application as heterogeneous catalyst for Suzuki–Miyaura cross-coupling reactions under ambient and ligand-free conditions. *Mater. Chem. Phys.*, **243**:122561, 2020.

[137] Böhm V.P.W. and Herrmann W.A. Nonaqueous ionic liquids: superior reaction media for the catalytic Heck-vinylation of chloroarenes. *Chem. Eur. J.*, **6**(6):1017–1025, 2000.

[138] Herrmann W.A. and Böhm V.P.W. Heck reaction catalyzed by phospha-palladacycles in non-aqueous ionic liquids. *J. Organomet. Chem.*, **572**(1):141–145, 1999.

[139] Xu L., Chen W., and Xiao J. Heck reaction in ionic liquids and the in situ identification of N-heterocyclic carbene complexes of palladium. *Organometallics*, **19**(6):1123–1127, 2000.

[140] Xiao J.C. and Shreeve J.M. Synthesis of 2,2'-biimidazolium-based ionic liquids: use as a new reaction medium and ligand for palladium-catalyzed Suzuki cross-coupling reactions. *J. Org. Chem.*, **70**(8):3072–3078, 2005.

[141] Okubo K., Shirai M., and Yokoyama C. Heck reactions in a non-aqueous ionic liquid using silica supported palladium complex catalysts. *Tetrahedron Lett.*, **43**(39):7115–7118, 2002.

[142] Zhao F., Shirai M., Ikushima Y., and Arai M. The leaching and re-deposition of metal species from and onto conventional supported palladium catalysts in the Heck reaction of iodobenzene and methyl acrylate in N-methylpyrrolidone. *J. Mol. Catal. A: Chemical*, **180**(1-2):211–219, 2002.

[143] LeBlond C.R., Andrews A.T., Sun Y., and Sowa J.R. Activation of aryl chlorides for Suzuki cross-coupling by ligandless, heterogeneous palladium. *Org. Lett.*, **3**(10):1555–1557, 2001.

[144] Ambulgekar G.V., Bhanage B.M., and Samant S.D. Low temperature recyclable catalyst for Heck reactions using ultrasound. *Tetrahedron Lett.*, **46**(14):2483–2485, 2005.

[145] Corma A., García H., and Leyva A. Bifunctional palladium-basic zeolites as catalyst for Suzuki reaction. *Appl. Catal. A Gen.*, **236**(1-2):179–185, 2002.

[146] Corma A., García H., Leyva A., and Primo A. Basic zeolites containing palladium as bifunctional heterogeneous catalysts for the Heck reaction. *Appl. Catal. A Gen.*, **247**(1):41–49, 2003.

[147] Dams M., Drijkoningen L., De Vos D.E., Jacobs P.A., Pauwels B., and Van Tendeloo G. Pd-zeolites as heterogeneous catalysts in Heck chemistry. *J. Catal.*, **209**(1):225–236, 2002.

[148] Shieh W.C., Shekhar R., Blacklock T., and Tedesco A. A simple, recyclable, polymer-supported palladium catalyst for Suzuki coupling - An effective way to minimize palladium contamination. *Synth. Commun.*, **32**(7):1059–1067, 2002.

[149] González-Arellano C., Corma A., Iglesias M., and Sánchez F. Pd(II)-Schiff base complexes heterogenised on MCM-41 and delaminated zeolites as efficient and recyclable catalysts for the Heck reaction. *Adv. Synth. Catal.*, **346**(13-15):1758–1764, 2004.

[150] Joo S.R., Kwon G.T., and Kim S.H. A combination of biocompatible room temperature ionic liquid and palladium catalyst for base- and ligand-free Suzuki coupling reactions. *Asian J. Org. Chem.*, **9**(4):584–587, 2020.

[151] Ramsingh Girase T., Bhilare S., Sankar Murthy Bandaru S., Chrysochos N., Schulzke C., Sanghvi Y.S., and Kapdi A.R. Carbazole-based N-heterocyclic carbenes for the promotion of copper-catalyzed palladium-free homo-/hetero-coupling of alkynes and Sonogashira reactions. *Asian J. Org. Chem.*, **9**(2):274–291, 2020.

[152] Thiyagamurthy P. and Khan F.R.N. A base-free Pd-precatalyst mediated Suzuki-Miyaura and Sonogashira cross-coupling in deep eutectic solvents. *ChemistrySelect*, **5**(8):2610–2617, 2020.

[153] Mhaldar P., Vibhute S., Rashinkar G., and Pore D. Highly effective cellulose supported 2-aminopyridine palladium complex (Pd(II)-AMP-Cell@Al_2O_3) for Suzuki-Miyaura and Mizoroki–Heck cross-coupling. *React. Funct. Polym.*, **152**:104586, 2020.

[154] Rajan P., Sarika V., Suku A., Krishnan A., and Saithalavi A. Amidoxime modified PAN supported palladium complex : a greener and efficient heterogeneous catalyst for Heck reaction. *Inorg. Chim. Acta*, **502**:119305, 2020.

[155] Mangaiyarkarasi R., Priyanga M., Santhiya N., and Umadevi S. In situ preparation of palladium nanoparticles in ionic liquid crystal microemulsion and their application in Heck reaction. *J. Mol. Liq.*, **310**:113241, 2020.

[156] Fang P.P., Jutand A., Tian Z.Q., and Amatore C. Au-Pd core-shell nanoparticles catalyze Suzuki-Miyaura reactions in water through Pd leaching. *Angew. Chem. Int. Ed.*, **50**(51):12184–12188, 2011.

[157] Peral D., Gómez-Villarraga F., Sala X., Pons J., Carles Bayón J., Ros J., Guerrero M., Vendier L., Lecante P., García-Antón J., and Philippot K. Palladium catalytic systems with hybrid pyrazole ligands in C-C coupling reactions. Nanoparticles versus molecular complexes. *Catal. Sci. Technol.*, **3**(2):475–489, 2013.

[158] Collins G., Schmidt M., O'Dwyer C., Holmes J.D., and McGlacken G.P. The origin of shape sensitivity in palladium-catalyzed Suzuki-Miyaura cross coupling reactions. *Angew. Chem. Int. Ed.*, **53**(16):4142–4145, 2014.

[159] Fusini G., Rizzo F., Angelici G., Pitzalis E., Evangelisti C., and Carpita A. Polyvinylpyridine-supported palladium nanoparticles : an efficient catalyst for Suzuki-Miyaura coupling reactions. *Catalysts*, **10**:330–342, 2020.

[160] Hübner S., de Vries J.G., and Farina V. Why does industry not use immobilized transition metal complexes as catalysts? *Adv. Synth. Catal.*, **358**(1):3–25, 2016.

[161] Deraedt C. and Astruc D. "Homeopathic" palladium nanoparticle catalysis of cross carbon-carbon coupling reactions. *Acc. Chem. Res.*, **47**(2):494–503, 2014.

[162] Bourouina A., Meille V., and Bellefon de C. About solid phase vs. liquid phase in Suzuki-Miyaura reaction. *Catalysts*, **9**(1):60–87, 2019.

[163] Jain S., Ji Y., and Davis R.J. Investigation of transition metal leaching from supported Pd catalysts during the Heck reaction. *AIChE Annual Meeting, Conference Proceedings*, page 9556, 2005.

[164] Kozuch S. and Martin J.M.L. "Turning over" definitions in catalytic cycles. *ACS Catal.*, **2**(12):2787–2794, 2012.

[165] Beletskaya I.P., Kashin A.N., Karlstedt N.B., Mitin A.V., Cheprakov A.V., and Kazankov G.M. NC-palladacycles as highly effective cheap precursors for the phosphine-free Heck reactions. *J. Organomet. Chem.*, **622**(1-2):89–96, 2001.

[166] Beletskaya I.P. and Cheprakov A.V. Heck reaction as a sharpening stone of palladium catalysis. *Chem. Rev.*, **100**(8):3009–3066, 2000.

[167] Jeffery T. Palladium-catalyzed vinylation of organic halides under solid-liquid phase transfer conditions. *J. Chem. Soc.Chem. Commun.*, **19**:1287–1289, 1984.

[168] Reetz M.T. and Westermann E. Phosphane-free palladium-catalyzed coupling reactions: the decisive role of Pd nanoparticles. *Angew. Chem. Int. Ed.*, **39**(1):165–168, 2000.

[169] Cassol C.C., Umpierre A.P., Machado G., Wolke S.I., and Dupont J. The role of Pd nanoparticles in ionic liquid in the Heck reaction. *J. Am. Chem. Soc.*, **127**(10):3298–3299, 2005.

[170] de Vries J.G. Ligand-free Heck reactions using low Pd-loading. *Chem. Commun.*, **4**(14):1559–1563, 2004.

[171] Kapdi A.R., Whitwood A.C., Williamson D.C., Lynam J.M., Burns M.J., Williams T.J., Reay A.J., Holmes J., and Fairlamb I.J.S. The elusive structure of $Pd_2(dba)_3$. Examination by isotopic labeling, NMR spectroscopy, and X-ray diffraction analysis: synthesis and characterization of $Pd_2(dba\text{-}Z)_3$ complexes. *J. Am. Chem. Soc.*, **135**(22):8388–8399, 2013.

[172] Zalesskiy S.S. and Ananikov V.P. $Pd_2(dba)_3$ as a precursor of soluble metal complexes and nanoparticles: determination of palladium active species for catalysis and synthesis. *Organometallics*, **31**(6):2302–2309, 2012.

[173] Zheng Q., Liu Y., Chen Q., Hu M., Helmy R., Sherer E.C., Welch C.J., and Chen H. Capture of reactive monophosphine-ligated palladium(0) intermediates by mass spectrometry. *J. Am. Chem. Soc.*, **137**(44):14035–14038, 2015.

[174] Braun M., Meletis P., and Fidan M. (S)-(–)-2-allylcyclohexanone. *Org. Synth.*, **86**:47–58, 2009.

[175] Carrillo J., Gómez A., Costa A.M., Fernández P., Isart C., Sidera M., and Vilarrasa J. A synthetic approach to palmerolides via Negishi cross coupling. The challenge of the C15-C16 bond formation. *Tetrahedron Lett.*, **55**(33):4623–4627, 2014.

[176] Düfert M.A., Billingsley K.L., and Buchwald S.L. Suzuki-Miyaura cross-coupling of unprotected, nitrogen-rich heterocycles: substrate scope and mechanistic investigation. *J. Am. Chem. Soc.*, **135**(34):12877–12885, 2013.

[177] Li W., Yang L., Tumbleston J.R., Yan L., Ade H., and You W. Controlling molecular weight of a high efficiency donor-acceptor conjugated polymer and understanding its significant impact on photovoltaic properties. *Adv. Mater.*, **26**(26):4456–4462, 2014.

[178] Doran R. and Guiry P.J. Catalytic asymmetric synthesis of sterically hindered tertiary α-aryl ketones. *J. Org. Chem.*, **79**(19):9112–9124, 2014.

[179] Hughes M., Boultwood T., Zeppetelli G., and Bull J.A. Palladium-catalyzed cross-coupling of aziridinylmetal species, generated by sulfinyl-magnesium exchange, with aryl bromides: reaction optimization, scope, and kinetic investigations. *J. Org. Chem.*, **78**(3):844–854, 2013.

[180] Imagawa N., Nagato Y., Ohmatsu K., and Ooi T. Multiple absolute stereocontrol in Pd-catalyzed [3+2] cycloaddition of oxazolidinones and trisubstituted alkenes using chiral ammoniumphosphine hybrid ligands. *Bull. Chem. Soc. Jpn.*, **89**(6):649–656, 2016.

[181] Kendall A.J., Zakharov L.N., and Tyler D.R. Steric and electronic influences of Buchwald-type alkyl-JohnPhos ligands. *Inorg. Chem.*, **55**(6):3079–3090, 2016.

[182] Lunn D.J., Gould O.E.C., Whittell G.R., Armstrong D.P., Mineart K.P., Winnik M.A., Spontak R.J., Pringle P.G., and Manners I. Microfibres and macroscopic films from the coordination-driven hierarchical self-Assembly of cylindrical micelles. *Nat. Commun.*, **7**:12371, 2016.

[183] Chandrasekhar S., Narsihmulu C., Shameem Sultana S., and Ramakrishna Reddy N. Poly(ethylene glycol) (PEG) as a reusable solvent medium for organic synthesis. Application in the Heck reaction. *Org. Lett.*, **4**(25):4399–4401, 2002.

[184] Wolfe J.P. and Buchwald S.L. A highly active catalyst for the room-temperature amination and Suzuki coupling of aryl chlorides. *Angew. Chem. Int. Ed.*, **38**(16):2413–2416, 1999.

[185] Pickett T.E. and Richards C.J. Synthesis of a C_3-symmetric ferrocenylphosphine and its application to the Suzuki reaction of aryl chlorides. *Tetrahedron Lett.*, **42**(22):3767–3769, 2001.

[186] Pickett T.E., Roca F.X., and Richards C.J. Synthesis of monodentate ferrocenylphosphines and their application to the palladium-catalyzed Suzuki reaction of aryl chlorides. *J. Org. Chem.*, **68**(7):2592–2599, 2003.

[187] Herrmann W.A., Broßmer C., Öfele K., Beller M., and Fischer H. Coordination chemistry and mechanisms of metal-catalyzed CC-coupling reactions [1]. Part 7. Heck vinylation of aryl halides with n-butyl acrylate: relevance of PC bond cleavage to catalyst deactivation. *J. Mol. Catal. A Chem.*, **103**(3):133–146, 1995.

[188] Kirchhoff J.H., Dai C., and Fu G.C. A method for palladium-catalyzed cross-couplings of simple alkyl chlorides: Suzuki reactions catalyzed by $[Pd_2(dba)_3]/PCy_3$. *Angew. Chem. Int. Ed.*, **41**(11):1945–1947, 2002.

[189] Hartwig J.F. Recent advances in palladium- and nickel- catalyzed chemistry provide new ways to construct C-N and C-O bonds . *Angew. Chem. Int. Ed.*, **37**:2046–2067, 1998.

[190] Baber R.A., Collard S., Hooper M., Orpen A.G., Pringle P.G., Wilkinson M.J., and Wingad R.L. Bulky triarylarsines are effective ligands for palladium catalysed Heck olefination. *Dalton Trans.*, **124**(8):1491–1498, 2005.

[191] Grasa G.A., Hillier A.C., and Nolan S.P. Convenient and efficient Suzuki-Miyaura cross-coupling catalyzed by a palladium / diazabutadiene system. *Org. Lett.*, **3**(7):1–4, 2001.

[192] Grasa G.A., Singh R., Ste E.D., and Nolan P. Catalytic activity of Pd(II) and Pd(II)/DAB-R systems for the Heck arylation of olefins. *J. Organomet. Chem.*, **687**(2):269–279, 2003.

[193] Huang M. and Liang L. Amido pincer complexes of palladium : synthesis , structure , and catalytic Heck reaction. *Organometallics*, **23**(11):2813–2816, 2004.

[194] Beletskaya I.P., Chuchuryukin A.V., Van Koten G., Dijkstra H.P., Van Klink G.P.M., Kashin A.N., Nefedov S.E., and Eremenko I.L. Synthesis and catalytic properties of di- and trinuclear palladium complexes with PCP-pincer ligands. *Russian J. Org. Chem.*, **39**(9):1268–1281, 2003.

[195] Beletskaya I.P. and Cheprakov A.V. Palladacycles in catalysis - A critical survey. *J. Organomet. Chem.*, **689**(24):4055–4082, 2004.

[196] Isai Ortega-Gaxiola J., Valdés H., Rufino-Felipe E., Toscano R.A., and Morales-Morales D. Synthesis of Pd(II) complexes with P-N-OH ligands derived from 2-(diphenylphosphine)-benzaldehyde and various aminoalcohols and their catalytic evaluation on Suzuki-Miyaura couplings in aqueous media. *Inorg. Chim. Acta*, **504**, 2020.

[197] Beller M. and Riermeier T.H. First efficient palladium-catalyzed Heck reactions of aryl bromides with alkyl methacrylate. *Tetrahedron Lett.*, **37**(36):6535–6538, 1996.

[198] Beller M. and Riermeier T.H. Phosphapalladacycle-catalyzed Heck reactions for efficient synthesis of trisubstituted olefins: evidence for palladium(0) intermediates. *Eur. J. Inorg. Chem.*, **1998**(1):29–35, 1998.

[199] Bergbreiter D.E., Osburn P.L., and Liu Y.S. Tridentate SCS palladium(II) complexes: new, highly stable, recyclable catalysts for the Heck reaction. *J. Am. Chem. Soc.*, **121**(41):9531–9538, 1999.

[200] Eberhard M.R. Insights into the Heck reaction with PCP pincer palladium(II) complexes. *Org. Lett.*, **6**(13):2125–2128, 2004.

[201] Bedford R.B., Hazelwood S.L., Horton P.N., and Hursthouse M.B. Orthopalladated phosphinite complexes as high-activity catalysts for the Suzuki reaction. *Dalton Trans.*, **3**(21):4164–4174, 2003.

[202] Schnyder A., Indolese A.F., Studer M., and Blaser H.U. A new generation of air stable, highly active Pd complexes for C-C and C-N coupling reactions with aryl chlorides. *Angew. Chem. Int. Ed.*, **41**(19):3668–3671, 2002.

[203] Navarro O., Kelly R.A., and Nolan S.P. A general method for the Suzuki-Miyaura cross-coupling of sterically hindered aryl chlorides: Synthesis of di- and tri-ortho-substituted biaryls in 2-propanol at room temperature. *J. Am. Chem. Soc.*, **125**(52):16194–16195, 2003.

[204] López-mosquera C., Grabulosa A., Rocamora M., and Font-bardia M. Cyclopalladated compounds with polyhalogenated benzylphosphanes for the Mizoroki-Heck reaction. *Eur. J. Inorg. Chem.*, **2020**:2470–2484, 2020.

[205] Nowotny M., Hanefeld U., Van Koningsveld H., and Maschmeyer T. Cyclopalladated imine catalysts in Heck arylation: search for the catalytic species. *Chem. Commun.*, **2**(19):1877–1878, 2000.

[206] Dupont J., Pfeffer M., and Spencer J. Palladacycles - An old organometallic family revisited: new, simple, and efficient catalyst precursors for homogeneous catalysis. *Eur. J. Inorg. Chem.*, **2001**(8):1917–1927, 2001.

[207] Rocaboy C. and Gladysz J.A. Thermomorphic fluorous imine and thioether palladacycles as precursors for highly active Heck and Suzuki catalysts; evidence for palladium nanoparticle pathways. *New J. Chem.*, **27**(1):39–49, 2003.

[208] Consorti C.S., Zanini M.L., Leal S., Ebeling G., and Dupont J. Chloropalladated propargyl amine: a highly efficient phosphine-free catalyst precursor for the Heck reaction. *Org. Lett.*, **5**(7):983–986, 2003.

[209] Kumar A., Rao G.K., Kumar S., and Singh A.K. Organosulphur and related ligands in Suzuki–Miyaura C–C coupling. *Dalton Trans.*, **42**(2):5200–5223, 2013.

[210] Kumar A., Rao G.K., Saleem F., and Singh A.K. Organoselenium ligands in catalysis. *Dalton Trans.*, **41**(39):11949–11977, 2012.

[211] Panda A. Chemistry of selena macrocycles. *Coord. Chem. Rev.*, **253**(7-8):1056–1098, 2009.

[212] Rao G.K., Kumar A., Kumar N., Kumar D., and Singh A.K. Palladium(II)-selenated Schiff base complex catalyzed Suzuki-Miyaura coupling: dependence of efficiency on alkyl chain length of ligand. *Dalton Trans.*, **41**(7):1931–1937, 2012.

[213] Nagalakshmi V., Sathya M., Premkumar M., Kaleeswaran D., Venkatachalam G., and Balasubramani K. Palladium(II) complexes comprising naphthylamine and biphenylamine based Schiff base ligands: synthesis, structure and catalytic activity in Suzuki coupling reactions. *J. Organomet. Chem.*, **914**:121220, 2020.

[214] Nandhini R., Vijayan P., and Venkatachalam G. Palladium(II) complexes containing sterically bulky O, N donor ligands: synthesis, characterization and catalytic activity in the Suzuki-Miyaura and Sonogashira coupling reactions. *J. Organomet. Chem.*, **907**:121080, 2020.

[215] Sünbül A.B., Inan A., Köse M., Evren E., Gürbüz N., Ozdemir İ., Ikiz M., Dağ A.K., and Ispir E. Azo-azomethine based palladium(II) complexes as catalysts for the Suzuki-Miyaura cross-coupling reaction. *J. Mol. Struct.*, **1216**:128279, 2020.

[216] Zhang H., Zhu J.H., Hou F., Quan Z.J., and Wang X.C. A catalytic system with high efficiency and recyclability based on Suzuki and Heck reaction in aqueous admicellar medium. *Appl. Organomet. Chem.*, **34**(4):1–7, 2020.

[217] Beller M., Fischer H., Herrmann W.A., Öfele K., and Brossmer C. Palladacycles as efficient catalysts for aryl coupling reactions. *Angew. Chem. Int. Ed.*, **34**(17):1848–1849, 1995.

[218] Herrmann W.A., Broßmer C., Öfele K., Reisinger C., Priermeier T., Beller M., and Fischer H. Palladacycles as structurally defined catalysts for the Heck olefination of chloro- and bromoarenes. *Angew. Chem. Int. Ed.*, **34**(17):1844–1848, 1995.

[219] Herrmann W.A., Reisinger C.P., Öfele K., Broßmer C., Beller M., and Fischer H. Facile catalytic coupling of aryl bromides with terminal alkynes by phospha-palladacycles. *J. Mol. Catal. A: Chemical*, **108**(2):51 – 56, 1996.

[220] Brunel J.M., Hirlemann M.H., Heumann A., and Buono G. New highly active chiral phospha-palladacycle catalysts. First isolation and characterization of a Pd(IV) intermediate. *Chem. Commun.*, **1869**(19):1869–1870, 2000.

[221] Miyazaki F., Yamaguchi K., and Shibasaki M. The synthesis of a new palladacycle catalyst. Development of a high performance catalyst for Heck reactions. *Tetrahedron Lett.*, **40**(41):7379–7383, 1999.

[222] Gruber A.S., Zim D., Ebeling G., Monteiro A.L., and Dupont J. Sulfur-containing palladacycles as catalyst precursors for the Heck reaction. *Org. Lett.*, **2**(9):1287–1290, 2000.

[223] Jung I.G., Son S.U., Park K.H., Chung K.C., Lee J.W., and Chung Y.K. Synthesis of novel Pd-NCN pincer complexes having additional nitrogen coordination sites and their application as catalysts for the Heck reaction. *Organometallics*, **22**(23):4715–4720, 2003.

[224] Yao Q., Kinney E.P., and Yang Z. Ligand-free Heck reaction: $Pd(OAc)_2$ as an active catalyst revisited. *J. Org. Chem.*, **68**(19):7528–7531, 2003.

[225] Heravi M.M., Asadi S., Hoseini Chopani S.M., and Jaderi E. N-heterocyclic carbene–palladium complex onto graphene oxide and poly (ethylene glycol) (PEG) applied as superior catalyst for the Suzuki-Miyaura cross-coupling reaction in water. *Appl. Organomet. Chem.*, **34**(9):1–13, 2020.

[226] Herrmann W.A., Reisinger C.P., and Spiegler M. Chelating N-heterocyclic carbene ligands in palladium-catalyzed Heck-type reactions. *J. Organomet. Chem.*, **557**(1):93–96, 1998.

[227] Weskamp T., Böhm V.P.W., and Herrmann W.A. Combining N-heterocyclic carbenes and phosphines: improved palladium(II) catalysts for aryl coupling reactions. *J. Organomet. Chem.*, **585**(2):348–352, 1999.

[228] Herrmann W.A., Bo V.P.W., Gsto C.W.K., Grosche M., Reisinger C.P., and Weskamp T. Synthesis, structure and catalytic application of palladium(II) complexes bearing N-heterocyclic carbenes and phopshines. *J. Organomet. Chem.*, **618**:616–628, 2001.

[229] Herrmann W.A., Böhm V.P.W., and Reisinger C.P. Application of palladacycles in Heck type reactions. *J. Organomet. Chem.*, **576**(1-2):23–41, 1999.

[230] Chen M.T., Hsieh B.Y., Liu Y.H., Wu K.H., Lussari N., and Braga A.A.C. N,N'-bridged binuclear NHC palladium complexes: a combined experimental catalytic and computational study for the Suzuki reaction. *Appl. Organomet. Chem.*, **34**(10):1–16, 2020.

[231] Zhang D. and Yu J. Fine tuning of chiral bis(N-heterocyclic carbene) palladium catalysts for asymmetric Suzuki-Miyaura cross-coupling reactions: exploring the ligand modification. *Organometallics*, **39**(8):1269–1280, 2020.

[232] Zhang Y., Zhang R., Ni C., Zhang X., Li Y., Lu Q., Zhao Y., Han F., Zeng Y., and Liu G. NHC-Pd(II)-azole complexes catalyzed Suzuki–Miyaura cross-coupling of sterically hindered aryl chlorides with arylboronic acids. *Tetrahedron Lett.*, **61**(10):151541, 2020.

[233] Dumesic J.A., Huber G.W., and Boudart M. *Principles of Heterogeneous Catalysis*, chapter 1.1, pages 1–15. American Cancer Society, 2008.

[234] Supriya S., Ananthnag G.S., Shetti V.S., Nagaraja B.M., and Hegde G. Cost-effective bio-derived mesoporous carbon nanoparticles-supported palladium catalyst for nitroarene reduction and Suzuki–Miyaura coupling by microwave approach. *Appl. Organomet. Chem.*, **34**(3):1–14, 2020.

[235] Tran T.P.N., Thakur A., Trinh D.X., Dao A.T.N., and Taniike T. Design of Pd@Graphene oxide framework nanocatalyst with improved activity and recyclability in Suzuki-Miyaura cross-coupling reaction. *Appl. Catal. A Gen.*, **549**:60–67, 2018.

[236] Mastalir Á., Hancsárik M., and Szabó T. Immobilization of a Pd(II) complex on hydrophilic graphite oxide and its catalytic investigation in the Heck coupling reaction. *Appl. Organomet. Chem.*, **34**:1–9, 2020.

[237] Shekarizadeh A. and Azadi R. Synthesis of Pd@graphene oxide framework nanocatalyst with enhanced activity in Heck-Mizoroki cross-coupling reaction. *Appl. Organomet. Chem.*, **34**(9):1–8, 2020.

[238] Mironenko R.M., Belskaya O.B., and Likholobov V.A. Approaches to the synthesis of Pd/C catalysts with controllable activity and selectivity in hydrogenation reactions. *Catal. Today*, pages 1–14, DOI: 10.1016/j.cattod.2019.03.023, 2019.

[239] Jawale D.V., Gravel E., Boudet C., Shah N., Geertsen V., Li H., Namboothiri I.N.N., and Doris E. Room temperature Suzuki coupling of aryl iodides, bromides, and chlorides using a heterogeneous carbon nanotube-palladium nanohybrid catalyst. *Catal. Sci. Technol.*, **5**(4):2388–2392, 2015.

[240] Cao N., Fei M., Feng Y., Chu W., Jiang C., and Sun W. Applied surface science density functional theory study of N-doping effect on the stability and activity of Pd/NCNT catalysts for Heck reaction. *Appl. Surf. Sci.*, **506**:144960, 2020.

[241] Védrine J.C. Heterogeneous catalysis on metal oxides. *Catalysts*, **7**(11):341–366, 2017.

[242] Augustine R.L. and O'Leary S.T. Heterogeneous catalysis in organic chemistry Part 8. The use of supported palladium catalysts for the Heck arylation. *J. Mol. Catal.*, **72**(2):229–242, 1992.

[243] de Barros S.D.T., Duarte J.P.P., Rocha L.D.S., Ramos V.S., Navarro M.I.R., Archanjo B.S., Medeiros M.E., De Campos J.B., Da Costa M.E.H.M., Lachter E.R., Senra J.D., and Malta L.F.B. Cyclodextrin - stabilized palladium nanoparticles on ceria: investigation of support interactions and pivotal promotion in the Suzuki-Miyaura reaction. *ChemistrySelect*, **5**(24):7227–7235, 2020.

[244] Kaneda K., Higuchi M., and Imanaka T. Highly dispersed Pd on MgO as catalyst for activation of phenyl-chlorine bonds leading to carbon-carbon bond formation. *J. Mol. Catal.*, **63**(3):33–36, 1990.

[245] Köhler K., Wagner M., and Djakovitch L. Supported palladium as catalyst for carbon-carbon bond construction (Heck reaction) in organic synthesis. *Catal. Today*, **66**(1):105–114, 2001.

[246] Wali A., Muthukumaru Pillai S., Kaushik V.K., and Satish S. Arylation of acrylonitrile with iodobenzene over Pd/MgO catalyst. *Appl. Catal. A Gen.*, **135**(1):83–93, 1996.

[247] Chen J., Zhang M., Pang C., Xiang F., Zhu M., Ma X., Chang G., and Yin W. Hydrophilic Pd/MgO nanosystem for the highly efficient aqueous-phase catalysis of Suzuki-Miyaura reactions. *Ind. Eng. Chem. Res.*, **59**(1):81–87, 2020.

[248] López M.I., Esquivel D., Jiménez-Sanchidrián C., Van Der Voort P., and Romero-Salguero F.J. Thiol-functionalized ethylene periodic mesoporous organosilica as an efficient scavenger for palladium: confirming the homogeneous character of the Suzuki reaction. *Materials*, **13**(3):623–637, 2020.

[249] Mennecke K. and Kirschning A. Polyionic polymers-heterogeneous media for metal nanoparticles as catalyst in Suzuki-Miyaura and Heck-Mizoroki reactions under flow conditions. *Beilstein J. of Org. Chem.*, **5**:1–6, 2009.

[250] Ichitsuka T., Suzuki N., Sairenji M., Koumura N., Ya Onozawa S., and Kobayashi K., Sato andS. Readily available immobilized Pd catalysts for Suzuki-Miyaura coupling under continuous-flow conditions. *ChemCatChem*, **11**(10):2427–2431, 2019.

[251] Yamamoto K., Nameki R., Sogawa H., and Takata T. Synthesis of polystyrene-supported Pd(II)-containing macrocyclic complex as a reusable catalyst for chemoselective Suzuki–Miyaura coupling reaction. *Tetrahedron Lett.*, **61**(21):151870, 2020.

[252] Gao P., Xiao Y., Dong Z., Pan H., and Wang W. Facile synthesis of palladium nanoparticles supported on urea-based porous organic polymers and its catalytic properties in Suzuki-Miyaura coupling. *J. Saudi Chem. Soc.*, **24**(2):282–287, 2020.

[253] Boztepe C., Künkül A., and Gürbüz N. Hydrogel supported vinylimidazole based PEPPSI-Pd-NHC catalysts: the catalytic activities in Heck and Suzuki-Miyaura coupling reactions. *J. Mol. Struct.*, **1209**:127948, 2020.

[254] Zhan K., Lu P., Dong J., and Hou X. Polymer hydrogel confined palladium nanoparticles as recyclable catalysts for Suzuki and Heck cross-coupling reactions. *Chin. Chem. Lett.*, **31**(6):1630–1634, 2019.

[255] Lei Y., Zhu W., Wan Y., Wang R., and Liu H. Pd nanoparticles supported on amphiphilic porous organic polymer as an efficient catalyst for aqueous hydrodechlorination and Suzuki-Miyaura coupling reactions. *Appl. Organomet. Chem.*, **34**(2):1–13, 2020.

[256] Chen J., Zhang J., Zhang Y., Xie M., and Li T. Nanoporous phenanthroline polymer locked Pd as highly efficient catalyst for Suzuki-Miyaura Coupling reaction at room temperature. *Appl. Organomet. Chem.*, **34**(2):1–11, 2020.

[257] Liu C., Zheng L., Xiang D., Liu S., Xu W., Luo Q., Shu Y., Ouyang Y., and Lin H. Palladium supported on triazolyl-functionalized hypercrosslinked polymers as a recyclable catalyst for Suzuki-Miyaura coupling reactions. *RSC Advances*, **10**(29):17123–17128, 2020.

[258] Crooks R.M., Zhao M., Sun L., Chechik V., and Yeung L.K. Dendrimer-encapsulated metal nanoparticles: synthesis, characterization, and applications to catalysis. *Acc. Chem. Res.*, **34**(3):181–190, 2001.

[259] Gan W., Xu H., Jin X., Cao X., and Gao H. Recyclable palladium-loaded hyperbranched polytriazoles as efficient polymer catalysts for Heck reaction. *ACS Appl. Polym. Mater.*, **2**:677–684, 2020.

[260] Nasrollahzadeh M., Bidgoli N.S.S., Issaabadi Z., Ghavamifar Z., Baran T., and Luque R. Hibiscus Rosasinensis L. aqueous extract-assisted valorization of lignin: preparation of magnetically reusable Pd NPs@Fe_3O_4-lignin for Cr(VI) reduction and Suzuki-Miyaura reaction in eco-friendly media. *Int. J. Biol. Macromol.*, **148**:265–275, 2020.

[261] Sargin I., Baran T., and Arslan G. Environmental remediation by chitosan-carbon nanotube supported palladium nanoparticles: conversion of toxic nitroarenes into aromatic amines, degradation of dye pollutants and green synthesis of biaryls. *Sep. Purif. Technol.*, **247**:116987, 2020.

[262] Wolfson A. and Levy-Ontman O. Recent developments in the immobilization of palladium complexes on renewable polysaccharides for Suzuki–Miyaura cross-coupling of halobenzenes and phenylboronic acids. *Catalysts*, **10**(1), 2020.

[263] Soltani S.S., Taheri-Ledari R., Farnia S.M.F., Maleki A., and Foroumadi A. Synthesis and characterization of a supported Pd complex on volcanic pumice laminates textured by cellulose for facilitating Suzuki-Miyaura cross-coupling reactions. *RSC Adv.*, **10**(39):23359–23371, 2020.

[264] Mosleh I., Shahsavari H.R., Beitle R., and Beyzavi M.H. Recombinant peptide fusion protein-templated palladium nanoparticles for Suzuki-Miyaura and stille coupling reactions. *ChemCatChem*, **12**(11):2942–2946, 2020.

[265] Hutchings G.J. and Védrine J.C. *Heterogeneous Catalyst Preparation*, pages 215–258. Springer Berlin Heidelberg, Berlin, Heidelberg, 2004.

[266] M., Ángeles Úbeda, Amorós P., Sánchez-Royo J.F., El Haskouri J., Dolores Marcos M., and Pérez-Pla F. Precatalyst or dosing-device? The $[Pd_2\{\mu\text{-}(C_6H_4)\ PPh_2\}_2\{\mu\text{-}O_2C(C_6H_5)\}_2]$ complex anchored on a carboxypolystyrene polymer as an effective supplier of palladium catalytically active nanoparticles for the Suzuki-Miyaura reaction. *J. Catal.*, **381**:26–37, 2020.

[267] Wang Y. and Sauer D.R. Use of polymer-supported Pd reagents for rapid and efficient Suzuki reactions using microwave heating. *Org. Lett.*, **6**(16):2793–2796, 2004.

[268] Uozumi Y. *Recent Progress in Polymeric Palladium Catalysts for Organic Synthesis*, pages 77–112. Springer Berlin Heidelberg, Berlin, Heidelberg, 2004.

[269] Terasawa M., Kaneda K., Imanaka T., and Teranishi S. A coordinatively unsaturated, polymer-bound palladium(0) complex. Synthesis and catalytic activities. *J. Organomet. Chem.*, **162**(3):403 – 414, 1978.

[270] Inada K. and Miyaura N. Synthesis of biaryls via cross-coupling reaction of arylboronic acids with aryl chlorides catalyzed by $NiCl_2$/triphenylphosphine complexes. *Tetrahedron*, **56**(44):8657–8660, 2000.

[271] Li X., Liu H., and Jiang Y. Olefinic substitution reaction catalyzed by sulfur-containing polymeric palladium complexes. *J. Mol. Catal.*, **39**(1):55–62, 1987.

[272] Hong L. and Ruckenstein E. Improving the cooperation of co-catalysts by locating them on different units of a copolymer. *J. Mol. Catal.*, **77**(3):273–282, 1992.

[273] Hong L. and Ruckenstein E. Preparation of polymer-supported catalysts containing phosphorus palladium complexes and quaternary onium groups, and their application to the vinylation reaction. *React. Polym.*, **16**(2):181–197, 1992.

[274] Bergbreiter D.E., Osburn P.L., Wilson A., and Sink E.M. Palladium-catalyzed C–C coupling under thermomorphic conditions. *J. Am. Chem. Soc.*, **122**(38):9058–9064, 2000.

[275] Schönfelder D., Fischer K., Schmidt M., Nuyken O., and Weberskirch R. Poly(2-oxazoline)s functionalized with palladium carbene complexes: soluble, amphiphilic polymer supports for C-C coupling reactions in water. *Macromolecules*, **38**(2):254–262, 2005.

[276] Bedford R.B., Coles S.J., Hursthouse M.B., and Scordia V.J.M. Polystyrene-supported dicyclohexylphenylphosphine adducts of amine- and phosphite-based palladacycles in the Suzuki coupling of aryl chlorides. *Dalton Trans.*, **2005**(5):991–995, 2005.

[277] Ooe M., Murata M., Mizugaki T., Ebitani K., and Kaneda K. Supramolecular catalysts by encapsulating palladium complexes within dendrimers. *J. Am. Chem. Soc.*, **126**(6):1604–1605, 2004.

[278] Dahan A. and Portnoy M. Remarkable dendritic effect in the polymer-supported catalysis of the Heck arylation of olefins. *Org. Lett.*, **5**(8):1197–1200, 2003.

[279] Janssen M., Müller C., and Vogt D. 'Click' dendritic phosphines : design , synthesis , application in Suzuki coupling , and recycling by nanofiltration. *Adv. Synth. Catal.*, **351**(3):313–318, 2009.

[280] Horniakova J., Raja T., Kubota Y., and Sugi Y. Pyridine-derived palladium complexes immobilized on ordered mesoporous silica as catalysts for Heck-type reactions. *J. Mol. Catal. A: Chemical*, **217**(1-2):73–80, 2004.

[281] Hardy J.J.E., Hubert S., Macquarrie D.J., and Wilson A.J. Chitosan-based heterogeneous catalysts for Suzuki and Heck reactions. *Green Chem.*, **6**(1):53–56, 2004.

[282] Liu N., Qiao N.N., Liu F.S., Wang S.H., and Liang Y. Bulky α-diimine palladium complexes supported graphene oxide as heterogeneous catalysts for Suzuki-Miyaura reaction. *J. Mol. Struct.*, **1218**:128537, 2020.

[283] Ibrahim A.A., Lin A., Adly M.S., and El-Shall M.S. Enhancement of the catalytic activity of Pd nanoparticles in Suzuki coupling by partial functionalization of the reduced graphene oxide support with p-phenylenediamine and benzidine. *J. Catal.*, **385**:194–203, 2020.

[284] Mehnert C.P., Weaver D.W., and Ying J.Y. Heterogeneous Heck catalysis with palladium-grafted molecular sieves. *J. Am. Chem. Soc.*, **120**(47):12289–12296, 1998.

[285] Mehnert C.P. and Ying J.Y. Palladium-grafted mesoporous MCM-41 material as heterogeneous catalyst for Heck reactions. *Chem. Commun.*, **1997**(22):2215–2216, 1997.

[286] Biffis A., Zecca M., and Basato M. Palladium metal catalysts in Heck C–C coupling reactions. *J. Mol. Catal. A Chem.*, **173**(1-2):249–274, 2001.

[287] Niknam E., Panahi F., and Khalafi-Nezhad A. Immobilized Pd on a NHC functionalized metal–organic framework MIL-101(Cr): an efficient heterogeneous catalyst in Suzuki-Miyaura coupling reaction in water. *Appl. Organomet. Chem.*, **34**(4):1–15, 2020.

[288] Julia M. and Duteil M. Condensation of aromatic halides with olefins, catalyzed by palladium. *Bull. Soc. Chim. Fr.*, (9-10):2790, 1973.

[289] Julia M., Duteil M., Grard C., and Kuntz E. Condensation of aryl halides with olefins catalyzed by palladium. *Bull. Soc. Chim. Fr.*, (9-10):2791–2794, 1973.

[290] Li J., Mau A.W.H., and Strauss C.R. The use of palladium on porous glass for catalytic coupling reactions. *Chem. Commun.*, **1997**(14):1275–1276, 1997.

[291] Walter J., Heiermann J., Dyker G., Hara S., and Shioyama H. Hexagonal or quasi two-dimensional palladium nanoparticles - Tested at the Heck reaction. *J. Catal.*, **189**(2):449–455, 2000.

[292] Mori K., Mizoroki T., and Ozaki A. Arylation of Olefin with Iodobenzene Catalyzed by Palladium. *Bull. Chem. Soc. Jpn.*, **46**(5):1505–1508, 1973.

[293] Nakayama M. and Mizoroki T. Stoichiometric carbonylation of aryl halide with nickel tetracarbonyl in the presence of potassium acetate. *Bull. Chem. Soc. Jpn.*, **44**(2):508–513, 1971.

[294] Augustine R.L. and O'Leary S.T. Heterogeneous catalysis in organic chemistry. Part 10. Effect of the catalyst support on the regiochemistry of the Heck arylation reaction. *J. Mol. Catal. A Chem.*, **95**(3):277–285, 1995.

[295] Swain S., Bhavya M., Kandathil V., Bhol P., Samal A.K., and Patil S.A. Controlled synthesis of palladium nanocubes as an efficient nanocatalyst for Suzuki-Miyaura cross-coupling and reduction of p-nitrophenol. *Langmuir*, **36**(19):5208–5218, 2020.

[296] Okumura K., Nota K., Yoshida K., and Niwa M. Catalytic performance and elution of Pd in the Heck reaction over zeolite-supported Pd cluster catalyst. *J. Catal.*, **231**(1):245–253, 2005.

[297] Ramchandani R.K., Uphade B.S., Vinod M.P., Wakharkar R.D., Choudhary V.R., and Sudalai A. Pd-Cu-Exchanged montmorillonite K10 clay: an efficient and reusable heterogeneous catalyst for vinylation of aryl halides. *Chem. Commun.*, **10**(21):2071–2072, 1997.

[298] Shimizu K.I., Maruyama R., Komai S.I., Kodama T., and Kitayama Y. Pd-sepiolite catalyst for Suzuki coupling reaction in water: structural and catalytic investigations. *J. Catal.*, **227**(1):202–209, 2004.

[299] Corma A., García H., Leyva A., and Primo A. Alkali-exchanged sepiolites containing palladium as bifunctional (basic sites and noble metal) catalysts for the Heck and Suzuki reactions. *Appl. Catal. A Gen.*, **257**(1):77–83, 2004.

[300] Smith M.D., Stepan A.F., Ramarao C., Brennan P.E., and Ley S.V. Palladium-containing perovskites: recoverable and reuseable catalysts for Suzuki couplings. *Chem. Commun.*, **3**(21):2652–2653, 2003.

[301] Villiger G., Marck andA. and Buchecker R. Aryl couplings with heterogeneous palladium catalysts. *Tetrahedron Lett.*, **35**(20):3277–3280, 1994.

[302] Heidenreich R.G., Kohler K., Krauter J.G.E., and Pietsch J. Pd/C as a highly active catalyst for Heck, Suzuki and Sonogashira reactions. *Synlett*, **2002**(7):1118–1122, 2002.

[303] Pröckl S.S., Kleist W., Gruber M.A., and Köhler K. In situ generation of highly active dissolved palladium species from solid catalysts - A concept for the activation of aryl chlorides in the Heck reaction. *Angew. Chem. Int. Ed.*, **43**(14):1881–1882, 2004.

[304] Gong X.F., Zhang L.Y., Zhang H.X., Cui Y.M., Jin F.C., Liu Y., Zhai Y.F., Li J.H., Liu G.Y., and Zeng Y.F. Highly active heterogeneous $PdCl_2$/MOF catalyst for Suzuki–Miyaura cross-coupling reactions of aryl chloride. *Z. Anorg. Allg. Chem.*, **646**(15):1–7, 2020.

[305] Ghobadi S., Burkholder M.B., Smith S.E., Gupton B.F., and Castano C.E. Catalytically sustainable, palladium-decorated graphene oxide monoliths for synthesis in flow. *Chem. Eng. J.*, **381**:122598, 2020.

[306] Ding G., Hao L., Xu H., Wang L., Chen J., Li T., Tu X., and Zhang Q. Atomically dispersed palladium catalyses Suzuki–Miyaura reactions under phosphine-free conditions. *Commun. Chem.*, **3**(1):1–8, 2020.

[307] Narayanan R. and El-Sayed M.A. Some aspects of colloidal nanoparticle stability, catalytic activity, and recycling potential. *Top. Catal.*, **47**(1-2):15–21, 2008.

[308] Reetz M.T., Breinbauer R., and Wanninger K. Suzuki and Heck reactions catalyzed by preformed palladium clusters and palladium/nickel bimetallic clusters. *Tetrahedron Lett.*, **37**(26):4499–4502, 1996.

[309] Reetz M.T., Lohmer G., and Schwickardi R. A new catalyst system for the Heck reaction of unreactive aryl halides. *Angew. Chem. Int. Ed.*, **37**(4):481–483, 1998.

[310] Narayanan R., Tabor C., and El-Sayed M.A. Can the observed changes in the size or shape of a colloidal nanocatalyst reveal the nanocatalysis mechanism type: homogeneous or heterogeneous? *Top. Catal.*, **48**(1-4):60–74, 2008.

[311] Liu Y., Khemtong C., and Hu J. Synthesis and catalytic activity of a poly(N,N-dialkylcarbodiimide)/palladium nanoparticle composite: a case in the Suzuki coupling reaction using microwave and conventional heating. *Chem. Commun.*, **2004**(4):398–399, 2004.

[312] Ornelas C., Ruiz Aranzaes J., Cloutet E., Alves S., and Astruc D. Click assembly of 1,2,3-triazole-linked dendrimers, including ferrocenyl dendrimers, which sense both oxo anions and metal cations. *Angew. Chem. Int. Ed.*, **46**(6):872–877, 2007.

[313] Percec V., Johansson G., Ungar G., and Zhou J. Fluorophobic effect induces the self-assembly of semifluorinated tapered monodendrons containing crown ethers into supramolecular columnar dendrimers which exhibit a homeotropic hexagonal columnar liquid crystalline phase. *J. Am. Chem. Soc.*, **118**(41):9855–9866, 1996.

[314] Diallo A.K., Boisselier E., Liang L., Ruiz J., and Astruc D. Dendrimer-induced molecular catalysis in water: the example of olefin metathesis. *Chem. Eur. J.*, **16**(39):11832–11835, 2010.

[315] Deraedt C., Salmon L., Etienne L., Ruiz J., and Astruc D. "Click" dendrimers as efficient nanoreactors in aqueous solvent: Pd nanoparticle stabilization for sub-ppm Pd catalysis of Suzuki–Miyaura reactions of aryl bromides. *Chem. Commun.*, **49**(74):8169–8171, 2013.

[316] Choudary B.M., Madhi S., Kantam M.L., Sreedhar B., and Iwasawa Y. Synthesis of surface organopalladium intermediates in coupling reactions: the mechanistic insight. *J. Am. Chem. Soc.*, **126**(8):2292–2293, 2004.

[317] Choudary B.M., Madhi S., Chowdari N.S., Kantam M.L., and Sreedhar B. Layered double hydroxide supported nanopalladium catalyst for Heck-, Suzuki-, Sonogashira-, and Stille-type coupling reactions of chloroarenes. *J. Am. Chem. Soc.*, **124**(47):14127–14136, 2002.

[318] Mandal S., Roy D., Chaudhari R.V., and Sastry M. Pt and Pd nanoparticles immobilized on amine-functionalized zeolite: excellent catalysts for hydrogenation and Heck reactions. *Chem. Mater.*, **16**(19):3714–3724, 2004.

[319] Gallon B.J., Kojima R.W., Kaner R.B., and Diaconescu P.L. Palladium nanoparticles supported on polyaniline nanofibers as a semi-heterogeneous catalyst in water. *Angew. Chem. Int. Ed.*, **46**(38):7251–7254, 2007.

[320] Han W., Liu C., and Jin Z.L. Aerobic ligand-free Suzuki coupling reaction of aryl chlorides catalyzed by in situ generated palladium nanoparticles at room temperature. *Adv. Synth. Catal.*, **350**(3):501–508, 2008.

[321] Han W., Liu C., and Jin Z.L. In situ generation of palladium nanoparticles: a simple and highly active protocol for oxygen-promoted ligand-free Suzuki coupling reaction of aryl chlorides. *Org. Lett.*, **9**(20):4005–4007, 2007.

[322] Yuan B., Pan Y., Li Y., Yin B., and Jiang H. A highly active heterogeneous palladium catalyst for the Suzuki-Miyaura and Ullmann coupling reactions of aryl chlorides in aqueous media. *Angew. Chem. Int. Ed.*, **49**(24):4054–4058, 2010.

[323] Wang F., Mielby J., Richter F.H., Wang G., Prieto G., Kasama T., Weidenthaler C., Bongard H.J., Kegnæs S., Fürstner A., and Schüth F. A polyphenylene support for Pd catalysts with exceptional catalytic activity. *Angew. Chem. Int. Ed.*, **53**(33):8645–8648, 2014.

[324] Du Y., Wei S., Tang M., Ye M., Tao H., Qi C., and Shao L. Palladium nanoparticles stabilized by chitosan/PAAS nanofibers : a highly stable catalyst for Heck reaction. *Appl. Organomet. Chem.*, **34**(5):1–12, 2020.

[325] Zhong S. Incorporation of palladium catalyst inside cross-linked chitosan hybrid nanofibers for the Sonogashira reaction. *Kin. Catal.*, **61**(3):480–485, 2020.

[326] Mirza-aghayan M., Mohammadi M., Addad A., and Boukherroub R. Pd nanoparticles supported on reduced graphene oxide as an effective and reusable heterogeneous catalyst for the Mizoroki–Heck coupling reaction. *Appl. Organomet. Chem.*, **34**:1–12, 2020.

[327] Yang P., Liu S., Ni H., and Shi J. Synthesis of the graphene supported Pd composites as catalyst for the Heck reaction of iodobenzene, acrylic acid and triethylamine. *Int. J. Nanosci.*, **19**(2):1950012, 2020.

[328] Zheng X., Zhao J., Xu M., and Zeng M. Preparation of porous chitosan/reduced graphene oxide microspheres supported Pd nanoparticles catalysts for Heck coupling reactions. *Carbohydr. Polym.*, **230**:115583, 2020.

[329] Xu J., Wilson A.R., Rathmell A.R., Howe J., Chi M., and Wiley B.J. Synthesis and catalytic properties of Au-Pd nanoflowers. *ACS Nano*, **5**(8):6119–6127, 2011.

[330] Wang F., Li C., Sun L.D., Wu H., Ming T., Wang J., Yu J.C., and Yan C.H. Heteroepitaxial growth of high-index-faceted palladium nanoshells and their catalytic performance. *J. Am. Chem. Soc.*, **133**(4):1106–1111, 2011.

[331] Movahed S.K., Miraghaee S., and Dabiri M. AuPd alloy nanoparticles decorated graphitic carbon nitride as an excellent photocatalyst for the visible-light-enhanced Suzuki–Miyaura cross-coupling reaction. *J. Alloys Compd.*, **819**:152994, 2020.

[332] Wang F., Li C., Chen H., Jiang R., Sun L.D., Li Q., Wang J., Yu J.C., and Yan C.H. Plasmonic harvesting of light energy for Suzuki coupling reactions. *J. Am. Chem. Soc.*, **135**(15):5588–5601, 2013.

[333] Sarina S., Zhu H., Jaatinen E., Xiao Q., Liu H., Jia J., Chen C., and Zhao J. Enhancing catalytic performance of palladium in gold and palladium alloy nanoparticles for organic synthesis reactions through visible light irradiation at ambient temperatures. *J. Am. Chem. Soc.*, **135**(15):5793–5801, 2013.

[334] Xiao Q., Sarina S., Jaatinen E., Jia J., Arnold D.P., Liu H., and Zhu H. Efficient photocatalytic Suzuki cross-coupling reactions on Au–Pd alloy nanoparticles under visible light irradiation. *Green Chem.*, **16**(9):4272–4285, 2014.

[335] Zhang Z., Rogers C.R., and Weiss E.A. Energy transfer from CdS QDs to a photogenerated pd complex enhances the rate and selectivity of a Pd-photocatalyzed Heck reaction. *J. Am. Chem. Soc.*, **142**:495–501.

[336] Evans J., O'Neill L., Kambhampati V.L., Rayner G., Turin S., Genge A., Dent A.J., and Neisius T. Structural characterisation of solution species implicated in the palladium-catalysed Heck reaction by Pd K-edge X-ray absorption spectroscopy: palladium acetate as a catalyst precursor. *J. Chem. Soc., Dalton Trans.*, **2002**(10):2207–2212, 2002.

[337] Bedford R.B., Cazin C.S.J., and Holder D. The development of palladium catalysts for C–C and C–heteroatom bond forming reactions of aryl chloride substrates. *Coord. Chem. Rev.*, **248**(21-24):2283–2321, 2004.

[338] Nájera C., Gil-Moltó J., and Karlström S. Suzuki-Miyaura and related cross-couplings in aqueous solvents catalyzed by di(2-pyridyl)methylamine-palladium dichloride complexes. *Adv. Synth. Catal.*, **346**(13-15):1798–1811, 2004.

[339] Kong F., Zhou C., Wang J., Yu Z., and Wang R. Water-soluble palladium click chelating complex: an efficient and reusable precatalyst for Suzuki-Miyaura and Hiyama reactions in water. *ChemPlusChem*, **78**(6):536–545, 2013.

[340] Diallo A.K., Ornelas C., Salmon L., Aranzaes J.R., and Astruc D. "Homeopathic" catalytic activity and atom-leaching mechanism in Miyaura-Suzuki reactions under ambient conditions with precise dendrimer-stabilized Pd nanoparticles. *Angew. Chem. Int. Ed.*, **46**(45):8644–8648, 2007.

[341] Köhler K., Heidenreich R.G., Soomro S.S., and Pröckl S.S. Supported palladium catalysts for Suzuki reactions : structure- property relationships , optimized reaction protocol and control of palladium leaching. *Adv. Synth. Catal.*, **350**(18):2930–2936, 2008.

[342] Soomro S.S., Ansari F.L., Chatziapostolou K., and Köhler K. Palladium leaching dependent on reaction parameters in Suzuki-Miyaura coupling reactions catalyzed by palladium supported on alumina under mild reaction conditions. *J. Catal.*, **273**(2):138–146, 2010.

[343] Narayanan R. and El-Sayed M.A. Effect of colloidal catalysis on the nanoparticle size distribution: dendrimer-Pd vs PVP-Pd nanoparticles catalyzing the Suzuki coupling reaction. *J. Phys. Chem. B*, **108**(25):8572–8580, 2004.

[344] Narayanan R. and El-Sayed M.A. Effect of colloidal nanocatalysis on the metallic nanoparticle shape: the Suzuki reaction. *Langmuir*, **21**(5):2027–2033, 2005.

[345] Narayanan R. and El-Sayed M.A. Effect of catalysis on the stability of metallic nanoparticles: Suzuki reaction catalyzed by PVP-palladium nanoparticles. *J. Am. Chem. Soc.*, **125**(27):8340–8347, 2003.

[346] Narayanan R. and El-Sayed M.A. FTIR study of the mode of binding of the reactants on the Pd nanoparticle surface during the catalysis of the suzuki reaction. *J. Phys. Chem. B*, **109**(10):4357–4360, 2005.

[347] Garcia-Martinez J.C., Lezutekong R., and Crooks R.M. Dendrimer-encapsulated Pd nanoparticles as aqueous, room-temperature catalysts for the Stille reaction. *J. Am. Chem. Soc.*, **127**(14):5097–5103, 2005.

[348] Pittelkow M., Moth-Poulsen K., Boas U., and Christensen J.B. Poly(amidoamine)-dendrimer-stabilized Pd(0) nanoparticles as a catalyst for the Suzuki reaction. *Langmuir*, **19**(18):7682–7684, 2003.

[349] Rahim E.H., Kamounah F.S., Frederiksen J., and Christensen J.B. Heck reactions catalyzed by PAMAM-dendrimer encapsulated Pd(0) nanoparticles. *Nano Lett.*, **1**(9):499–501, 2001.

[350] Ishida J., Nakatsuji M., Nagata T., Kawasaki H., Suzuki T., and Obora Y. Synthesis and characterization of N, N-dimethylformamide-protected palladium nanoparticles and their use in the Suzuki-Miyaura cross-coupling reaction. *ACS Omega*, **5**(16):9598–9604, 2020.

[351] Ananikov V.P. and Beletskaya I.P. Toward the ideal catalyst: from atomic centers to a "cocktail" of catalysts. *Organometallics*, **31**(5):1595–1604, 2012.

[352] Schmidt A.F., Al Halaiqa A., and Smirnov V.V. Interplays between reactions within and without the catalytic cycle of the Heck reaction as a clue to the optimization of the synthetic protocol. *Synlett*, **2006**:2861–2878, 2006.

[353] Zvereva E.E., Katsyuba S.A., Dyson P.J., and Aleksandrov A.V. Solvation of Palladium Clusters in an Ionic Liquid: a QM/MM Molecular Dynamics Study. *J. Phys. Chem. C Nanomater. Interfaces*, **120**(8):4596–4604, 2016.

[354] Loh N.D., Sen S., Bosman M., Tan S.F., Zhong J., Nijhuis C.A., Král P., Matsudaira P., and Mirsaidov U. Multistep nucleation of nanocrystals in aqueous solution. *Nat. Chem.*, **9**(1):77–82, 2017.

[355] Vidhani D.V., Krafft M.E., and Alabugin I.V. Rh(I)-catalyzed transformation of propargyl vinyl ethers into (E,Z)-dienals: stereoelectronic role of trans effect in a metal-mediated pericyclic process and a shift from homogeneous to heterogeneous catalysis during a one-pot reaction. *J. Org. Chem.*, **79**(1):352–364, 2014.

[356] Collins G., Schmidt M., Odwyer C., McGlacken G., and Holmes J.D. Enhanced catalytic activity of high-index faceted palladium nanoparticles in Suzuki-Miyaura coupling due to efficient leaching mechanism. *ACS Catal.*, **4**(9):3105–3111, 2014.

[357] Aufiero M., Scattolin T., Proutière F., and Schoenebeck F. Air-stable dinuclear iodine-bridged Pd(I) complex - catalyst, precursor, or parasite? The additive decides. Systematic nucleophile-activity study and application as precatalyst in cross-coupling. *Organometallics*, **34**(20):5191–5195.

[358] Johansson Seechurn C.C.C., Sperger T., Scrase T.G., Schoenebeck F., and Colacot T.J. Understanding the unusual reduction mechanism of Pd(II) to Pd(I): Uncovering hidden species and implications in catalytic cross-coupling reactions. *J. Amer. Chem. Soc.*, **139**(14):5194–5200, 2017.

[359] Bej A., Ghosh K., Sarkar A., and Knight D.W. Palladium nanoparticles in the catalysis of coupling reactions. *RSC Adv.*, **6**(14):11446–11453, 2016.

[360] European medicines agency: Scientific guideline on impurities in drug products, ref: Cpmp/ich/2738/99. Available at `http://www.ema.europa.eu/ema/index.jsp?curl=pages/regulation/general/general_content_000356.jsp&mid=WC0b01ac0580028e8c`.

[361] Therapeutic goods administration: Scientific guideline on impurities in drug products, ref: Cpmp/ich/2738/99. Available at `https://www.tga.gov.au/book/182-related-impurities-drug-substances-and-drug-products`.

[362] Lin K., Song M., Cai D., Hao X., and Wu Y. Polymer (fiber)-supported palladium catalyst containing imidazolinyl rings and its application to the Heck reaction. *Tetrahedron Lett.*, **44**(20):3955–3957, 2003.

[363] Stevens P.D., Fan J., Gardimalla H.M.R., Yen M., and Gao Y. Superparamagnetic nanoparticle-supported catalysis of Suzuki cross-coupling reactions. *Org. Lett.*, **7**(11):2085–2088, 2005.

[364] Stevens P.D., Li G., Fan J., Yen M., and Gao Y. Recycling of homogeneous Pd catalysts using superparamagnetic nanoparticles as novel soluble supports for Suzuki, Heck, and Sonogashira cross-coupling reactions. *Chem. Commun.*, **2005**(35):4435–4437, 2005.

[365] Tamoradi T., Daraie M., and Heravi M.M. Synthesis of palladated magnetic nanoparticle (Pd@Fe_3O_4/AMOCAA) as an efficient and heterogeneous catalyst for promoting Suzuki and Sonogashira cross-coupling reactions. *Appl. Organomet. Chem.*, **34**(4):1–10, 2020.

[366] Nouri K., Ghassemzadeh M., Mohsenzadeh F., and Afsharpour M. Pd(0) complex of fuberidazole modified magnetic nanoparticles: a novel magnetically retrievable high-performance catalyst for Suzuki and Stille C–C coupling reactions. *Appl. Organomet. Chem.*, **34**(9):1–15, 2020.

[367] Rangraz Y., Nemati F., and Elhampour A. A novel magnetically recoverable palladium nanocatalyst containing organoselenium ligand for the synthesis of biaryls via Suzuki-Miyaura coupling reaction. *J. Phys. Chem. Sol.*, **138**:109251, 2020.

[368] Hasan K. Methyl salicylate functionalized magnetic chitosan immobilized palladium nanoparticles: an efficient catalyst for the Suzuki and Heck coupling reactions in water. *ChemistrySelect*, **5**(23):7129–7140, 2020.

[369] Veisi H., Ozturk T., Karmakar B., Tamoradi T., and Hemmati S. In situ decorated Pd NPs on chitosan-encapsulated Fe_3O_4/SiO_2-NH_2 as magnetic catalyst in Suzuki-Miyaura coupling and 4-nitrophenol reduction. *Carbohydr. Polym.*, **235**:115966, 2020.

[370] Bartholomew C.H. Mechanisms of catalyst deactivation. *Appl. Catal. A Gen.*, **212**(1-2):17–60, 2001.

[371] Besson M. and Gallezot P. Deactivation of metal catalysts in liquid phase organic reactions. *Catal. Today*, **81**(4):547–559, 2003.

[372] Sádaba I., López Granados M., Riisager A., and Taarning E. Deactivation of solid catalysts in liquid media: the case of leaching of active sites in biomass conversion reactions. *Green Chem.*, **17**(8):4133–4145, 2015.

[373] Luo N., Ouyang K., Cao F., and Xiao T. Hydrogen generation from liquid reforming of glycerin over Ni-Co bimetallic catalyst. *Biomass Bioenergy*, **34**(4):489–495, 2010.

[374] Ding Y., Zheng H., Li J., Zhang S., Liu B., and Ekberg C. An efficient leaching of palladium from spent catalysts through oxidation with Fe(III). *Materials*, **12**(8), 2019.

[375] Benavidez A.D., Kovarik L., Genc A., Agrawal N., Larsson E.M., Hansen T.W., Karim A.M., and Datye A.K. Environmental transmission electron microscopy study of the origins of anomalous particle size distributions in supported metal catalysts. *ACS Catal.*, **2**(11):2349–2356, 2012.

[376] Challa S.R., Delariva A.T., Hansen T.W., Helveg S., Sehested J., Hansen P.L., Garzon F., and Datye A.K. Relating rates of catalyst sintering to the disappearance of individual nanoparticles during Ostwald ripening. *J. Am. Chem. Soc.*, **133**(51):20672–20675, 2011.

[377] Langmuir I. The vapor pressure of metallic tungsten. *Phys. Rev.*, **2**(5):329–342, Nov 1913.

[378] Harris P.J.F. The sintering of platinum particles in an alumina-supported catalyst: further transmission electron microscopy studies. *J. Catal.*, **97**(2):527–542, 1986.

[379] Harris P.J.F., Boyes E.D., and Cairns J.A. The sintering of an alumina-supported platinum catalyst studied by transmission electron microscopy. *J. Catal.*, **82**(1):127–146, 1983.

[380] Hansen T.W., Delariva A.T., Challa S.R., and Datye A.K. Sintering of catalytic nanoparticles: particle migration or Ostwald ripening? *Acc. Chem. Res.*, 46(8):1720–1730.

[381] Wynblatt P. and Gjostein N.A. Supported metal crystallites. *Prog. Solid State. Ch.*, **9**(C):21–58, 1975.

[382] Ouyang R., Liu J.X., and Li W.X. Atomistic theory of ostwald ripening and disintegration of supported metal particles under reaction conditions. *J. Am. Chem. Soc.*, **135**(5):1760–1771, 2013.

[383] Simonsen S.B., Chorkendorff I., Dahl S., Skoglundh M., Sehested J., and Helveg S. Ostwald ripening in a Pt/SiO_2 model catalyst studied by in situ TEM. *J. Catal.*, **281**(1):147–155, 2011.

[384] Pentsak E.O., Gordeev E.G., and Ananikov V.P. Noninnocent nature of carbon support in metal/carbon catalysts: etching/pitting vs nanotube growth under microwave irradiation. *ACS Catal.*, **4**(11):3806–3814, 2014.

[385] Bartholomew C.H. Sintering kinetics of supported metals: new perspectives from a unifying GPLE treatment. *Appl. Catal. A Gen.*, **107**(1):1–57, 1993.

[386] Davis J.J. and Hanyu Y. Mechanistic studies of AFM probe-driven Suzuki and Heck molecular coupling. *Nanotechnology*, **21**(26), 2010.

[387] Ellis P.J., Fairlamb I.J.S., Hackett S.F.J., Wilson K., and Lee A.F. Evidence for the surface-catalyzed Suzuki-Miyaura reaction over palladium nanoparticles: an operando XAS study. *Angew. Chem. Int. Ed.*, **49**(10):1820–1824, 2010.

[388] Lee A.F., Ellis P.J., Fairlamb I.J.S., and Wilson K. Surface catalysed Suzuki–Miyaura cross-coupling by Pd nanoparticles: an operando XAS study. *Dalton Trans.*, **39**(43):10473–10482, 2010.

[389] Newton M.A., Nicholls R., Brazier J.B., Nguyen B.N., Mulligan C.J., Hellgardt K., Barreiro E.M., Emerich H., Hii K.K., Snigireva I., and Thompson P.B.J. Effect of retained chlorine in ENCAT™ 30 catalysts on the development of encapsulated Pd: insights from in situ Pd K, L3 and Cl K-edge XAS. *Catalysis, Structure and Reactivity*, **3**(4):149–156, 2017.

[390] Lati M.P., Naeem M.I., Alinia-Asli M., Shirini F., Rezvani M.A., Åkermark B., Johnston E.V., and Verho O. Palladium nanoparticles immobilized on an aminopropyl-functionalized silica-magnetite composite as a recyclable catalyst for Suzuki-Miyaura reactions. *ChemistrySelect*, **3**(27):7970–7975, 2018.

[391] Thathagar M.B., Ten Elshof J.E., and Rothenberg G. Pd nanoclusters in C-C coupling reactions: proof of leaching. *Angew. Chem. Int. Ed.*, **45**(18):2886–2890, 2006.

[392] Barreiro E.M., Hao Z., Adrio L.A., van Ommen J.R., Hellgardt K., and Hii K.K. Spatial, temporal and quantitative assessment of catalyst leaching in continuous flow. *Catal. Today*, **308**:64–70, 2018.

[393] Davies I.W., Matty L., Hughes D.L., and Reider P.J. Are heterogeneous catalysts precursors to homogeneous catalysts? *J. Am. Chem. Soc.*, **123**(41):10139–10140, 2001.

[394] Budroni G., Corma A., García H., and Primo A. Pd nanoparticles embedded in sponge-like porous silica as a Suzuki-Miyaura catalyst: similarities and differences with homogeneous catalysts. *J. Catal.*, **251**(2):345–353, 2007.

[395] Crudden C.M., Sateesh M., and Lewis R. Mercaptopropyl-modified mesoporous silica: a remarkable support for the preparation of a reusable, heterogeneous palladium catalyst for coupling reactions. *J. Am. Chem. Soc.*, **127**(28):10045–10050, 2005.

[396] Gorunova O.N., Novitskiy I.M., Grishin Y.K., Gloriozov I.P., Roznyatovsky V.A., Khrustalev V.N., Kochetkov K.A., and Dunina V.V. When applying the mercury poisoning test to palladacycle-catalyzed reactions, one should not consider the common misconception of mercury(0) selectivity. *Organometallics*, **37**(17):2842–2858, 2018.

[397] Widegren J.A. and Finke R.G. A review of soluble transition-metal nanoclusters as arene hydrogenation catalysts. *J. Mol. Catal. A Chem.*, **191**(2):187–207, 2003.

[398] Górna M., Szulmanowicz M.S., Gniewek A., Tylus W., and Trzeciak A.M. Recyclable Pd(0)-Pd(II) composites formed from Pd(II) dimers with NHC ligands under Suzuki-Miyaura conditions. *J. Organomet. Chem.*, **785**:92–99, 2015.

[399] Snelders D.J.M., Van Koten G., and Klein Gebbink R.J.M. Hexacationic dendriphos ligands in the Pd-catalyzed Suzuki-Miyaura cross-coupling reaction: scope and mechanistic studies. *J. Am. Chem. Soc.*, **131**(32):11407–11416, 2009.

[400] Scrivanti A., Bertoldini M., Matteoli U., Beghetto V., Antonaroli S., Marini A., and Crociani B. Highly efficient Heck olefin arylation in the presence of iminophosphine-palladium(0) complexes. *J. Mol. Catal. A: Chem.*, **235**:12–16, 2005.

[401] Caporusso A.M., Innocenti P., Aronica L.A., Vitulli G., Gallina R., Biffis A., Zecca M., and Corain B. Functional resins in palladium catalysis: promising materials for Heck reaction in aprotic polar solvents. *J. Catal.*, **234**(1):1–13, 2005.

[402] Huang L., Ang T.P., Wang Z., Tan J., Chen J., and Wong P.K. On the roles of solid-bound ligand scavengers in the removal of palladium residues and in the distinction between homogeneous and heterogeneous catalysis. *Inorg. Chem.*, **50**(6):2094–2111, 2011.

[403] Richardson J.M. and Jones C.W. Strong evidence of solution-phase catalysis associated with palladium leaching from immobilized thiols during Heck and Suzuki coupling of aryl iodides, bromides, and chlorides. *J. Catal.*, **251**(1):80–93, 2007.

[404] Kurokhtina A.A., Larina E.V., and Shmidt A.F. Study of the differential selectivity of cross-coupling reactions for elucidating the nature of the true catalyst. *Kinet. Catal*, **56**(2):190–196, 2015.

[405] Schmidt A.F. and Kurokhtina A.A. Distinguishing between the homogeneous and heterogeneous mechanisms of catalysis in the Mizoroki-Heck and suzuki-miyaura reactions: problems and prospects. *Kinet. Catal*, **53**(6):714–730, 2012.

[406] Wan Y., Wang H., Zhao Q., Klingstedt M., Terasaki O., and Zhao D. Ordered mesoporous Pd/silica-carbon as a highly active heterogeneous catalyst for coupling reaction of chlorobenzene in aqueous media. *J. Am. Chem. Soc.*, **131**(12):4541–4550, 2009.

[407] Kurokhtina A.A., Larina E.V., Schmidt A.F., Malaika A., Krzyzyńska B., Rechnia P., and Kozłowski M. Mechanistic studies of the Suzuki-Miyaura reaction with aryl bromides using Pd supported on micro- and mesoporous activated carbons. *J. Mol. Catal. A Chem.*, **379**:327–332, 2013.

[408] De La Rosa M.A., Esperanza V., and Angel G. Cross-coupling reactions of monosubstituted acetylenes and aryl halides catalyzed by palladium on charcoal. *Synth. Commun.*, **20**(13):2059–2064, 1990.

[409] Duplais C., Forman A.J., Baker B.A., and Lipshutz B.H. UC Pd: a new form of PdVC for Sonogashira couplings. *Chem. Eur. J.*, **16**(11):3366–3371, 2010.

[410] Komáromi A., Szabó F., and Novák Z. Activity of palladium on charcoal catalysts in cross-coupling reactions. *Tetrahedron Lett.*, **51**(41):5411–5414, 2010.

[411] Komáromi A. and Novák Z. Efficient copper-free sonogashira coupling of aryl chlorides with palladium on charcoal. *Chem. Commun.*, **2008**(40):4968–4970, 2008.

[412] Shmidt A.F. and Mametova L.V. Main features of catalysis in the styrene phenylation reaction. *Kinet. Catal*, **37**(3):406–408, 1996.

[413] Djakovitch L., Wagner M., Hartung C.G., Beller M., and Koehler K. Pd-catalyzed Heck arylation of cycloalkenes - Studies on selectivity comparing homogeneous and heterogeneous catalysts. *J. Mol. Catal. A: Chemical*, **219**(1):121–130, 2004.

[414] Zhao F. and Arai M. Reactions of chlorobenzene and bromobenzene with methyl acrylate using a conventional supported palladium catalyst. *React. Kinet. Catal. Lett.*, **81**(2):281–289, 2004.

[415] Gnad C., Abram A., Ursto A., Weigl F., Schuster M., and Köler K. Leaching mechanism of different palladium surface species in Heck reactions of aryl bromides and chlorides. *ACS Catal.*, **10**:6030–6041, 2020.

[416] Schmidt A.F., Smirnov V.V., and Al-Halaiga A. Kinetics of the Heck reactions of styrene with bromobenzene and iodobenzene in the presence of ligandless catalytic systems: a comparative study. *Kinet. Catal*, **48**(3):390–397, 2007.

[417] Le Bars J., Specht U., Bradley J.S., and Blackmond D.G. Catalytic probe of the surface of colloidal palladium particles using Heck coupling reactions. *Langmuir*, **15**(22):7621–7625, 1999.

[418] Briggs B.D., Bedford N.M., Seifert S., Koerner H., Ramezani-Dakhel H., Heinz H., Naik R.R., Frenkel A.I., and Knecht M.R. Atomic-scale identification of Pd leaching in nanoparticle catalyzed C-C coupling: effects of particle surface disorder. *Chem. Sci.*, **6**(11):6413–6419, 2015.

[419] Pathak S., Greci M.T., Kwong R.C., Mercado K., Prakash G.K.S., Olah G.A., and Thompson M.E. Synthesis and applications of palladium-coated poly(vinylpyridine) nanospheres. *Chem. Mater.*, **12**(7):1985–1989, 2000.

[420] Li Y., Boone E., and El-Sayed M.A. Size effects of PVP-Pd nanoparticles on the catalytic Suzuki reactions in aqueous solution. *Langmuir*, **18**(12):4921–4925, 2002.

[421] Hiebler K., Lichtenegger G.J., Maier M.C., Park E.S., Gonzales-Groom R., Binks B.P., and Gruber-Woelfler H. Heterogeneous Pd catalysts as emulsifiers in Pickering emulsions for integrated multistep synthesis in flow chemistry. *Beilstein J. Org. Chem.*, **14**:648–658, 2018.

[422] Lipshutz B.H., Tasler S., Chrisman W., Spliethoff B., and Tesche B. On the nature of the 'heterogeneous' catalyst: nickel-on-charcoal. *J. Org. Chem.*, **68**(4):1177–1189, 2003.

[423] Del Zotto A. and Zuccaccia D. Metallic palladium, PdO, and palladium supported on metal oxides for the Suzuki–Miyaura cross-coupling reaction: a unified view of the process of formation of the catalytically active species in solution. *Catal. Sci. Technol.*, **7**(18):3934–3951, 2017.

[424] Biffis A., Zecca M., and Basato M. Metallic palladium in the Heck reaction: active catalyst or convenient precursor? *Eur. J. Inorg. Chem.*, **2001**(5):1131–1133, 2001.

[425] Andrews S.P., Stepan A.F., Tanaka H., Ley S.V., and Smith M.D. Heterogeneous or homogeneous? A case study involving palladium-containing perovskites in the Suzuki reaction. *Adv. Synth. Catal.*, **347**(5):647–654, 2005.

[426] Srivastava R., Venkatathri N., Srinivas D., and Ratnasamy P. Pd-SAPO-31, an efficient, heterogeneous catalyst for Heck reactions of aryl chlorides. *Tetrahedron Lett.*, **44**(18):3649–3651, 2003.

[427] Djakovitch L. and Rollet P. Sonogashira cross-coupling reactions catalysed by copper-free palladium zeolites. *Adv. Synth. Catal.*, **346**(13-15):1782–1792, 2004.

[428] Costantino F., Vivani R., Bastianini M., Ortolani L., Piermatti O., Nocchetti M., and Vaccaro L. Accessing stable zirconium carboxy-aminophosphonate nanosheets as support for highly active Pd nanoparticles. *Chem. Commun.*, **51**(88):15990–15993, 2015.

[429] Kozell V., Giannoni T., Nocchetti M., Vivani R., Piermatti O., and Vaccaro L. Immobilized palladium nanoparticles on zirconium carboxy-aminophosphonates nanosheets as an efficient recoverable heterogeneous catalyst for Suzuki–Miyaura and Heck coupling. *Catalysts*, **7**(6):186, 2017.

[430] MacQuarrie S., Horton J.H., Barnes J., McEleney K., Loock H.P., and Crudden C.M. Visual observation of redistribution and dissolution of palladium during the Suzuki-Miyaura reaction. *Angew. Chem. Int. Ed.*, **47**(17):3279–3282, 2008.

[431] Rossy C., Majimel J., Fouquet E., Delacôte C., Boujtita M., Labrugère C., Tréguer-Delapierre M., and Felpin F.X. Stabilisation of carbon-supported palladium nanoparticles through the formation of an alloy with gold: application to the Sonogashira reaction. *Chem. Eur. J.*, **19**(42):14024–14029, 2013.

[432] Shimizu K.I., Koizumi S., Hatamachi T., Yoshida H., Komai S., Kodama T., and Kitayama Y. Structural investigations of functionalized mesoporous silica-supported palladium catalyst for Heck and Suzuki coupling reactions. *J. Catal.*, **228**(1):141–151, 2004.

[433] Baleizão C., Corma A., García H., and Leyva A. Oxime carbapalladacycle covalently anchored to high surface area inorganic supports or polymers as heterogeneous green catalysts for the Suzuki reaction in water. *J. Org. Chem.*, **69**(2):439–446, 2004.

[434] Gaikwad A.V., Holuigue A., Thathagar M.B., Ten Elshof J.E., and Rothenberg G. Ion- and atom-leaching mechanisms from palladium nanoparticles in cross-coupling reactions. *Chem. Eur. J.*, **13**(24):6908–6913, 2007.

[435] Leyva-Pérez A., Oliver-Meseguer J., Rubio-Marqués P., and Corma A. Water-stabilized three- and four-atom palladium clusters as highly active catalytic species in ligand-free C-C cross-coupling reactions. *Angew. Chem. Int. Ed.*, **52**(44):11554–11559, 2013.

[436] Pahlavani M.R. *Theoretical Concepts of Quantum Mechanics.* InTech, Janeza Trdine, Croatia, 2012.

[437] Eschrig H. The fundamentals of density functional theory (revised and extended version). Institute for Solid State and Materials Research Dresden and University of Technology Dresden. Preprint on webpage at `http://puccini.chimica.uniba.it/didattica/corsi/solid{_}state{_}chem/dft.pdf`, 2003.

[438] Koch W. and Holthausen M.C. *A Chemist's Guide to Density Functional Theory.* Wiley-VCH, Weinheim, Germany, 2001.

[439] Vosko S.H., Wilk L., and Nusair M. Accurate spin-dependent electron liquid correlation energies for local spin density calculations: a critical analysis. *Can. J. Phys.*, **58**(8):1200–1211, 1980.

[440] Perdew J.P., Chevary J.A., Vosko S.H., Jackson K.A., Pederson M.R., Singh D.J., and Fiolhais C. Atoms, molecules, solids, and surfaces: applications of the generalized gradient approximation for exchange and correlation. *Phys. Rev. B*, **46**:6671–6687, 1992.

[441] Becke A.D. Density-functional exchange-energy approximation with correct asymptotic behavior. *Phys. Rev. A*, **38**:3098–3100, 1988.

[442] Perdew J.P. *Unified Theory of Exchange and Correlation Beyond the Local Density Approximation.* Ziesche, P. and Eschrig, H., Akademie Verlag, Berlin, 1991.

[443] Lee C., Yang W., and Parr R.G. Development of the Colle-Salvetti correlation-energy formula into a functional of the electron density. *Phys. Rev. B*, **37**:785–789, 1988.

[444] Becke A.D. Density-functional thermochemistry. III. the role of exact exchange. *J. Chem. Phys.*, **98**:5648, 1993.

[445] Stephens P.J., Devlin F.J., Chabalowski C.F., and Frisch M.J. Ab Initio calculation of vibrational absorption and circular dichroism spectra using density functional force fields. *J. Phys. Chem.*, **98**(45):11623–11627, 1994.

[446] Woods N.D., Payne M.C., and Hasnip P.J. Computing the self-consistent field in Kohn-Sham density functional theory. *J. Phys. Condens. Matter*, **31**(45):453001, 2019.

[447] Ditchfield R., Hehre W.J., and Pople J.A. Self-consistent molecular-orbital methods. IX. An extended gaussian-type basis for molecular-orbital studies of organic molecules. *J. Chem. Phys.*, **54**(2):720–723, 1971.

[448] Hehre W.J., Ditchfield R., and Pople J.A. Self–consistent molecular orbital methods . XII . Further extensions of Gaussian–type basis sets for use in molecular orbital studies of organic molecules. *J. Chem. Phys.*, **56**(5):2257–2261, 1972.

[449] Francl M.M., Pietro W.J., Hehre W.J., Binkley J.S., Gordon M.S., DeFrees D.J., and Pople J.A. Self-consistent molecular orbital methods. XXIII. A polarization-type basis set for second-row elements. *J. Chem. Phys.*, **77**(7):3654–3665, 1982.

[450] Binning R.C. and Curtiss L.A. Compact contracted basis sets for third-row atoms: Ga–Kr. *J. Comput. Chem.*, **11**(10):1206–1216, 1990.

[451] Blaudeau J.P., McGrath M.P., Curtiss L.A., and Radom L. Extension of Gaussian-2 (G2) theory to molecules containing third-row atoms K and Ca. *J. Chem. Phys.*, **107**(13):5016–5021, 1997.

[452] Rassolov V.A., Pople J.A., Ratner M.A., and Windus T.L. 6-31G* basis set for atoms K through Zn. *J. Chem. Phys.*, **109**(4):1223–1229, 1998.

[453] Rassolov V.A., Ratner M.A., Pople J.A., Redfern P.C., and Curtiss L.A. 6-31G* basis set for third-row atoms. *J. Comput. Chem.*, **22**(9):976–984, 2001.

[454] Hariharan P.C. and Pople J.A. The influence of polarization functions on molecular orbital hydrogenation energies. *Theor. Chim. Acta*, **28**(3):213–222, 1973.

[455] Kahn L.R. and Goddard W.A. Ab initio effective potentials for use in molecular calculations. *J. Chem. Phys.*, **56**(6):2702–2712, 1972.

[456] Hay P.J. and Wadt W.R. Ab initio effective core potentials for molecular calculations. Potentials for K to Au including the outermost core orbital. *J. Chem. Phys.*, **82**(1):299–310, 1985.

[457] Hay P.J. and Wadt W.R. Ab initio effective core potentials for molecular calculations. Potentials for the transition metal atoms Sc to Hg. *J. Chem. Phys.*, **82**(1):270–283, 1985.

[458] Wadt W.R. and Hay P.J. Ab initio effective core potentials for molecular calculations. Potentials for main group elements Na to Bi. *J. Chem. Phys.*, **82**(1):284–298, 1985.

A Appendix

A.I The laboratory

The lab-bench experiments started with some model batch reactions between 4-iodoacetophenone and phenylboronic acid, according to a Suzuki-Miyaura coupling scheme (Section 2.1). The reactions were performed in the presence of Na_2CO_3 as the base and in a solvent mixture of 1:1 THF:water. The reaction mixture was heated under reflux through an oil bath at a fixed temperature of 95°C (66°C within the medium) and catalyzed by $3\%_{wt}$ loaded Pd/C coil synthesized by a colleague.
The aim of the model reaction was to reproduce in batch, the reaction conditions under which other continuous-flow experiments would have been carried out. For this purpose, two reactors were envisaged to be tested: Mark II and microfluidic Mark IV. The latter being under assembly, Mark II was prepared to launch the first reactions, which were, unfortunately, not performed due to an early departure. However, Figure 47 shows Mark II reactor's set up. One should note that the description includes some devices, employed in liquid-gas phase reactions, namely hydrogenations, which were not envisaged for our application, though, the reactor's setup is apt to carry out these reactions, too.

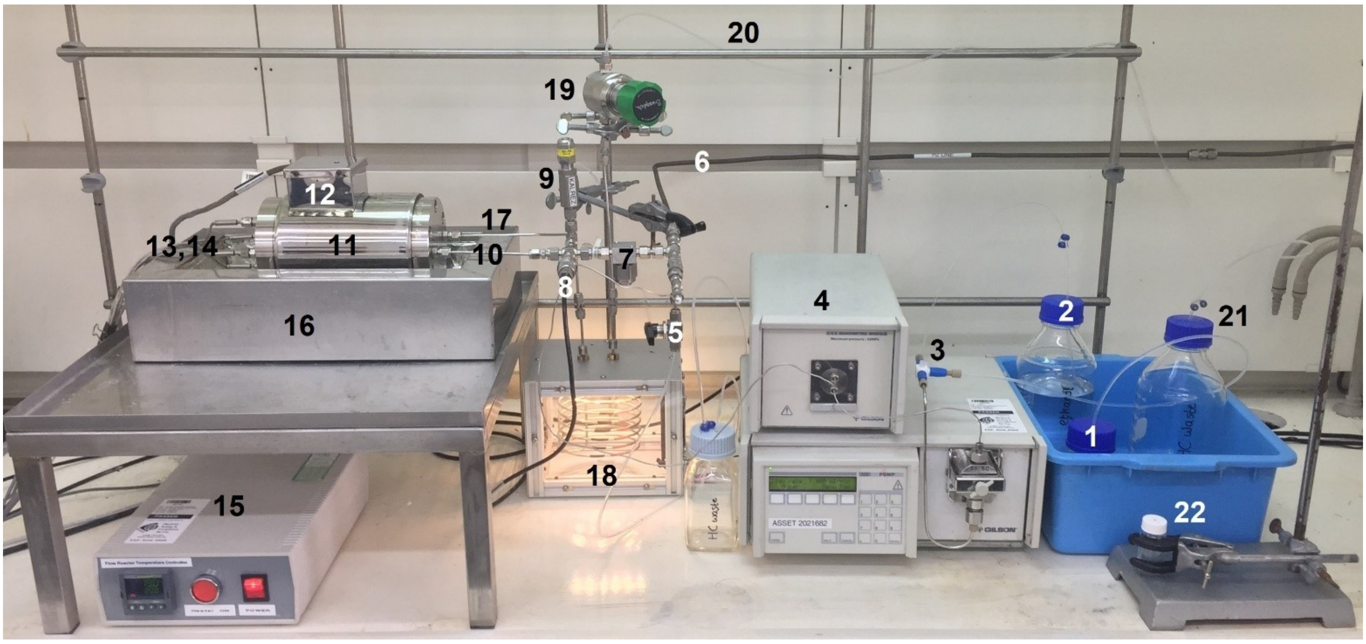

Figure 47: Schematic photograph of the setup of the Mark II C–C coupling reactor. (1) Inlet leading to Schott bottle containing first solution of C–C coupling substrate. (2) Inlet leading to Schott bottle containing second solution of C–C coupling substrate. (3) T-piece. (4) Gilson pump to deliver the liquid stream into the reactor (flow-rate 0.01-45 [ml/min]). (5) Purge valve to allow removal of air bubbles from the pump. (6) Gas inlet for 3-phase experiments. (7) Mixer. (8) Pressure transducer leading to external data-logger and computer. (9) Pressure relief valve which opens if the reactor pressure exceeds 28 bar. (10) Reactor inlet. (11) Reactor body containing 12 channels of ID = 6 mm, into which static mixers may be inserted. (12) Heating block. (13) Thermocouples leading to external data-logger and computer. (14) Gas flow rate detector leading to external data-logger and computer. (15) Heating controller leading to external data-logger and computer. (16) Heat-retaining container for reactor. (17) Reactor outlet. (18) Fan-assisted air cooler. (19) Back-pressure regulator to control reactor pressure, which can range from 1 to 30 bar. (20) Outlet tubing. (21) Outlet collection Schott bottle. (22) Sample collection vial with specially drilled cap to clamp the outlet and allow gas venting.

Some photos (Figure 48) describe the internal setup of the reactor, too. The inner construction of Mark II consists of a continuous pathway dug into a steel-monolith structure. 12 cylindrical tube-like channels have been created in order to host an equal maximum number of Catalytic Static Mixers (CSMs), playing the role of the carriers for palladium catalytic species (*vide infra*). The liquid solution containing the substrates, travels through each channel and changes direction towards the following one, thanks to the grooves in the back and front end-plates. This scheme built a continuous pathway between the inlet and the outlet allowing the intermittent contact with the catalyst, supported on the CSMs (*vide infra*).

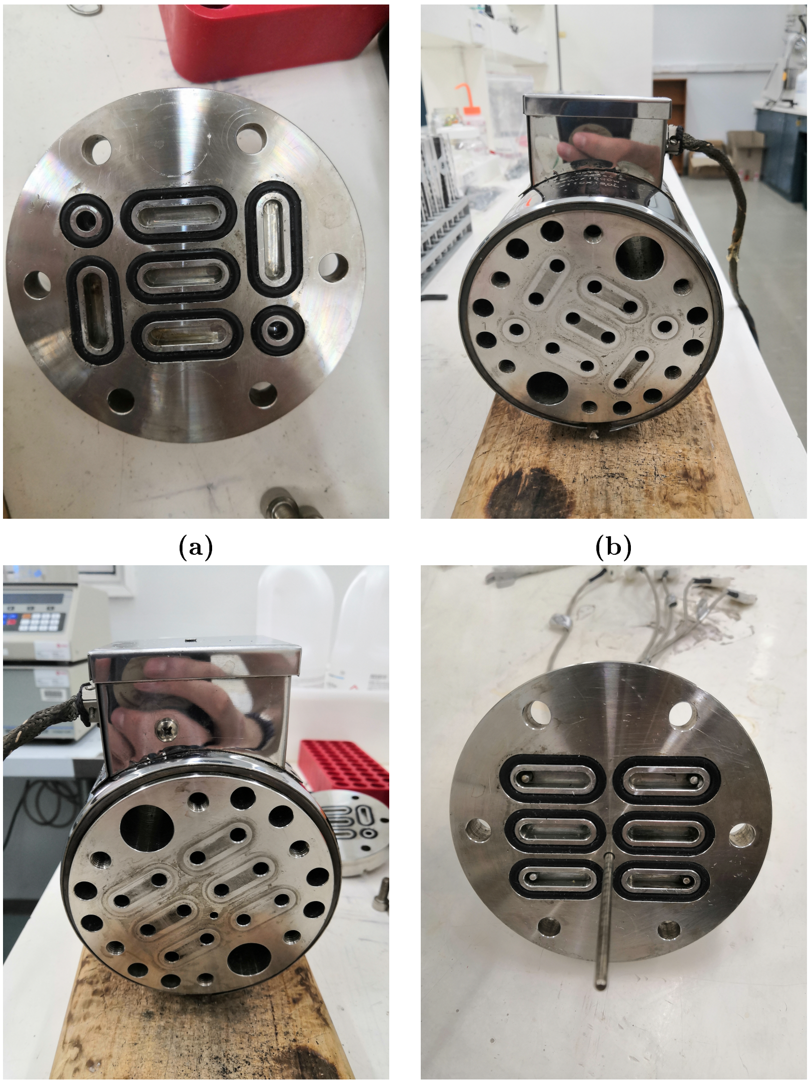

(a) **(b)** **(c)** **(d)**

Figure 48: Main parts of Mark II reactor. (a) Front end-plate of the reactor including the holes for inlet and outlet in addition to the reversing-flow channel for continuous pathway. (b) Main body of Mark II (front view). (c) Main body of Mark II (back view). (d) Back end-plate of the reactor including five thermocouple-inlets in addition to the reversing-flow channels for continuous pathway.

A.II The Catalytic Static Mixers (CSMs)

In 2016, CSIRO patented the metallic modular structures called "static mixers", which can be coated with active metal catalysts. The design of the mixer was optimized computationally in order to enhance its mixing ability. It consists of a complex repeated-unit framework, manufactured thanks to metal 3D printing, which offers flexibility over the design.

Coating techniques include electroplating, metal cold spraying and wash coating. The treatment with metal precursors turns them into Catalytic Static Mixers (CSMs).

Several advantages characterize these modern structures. First of all, their length-to-diameter ratio promotes mass and heat transfer, contrarily to packed beds, resulting in more uniform concentration and temperature gradients. Moreover, their monolith nature and the perfect fitting into the reactor channels, reduce long-term mechanical disruption through attrition and shocks of both the support and the reactor walls, as well as channeling, dead zones ad restructuring phenomena. Furthermore, they are easier to replace than packed beds. After removal, the metal static mixer body can be recycled by re-coating with a fresh catalyst. Last but not least, CSMs are highly scalable.
Figure 49 shows the metallic framework of a typical CSIRO's CSM.

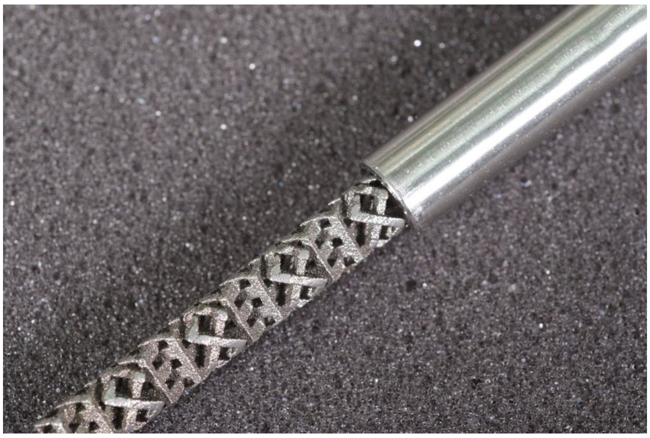

Figure 49: CSMs structure design, as patented by CSIRO. Structure manufactured by metal 3D printing.

Acknowledgments

Going through this year's difficulties and sad news while having to face the conception and drafting of this work, has been tough. Some dreams have been crushed, some opportunities born. Anyway, no work like this would have been concluded without the aid of all the people I knew.
First of all I would like to thank the whole CSIRO's Manufacturing business unit for letting me join their team during this wonderful yet short experience; the CSIRO in general for accepting my work and my further requests related to the COVID-19 health emergency.
I am particularly thankful to my research group, namely Simon, Christian, Tom, Christopher, Yutong, Xindong, but above all my tutor Ivan Martinez Botella, researcher at CSIRO of Clayton (Vic, Australia). Through these months, he took care of me and my work and interceded with the laboratory in order to organize my early departure. Even when I came back to Italy he always asked me for updates and efficiently and carefully read this report.
Thank you all guys for your care and kindness! Thanks to you, my experience in Melbourne has been even more likable than expected. Now I know that if I ever come back, I will find part of a family, there.
I also thank both my universities: the ENSCM of Montpellier and the Politecnico of Turin, for the concern showed towards students studying and living abroad. A special mention goes to Professors: Délphine Paolucci, Anne Filippi, Vasile Hulea and Stefania Specchia, for their help during these two years of French double degree.
In addition to them, thanks to my Italian supervisor, prof. Mauro Banchero for accepting my work which had neither shape nor direction at the beginning, for his advice and patience.

To my ENSCM's family, I would like to dedicate a tender virtual embrace, just like they devoted their time and patience to include me and make me feel home. We spent such a great time together! I will always remember that time as one of the best periods of my life...with a little melancholy for what I lost and gratefulness for what I found.
I would like to mention one by one, my dearest "Sultans" and friends: "Ma belle marraine", Moooorgaaaane, Erwi, Laura, Tatane, Kantin, Alexis, Elise, Seb, Caro, Gaëlle, Matthieu, Konter, Laure...and... Soraya, Christelle, Julián, Henrique, Ramon. I love you!
Moreover, the "Stones" (cc Beubeu), the "Incas", the "Wilds", "Tikis", "Wizards"...and more...my team NAECO (Roxane, Camille L., Camille A., Elina, Robin, Clément etc), the "Club Arc-en-ciel" (Katya vous aime)...and Iñigo for the good moments...Thank you all!

Though, the greater thanks goes to my parents, who bore and supported me during these lock-down months, whatever the issue or concern.
Together with them, they come my friends. In particular, I would like to thank Guillerme and Giovanni for being so helpful and welcoming, once I arrived in Australia and did not know anyone.
Then, thanks to Carlotta, Rebecca, Nicolò, together with my "Monregafamily", I know we went through hard times, but hopefully everything will get fixed. I really love you all!
One last special mention is for Marcella, my good old friend (not that old though), who looked after me when everything seemed to go wrong. You usually do not want me to be that sweet but I will remember your "rude" words and lectures, as a proof of affection and with a smile.